Hawaii Ocean Time-series
Data Report 5
1993

Luis Tupas

Fernando Santiago-Mandujano

Dale Hebel

Eric Firing

Frederick Bingham

Roger Lukas

David Karl

University of Hawaii

School of Ocean and Earth Science and Technology

1000 Pope Road

Honolulu, Hawaii 96822

U. S.A.

SOEST TECHNICAL REPORT 94-5

Preface

Scientists working within the Hawaii Ocean Time-series (HOT) project have been making repeated observations of the hydrography, chemistry and biology at a station north of Oahu, Hawaii since October 1988. The objective of this research is to provide a comprehensive description of the ocean at a site representative of the central North Pacific subtropical gyre. Cruises are made approximately once a month to the HOT deep-water station (22 45' N, 158 W) located about 100 km north of Oahu, Hawaii. Measurements of the thermohaline structure, water column chemistry, currents, primary production and particle sedimentation rates are made over a 72-hour period on each cruise.

This document reports the data collected during 1993. However, we have included some data from 1988 - 1992 in order to place the 1993 measurements within the context of our time-series observations. The data reported here are a screened subset of the complete data set. Summary plots are given for CTD, biogeochemical, optical, meteorological and ADCP observations.

In order to conserve paper and to provide easy computer access to our data, CTD data at National Oceanographic Data Center (NODC) standard pressures for temperature, potential temperature, salinity, oxygen and potential density are provided in ASCII files on the enclosed diskette. Chemical measurements are also summarized in a set of Lotus-123™ files on the enclosed diskette. The complete data set resides on a Sun workstation at the University of Hawaii. These data are in ASCII format, and can easily be accessed using anonymous ftp via Internet. Instructions for using the Lotus files and for obtaining the data from the network are presented in Section 8. The entire data set will also be submitted to the NODC and will eventually be available through that service.

Acknowledgments

Many people have participated in the 1993 cruises sponsored by the HOT program. They are listed in Table 1.4. We gratefully acknowledge their contributions and support.

Thanks are due to James Christian, John Dore, Charles Holloway, Terrence Houlihan, Ricardo Letelier, Hongbin Liu, Richard Muller, Jefrey Snyder and Jinchun Yuan for participating in many of the 1993 cruises and for the tremendous amount of time and effort they have put into the program. Special thanks is due to Lisa Lum and Caroline Kohan for their excellent administrative support of the program. In addition, we would like to acknowledge the contributions made by Sharon DeCarlo and Lance Fujieki for programming and data management and Julie Ranada and Xiaomei Zhou for ADCP processing. Nava Zvaig and Venugopal Sanaka provided additional computer support. Ursula Magaard performed many of the routine chemical analyses. Ted Walsh performed the nutrient analyses, Sophia Asghar and Reka Domokos the salinity measurements and Jason Killam provided additional technical support. We also would like to thank the captains and crew members of the R/V Townsend Cromwell, R/V Moana Wave, R/V Thomas G. Thompson, R/V Wecoma, R/V New Horizon and R/V Na'Ina, and the UH Marine Center staff for their efforts. Don Wright, Nancy Koike, Karen Parayno and Brenda Lee-Ha were responsible for producing this document. Without the assistance of these people, the data presented in this report could not have been collected, processed, analyzed and reported.

This data set was acquired with funding from the National Science Foundation (NSF). The specific grants which have supported this work are NSF grants OCE-8717195 (WOCE), OCE-8800329 (JGOFS), OCE-9016090 (JGOFS), OCE-9303094 (WOCE), and OCE-9301368 (JGOFS). We also acknowldege the contributions of Dr. Christopher Winn (OCE-9315392), and Dr. Robert Bidigare (OCE-9315311) and their staff to the scientific efforts of HOT.

1. Introduction

In 1987, the National Science Foundation established a special-focus research initiative termed "The Global Geosciences Program." This program was intended to support studies of the earth as a system of interrelated physical, chemical and biological processes that act together to regulate the habitability of our planet. The stated goals of this program were two-fold. The first goal was to understand the earth-ocean-atmosphere system and how it functions. The second goal was to describe, and eventually predict, major cause-and-effect relationships. Two components of the Global Geosciences Program are the World Ocean Circulation Experiment (WOCE) and the Joint Global Ocean Flux Study (JGOFS). The former is focused on physical oceanographic processes and the latter on biogeochemical processes.

The Hawaii Ocean Time-series (HOT) project was initially funded in 1988 under the sponsorship of both the WOCE and JGOFS programs to make repeated observations of the physics, chemistry and biology of the water column for five years at a station north of Hawaii. Funding from NSF has been received to continue these observations until 1998. The objectives of HOT are to describe and understand the physical oceanography, and to identify and quantify the processes controlling biogeochemical cycling in the ocean at a site representative of the oligotrophic North Pacific Ocean.

Time-series cruises are made on approximately monthly intervals with two stations routinely occupied each month. The HOT deep-water station, also known as Station ALOHA (A Long-term Oligotrophic Habitat Assessment), is approximately 100 km north of Kahuku Point, Oahu, Hawaii (Figure 1.1; Table 1.1). Along the transit route to Station ALOHA, another station is occupied at 21° 20.6' N, 158° 16.4' W, off Kahe Point, Oahu. Station Kahe (also referred to as Station 1) is used primarily to test the CTD and other equipment, but it also provides additional time-series data at a near-shore site. Station Kahe is located in approximately 1500 m of water about 16 km from shore (Figure 1.1).

Station ALOHA (also referred to as Station 2) is defined as a circle with a 6 nautical mile radius centered at 22°45' N, 158° 00 W. All sampling at Station ALOHA is conducted within this circle (Figure 1.1). The maximum depth at Station ALOHA is about 4800 m. On several cruises in 1993, other stations were occupied along longitude 158°W at 22° 25' N (Station 3), 21° 57.8' N (Station 4) and 21° 46.6' N (Station 5) and at 21°50.8' N, 158° 21.8' W, near Kaena Point, Oahu (Station 6).

The JGOFS and WOCE components of the program measure a variety of parameters during the regular monthly sampling work at Station ALOHA (Table 1.1). Sampling includes a 36-hour burst of CTD casts at roughly 3-hour intervals to obtain temperature, salinity and oxygen profiles from 0 to 1000 meters. Sampling also includes a deep CTD cast as close to the bottom as possible. In addition, primary production, particle flux and a variety of chemical determinations at discrete depths with continuous profiles of optical parameters are conducted. Current measurements are made on HOT cruises using shipboard Acoustic Doppler Current Profiler (ADCP) when available. In addition, lowered ADCP measurements have been made on several HOT cruises. HOT cruises have continued to provide logistical support to several ancillary projects (Table 1.2).

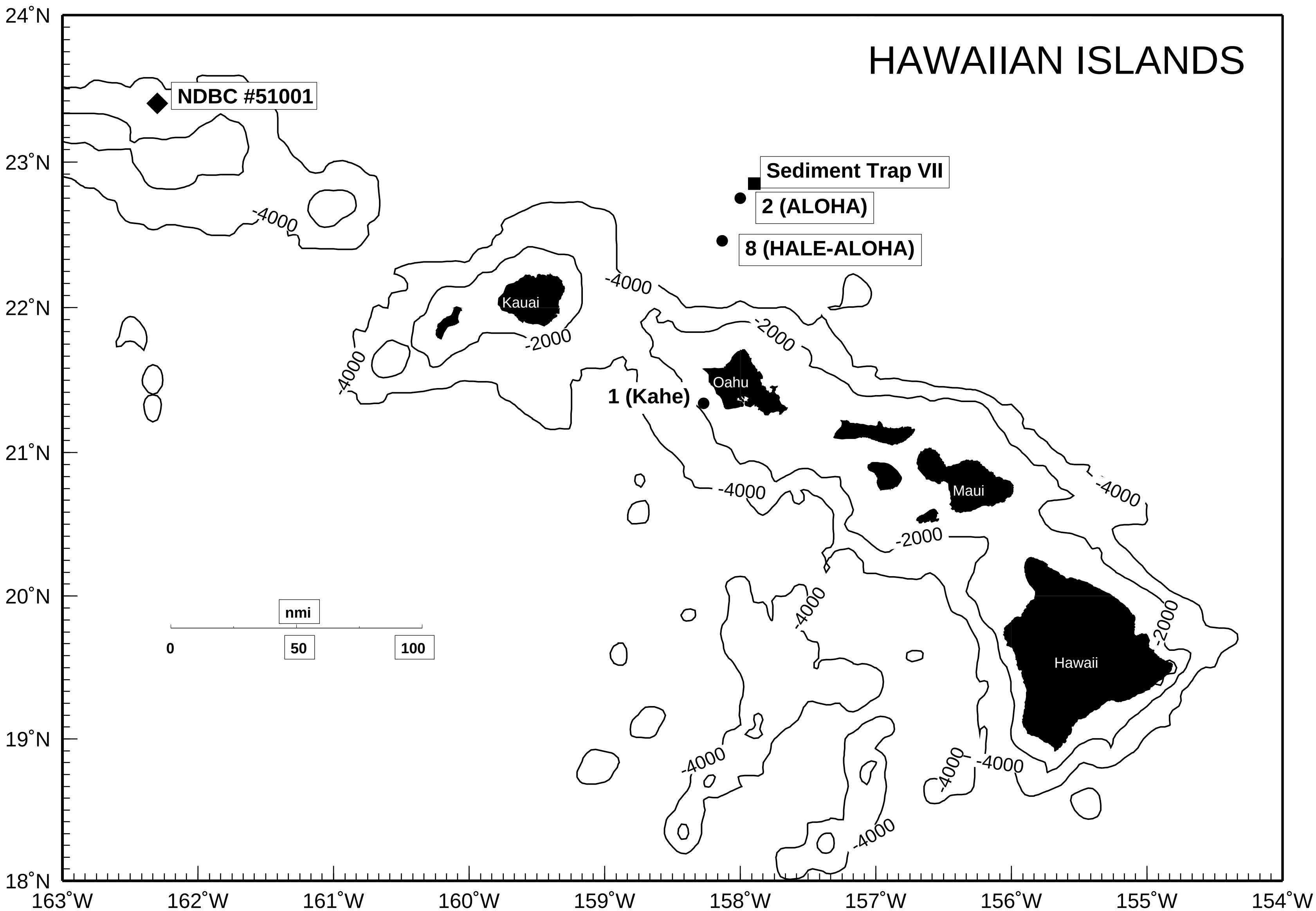

Figure 1.1: **Map of the Hawaiian Islands showing the locations of Station ALOHA, Station Kahe and the NDBC weather buoy. Also shown are Stations 3, 4, 5 and Station Kaena. Lower panel: Expanded view of Station ALOHA (a 6 nautical mile radius circle centered at 22°45'N, 158°W) and the location of the inverted echo sounders (N, C, E, SW, SE) and the bottom-moored sediment trap (ST-I & ST-II).**

Table 1.1. Locations of the HOT water column and bottom stations

Station	Coordinates	Approximate bottom depth (m)	Comments
1 (Kahe)	21°20.6'N 158°16.4'W	1,500	HOT Program coastal time-series station
2 (ALOHA)	22°45'N 158°00'W	4,800	HOT Program open ocean time-series station, confined to a circle with a 6 nmi radius, centered at ALOHA
3	23°25'N 158°00'W	4,800	One of three onshore to offshore transect sites, established
4	21°57.8'N 158°00'W	4,000	One of three onshore to offshore transect sites, established
5	21°46.6'N 158°00'W	45 0	One of three onshore to offshore transect sites, established
6 (Kaena)	21°50.8'N 158°21.8'W	2,500	Location of a long-term IES May 93-Jun 95
IES Network			
N	23°00.7'N 157°59.9'W	4,800	Feb 91-Feb 92, Jun 92- May 93
C	22°44.9'N 157°59.9'W	4,800	Feb 91-Feb92, Jun 92-present
SW	22°37.0'N 158°14.7'W	4,800	Feb 91-Feb 92, Jun 92- May 93
SE	22°30.0'N 157°45.2'W	4,800	Feb 91-Feb 92, Jun 92- May 93
E	22°44.8'N 157°54.0'W	4,800	Feb 91- Feb 92
ST-I	22°57.3'N 158°06.2'W	4,800	1st deployment of bottom-moored sequencing sediment trap, June 92-Oct 93
ST-II	23°6.7'N 157°55.8'W	4,800	2nd deployment of bottom-moored sequencing sediment trap, Oct 93 - Oct 94
Buoy #51001	23°24'N 162°18'W		NOAA-NDBC meteorological buoys closest to Sta. ALOHA

Table 1.2: Time-Series Parameters Measured at Station ALOHA

Parameter	Depth Range (m)	Analytical Procedure
1. CTD Measurements		
Depth (pressure)	0-4800	Pressure transducer on SeaBird CTD-rosette package
Temperature	0-4800	Thermistor on Sea-Bird CTD package with frequent calibration
Salinity	0-4800	Conductivity sensor on Sea-Bird CTD package, standardization with Guildline AutoSal #8400 against Wormley standard seawater
Oxygen	0-4800	Polarographic sensor on Sea-Bird CTD package with Winkler standardization
Fluorescence	0-1000	Sea-Tech Flash Fluorometer on Sea-Bird CTD package
Beam Transmission	0-1000	Sea-Tech 25 cm path length beam transmissometer on Sea-Bird CTD package
II. Optical Measurements		
Solar Irradiance (PAR)	Surface	Licor Cosine Collector and Biospherical 2 pi Collector
Underwater Irradiance (PAR)	0-150	Biospherical Profiling Natural Fluorometer 4 pi Collector
Solar Stimulated Fluorescence (683nm)	0-150	Biospherical Profiling Natural Fluorometer
III. Water Column Chemical Measurements		
Oxygen	0-4750	Winkler Titration
Total Dissolved Inorganic Carbon	0-4750	Coulometry
Titration Alkalinity	0-4750	Automated Titration
PH	0-4750	Potentiometry, Spectrophotometric
Dissolved Inorganic Nitrate Plus Nitrite	0-4750	Autoanalyzer
Dissolved Inorganic Phosphorus	0-4750	Autoanalyzer
Dissolved Silica	0-4750	Autoanalyzer
Low Level Nitrate Plus Nitrite	0-200	Chemiluminescence
Low Level Phosphorus	0-200	Magnesium-induced Coprecipitation
Low Level Silica	0-200	Magnesium-induced Coprecipitation
Dissolved Organic Carbon	0-1000	High Temperature Catalytic Oxidation
Total Dissolved Nitrogen	0-1000	U.V. oxidation
Total Dissolved Phosphorus	0-1000	U.V. oxidation
Particulate Carbon	0-1000	High Temperature Combustion
Particulate Nitrogen	0-1000	High Temperature Combustion
Particulate Phosphorus	0-1000	High Temperature Combustion
IV. Water Column Biomass Measurements		
Chlorophyll *a* and Phaeopigments	0-200	Fluorometric Analysis
Chlorophyll *a*, *b*, *c* and Accessory Pigme	0-200	High Performance Liquid Chromatography
Adenosine 5'-Triphosphate	0-1000	Firefly Bioluminescence
Bacteria and Cyanobacteria	0-1000	Flow Cytometry

Table 1.2: Continued

V. Carbon Assimilation and Particle Flux		
Primary Production	0-175	"Clean" ^{14}C Incubations
Carbon, Nitrogen, Phosphorus and Mass Flux	150, 300, 500	Free-Floating Particle Interceptor Traps
VI. Currents		
Acoustic Doppler Current Profiler	0-300	Hull Mounted, RDI #VM-150
Acoustic Doppler Current Profiler	0-4750	Lowered
VII. Moored Instruments		
Inverted Echo Sounder Network (Dynamic height)	100-1000	Acoustic telemetry, CTD calibration
Sequencing Sediment Traps (Particle Flux)	800, 1500, 3000, 4000	Honjo type

Table 1.3: Ancillary Projects Supported by HOT

Principal Investigator	Institution	Funding Agency	Duration	Title
Charles Keeling	Scripps Inst. of Oceanog.	National Science Foundation (NSF)	12/88-12/95	A Study of the Abundance and C13/C12 Ratio of Atmosphere Carboni Dioxide and Oceanic Carbon in Relation to the Global Carbon Cycle
George Luther	University of Delaware	NSF	2/93- 1/96	Iodine Speciation as a Primary Productivity Indicator
Marlin Atkinson	University of Hawaii	NSF	12/92-11/93	Calibration Stability of Two New Oxygen Sensors for CTDs
Lisa Campbell	University of Hawaii	NSF	3/91- 2/94	Phytoplankton Population Dynamics at the Hawaii Ocean Time-series Station
James Cowen	University of Hawaii	NSF	8/92- 12/94	Studies on the Dynamics of Marine Snow and Particle Aggregation in the North Pacific Central Gyre
Christopher Measures	University of Hawaii	Office of Naval Research	4/93-12/95	Temporal Variation of Dissolved Trace Element Concentrations in Response to Asian Dust Inputs
Brian Popp	University of Hawaii	NSF	6/91- 5/94	Isotopic Analyses of DOC and Cell Concentrates
Craig Smith	University of Hawaii	NSF	10/91- 9/94	The Relationship of Bioturbation, Macrobenthos and Seabed Radio-nuclides to the Flux and Fate of Organic Carbon Along the JGOFS Equatorial Pacific Transect

Table 1.3: Continued

Steve Emerson	University of Washington	NSF	10/93- 9/96	Ocean Oxygen Fluxes
Paul Quay	University of Washington	National Oceanographic and Atmospheric Administration	6/93- 6/96	13C/12C of Dissolved Inorganic Carbon in the Ocean
Hans Thierstein	Geo. Inst. Switzerland	Federal Institute of Technology	1/93- 12/95	Calcareous Phytoplankton Dynamics

This report presents selected core data collected during the fifth year of the HOT Program (January-December 1993). During this period, 7 cruises were conducted using six research vessels (Table 1.4) and a total field scientific crew of 50 (Table 1.5). The R/V Moana Wave, R/V New Horizon, R/V Wecoma and R/V Thomas G. Thompson are UNOLS vessels operated by the University of Hawaii, Scripps Institution of Oceanography, Oregon State University and the University of Washington, respectively. The R/V Townsend Cromwell is a National Oceanic & Atmospheric Administration owned and operated research vessel. The R/V Na'Ina is a motorized work vessel owned and operated by Uaukewai Diving Salvage & Fishing Inc. which was chartered by the University of Hawaii and U.S. Coast Guard certified as a research vessel for one ill-fated cruise.

Table 1.4: Summary of HOT Cruises, 1993

HOT	Ship	Depart	Return
44	R/V Townsend Cromwell	18 January 1993	23 January 1993
45	R/V Thomas G. Thompson	15 February 1993	20 February 1993
46	R/V Wecoma	12 April 1993	17 April 1993
47	R/V New Horizon	18 May 1993	23 May 1993
48	R/V Na'Ina	24 July 1993	30 July 1993
49A	R/V Moana Wave	9 September 1993	12 September 1993
49B	R/V Moana Wave	12 September 1993	17 September 1993
50	R/V Moana Wave	27 October 1993	01 November 1993

Table 1.5: University of Hawaii Cruise Personnel

	44	45	46	47	48	49a	49b	50
F. Bingham, P. I.							▒	
D. Hebel, P. I.	▒	▒	■	▒	▒	▒	■	▒
D. Karl, P. I.					▒	■		
L. Tupas, P. I.		■	▒	■	■	▒	▒	■
M. Atkinson, Scientist		▒						
L. Campbell, Scientist							▒	
M. Latasa, Scientist			▒					
C. Measures, Scientist				▒				
F. Thomas, Scientist				▒				
C. Winn, Scientist	■						▒	
N. Ahmed, Visiting Scientist			▒					
D. Bird, Visiting Scientist								▒
S. Emerson, Visiting Scientist		▒						
M. Keller, Visiting Scientist			▒					
M. Mulroney, Visiting Scientist				▒				
C. Stump, Visiting Scientist							▒	
C. Carrillo, Research Associate	▒			▒				
D. Copson, Research Associate						▒		
T. Houlihan, Research Associate	▒	▒			▒	▒	▒	▒
U. Magaard, Research Associate			▒					
R. Muller, Research Associate		▒	▒	▒	▒	▒	▒	▒
M. Rand, Research Associate								▒
F. Santiago-Mandujano, Research Associate							▒	▒
J. Snyder, Research Associate	▒		▒	▒	▒		▒	▒
S. Asghar, Graduate Student			▒					
J. Bower, Graduate Student			▒					
R. Bregman, Graduate Student								▒
J. Christian, Graduate Student	▒	▒				▒	▒	▒
R. Domokos, Graduate Student				▒				
J. Dore, Graduate Student	▒	▒			▒			▒
S. Evans, REU Student		▒						
L. Fujieki, Graduate Student				▒		▒		
C. Holloway, Graduate Student		▒	▒	▒		▒	▒	▒
D. Hoover, Graduate Student		▒						
S. Kennan, Graduate Student	▒	▒			▒			
R. Letelier, Graduate Student			▒	▒	▒		▒	
H. Liu, Graduate Student		▒	▒	▒			▒	▒
S. Reid, Graduate Student						▒	▒	
	44	45	46	47	48	49a	49b	50

Shaded area = cruise participant Solid area = Chief Scientist

Table 1.5: Continued

	44	45	46	47	48	49a	49b	50
D. Sadler, Graduate Student		■	■	■				■
K. Selph, Graduate Student								■
S. Siddiqui, Graduate Student						■		
P. Troy, Graduate Student		■						
D. Walsh, Graduate Student		■						
J. Yuan, Graduate Student	■	■		■			■	■
A. Farrenkopf, Visiting Graduate Student								■
K. Bjorkman, Visiting Graduate Student					■			
R. Hamme, Visiting Graduate Student							■	
	44	45	46	47	48	49a	49b	50

2. Sampling Procedures and Analytical Methods

2.1. CTD Profiling

Continuous measurements of temperature, salinity, oxygen, fluorescence and beam transmission are made with a Sea-Bird SBE-09 CTD package described in Tupas et al. (1993). A CTD cast to 1000 meters is made at Station Kahe on each cruise. At Station ALOHA a burst of consecutive CTD casts to 1000 meters is made over 36 hours to span the local inertial period and three semi-diurnal tidal cycles. One deep cast close to the bottom is made on each cruise to satisfy WOCE requirements. During HOT-44, CTD operations were conducted with a 12-place rosette and limited to 1000 m casts (see 3.1.). On HOT-48, only Station Kahe was occupied (see 3.5.).

2.1.1. Data Acquisition and Processing

CTD data were acquired at a rate of 24 samples per second. Digital data were stored on an IBM-compatible PC and the analog signal recorded on VHS video tapes. Backups of CTD data were made onto Bernoulli disks and later onto DAT tapes. The raw CTD data were quality controlled and screened for spikes as described in Winn et al. (1993). Data alignment, averaging, correction and reporting were done as described in Tupas et al. (1993). Temperature is reported in the ITS-90 scale and oxygen is reported in µmol kg^{-1}.

2.1.2. Sensor Corrections and Calibrations

Pressure

Pressure sensor calibration strategies and procedures are described in Winn et al. (1993) and Tupas et al. (1993). Briefly, this strategy used a high quality quartz pressure transducer as the laboratory transfer standard and a Russka precision dead-weight pressure tester as a primary standard. The primary standard met National Institute of Standards and Technology specifications and was operated under controlled conditions. The transfer standard was a Paroscientific Model 760 pressure gauge equipped with a 10,000 psi transducer. The transfer standard was calibrated by the Oceanographic Data Facility at Scripps Institution of Oceanography against their primary standard in May 1991, which showed an offset at 0 dbar of

0.3 dbar, and a 0.6 dbar increase in pressure difference, with our standard reading high, over the range of 0-4500 dbar. Hysteresis was less than 0.1 dbar throughout the entire range. A recent calibration at the Northwest Regional Calibration Center on 27 September 1994 showed no major change in our standard. The offset at 0 dbar was 0.3 dbar and the pressure difference over the 0-4500 dbar range was 1.2 dbar. Hysteresis was 0.2 dbar.

Pressure transducer #26448 was used on all the cruises in 1993. Calibrations against the transfer standard in 1993 are given in Table 2.1. These values have been corrected in the shift of the standard. The 28 January and 30 June offsets were used for the cruises in 1993. These offsets were used only for real-time data acquisition as a more accurate offset was determined at the time the CTD first enters the water on each cast. The drift of nearly 2 dbar yr^{-1} in offset observed between 30 June 1993 and 3 January 1994 can be considered normal for this sensor (see Tupas et al. 1993).

Table 2.1: CTD Pressure Calibrations (decibars)
Sea-Bird SBE-09 #91361 / Pressure Transducer #26448

Calibration date	Offset @ 0 dbar	slope offset @ 4500 dbar	hysteresis
28 January 1993	-5.29	-0.70	N/A
30 June 1993	-5.18	-0.83	0.14
3 January 1994	-6.19	-1.04	0.02

Temperature

Three Sea-Bird SBE-3-02/F temperature transducers were used in 1993 and were calibrated at the Northwest Regional Calibration Center (NWRCC) during the early part of the year. In May 1993 Sea-Bird commenced temperature calibrations in their own calibration bath. Cross-calibration checks with NWRCC for almost two years have shown that the Sea-Bird calibration facility is within ± 1 m°C of NWRCC's long term mean (N. Larson, personal communication, 1993). The history of the sensors is well-documented in Tupas et al. (1993). In 1992 sensor #961 was used only as a transfer standard during intercomparisons with two sensors in our laboratory.

Sensor #961

We modeled the drift of sensor #961 as a linear function of time using the calibrations on Table 2.2. A linear fit to the 0-30 °C average offset from each calibration relative to that on 31 July 1992 gave an intercept of 0.17 m°C with a slope of 0.00514 °C day^{-1}. The RMS deviation of the offsets from this fit was 0.16 m°C.

Sensor #866

A linear model of the drift from the calibrations on Table 2.2 was obtained with an intercept of 0.07 m°C and a slope of 0.00766 m°C day^{-1}. The RMS deviation of the fit was 0.56 m°C.

The 18 December 1992 calibration was used to calculate temperature from the sensor frequency data of all 1993 cruises, except HOT 49 station 2, cast 2 in which sensor #741 was used. When corrected for linear drift to 20 May 1993, this calibration gave the smallest deviation in the 0-5 °C temperature range from the set of all the calibrations in Table 2.2 (also corrected for linear drift to 20 May 1993). In the 0-5 °C range, the mean deviation of this calibration was approximately 0.2 m°C with about ± 0.2 m°C standard deviation. The deviation from this and the other calibrations for 1993 HOT cruises was ± 0.4 m°C. The corrections applied to sensor #886 are presented in Table 2.3.

Sensor #741

The steady drift followed for this sensor since 5 March 1991 suddenly started to decrease after June 1992, as documented in Tupas et al. (1993). A series of tests conducted at Sea-Bird from May to July 1993 confirmed that this change in sensor behaviour was due to aging, as experience with other sensors has shown that they become more stable with time. Using only the calibrations that reflected the drift change (Table 2.2), we estimated a sensor drift of -0.00210 m°C day^{-1} with an intercept of -0.03 m°C and a RMS deviation of 0.26 m°C in the fit. The 13 May 1993 calibration was used to recalculate temperature for HOT 49, station 2, cast 2. The correction applied to this cast is in Table 2.3.

Laboratory Calibrations

During 1993 we were able to perform intercalibrations among our three sensors after every cruise in the 10-20 °C range. The procedure is documented in Tupas et al. (1993). Using sensor #961 as the transfer sensor, with the linear drift correction obtained as described above, sensor #886 gave a drift of 0.00723 m°C day^{-1} with a RMS residual of 0.05 m°C from 4 intercalibrations. This is comparable to the 0.00766 m°C day^{-1} from NWRCC and Sea-Bird calibrations. For sensor #741, we obtained a drift of -0.00173 m°C day^{-1} with a RMS residual of 1.05 m°C from 5 intercalibrations. This is comparable to the -0.00210 m°C day^{-1} from NWRCC and Sea-Bird calibrations.

Conductivity

Conductivity cell #679 was used during HOT 44 to 48 and 50, and was calibrated at NWRCC on 11 August 1993. At the beginning of HOT 49, sensor #679 gave erratic measurements and failed at the bottom of station 2, cast 1, after which it was replaced by sensor #527. A post-cruise inspection of the sensor at Sea-Bird revealed an irreparable crack in the cell of #679. The cell was replaced and the sensor recalibrated on 14 October 1993. Sensor #527 was used for the rest of HOT 49 and was calibrated on 24 September 1993 and 8 October 1993. The calibration procedure is described in Winn et al. (1991).

Table 2.2: Calibration Coefficients for Sea-Bird Temperature Transducers. RMS Residuals from Calibration Give an Indication of Quality of the Calibration.

SN	YYMMDD	f_0	a	b	c	d	RMS (m°C)
961	940108	6718.08	3.68104129E-3	6.00719211E-4	1.56735492E-5	2.62306433E-6	0.05
961	930506	6719.05	3.68096927E-3	6.00707448E-4	1.56310803E-5	2.57218188E-6	0.06
961	930114	6791.28	3.67456115E-3	6.00413807E-4	1.56851516E-5	2.78999142E-6	0.43
961	920731	6782.47	3.67533262E-3	6.00279865E-4	1.51877355E-5	2.26314932E-6	0.24
961	920129	6789.88	3.67467693E-3	6.00392638E-4	1.56716646E-5	2.72527915E-6	0.09
886	931216	5904.70	3.68108073E-3	5.96027290E-4	1.48092022E-5	2.31314120E-6	0.05
886	930605	5905.69	3.68098370E-3	5.96013394E-4	1.47882243E-5	2.29755837E-6	0.06
886	921218	5967.82	3.67476787E-3	5.95715773E-4	1.48206068E-5	2.52835250E-6	0.39
886	920820	5935.78	3.67798061E-3	5.95648169E-4	1.41980725E-5	1.94572339E-6	0.60
886	920129	5969.00	3.67467842E-3	5.95638784E-4	1.45242521E-5	2.12848528E-6	0.20
741	931216	6169.60	3.68108398E-3	6.02142067E-4	1.53434585E-5	2.47225482E-6	0.26
741	930513	6170.47	3.68098624E-3	6.02116588E-4	1.52577583E-5	2.38750692E-6	0.26
741	921218	6234.70	3.67477118E-3	6.01755208E-4	1.48365899E-5	2.06062301E-6	0.38
741	920626	6246.37	3.67361468E-3	6.01608285E-4	1.48891820E-5	2.32038514E-6	0.26

The nominal calibrations were used for data acquisition and final calibration was determined empirically by comparing salinity determinations of discrete water samples acquired during each cast. Prior to empirical calibration of conductivity data with water bottle salinities, conductivity was corrected for thermal inertia of the glass conductivity cell as described in Chiswell et al. (1990). Table 2.3 lists the value of α used for each cruise.

Preliminary screening of bottle samples and empirical calibration of the conductivity cell are described in Tupas et al. (1993). The procedure for screening the bottles against calibrated CTD salinities has been improved to avoid excessive flagging of bottles with moderate CTD minus bottle salinity differences due to bottle closure and mark pressure mismatch, especially in high gradient regions.

The new method includes the calculation of the local vertical salinity gradient from a least square fit to 5 levels of the 2 dbar averaged data on both sides of the mark. The absolute value of the CTD minus bottle salinity difference (S) divided by the absolute value of the gradient yields a pressure Δp that is used as an additional parameter to determine the bottle quality.

The quality of each bottle is determined by comparing ΔS against the standard deviation

(SD) of "good data" and comparing Δp against a pressure cutoff value (P) as follows:

Bottle is flagged bad if $\Delta S > 4*SD$ and $\Delta p > P$

Bottle is flagged suspect if $\Delta S \geq 4*SD$ and $\Delta p \geq P$

or if $3*SD < \Delta S < 4*SD$ and $\Delta p > P$

Bottle is flagged good if $\Delta S > 3*SD$ and $\Delta p \leq P$

or if $\Delta S \leq 3*SD$

We selected a pressure cutoff value of 7 dbar, which is consistent with the objective of this new flagging method. This cutoff value represents the maximum vertical distance that a bottle can travel between the time of the mark and the closing of the bottles as a result of a ship roll or changing wire angle. A greater value would imply vertical movement of more than 7 dbars which is unlikely.

This new screening procedure was also applied to previous cruises (HOT 13 to 41) and the affected bottles were re-flagged. For HOT 44 to 50 the standard deviations within the 4 pressure ranges were: 0.0036 (surface-150 dbar), 0.0050 (150-500 dbar), 0.0022 (500-1050 dbar) and 0.0011 (1050-5000 dbar).

The conductivity calibration coefficients resulting from the least squares fit of the CTD minus bottle conductivities as a function of conductivity are given in Table 2.4. The quality of the CTD calibration is illustrated in Figure 2.1, which shows the differences between the corrected CTD salinities and the bottle salinities as a function of pressure for each cruise. The calibrations were best below 500 dbar because the weaker vertical salinity gradients at depth lead to less error if the bottle and CTD pressures are slightly mismatched.

The final step of conductivity calibration was a cast-dependent bias correction as described in Tupas et al (1993) to allow for drift during each cruise or for suddent offsets due to fouling. This offset was determined by taking the median valve of CTD minus bottle salinity differences for each profile at temperatures below 5°C (Table 2.5). Note that a change of 1×10^{-4} s m^{-1} in conductivity was approximately equivalent to 0.001 in salinity. The conductivity cell seemed to drift during HOT-47 for unknown reasons. For this cruise various casts required correction for their individual drifts. The cell functioned normally in succeeding cruises. Table 2.6 gives the mean and standard deviations for the final calibrated CTD minus water sample values.

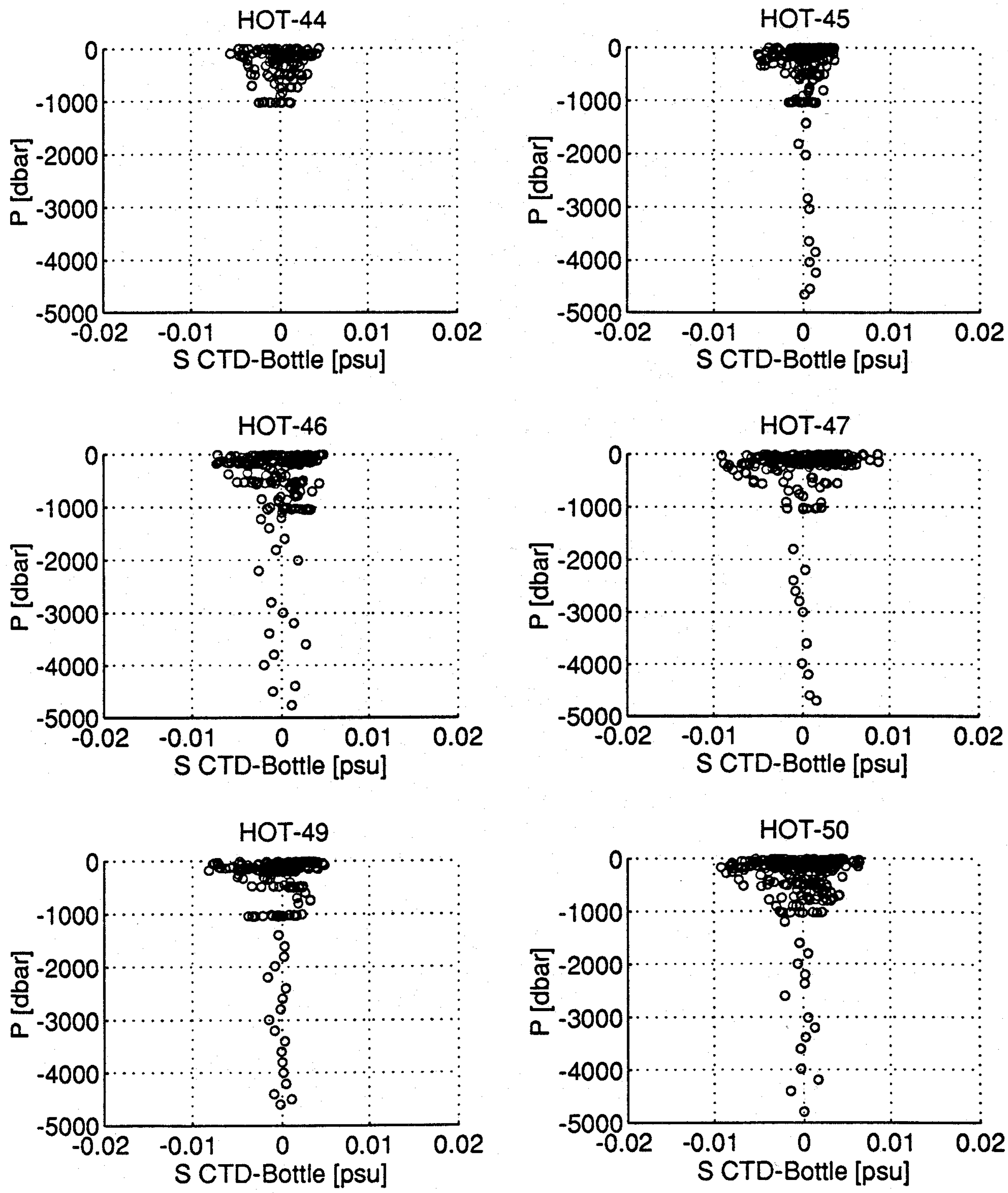

Figure 2.1: Differences between calibrated CTD salinities and bottle salinities for Station ALOHA, HOT-44 to 47, 49 and 50.

Table 2.3: Temperature and Conductivity Sensor Corrections

HOT	Temp #	T Correction °C	Cond #	α
44	886	-0.00100	679	0.028
45	886	-0.00080	679	0.037
46	886	-0.00040	679	0.028
47	886	-0.00010	679	0.028
48	886	0.00040	679	0.037
49	741	0.00020	679	0.037
49	886	0.00080	527	0.037
50	886	0.00110	679	0.037

Table 2.4: Table of Conductivity Calibration Coefficients

Cruise	b0	b1
HOT-44	0.001580438	-0.000895365
HOT-45	0.001188558	-0.000772499
HOT-46	0.001414603	-0.000920932
HOT-47	0.000478261	-0.000659599
HOT-48	0.000971945	-0.000787944
HOT-49	0.000763186	-0.000195160
HOT-49	0.000472153	-0.000160327
HOT-50	0.000802341	-0.000458807

Table 2.5: Individual Cast Conductivity Offsets

Cruise	Station	Cast	Offset
HOT-44	2	8	2.8414
	2	11	-2.2588
HOT-46	2	1	0.2229
HOT-47	2	1	3.5745
	2	5	-5.7573
	2	8	-7.0295
	2	11	-4.4674
	2	12	-7.0427
	2	13	-8.1657
	3	1	4.6391
	4	1	4.1929
HOT-49	2	18	2.5449
HOT-50	2	2	3.2589
	2	18	2.5569

Table 2.6: CTD-Bottle Salinity Comparison for Each Cruise

	0 < P < 4700 db		500 < P < 4700 db	
Cruise	Mean	St. Dev.	Mean	St. Dev.
HOT-44	-0.0000	0.0021	-0.0002	0.0016
HOT-45	0.0000	0.0018	0.0003	0.0010
HOT-46	-0.0000	0.0027	0.0003	0.0020
HOT-47	0.0002	0.0032	-0.0001	0.0018
HOT-48	-0.0000	0.0012	-0.0002	0.0006
HOT-49	-0.0002	0.0025	0.0002	0.0015
HOT-50	-0.0002	0.0033	0.0001	0.0023

Oxygen

A YSI Inc. oxygen probe was used for all cruises in 1993. Water bottle oxygen data were screened and the sensor was calibrated for all cruises in 1993 as described previously (Winn et al. 1991). Very low oxygen values were observed in the upper 50-80 m of several casts, specifically, HOT-44, station 1, cast 1 and station 2, casts 10 to 20; HOT-45, station 2 casts 8, 14, 15 and 16; and the single cast made stations 4, 8, 10, 13 and 14; HOT-47, station 2, cast 2. In addition, station 2 cast 2 of HOT-46 showed an abrupt offset in the oxygen trace of about 20 µmol kg^{-1} between 440 and 750 dbar. These oxygen values were flagged as suspect. Analysis of water bottle samples are described in section 2.2.2. Screening of bottle samples and empirical calibrations are described in Tupas et al. (1993). Table 2.7 gives the means and standard deviations for the final calibrated CTD values minus the water sample values.

Table 2.7: CTD minus Bottle O_2 (µmol kg^{-1}) Comparison for Each Cruise

	Station 1, Kahe Point 0 to 1500 dbar		Station 2, ALOHA 0 to 4700 dbar		Station 2, ALOHA 500 to 4700 dbar	
Cruise	Mean	St. Dev.	Mean	St. Dev.	Mean	St. Dev.
HOT-44	0.64	3.42	0.01	1.22	0.24	1.27
HOT 45	0.01	1.29	0.02	2.27	0.08	1.95
HOT-46	0.00	1.26	0.03	1.37	0.03	1.07
HOT-47	0.02	1.64	0.04	1.97	0.11	1.76
HOT-48	0.00	0.98				
HOT-49	0.00	1.84	0.09	2.94	0.12	2.71
HOT-50	0.02	2.58	0.05	2.11	-0.019	2.17

Flash Fluorescence

Flash fluorescence was measured with a Sea Tech Model ST0250 flash fluorometer and the data collected with the Sea Bird CTD system. Flash fluorescence traces were collected on as many casts as possible. Because an absolute radiometric standard is not available for flash fluorometers, instrument drift was corrected by checking the relative response of the instrument between cruises using fluorescent plastic sheeting as described in Tupas et al. (1993). The constants used to correct the fluorescence data for 1993 are given in Table 2.8.

Table 2.8: Fluorescence Calibration Factors

Cruise #	a	b
44	2.9318	0.3112
45	2.9318	0.3112
46	2.9318	0.3112
47	2.9318	0.1556
48	2.9318	0.3112
49	2.9318	0.3112
50	2.9318	0.3112

Beam Transmission

Beam transmission was measured with a Sea Tech 25 cm path length transmissometer. Transmission data were collected using the Sea Bird CTD system in a fashion analogous to that described for flash fluorescence. The transmissometer was calibrated as described by the manufacturer before each cruise to correct for instrument drift.

2.2. Discrete Water Column Measurements

Water samples for chemical analyses were collected at Station Kahe and ALOHA as well as the other irregularly occupied stations. Sampling strategies and procedures are well documented in the previous data reports (Tupas et al. 1993, Winn et al. 1993) and in the HOT-JGOFS protocol manual (Karl et al. 1990; available over Internet, see Section 8). This data report contains only a subset of the total data base which can be extracted from the accompanying diskette or via anonymous ftp over Internet. To assist in the interpretation of these data and to save users the time to estimate the precision of individual chemical analysis, we have summarized precision estimates from replicate determinations for each constituent on each HOT cruise in 1993.

2.2.1. Salinity

Salinity samples were collected, stored and analyzed as described in Tupas et al. (1993). The results of laboratory standard analyses run for each cruise are presented in Table 2.9. The typical precision estimate for salinity measurements made in 1993 are about 0.001.

Table 2.9: Precision of salinity measurements using lab standards

HOT	Mean Salinity & number of samples		
	Mean salinity ± standard deviation	# samples	batch #
44	34.49784 ± 0.00011	8	6
45	34.47292 ± 0.00165	14	6
46	34.46888 ± 0.00051	13	7
47	34.47368 ± 0.00488	7	7
48	34.46790 ± 0.00028	2	7
49	34.46694 ± 0.00066	30	7
50	34.47104 ± 0.00094	17	7

2.2.2. Oxygen

Oxygen samples were collected and analyzed using a computer controlled potentiometric end-point titration procedure as described in Tupas et al. (1993). As in previous years we measured, using a calibrated digital thermistor, the temperature of the seawater sample within the individual Niskin bottles at the time the iodine flask was filled. This was done to evaluate the magnitude of oxygen sample temperature error which affects the calculation of oxygen concentrations in units of µmol kg^{-1}. Figure 2.2 (top panel) shows a plot of the difference between on-deck sample temperature and potential temperature, computed from the in-situ measured at the time of bottle trip, versus pressure. The bottom panel of the same figure shows a plot of the difference between oxygen concentration using on-deck and potential temperatures versus pressure. The depth dependent variability in Δ oxygen is a result of the absolute magnitude of the oxygen concentration and the time-series subsampling strategy. For work of the highest accuracy, this error should be considered.

The precision of our oxygen analyses was assessed from both an analytical and field perspective and is presented in Table 2.10. The mean analytical and field precision of our oxygen analyses in 1993 was 0.13% and 0.08% with a mean standard deviation of 0.17 and 0.13 µmol l^{-1}, respectively. Oxygen concentrations measured over the five years of the program are plotted at three constant potential density horizons in the deep ocean along with their mean and 95% confidence intervals (Figure 2.3). The values range from 1.83 at 22.78 kg m^{-3} to 4.26 at 27.67 kg m^{-3}, indicating that analytical consistency has been maintained throughout the program.

Table 2.10: Precision of Winkler Titration

HOT	Analytical			Field		
	CV %	SD µmol l^{-1}	n	CV %	SD µmol l^{-1}	n
44	0.10	0.11	5	0.12	0.23	8
45	0.10	0.07	8	0.08	0.13	10
46	0.10	0.19	9	0.06	0.11	9
47	0.18	0.25	7	0.09	0.11	12
48	0.10	0.18	6	not determined		
49	0.14	0.19	4	0.14	0.21	13
50	0.16	0.20	7	0.06	0.11	12

2.2.3. Dissolved Inorganic Carbon and Titration Alkalinity

Samples for dissolved inorganic carbon (DIC) were measured using a Single Operator Multi-parameter Metabolic Analyzer (SOMMA) which was manufactured at the University of Rhode Island and standardized at the Brookhaven National Laboratory. Analyses of primary DIC standards (Tupas et al. 1993) indicated that the precision of replicate samples is approximately 1 µmol kg $^{-1}$. Titration alkalinity was determined using the Gran titration method as described in Tupas et al. (1993). The precision of the titration procedure was approximately 5 µequiv kg^{-1}. Accuracy was established through intercalibration with Scripps Institution of Oceanography.

2.2.4. pH

In 1993, pH was determined spectrophotometrically using the indicator m-cresol purple following the methods described in Tupas et al. (1993). The absorbance of the dye/seawater mixture was measured at 578 and 434 nm on a Perkin Elmer Model 3 dual-beam spectrophotometer and converted to pH on the total hydrogen scale according to Clayton and Byrne (1993).

2.2.5. Dissolved Inorganic Nutrients

Samples for the determination of dissolved inorganic nutrients (phosphate, [nitrate+nitrite], silicate) were collected as described in Tupas et al. (1993). Analyses were conducted at room temperature on a four-channel Technicon Autoanalyzer II continuous flow system (Winn et al. 1991). A summary of the precision of analyses for 1993 is shown in Table 2.11. Figures 2.4-2.6 show the mean and 95% condifence limits of nutrient concentrations measured at three potential density horizons for the 5 years of the program. In addition to standard automated nutrient analyses, specialized chemical methods (2.2.7) were used to determine concentration of nutrients that are normally below the detection limits of autoanalyzer methods.

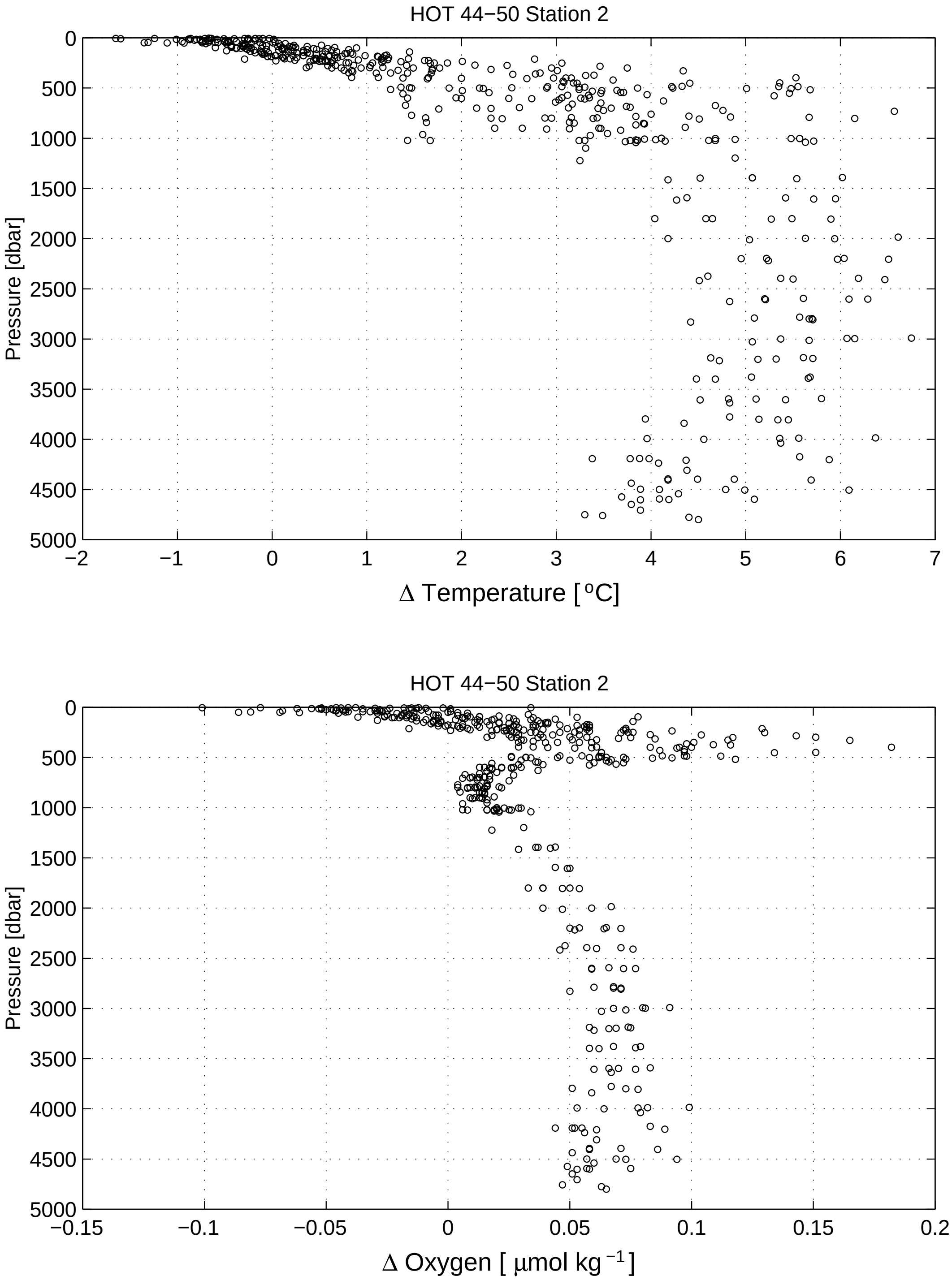

Figure 2.2: Upper Panel: Difference between sample temperature at the time of sample collection and potential temperature calculated from *in situ* temperature at the time of bottle trip. Lower Pannel: Difference in oxygen concentration in units of μmol kg^{-1} using temperatures measured at the time of sample collection and potential temperature computed from *in situ* temperature.

Figure 2.3: Oxygen versus time at three density horizons at Station ALOHA. Upper panel: Oxygen concentration at potential densities of 27.782, 27.758 and 27.675 during1993. Lower panel: Oxygen at these same three density horizons including all four years of the time-series program.

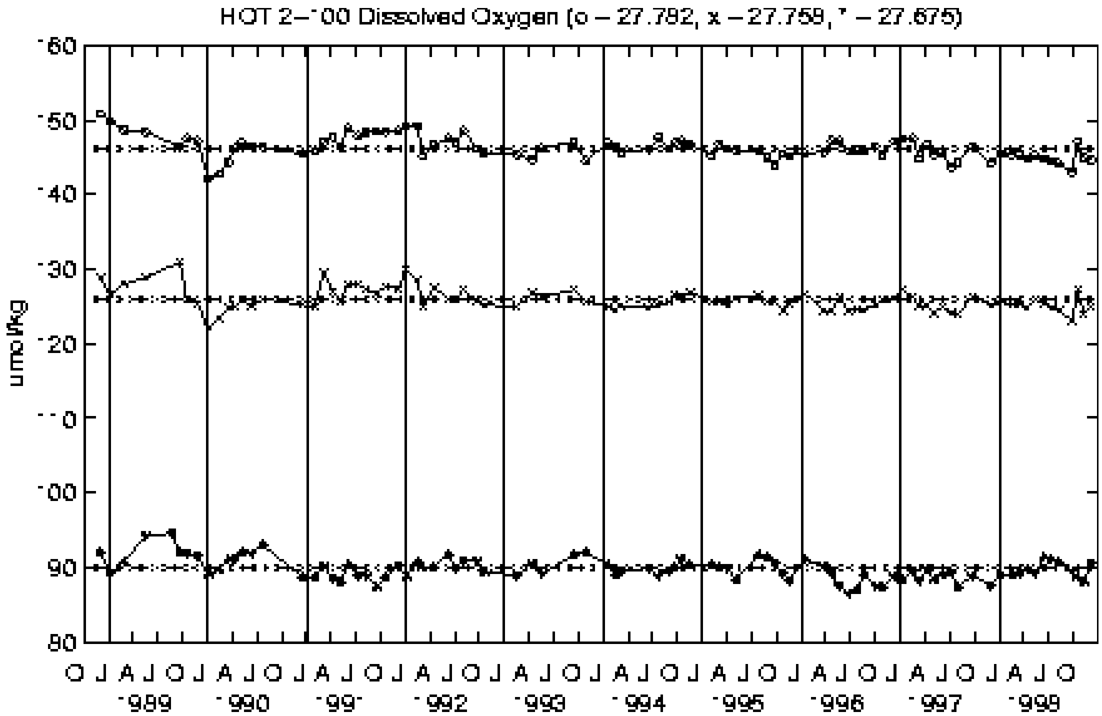

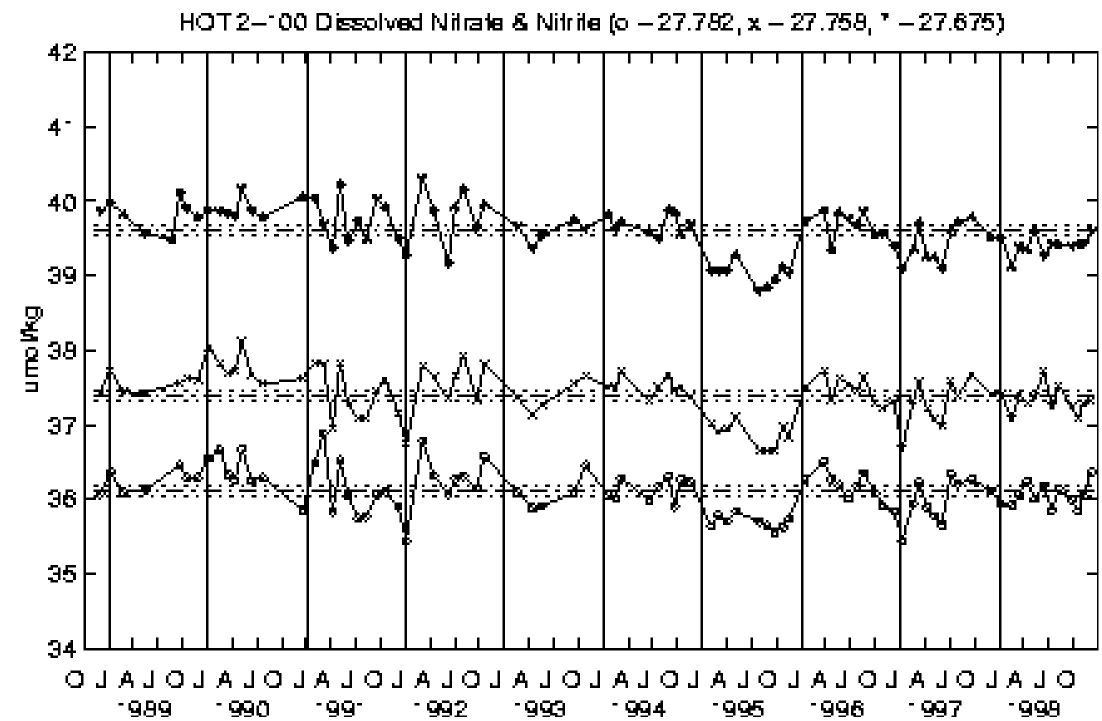

Figure 2.4: As in Figure 2.3, except for concentrations of dissolved [nitrate+nitrite].

2.2.6. Dissolved Organic Nutrients

Dissolved organic carbon (DOC) was determined by the high temperature catalytic oxidation method as described in Tupas et al. (1994). Water samples were collected in acid-washed polyethylene tubes and were stored frozen until analyzed. The oxidation method used a pure platinum catalyst with infrared detection on a LICOR 6252 carbon dioxide analyzer. Dissolved organic nitrogen (DON) was calculated as the difference between total dissolved nitrogen (TDN) and [nitrate+nitrite] concentrations determined by the autoanalyzer (2.2.5.). TDN and [nitrate+nitrite] were determined as described in Tupas et al. (1993). Ammonium was determined to be a very minor portion of TDN (Tupas et al. 1993). Total dissolved phophorous (TDP) and soluble reactive phosphorous (SRP) were determined as described in Tupas et al. (1993). A summary of the precision of these analyses is given in Table 2.12.

Table 2.11: Precision of Dissolved Nutrient Analyses

	Phosphate				Nitrate + Nitrite				Silicate			
	Analytical[a]		Field[b]		Analytical[a]		Field[b]		Analytical[a]		Field[b]	
HOT	mean cv[c]	mean sd[d]	mean cv[c]	mean sd[d]	mean cv[c]	mean sd[d]	mean cv[c]	mean sd[d]	mean cv[c]	mean sd[d]	mean cv[c]	mean sd[d]
44	0.2	0.004	0.4	0.006	0.8	0.093	0.8	0.031	0.3	0.087	0.6	0.120
45	0.7	0.015	0.5	0.012	0.3	0.074	0.3	0.097	0.2	0.082	0.9	0.149
46	0.4	0.007	0.3	0.007	0.3	0.092	0.3	0.038	0.4	0.242	0.4	0.150
47	0.0	0.000	0.5	0.013	0.1	0.007	0.5	0.147	0.3	0.049	0.8	0.897
48	0.3	0.011	NR	NR	0.3	0.127	NR	NR	0.2	0.233	NR	NR
49	NR[e]	NR	0.3	0.007	NR	NR	0.1	0.037	NR	NR	0.1	0.109
50	0.2	0.007	0.6	0.011	0.1	0.064	0.2	0.073	0.1	0.092	0.3	0.211

[a]Average coefficient of variation (i.e., standard deviation as a percentage of the mean) for analytical replicates (i.e., replicate analysis of a single sample) for phosphate concentrations 0.4 µM, nitrate plus nitrite 0.2 µ M and silicate concentrations 2.0 µM..

[b]Average coefficient of variation for field replicates (i.e., analysis of replicate samples from the same Niskin) for the above concentration ranges.

[c]%

[d]µmol kg^{-1}

[e]No replicate analysis performed

Figure 2.5: As in Figure 2.3, except for concentrations of dissolved phosphate.

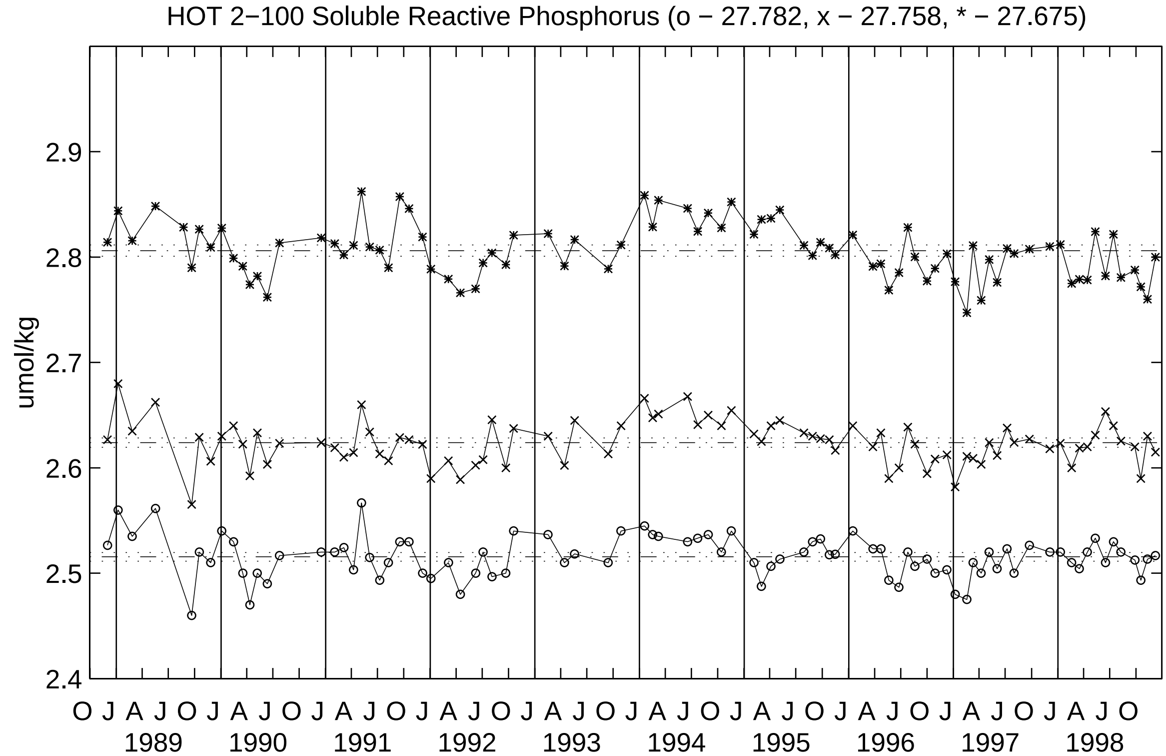

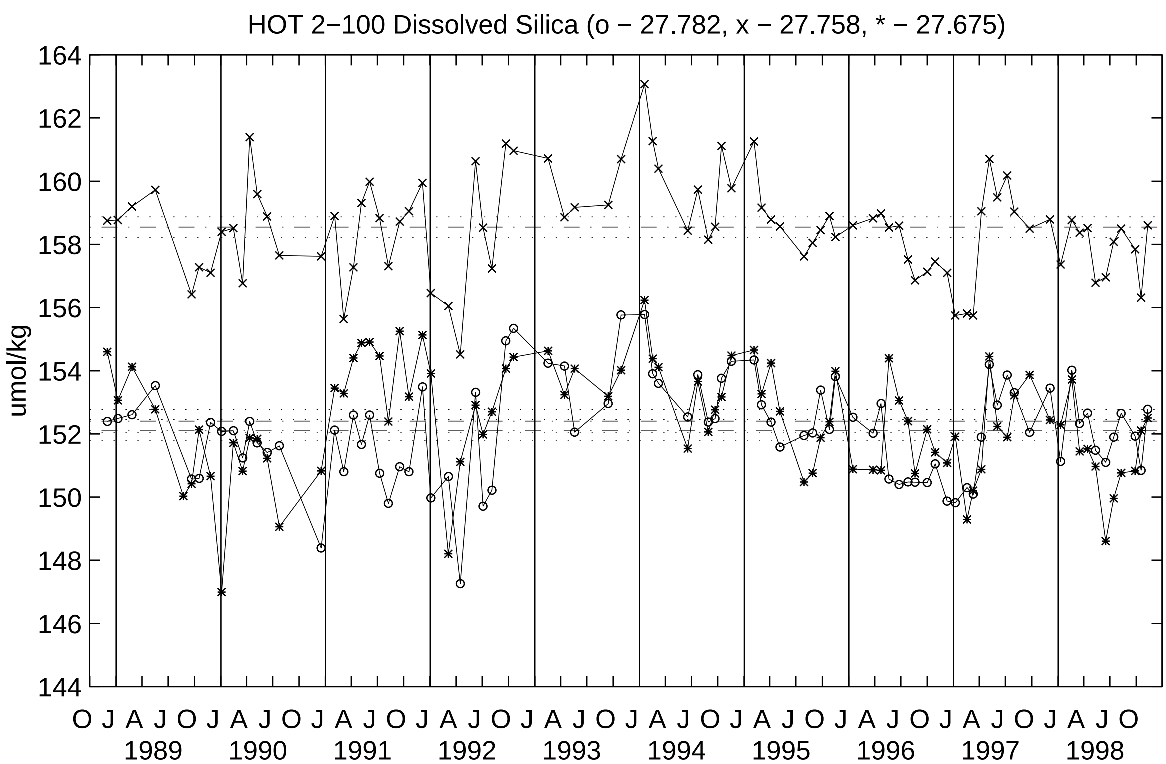

Figure 2.6: As in Figure 2.3, except for concentrations of dissolved silica.

Table 2.12: Precision of Dissolved Organic Nutrient Analyses

HOT	DOC FIELD mean cv (%)	DOC FIELD mean sd ($\mu mol\ kg^{-1}$)	DON FIELD mean cv (%)	DON FIELD mean sd ($\mu mol\ kg^{-1}$)	DOP FIELD mean cv (%)	DOP FIELD mean sd ($\mu mol\ kg^{-1}$)
44	2.81	2.66	7.1	0.255	9.3	0.021
45	3.89	1.98	5.6	0.133	6.0	0.007
46	2.62	1.83	6.4	0.154	11.1	0.014
47	3.55	2.25	8.9	0.190	6.7	0.014
49	1.96	1.46	10.0	0.276	17.9	0.021
50	2.26	1.56	7.4	0.184	3.4	0.007

2.2.7. Low-Level Nutrients

The chemiluminescent method of Cox (1980) as modified for seawater by Garside (1982) was used to determine the [nitrate+nitrite] content of surface to 100 m water samples (Tupas et al. 1993). The limit of detection for [nitrate+nitrite] was approximately 2 nM with a precision and accuracy of ±1 nM.

Low level soluble reactive phosphorus (SRP) concentrations in the euphotic zone were determined according to the magnesium induced coprecipitation method of Karl and Tien (1992). Typical precision estimates for triplicate determinations of SRP are from 1-3% with a limit of detection of 10 nmol l^{-1} sample.

2.2.8. Particulate Material

Samples for analysis of particulate metter were prefiltered through 202- µm Nitex mesh to remove large zooplankton and collected onto combusted GF/F glass fiber filters. Particulate carbon (PC) and nitrogen (PN) on the filters were analyzed using a Perkin-Elmer 2400 CHN analyzer. Particulate phosphorus (PP) was analyzed by converting the material to orthophosphate by high temperature ashing followed by acid hydrolysis and determining the orthophosphate content by spectrophotometry.

2.2.9. Pigments

Chlorophyll a (chl a) and phaeopigments were measured fluorometrically using acetone and standard techniques (Strickland and Parsons, 1972). Analytical precision for this analysis is presented in Table 2.13. Integrated values for pigment concentrations were calculated using the trapezoid rule. We also measured chl a and accessory photosynthetic pigments (Table 2.14) by high performance liquid chromatography (HPLC) according to Bidigare et al. (1990).

2.2.10. Adenosine 5'-Triphosphate

Water column adenosine 5'-triphosphate (ATP) concentrations were determined using the firefly bioluminesence technique as described by Karl and Holm-Hansen (1978). The precision of

ATP determinations in 1993 are given in Table 2.15.

Table 2.13: Precision of Fluorometric Analyses of Chlorophyll *a* and Phaeopigment

Cruise	Chl *a* CV(%)	Std. ($\mu g\ l^{-1}$)	Phaeo CV(%)	Std. ($\mu g\ ^{-1}$)
44	5.0	0.005	5.0	0.008
45	2.7	0.004	5.0	0.012
46	1.9	0.004	3.2	0.009
47	3.9	0.008	6.1	0.012
48	1.9	0.003	8.0	0.015
49	3.9	0.006	5.6	0.013
50	4.2	0.007	5.4`	0.016

Table 2.14: HPLC Pigment Analysis

Pigment	RF[a]	RT[b]
Chlorophyll c_3	0.000455	
Chlorophyll (c_1 + c_2) & Mg 3,8 DVP4A5	0.000455	
Peridinin	0.000587	.316
19'-Butanoyloxyfucoxanthin	0.000421	.380
Fucoxanthin	0.000454	.415
19'-Hexanoyloxyfucoxanthin	0.000401	.450
Prasinoxanthin	0.000434	.487
Diadinoxanthin	0.000261	.635
Zeaxanthin	0.000305	.766
Chlorophyll *b*	0.001423	.888
Chlorophyll *a*	0.000729	1.000
Chlorophyll c_4	0.000455	
Carotens	0.000264	1.612

[a]RF - Response Factor (mg pigment per unit absorbance peak area at 436 nm).
[b]RT - Retention Time (relative to chlorophyll *a*)

Table 2.15: Precision of ATP Analyses

Cruise	CV* (%)	Std($\mu g\ m^{-3}$)
44	10.0	1.068
45	12.7	2.920
46	12.5	2.049
47	13.9	4.893
49	16.6	2.204
48	no replicates	no replicates
50	13.8	1.893

*Coefficient of variation as the percent of mean of all triplicate dterminations for each cruise.

2.3. Biogeochemical Rate Measurements

2.3.1. Primary Productivity

Photosynthetic production of organic matter was measured by a trace-metal clean, C^{14} method. Incubations were conducted in-situ at eight depths (Table 1.1) for at least 12 hours using a free-drifting array as described by Winn et al. (1991). Integrated carbon assimilation rates were calculated using the trapezoid rule with the shallowest values extended to 0 m and the deepest extrapolated to a value of zero at 200 m.

2.3.2. Particle Flux

Particle flux was measured at reference depths of 150, 300 and 500 meters using sediment traps deployed on a free-floating array for approximately 72 hours during each cruise. Sediment trap design and collection methods, as well as sample analysis, are described in Winn et al. (1991). The drifts of the sediment trap arrays are shown in Figure 6.1.1.-5.

2.4. ADCP Measurements

Of the seven HOT cruises, shipboard ADCP's were available and used on five: on the R/V Townsend Cromwell (HOT-44), the R/V Wecoma (HOT-46), the R/V New Horizon (HOT-47) and the R/V Moana Wave (HOT-49 and HOT-50). Shipboard ADCP on the R/V Thomas G. Thompson was under repair during HOT-45 and R/V Na'ina had no ADCP capability. All ADCPs used were RDI model VM-150 but different transducers were used for the two R/V Moana Wave cruises. ADCP and navigation data were recorded successfully throughout most of the cruises. Major ADCP recording gaps occurred on HOT-47 while on station and during the return transit to Honolulu, and on HOT-49 in the middle of the on station period.

All position fixes were from GPS receivers. The receiver on R/V New Horizon was not working properly; fix messages were emitted at infrequent and irregular intervals. There was also a short GPS gap, about 0.87 hour, at the beginning of HOT-44 cruise. Otherwise, the raw reference layer velocity estimates for all cruises display the typocal level of noise (data not shown).

2.5. Optical Measurements

Incident irradiance at the sea surface was measured on each HOT cruise with a LICOR LI-200 data logger and cosine collector. Vertical profiles of Photosynthetically Available Radiation (PAR) were also obtained using a Biospherical Instrument model PNF-300 optical profiler. The entire data set is available via Internet as described in Section 8.

2.6. Meteorology

Wind speed and direction, atmospheric pressure, wet- and dry-bulb air temperature, sea surface temperature, cloud cover and sea state were collected at four-hour intervals while on station. Additionally, air and sea surface temperature, atmospheric pressure, wind speed and direction are obtained from NDBC buoy 51001 located at 23.4°N, 162.3°W.

2.7. Inverted Echo Sounder Network

In 1991, a 50-km array of 5 inverted echo sounders (IESs) was deployed as part of the WOCE deep water station (Fig. 1.1). IESs record the round-trip acoustic travel time from the sea-floor to the sea surface, which is known to correlate well with dynamic height. The purpose of these observations was to resolve the synoptic variability which may not be resolved by the monthly sampling.

The IES were named according to their location with respect to the center of Station ALOHA (C: center, N: north, E: East, SE: Southeast, SW: Southwest) and recorded data from February 1991 to March 1992 when they were recovered. IESs N, SW and SE were redeployed in June 1992 and recorded data until their recovery in May 1993.

CTD casts made during 25 monthly cruises to the deep-water station were used to calibrate the IES. The conversion factor from travel time to dynamic height was found to be -54 dyn m s^{-1}. The time-series from the IESs show that there are many fluctuations in dynamic height having timescales from weeks to months that are not well resolved with the CTD sampling.

3. Cruise Summaries

3.1. HOT-44: January 18-22, 1993; R/V Townsend Cromwell; C.D. Winn

Ship departed Snug Harbor at 0930, January 18 with 9 scientists . Weather was generally calm for the duration of the cruise. Station Kahe was occupied enroute to Station ALOHA. The ship returned to Honolulu after work at Station ALOHA was accomplished and docked at 1400 on January 22.

CTD operations were conducted with a 12-place rosette and limited to 1000 m casts due to lack of a longer conducting cable. Problems were encountered during the test CTD cast at Station Kahe but were solved at Station ALOHA. A total of 17 casts were conducted at Station ALOHA with no major problems.

All water samples for WOCE and JGOFS measurements were obtained. A Go-Flo cast was conducted to collect water at eight depths for the primary production experiment. Sediment trap and primary production arrays were deployed and recovered without incident. All traps and incubation bottles were recovered.

Water samples were collected for C. Keeling (SIO-UCSD), F. Millero (RSMAS-U.Miami), R. Wanninkhof (NOAA) and T. Takahashi (LDEO) for inorganic carbon measurements and L. Campbell (UH) for flow cytometric analysis of microorganisms.

3.2. HOT-45: February 15-20, 1993; R/V Thomas G. Thompson; L.M. Tupas

Ship departed Snug Harbor at 0830, February 15 with 17 scientists. Weather was generally calm for the duration of the cruise. Station Kahe was occupied enroute to Station ALOHA. After core work at Station ALOHA was accomplished, the ship proceeded to the vicinity of the sediment trap array. After the array was sighted, the ship moved a few miles downcurrent to conduct 2 deep CTD casts for oxygen sensor work (M. Atkinson) and 2 box cores for sediment samples (D. Hoover). After these operations, the sediment trap array was recovered. The ship returned to the center of Station ALOHA to start a transect towards Kahuku Point interspaced with 1000 m CTD casts (S. Kennan). At the end of the transect, the ship returned to Honolulu and docked at 0730 on February 20

CTD operations were conducted with a 24-place rosette. No problems were encountered during the test CTD cast at Station Kahe, Station ALOHA and during the CTD survey. A total of 17 casts were conducted at Station ALOHA. During the transect, 11 CTD casts were conducted.

All water samples for WOCE and JGOFS measurements were obtained. A Go-Flo cast was conducted to collect water at eight depths for the primary production experiment. Sediment trap and primary production arrays were deployed and recovered without incident. All traps and incubation bottles were recovered. Additional sediment traps were deployed for thorium samples (C. Holloway) and the sediment trap line was extended to 1000 m for a carbonate dissolution experiment (P. Troy).

S. Emerson collected water samples with an online Niskin for respiration experiments and collected water samples for oxygen measurements. J. Dore conducted experiments on denitrification, J. Christian on microbial enzymes and H. Liu on bacterial grazing. J. Yuan collected water samples for trace metal analysis and C. Holloway for thorium analysis. Water samples were collected for P. Quay (UW) and C. Keeling (SIO-UCSD) for inorganic carbon measurements and L. Campbell (UH) for flow cytometric analysis of microorganisms.

3.3. HOT-46: April 12-17, 1993; R/V Wecoma; D.V. Hebel

Ship departed Snug harbor at 1015 on April 12 with 15 scientists . Weather was generally calm for the duration of the cruise. Station Kahe was occupied enroute to Station ALOHA. The ship returned to Honolulu after work at Station ALOHA was accomplished and docked at 0700 on April 17.

CTD operations were conducted with a 24-place rosette. Problems with the conducting cable and the CTD winch were encountered at Station ALOHA and persisted until the end of the cruise. The CTD winch frequently stopped due to overheating and could not maintain the required 60 m min^{-1} of wire speed. The only solution to this problem was to run the winch at a reduced speed of 40 m min^{-1}.The conducting cable on the other hand frequently came out twisted. After several reterminations, a single conducting cable which terminated in a swivel attachment to the package was used. The delays caused by the equipment problems required the burst sampling period to be restarted at the time the swivel was installed. A total of 21 casts were conducted at Station ALOHA.

All water samples for WOCE and JGOFS measurements were obtained. A Go-Flo cast was conducted to collect water at eight depths for the primary production experiment. Sediment trap and primary production arrays were deployed and recovered without incident. All traps and incubation bottles were recovered.

M. Keller (Bigelow) and M. Latasa (UH) collected water samples for pigment measurements. J. Yuan collected samples for trace metal analysis and C. Holloway collected samples for thorium analysis. R. Letelier conducted studies on *Trichodesmium*, D. Sadler on time-series pH measurements and J. Bower on squid population. Water samples were collected for T. Takahashi (LDEO), P. Quay (UW) and C. Keeling (SIO-UCSD) for inorganic carbon measurements and L. Campbell (UH) for flow cytometric analysis of microorganisms.

3.4. HOT-47: May 18-23, 1993; R/V New Horizon; L.M. Tupas

Ship departed Snug Harbor at 0800 on May 18 with 15 scientists. Weather was generally calm for the duration of the cruise. Station Kahe was occupied enroute to Station ALOHA. After operations at Station Kahe were accomplished, the ship proceeded to the vicinity of Station ALOHA. Aside from the standard HOT operations, 3 inverted echo sounders (IES) were retrieved (N, SW and SE). The IES at the center of Station ALOHA (C) could not be located. One IES was deployed at the center of Station ALOHA. On the return leg to Honolulu, the ship stopped near Kaena Point to conduct a bathymetrc survey and deploy another IES. The ship docked at 1630 on May 23.

CTD operations were conducted with a 24-place rosette. No problems were encountered during the test CTD cast at Station Kahe, Station ALOHA and during the CTD survey. A total of 20 casts were conducted at Station ALOHA.

All water samples for WOCE and JGOFS measurements were obtained. A Go-Flo cast was conducted to collect water at eight depths for the primary production experiment. Sediment trap and primary production arrays were deployed and recovered without incident. All traps and incubation bottles were recovered.

F. Thomas collected deep water samples for oxygen sensor calibration. J. Yuan collected samples for trace metal analysis and C. Holloway collected samples for thorium analysis. H. Liu conducted bacterial grazing experiments. Water samples were collected for P. Quay (UW) and C. Keeling (SIO-UCSD) for inorganic carbon measurements and L. Campbell (UH) for flow cytometric analysis of microorganism.

3.5. HOT-48: July 24-30, 1993; R/V Na'Ina; L.M. Tupas

A charter agreement was made with Uaukewai Diving Salvage and Fishing Inc. for the use of their workboat Na'Ina to conduct a HOT cruise. The vessel was reclassified as a research vessel after U.S. Coast Guard inspection. It took 3 days to complete the installation of all necessary equipment on the back deck of the ship. A test cruise at Barber's Point was conducted on July 24th. Inclement weather was encountered and operations were difficult, several tests were actually aborted. Further modifications of the ship and equipment were made on July 25 to alleviate certain problems. A HOT cruise was attempted on July 26, however, problems were encountered with the CTD system at Station Kahe and the ship returned to Snug harbor. The hydrowinch was inspected and operational guidelines were made as to its operation. A second attempt was made on July 28 but sea-conditions were bad and the cruise was aborted. A third attempt scheduled for July 30 was aborted due to new problems and it was decided to end the charter.

3.6. HOT-49A: Sept. 9-12, 1993; R/V Moana Wave; D.M. Karl

HOT-49 was the first cruise of the second 5-year phase of the HOT Program. The cruise was divided into 2 legs; leg 1 was devoted to the retrieval and redeployment of the moored sediment trap near Station ALOHA, leg 2 was a standard HOT cruise.

HOT 49A departed Snug harbor at 1500 on Sept. 9 with 11 scientists on board. After deployment of the floating sediment traps, the ship steamed to the location of the moored traps. The array was successfully recovered. During the sampling and reconfiguration of the array, the continuous water sampler (CWS) system was tested. After the sediment trap array was reconfigured, the CWS test was terminated. The ship transited a short distance away from the original site and the sediment traps were successfully deployed. Ship transited back to Snug Harbor to exchange science personnel. Ship arrived at Snug Harbor at 0800 on Sept. 12.

3.7. HOT-49B: Sept. 12-17, 1993; R/V Moana Wave; D.V. Hebel

Ship departed at 0900 with 17 scientist on board and returned on Sept. 17 at 0800. Station Kahe was occupied enroute to Station ALOHA. Ship proceeded directly to the center of the station and commenced with the standard sampling operations.

CTD operations were conducted with a 24-place rosette. No problems were encountered during the test CTD cast at Station Kahe and during the CTD survey.

At Station ALOHA the conductivity sensor failed at the bottom of cast 1. The sensor was replaced with sensor #527 and the rest of the casts were conducted without further problems. Since station 2 cast 1 did not have up-cast conductivities, we used the potential temperature data to map the down-cast conductivities at the bottle marks.

Temperature sensor #886 was replaced by #741 and used during cast 2 while the primary sensor was being inspected. Sensor #886 was returned to the CTD after this cast and performed well the rest of the cruise. A total of 22 casts were conducted at Station ALOHA, one at Station 3 and one at Station Kaena.

All water samples for WOCE and JGOFS measurements were obtained. A Go-Flo cast was conducted to collect water at eight depths for the primary production experiment. Sediment trap and primary production arrays were deployed and recovered without incident. All traps and incubation bottles were recovered. Additional sediment traps were deployed for thorium samples (C. Holloway).

Water samples were collected for P. Quay (UW) and C. Keeling (SIO-UCSD) for inorganic carbon measurements, L. Campbell (UH) for flow cytometric analysis of microorganism, R. Bidigare (UH) for pigments. Particulate samples were collected for H. Thierstein (ITH) for microscopic analysis.

3.8. HOT-50: Oct. 27 - Nov. 1, 1993; R/V Moana Wave; L.M. Tupas

Ship departed at 0900 on Oct. 27 with 17 scientists on board and returned on Nov. 1 at 0800. Station Kahe was occupied enroute to Station ALOHA. Ship proceeded directly to the center of the station and commenced with the standard sampling operations.

CTD operations were conducted with a 24-place rosette. No problems were encountered during the test CTD cast at Station Kahe, Station ALOHA and during the CTD survey. A total of 22 casts were conducted at Station ALOHA, one at Station 3 and one at Station Kaena.

All water samples for WOCE and JGOFS measurements were obtained. A Go-Flo cast was conducted to collect water at eight depths for the primary production experiment. Sediment trap and primary production arrays were deployed and recovered without incident. All traps and incubation bottles were recovered.

Additional sediment traps were deployed for thorium samples (C. Holloway). Water samples were collected for P. Quay (UW) and C. Keeling (SIO-UCSD) for inorganic carbon measurements, L. Campbell (UH) for flow cytometric analysis of microorganism, R. Bidigare (UH) for pigments. Particulate samples were collected for H. Thierstein (ITH) for microscopic analysis.

4. Results

4.1. Hydrography

4.1.1. 1993 CTD Profiling Data

Profiles of temperature, salinity, oxygen and potential density (σ_θ) were collected at both Station Kahe and Station ALOHA. The profiles from Station ALOHA during 1993 are presented in Figure 6.2.1. The results of bottle determinations of oxygen, salinity and inorganic nutrients are also shown. In addition, stack plots of CTD temperature and salinity profiles for all 1000 m casts conducted at Station ALOHA are presented (Fig. 6.2.2). The data collected for Station Kahe during 1993 are presented in Figures 6.2.3. The temperature, salinity and oxygen profiles obtained from the deep casts at Station ALOHA during 1993 are presented in Figures 6.2.4-6.

4.1.2. Time-series Hydrography, 1988-1993

The hydrographic data collected during the first five years of HOT are presented in a series of contour plots (Figures 6.3.1-14). These figures show the data collected in 1993 within the context of the longer time-series database. The CTD data used in these plots are obtained by averaging the data collected during the 36-hour period of burst sampling. Therefore, much of the variability which would otherwise be introduced by internal tides in the upper ocean has been removed. Figures 6.3.1 and 6.3.2 show the contoured time-series record for potential temperature and density in the upper 1000 dbar for all HOT cruises through 1993. Seasonal variation in temperature for the upper ocean is apparent in the maximum of near-surface temperature of about 26°C and the minimum of approximately 23°C. Oscillations in the depth of the 5°C isotherm below 500 dbar appear to be relatively large with displacements up to 75 dbar. The main pycnocline is observed between 100 and 600 dbar, with a seasonal pycnocline developing between June and December in the 50-100 dbar range (Figure 6.3.2). The cruise-to-cruise changes between February and July 1989 in the upper pycnocline illustrate that variability in density is not always resolved by our quasi-monthly sampling.

Figures 6.3.3-6 show the contoured time-series record for salinity in the upper 1000 dbar for all HOT cruises through 1993. The plots show both the CTD and bottle results plotted against pressure and potential density. Most of the differences between the contoured sections of bottle salinity and CTD salinity are due to the coarse distribution of bottle data in the vertical as compared to the CTD observations. Some of the bottles in Figure 6.3.6 are plotted at density values lower than the indicated sea surface density. This is due to surface density changing from cast to cast within each cruise, and even between the downcast and upcast during a single cast.

Surface salinity is variable from cruise-to-cruise, with no obvious seasonal cycle and some substantial interannual variability. The surface salinity is low in late 1989, increases to a maximum in late 1991, decreases again during 1991 and 1992 and rises to an extreme high in late 1993. The salinity maximum is generally found between 50 and 150 dbar, and within the potential density range 24-25 kg m^{-3}. A salinity maximum region extends to the sea surface in the latter part of 1988, 1990 and 1993, as indicated by the 35.2 contour reaching the surface. This contour nearly reaches the surface late in 1989. The maximum value of salinity in this feature is subject to short-term variations of about 0.1 which is probably due to the proximity of Station ALOHA to the region where this water is formed at the sea surface (Tsuchiya, 1968). The variability of this feature is itself variable. Throughout 1989 there were extreme variations of a couple of months duration with 0.2 amplitude. The variability was much smaller and slower, thereafter, except for a few months of rapid variation in earlier 1992. The salinity minimum is found between 400 and 600 dbar (26.35-26.85 kg m^{-3}). There is no obvious seasonal variation of this feature, but there are distinct periods of higher than normal minimum salinity in early 1989, in the fall of 1990 and early 1992. These variations are related to the episodic appearance at Station ALOHA of energetic fine structure and submesoscale water mass anomalies (Lukas and Chiswell, 1991).

Figures 6.3.7 and 6.3.8 show contoured time-series data for oxygen in the upper 1000 dbar at Station ALOHA. The oxygen data show a strong oxycline between 400 and 625 dbar (26.25-27.0 kg m^{-3}), and an oxygen minimum centered near 800 dbar (27.2 kg m^{-3}). During 1989, there was a persistent oxygen maximum near 300 dbar (25.75 kg m^{-3}), which appeared only weakly afterward. The oxygen minimum exhibited some interannual variability as well, with values less than 30 µmol kg^{-1} appearing in the last half of 1989 and the first half of 1990, reappearing, less intensely, in 1991 and 1992 and again strongly in 1993. The surface layer shows a seasonality in oxygen concentrations, with highest values in the winter. This roughly corresponds to the minimum in surface layer temperature (Figure 6.3.1). An oxygen maximum at about 100 m appears in the latter half of 1991 and persists through 1992.

Figures 6.3.9-14 show [nitrate+nitrite], phosphate and silica at Station ALOHA plotted against both pressure and potential density. The nitricline is located between about 200 and 600 dbar (25.75-27 kg m^{-3}; Figures 6.3.9-10). Most of the variations seen in these data are associated with vertical displacements of the density structure, and when [nitrate+nitrite] is plotted versus potential density, most of the contours are level. The upper reaches of the water column show considerable variability in density space. The record is dominated by a few short events where nutrients appear to be brought up into the surface layers. These events occurred in March-April, 1990, January, 1992, February 1993 and possible smaller events in September, 1989 and March, 1991. These events are probably important in the upper ocean nutrient balance, but are of such short duration that it is difficult to capture then with quasi-monthly sampling. The phosphate and silicic acid records are similar to the [nitrate + nitrite].

4.1.3. Mixed Layer Observations

Figure 4.1 displays the surface temperature, salinity and density averaged over 6-10 dbars, the mixed layer depth calculated using a density difference criterion, and surface bottle oxygen and surface oxygen saturation averaged over the top 20 dbars for the duration of the HOT program. The density difference for the mixed layer calculation is 0.3 kg m^{-3}, which corresponds approximately to 1°C. The error bars are one standard deviation from the mean. Cruises 32 and 49 showed a large spread in the near-surface oxygen values in comparison to the other cruises, which is reflected in the large error bars in the oxygen and oxygen saturation plot.

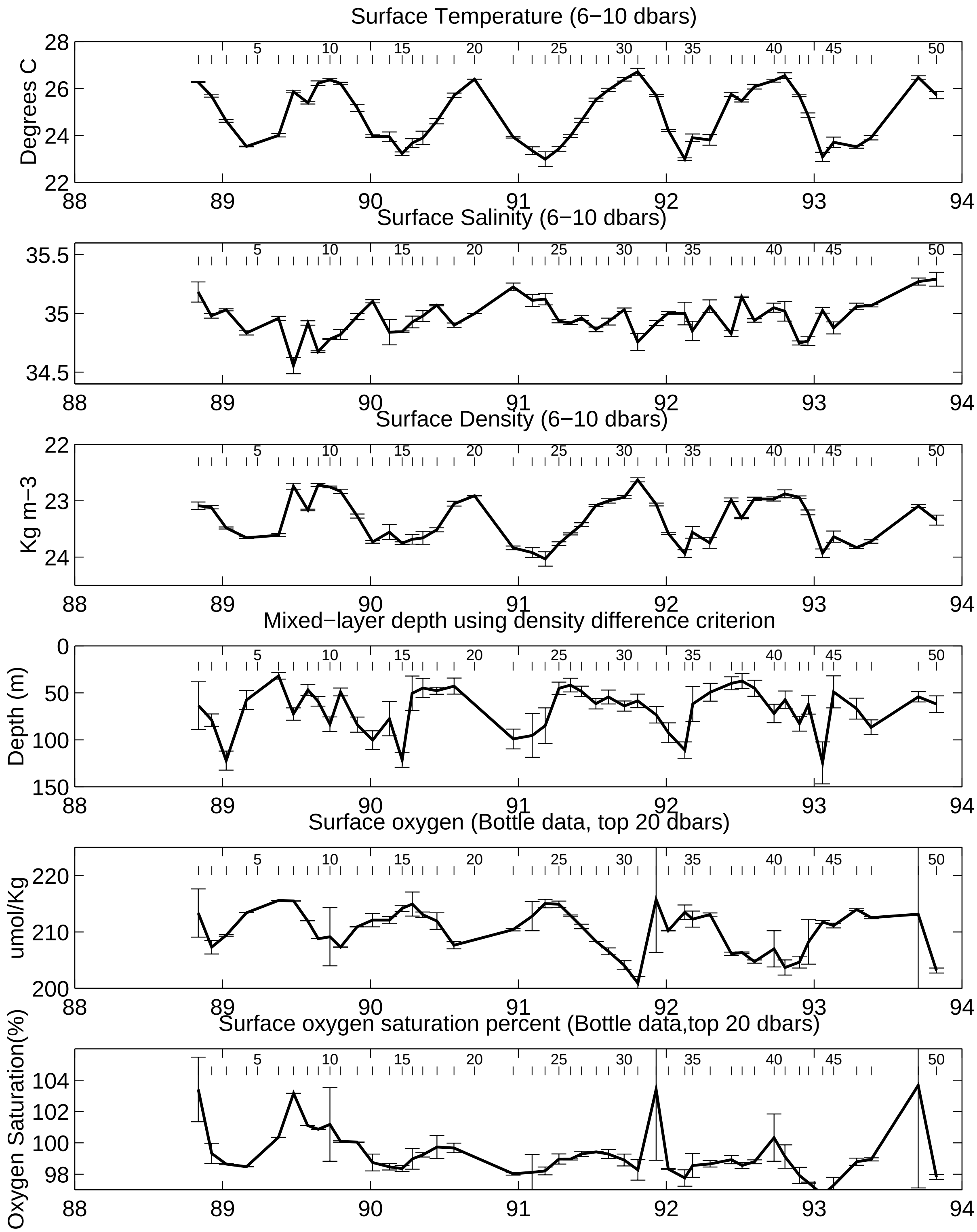

Figure 4.1: Surface CTD temperature, salinity and density averaged over 6-10 dbars, the mixed layer depth calculated using a density difference critereon, and surface bottle oxygen and surface oxygen saturation averaged over the top 20 dbars for the duration of the HOT program. The horizontal axis above each plot shows the HOT cruise numbers.

Surface temperature and density have strong seasonal cycles with some interannual variability superimposed. The amplitude of the seasonal cycle grew between October 1988 and October 1992, with an increase in amplitude of 1°C peak-to-peak. The densest isopycnal to outcrop at station ALOHA was 24 kg m^{-3} in early 1991. This is in contrast to the winter of 1988/89, where the densest isopycnal to outcrop was 23.7 kg m^{-3}. The surface density is dominated by seasonal cycles but is modulated by variations in the surface salinity, which have no significant annual component, and interannual variability in the seasonal cycle of temperature. The surface salinity exhibits mostly interannual variations, with periods of a couple of years. The maximum surface salinity was observed in early 1991 and late 1993 and the minima in mid-1989.

The oxygen concentration in the surface layer had strong seasonal variations in the first three years of HOT with maximum oxygen in mid-summer, average values around 212 umol kg^{-1} and peak-to-peak variations of about 7 umol kg^{-1}. However, in mid-1991, the seasonal cycle was interrupted and the oxygen concentration decreased steadily. This disruption of the seasonal cycle may be related to the onset of the 1991-92 El Niño Southern Oscillation (ENSO) event and a consequent decrease in local wind stirring. The oxygen saturation has a strong seasonal cycle as well. Curiously, oxygen is less than 100% saturation for most of the HOT program to date, with a downward trend starting in mid-1989.

Mixed-layer thickness shows interannual variations as well, with shallowest late-winter mixed layers observed in early 1991, coincident with the densest isopycnal outcrop. Mixed layer thickness is related to net surface heat flux, as the deepest winter layers occur in years with large winter heat loss to the atmosphere. Heat flux estimates were obtained using the wind data from the comprehensive ocean-atmosphere data set (Woodroff et al. 1987). The impulsive nature of the appearance of the deepest late-winter mixed layers, most apparent in the winters of 1989-90 and 1992-93, leads one to the conclusion that the mixed layer is deepened by one or several storm events. These events may be undersampled by our nominal monthly cruises.

4.2. Flash Fluorescence and Beam Transmission

Stack plots of the flash fluorescence and beam transmission results from each HOT cruise in 1993 are presented in Figures 6.4.1-6. *In situ* flash fluorescence profiles show the fluorescence maximum at the base of the euphotic zone, characteristic of the central North Pacific Ocean. Percent transmission profiles consistently show increased attenuation due to increased particle load at depths shallower than 100 dbar. Both fluorescence and beam transmission profiles show the influence of internal waves when plotted against pressure, but remain relatively constant within a cruise when plotted in density space. However, both data sets show substantial cruise-to-cruise variability in these properties.

Representative fluorescence profiles for a period of five years are shown in Figures 6.4.7 and 8. In order to facilitate comparison, only night-time profiles are presented after normalization to the average density profile obtained from the CTD burst sampling for each cruise. Month-to-month variability in the average depth of the fluorescence maximum is apparent. This is particularly evident in year 3 where the depth of the fluorescence maximum appears to increase in mid to late summer and in year 4 from summer to winter (Figure 6.4.7). The depth of the fluorescence max decreased significantly from spring to fall in 1993. Beam transmission profiles for cruises in 1993 are shown in Figure 6.4.9. These profiles were collected at approximately midnight and were normalized to the average density profile obtained for each cruise. Beam transmission profiles also show considerable variability on monthly time scales (Figure 6.4.10).

4.3. Biogeochemistry

Biogeochemical data collected during 1993 are summarized in Figures 6.5.1-9. In some cases the results from the first four years of the program have been combined to produce these figures.

4.3.1. Dissolved Inorganic Carbon and Titration Alkalinity

Dissolved inorganic carbon (DIC) and titration alkalinity measured in the upper 1000 dbar of the water column over the 5 years of the time-series program are presented in Figures 6.5.1 and 2. Time-series of titration alkalinity and DIC in the mixed layer are presented in Figure 6.5.3. Titration alkalinity normalized to 35 ppt salinity averages approximately 2305 µmol kg^{-1} and, within the precision of the analysis, appears to remain relatively constant at Station ALOHA. This observation is consistent with the results of Weiss et al. (1982) who conclude that titration alkalinity normalized to salinity remains constant in both the North and South Pacific subtropical gyres. In contrast to titration alkalinity, the concentration of DIC varies annually. DIC in the mixed layer is highest in winter and lowest in summer. This oscillation is consistent with an exchange of carbon dioxide across the air-sea interface driven by temperature dependent changes in mixed layer pCO_2.

Titration alkalinity shows considerable time dependent variability around the shallow salinity maximum, centered at about 125 dbar, and the salinity minimum, centered at about 400 dbar. These variations are largely associated with variability in salinity at these depths and disappear when alkalinity is normalized to 35 ppt. Titration alkalinity normalized to 35 ppt salinity is elevated in surface waters in spring of 1990. This corresponds to the appearance of mesoscale eddies at Station ALOHA at this time (Winn et al., 1991).

4.3.2. Low Level Nutrient Profiles

Euphotic zone nutrient concentrations at Station ALOHA are at or well below the detection limits of the autoanalyzer methods. Other analytical techniques and instrumentation are used to measure the nanamolar levels of [nitrate+nitrite] and phosphorus (Section 2.2.7) in these waters. Figures 6.5.4 and 6.5.5 show the profiles obtained from our low level nutrient analyses in 1993. At depths shallower than 100 dbar, phosphate is typically less than 150 nmol kg^{-1} and on occasion, as low as 15 nmol kg^{-1}. Phosphate concentrations appear to vary by at least 3-fold in this region (Figure 6.5.4). Concentrations of [nitrate+nitrite] at depths less than 100 meters are always less than 10 nmol kg^{-1} and are often less the 5 nmol kg^{-1} (Figure 6.5.5).

4.3.3. Pigments

A contour plot of chl *a* concentrations measured using standard fluorometric techniques from 0 to 200 dbar over the first five years of the program is shown in Figure 6.5.6. As expected a chlorophyll maximum with concentrations up to 300 µg m^{-3} is observed at approximately 100 dbar. No strong seasonal cycle is observed in the chlorophyll maximum layer. The chl a concentrations at depths shallower than 50 meters appear to have steadily decreased from January 1989 to mid 1990. There is some indication that the chl a concentrations in surface waters are increasing again toward the end of 1991 then decrease towards the summer of 1992.

4.3.4. Particulate Carbon, Nitrogen and Phosphorus

Particulate carbon (PC), nitrogen (PN) and phosphorus (PP) in the surface ocean over the first five years of the program are shown in Figures 6.5.7-9. PC varies between 1.3 - 3.0 µmol kg^{-1}, PN between 0.08 -0.45 µmol kg^{-1} and PP between 12 - 30 nmol kg^{-1} in the upper 50 meters of the water column. PC and PN show a clear annual cycle with peaks in particulate concentrations in summer of 1989, and 1990-92. A significantly larger PN concentration was observed in the late fall of 1993 with only a slight increase in PC and a decrease in PP.

4.4. Primary Production and Particle Flux

4.4.1. Primary Productivity

The results of the ^{14}C incubations and pigment determinations for samples collected from Go-Flo casts in 1993 are presented in Tables 4.4.1 and 4.4.2. Table 4.4.1 presents the primary production and pigment measurements made at individual depths on all 1993 cruises. Table 4.4.2 presents integrated values for irradiance, pigment concentration and primary production rates. The pigment concentrations and ^{14}C incorporation rates reported are the average of triplicate determinations. Integrated primary production rates measured over all five years of the program are shown in Figure 6.6.1 in order to place the 1993 results within the context of the time-series data set.

Variability in rates of primary production, integrated over the euphotic zone during the first five years of the time-series program, appear to be stochastic with no evidence of a seasonal cycle. Measured rates ranged between approximately 250 and 1100 mgC m^{-2} day^{-1} with the highest rate being observed in August 1989. This high rate of primary production coincided with a cyanobacterial bloom observed in surface waters near Station ALOHA on HOT cruise #9 (Karl et al. 1992). This variability, with a range of almost a factor of 5, is surprisingly large. However, the majority of the primary production estimates were between 250 and 600 mg C m^{-2} d^{-1}, and the average rate of primary production was approximately 450 mg C m^{-2} d^{-1}. Although this value is higher than historical measurements for the central ocean basins (Ryther, 1969), it is consistent with more recent measurements using modern methodology (Martin et al. 1987; Laws et al. 1989; Knauer et al. 1990).

4.4.2. Particle Flux

Particulate carbon (PC), nitrogen (PN), phosphorus (PP) and mass fluxes (150, 300 and 500 m) are presented in Table 4.4.3 and Figures 6.6.2-9 for the first five years of the program. Carbon flux displays a clear annual cycle with peaks in both the early spring and in the late summer months. The magnitude of particle flux varies by a factor of approximately 3. With the exception of anomalous PP fluxes measured on the first two HOT cruises, temporal variability in PN, PP and mass flux show similar temporal trends, and also vary between cruises by about a factor of three. Elemental ratios of carbon-to-nitrogen (atom:atom) at 150 m are typically between 6 - 10 and show no obvious temporal pattern. These particle flux measurements and elemental ratios are consistent with those measured in the central North Pacific Ocean by the VERTEX program (Martin et al. 1987, Kanuer et al. 1990)). Nitrogen flux at 150 m, as a percent of photosynthetic nitrogen assimilation (calculated from ^{14}C primary production values assuming a C:N ratio [atom:atom] of 6.6) ranges between 2 - 10%. The average value (approximately 6.5%) is consistent with the estimate of new production for the oligotrophic central gyres made by Eppley and Peterson (1979) and with field data from the VERTEX program (Knauer *et al.*, 1990). Average fluxes of PC, PN, PP and mass at 150 m from the first five years of the time-series observations are shown in Figures 6.6.2-5. Contour plots of concentration are shown in Figures 6.6.6-9. For carbon, nitrogen, phosphorus and total mass, the flux declines rapidly with depth, presumably due to the rapid dissolution and remineralization of organic particles sinking through the water column. The flux of carbon at 500 m is less than 50% of the flux at 150 m.

4.5. ADCP Measurements

An overview of the shipboard ADCP data is given by the plots of velocity as a function of time and depth wjhile on station (Figures 6.7.1) and the velocity as a function of latitutde and depth during transit to and from Station ALOHA (Figures 6.7.2). As in the previous four years, currents were highly variable from cruise to cruise and within each cruise.

4.6. Meteorology

The meteorological data collected by HOT program scientists include atmospheric pressure, sea-surface temperature and wet and dry bulb air temperature. These data are presented in Figures 6.8.1-3. As described by Winn et al. (1991), parameters show evidence of annual cycles, although the daily and weekly ranges are nearly as high as the annual range for some variables. Wind speed and direction are also collected on HOT cruises. These data are presented in Figures 6.8.4-9.

4.7. Light Measurements

Integrated irradiance measurements made with the on-deck cosine collector on days that primary production experiments were conducted are presented in Table 4.4.2.

Table 4.4.1: Primary Production and Pigment Summary

Cruise[a]	Depth (m)	Mean Chl *a* [b] mg m^{-3}	Std. Dev. Chl *a* [c] mg m^{-3}	Mean Phaeo[b] mg m^{-3}	Std. Dev. Phaeo[c] mg m^{-3}	Light[d] mg C m^{-3} Rep #1	Light[d] mg C m^{-3} Rep #2	Light[d] mg C m^{-3} Rep #3	Dark[d] mg C m^{-3} Rep #1	Dark[d] mg C m^{-3} Rep #2	Dark[d] mg C m^{-3} Rep #3
44	5	0.118		0.099		3.97	4.25	4.62	0.27	0.13	0.14
44	25	0.180		0.156		4.44	6.25	5.80	0.40	0.29	0.29
44	45	0.179		0.157		4.51	5.69	5.09	0.17	0.15	0.07
44	75	0.191		0.179		2.85	2.46	1.73	0.38	0.19	0.14
44	100	0.198		0.145		0.98	0.91	0.96	0.04	0.05	0.06
44	125	0.152		0.145		0.25		0.27	0.14	0.14	0.13
44	150	0.079		0.152		0.10	0.10	0.18	0.04	0.04	0.06
44	175	0.084		0.144			0.05	0.05	0.07	0.07	0.05
45	5	0.086	0.001	0.065	0.003	5.90	7.55	5.71	0.19	0.11	0.11
45	25	0.086	0.003	0.077	0.004	6.27	3.88	2.94	0.22	0.20	0.23
45	45	0.081	0.001	0.066	0.005	3.95	3.56	4.96	0.14	0.14	0.02
45	75	0.100	0.002	0.087	0.005	0.27	0.50	0.63	0.12	0.15	0.14
45	100	0.137	0.005	0.257	0.008	1.37	1.19	0.66	0.06	0.06	0.07
45	125	0.088	0.003	0.205	0.007	0.34	0.24	0.34	0.07	0.05	0.05
45	150	0.037	0.000	0.094	0.003	0.09	0.10	0.09	0.03	0.03	0.04
45	175	0.012	0.001	0.032	0.004	0.03	0.03	0.04	0.03	0.03	0.03
46	5	0.075	0.003	0.056	0.001	0.35	6.06	6.22	0.22	0.12	0.13
46	25	0.070	0.005	0.051	0.005	5.28	5.08	5.97	0.24	0.21	0.22
46	45	0.069	0.002	0.048	0.004	4.59	4.97	4.76	0.14	0.15	0.06
46	75	0.091	0.028	0.079	0.019	3.26	3.23	3.47	0.16	0.17	0.15
46	100	0.219	0.018	0.254	0.024	3.71	3.71	0.99	0.12	0.13	0.11
46	125	0.070	0.005	0.051	0.004	0.19	0.19	0.17	0.17	0.15	0.14
46	150	0.077	0.002	0.054	0.001	0.16	0.23	0.17	0.20	0.21	0.27
46	175	0.089	0.006	0.071	0.008	0.15	0.21	0.14	0.30	0.21	0.20
47	5	0.083	0.002	0.066	0.013	7.69	7.38	6.69	0.27	0.26	0.17
47	25	0.090	0.003	0.065	0.004	7.43	7.76	7.58	0.25	0.35	0.24
47	45	0.094	0.001	0.071	0.004	6.68	7.18	5.95	0.15	0.17	0.05
47	75	0.199	0.023	0.142	0.013	5.59	5.39	6.06	0.15	0.16	0.23
47	100	0.203	0.052	0.291	0.083	3.25	0.68	3.40	0.12	0.13	0.15
47	125	0.171	0.002	0.410	0.011	1.28	1.50	1.19	0.11	0.11	0.17
47	150	0.112	0.013	0.306	0.034	0.34	0.38	0.37	0.07	0.08	0.10
47	175	0.042	0.005	0.108	0.000	0.13	0.11	0.20	0.06	0.22	

Table 4.4.1: (continued)

Cruise[a]	Depth (m)	Mean Chl *a* [b] mg m^{-3}	Std. Dev. Chl *a* [c] mg m^{-3}	Mean Phaeo[b] mg m^{-3}	Std. Dev. Phaeo[c] mg m^{-3}	Light[d] mg C m^{-3} Rep #1	Light[d] mg C m^{-3} Rep #2	Light[d] mg C m^{-3} Rep #3	Dark[d] mg C m^{-3} Rep #1	Dark[d] mg C m^{-3} Rep #2	Dark[d] mg C m^{-3} Rep #3
49	5	0.072	0.002	0.049	0.004	7.99	8.59	7.32	0.24	0.19	0.19
49	25	0.074	0.001	0.052	0.008	7.46	7.12	8.00	0.24	0.28	0.21
49	45	0.080	0.002	0.052	0.003	5.93	5.37	4.59	0.17	0.20	0.07
49	75	0.131	0.002	0.113	0.007	3.07	3.25	2.83	0.13	0.15	0.13
49	100	0.206	0.002	0.205	0.010	1.30	1.32	1.14	0.08	0.14	0.12
49	125	0.195	0.022	0.454	0.006	0.38	0.54	0.52	0.09	0.11	0.10
49	150	0.131	0.009	0.347	0.002	0.21	0.26	0.26	0.08	0.13	0.21
49	175	0.077	0.001	0.061	0.001	0.18	0.22	0.24	0.18	0.15	0.20
50	5	0.074	0.009	0.060	0.010	3.17	4.84	3.05	0.30	0.17	0.15
50	25	0.077	0.003	0.054	0.005	2.85	2.86	2.42	0.49	0.23	0.30
50	45	0.057	0.009	0.044	0.005	1.57	1.18	2.59	0.14	0.13	0.03
50	75	0.145	0.011	0.125	0.014	0.74	1.30	1.57	0.14	0.13	0.17
50	100	0.167	0.001	0.400	0.005	0.82	1.01	0.96	0.04	0.05	0.04
50	125	0.127	0.006	0.320	0.004	0.25	0.21	0.22	0.06	0.05	0.09
50	150	0.033	0.000	0.099	0.001	0.08	0.07	0.12	0.05	0.17	0.04
50	175	0.017	0.002	0.044	0.009	0.03	0.05	0.03	0.06	0.04	0.10

[a]IS = *in situ* incubations

[b]Generally average of 2 or more replicates

[c]SD (standard deviation) computed only at depths with three replicate subsamples

[d]Incubation times are approximations only (i.e., half day or full day). Actual incubation time for each measurement is given in Table 4.4.2.

[e]Not determined

Table 4.4.2: *In Situ* Primary Production and Pigment Summary (0-200 m)

Cruise	Incident Irradiance ($E\ m^{-2}\ d^{-1}$) cosine[a]	hemi[b]	Pigments ($mg\ m^{-2}$) Chl *a*	Phaeo	Incubation (hrs)	Carbon Assimilation Rates ($mgC\ m^{-2}\ d^{-1}$) light	dark
44	35.84	74.5	28.973	29.903	12.3	401	27
45	41.95	72.5	14.785	21.658	13.8	338	18
46	57.32	92.1	19.240	16.870	11.8	466	36
47	58.21	88.9	24.593	37.195	13.7	689	31
49	51.14	94.7	24.350	33.620	13.7	541	31
50	21.53	NA*	16.875	28.643	11.8	219	24

*not available

Table 4.4.3: Station ALOHA Sediment Trap Flux Data

Cruise	Depth (m)	Carbon mg $m^{-2}\ day^{-1}$	SD	n	Nitrogen mg $m^{-2}\ day^{-1}$	SD	n	Phosphorus mg $m^{-2}\ day^{-1}$	SD	n	Mass Flux mg $m^{-2}\ day^{-1}$	SD	n
44	150	25.2	2.8	6	3.69	0.51	6	0.31	0.04	3	31.8	7.7	3
44	300	18	2.1	6	2.04	0.09	6	0.16	0.02	3	22.5	9.1	3
44	500	12.8	2.6	4	1.58	0.48	4	0.1	0.01	3	19.3	6.8	3
45	150	37.2	10.1	5	3.67	0.81	5	0.63	0.01	3	103.3	15.3	3
45	300	15.5	3.5	6	1.53	0.49	6	0.13	0.06	3	54.5	11.6	3
45	500	11.6	0.7	6	0.92	0.09	6	0.09	0.02	3	34.3	6.3	3
46	150	20.6	3.0	6	3.18	0.51	6	0.47	0.01	3	87.8	1.4	3
46	300	9.0	1.4	6	1.16	0.19	6	0.14	0.01	3	46.8	1.9	3
46	500	9.1	2.2	6	1.18	0.34	6	0.09	0.05	3	41.9	7.6	3
47	150	21.9	2.2	4	2.83	0.27	4	0.36	0.03	3	74.5	6.7	3
47	300	10.1	1.0	4	0.87	0.12	4	0.13	0.01	3	45.6	4.0	3
47	500	7.9	0.6	4	0.55	0.06	4	0.08	0.06	3	27.2	5.5	3
49	150	18.1	4.0	6	2.21	0.46	6	0.20	0.02	3	42.0	5.5	3
49	300	7.9	1.7	6	0.67	0.16	6	0.06	0.02	3	16.9	5.7	3
49	500	6.6	1.8	5	0.59	0.13	5	0.07	0.02	3	19.9	5.8	3
50	150	25.8	0.1	3	3.83	0.32	3	0.46	0.35	3	32.3	7.3	3
50	300	15.0	4.9	6	1.56	0.45	6	0.11	0.03	3	22.3	0.4	3
50	500	14.3	3.8	6	1.23	0.46	6	ND*	ND*	3	9.3	1.2	3

*not determined

4.8. Buoy and Shipboard Observations

A National Data Buoy Center (NDBC) meteorological buoy is located about 400 km west of Station ALOHA at 23°24'N, 162°18'W. This buoy collects hourly observations of air temperature, sea surface temperature, atmospheric pressure, wind speed and direction and significant wave height. The coherence of these data with the data collected on HOT cruises was examined and reported in Tupas et al. (1993). We concluded from these analyses, that the buoy data can be used to get useful estimates of air temperature, sea-surface temperature and atmospheric pressure at Station ALOHA.

4.9. Inverted Echo Sounder Observations

Fig. 4.2 shows dynamic height from the IESs after removal of the semi-diurnal and diurnal tides and other variability with time-scales less than 1 day. The tidal range in dynamic height is about 8 dyn-cm, which is relatively large compared to the annual range (about 25 dyn-cm), and illustrates the importance of the "burst" CTD sampling.

It is immediately apparent from Fig. 4.2 that there are large events with time-scales from weeks to months which dominate dynamic height to such an extent that there is no clearly defined annual cycle - the highest and lowest dynamic height in 1991 occurred within the space of about a month. These events are not well sampled with the monthly spacing of the HOT cruises; the events occurring in the first half of 1991 were poorly sampled.

Some indication of the spatial scales of the dynamic height variability can be inferred from the differences between the IES signals, remembering that the IES spacing was about 50 km. At time-scales of several months, the records appear similar; for example the large event in late 1992, having peak-to-peak amplitudes of 25 dyn-cm, appears in all records. But at periods of one month or less, there can be differences between the records; for example during the first half of 1991. Cross-spectra between the various IES pairs indicate that dynamic height was coherent across the entire array for periods greater than about 25 days during both deployments, and that at these periods, phase propagation was from east to west. The synoptic time-scale oscillations may well be associated with Rossby waves arriving from the east.

The array of dynamic height can be used to compute geostrophic currents, which are shown to be reasonably well correlated with Acoustic Doppler Current Profiler measurements.

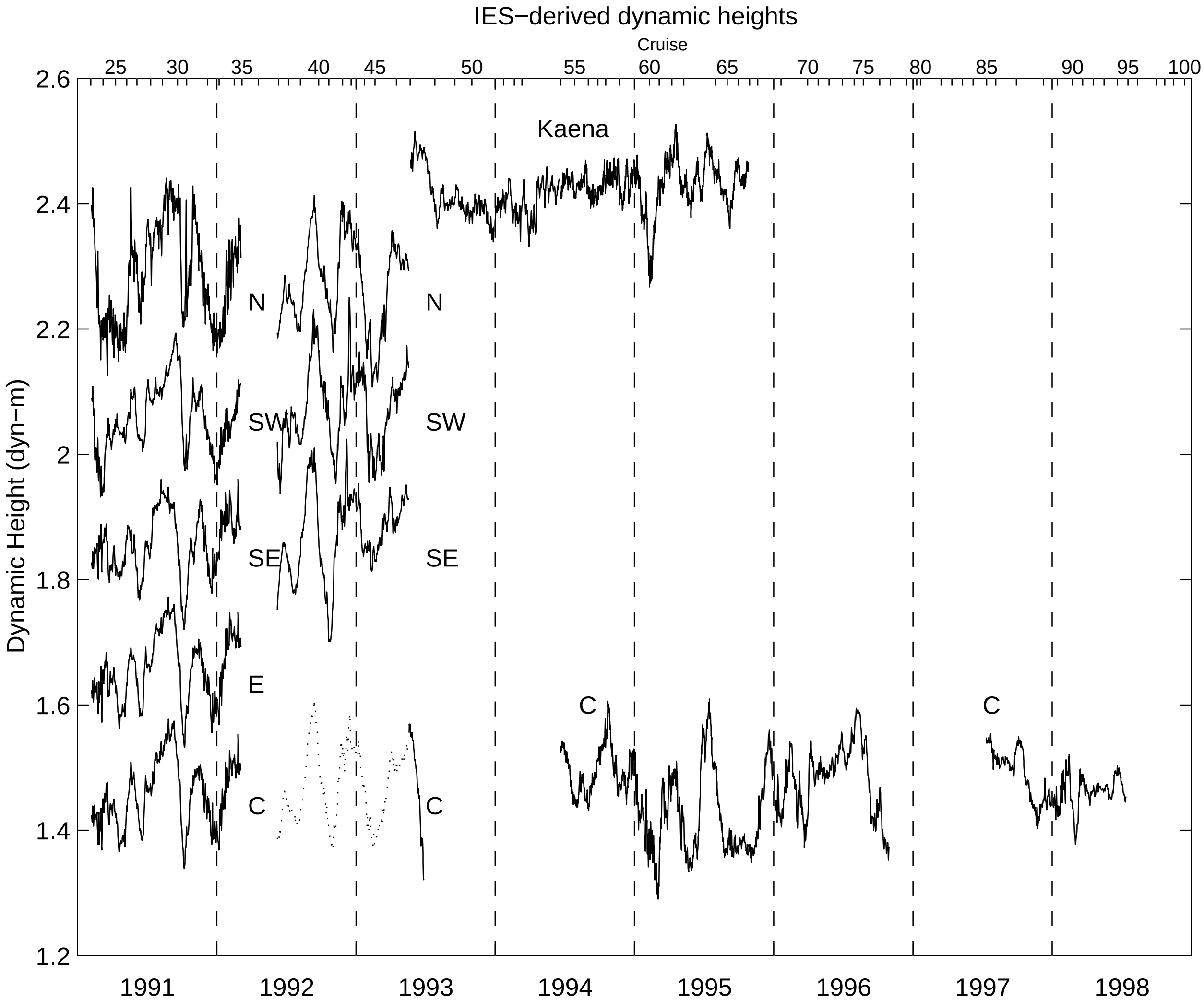

Figure 4.2: Dynamic height from the inverted echo sounders after removal of the semi-diurnal, diurnal tides and variability with time-scales less than one day. The plots are staggered at 0.2 dyn-m intervals. The dotted line is an average of the N, SW and SE records between June 1992 and May 1993. Horizontal axis above shows the cruise numbers.

5. References

Bidigare, R.R., J. Marra, T.J. Dickey, R. Iturriaga, K.S. Baker, R.C. Smith and H. Pak, 1990: Evidence for phytoplankton succession and chromatic adaptation in the Sargasso Sea during Spring 1985. *Marine Ecology Progress Series*, **60**, 113-122.

Chiswell, S.M., E. Firing, D. Karl, R. Lukas, C. Winn, 1990: Hawaii Ocean Time-series Program Data Report 1, 1988-1989. School of Ocean and Earth Science and Technology, University of Hawaii, 269 pp.

Clayton, T.D. and R.H. Byrne, 1993: Spectrophotometric seawater pH measurements: total hydrogen ion concentration scale calibration of m-cresol purple and at-sea results. *Deep-Sea Research*, **40**, 2115-2129.

Cox, R.D., 1980: Determination of nitrate at the parts per billion level by chemiluminescence. *Analytical Chemistry*, **52**, 332-335.

Eppley, R.W. and B.J. Peterson, 1979: Particulate organic matter flux and planktonic new production in the deep ocean. *Nature*, **282**, 677-680.

Garside, C., 1982: A chemiluminescent technique for the determination of nanomolar concentrations of nitrate and nitrite in seawater. *Marine Chemistry*, **11**, 159-167.

Karl, D.M. and O. Holm-Hansen, 1978: Methodology and measurement of adenylate energy charge ratios in environmental samples. *Marine Biology*, **48**, 185-197.

Karl, D. M., R. Letelier, D. V. Hebel, D. F. Bird and C. D. Winn, 1992: *Trichodesmium* blooms and new nitrogen in the North Pacific gyre. In: E. J. Carpenter et al. (eds.), Marine Pelagic Cyanobacteria: Trichodesmium and Other Diazotrophs, pp. 219-237. Kluwer Academic Publishers, Netherlands.

Karl, D.M. and G. Tien, 1992: MAGIC: A sensitive and precise method for measuring dissolved phosphorus in aquatic environments. *Limnology and Oceanography*, **37**, 105-116.

Karl, D.M., C.D. Winn, D.V.W. Hebel and R. Letelier, 1990: Hawaii Ocean Time-series Program Field and Laboratory Protocols, September 1990.

Knauer, G.A., D.G. Redalje, W.G. Harrison and D.M. Karl, 1990: New production at the VERTEX time-series site. *Deep-Sea Research*, **37**, 1121-1134.

Laws, E.A., G.R. DiTullio, P.R. Betzer, D.M. Karl and R.L. Carder, 1989: Autotrophic production and elemental fluxes at 26°N, 155°W in the North Pacific subtropical gyre. *Deep-Sea Research*, **36**, 103-120.

Lukas, R. and S. Chiswell, 1991: Submesoscale water mass variations in the salinity minimum of the north Pacific near Hawaii. *WOCE Notes*, **3(1)**, 1,6-8.

Martin, J.H., G.A. Knauer, D.M. Karl and W.W. Broenkow, 1987: VERTEX: Carbon cycling in the northeast Pacific. *Deep-Sea Research*, **34**, 267-285.

Strickland, J.D.H. and T.R. Parsons, 1972: A practical handbook of seawater analysis. Fisheries Research Board of Canada, 167 pp.

Tsuchiya, M., 1968: Upper waters of the intertropical Pacific Ocean. Johns Hopkins Oceanographic Studies, **4**, 49 pp.

Tupas, L., F. Santiago-Mandujano, D. Hebel, R. Lukas, D. Karl and E. Firing, 1993: Hawaii Ocean Time-series Program Data Report 4, 1992. School of Ocean and Earth Science and Technology, University of Hawaii, 248 pp.

Tupas, L.M., B.N. Popp and D.M. Karl, 1994: Dissolved organic carbon in oligotrophic waters: experiments on sample preservation, storage and analysis. *Marine Chemistry*, **48**, 207-216.

Weiss, R.F., R.A. Jahnke and C.D. Keeling, 1982: Seasonal effects of temperature and salinity on the partial pressure of CO_2 in seawater. *Nature*, **300**, 511-513.

Winn, C., S.M. Chiswell, E. Firing, D. Karl, R. Lukas, 1991: Hawaii Ocean Time-series Program Data Report 2, 1990. School of Ocean and Earth Science and Technology, University of Hawaii, 175 pp.

Winn, C., R. Lukas, D. Karl, E. Firing, 1993: Hawaii Ocean Time-series Program Data Report 3, 1991. School of Ocean and Earth Science and Technology, University of Hawaii, 228 pp.

Woodroff, J., R.J. Slotz, R.L. Jenne and P.M. Steurer, 1987: A comprehensive ocean-atmosphere data set. *Bulletin of the American Meteorological Society*, **68**, 1239-1250.

6. Figures

6.1. CTD Station Locations and Sediment Trap Drift Tracks

Figure6.1.1: CTD station locations on HOT-44 and 45. CTD stations represented by open circles relative to Station ALOHA. Solid lines connect casts taken in sequence and numbers show location of first and last casts. Dashed line shows area nominally defined as Station ALOHA. Drift track for the sediment trap array during the 72-hour deployment period is indicated by a solid line with the start point indicated by an S.

Figure 6.1.2: As in Figure 6.1.1, except for HOT-46 and 47.

Figure 6.1.3: As in Figure 6.1.1, except for HOT-49 and 50.

Figure 6.1.4: Other CTD locations on HOT-45 and HOT-47.

Figure 6.1.5: Other CTD locations on HOT-49 and HOT-50.

HOT−44

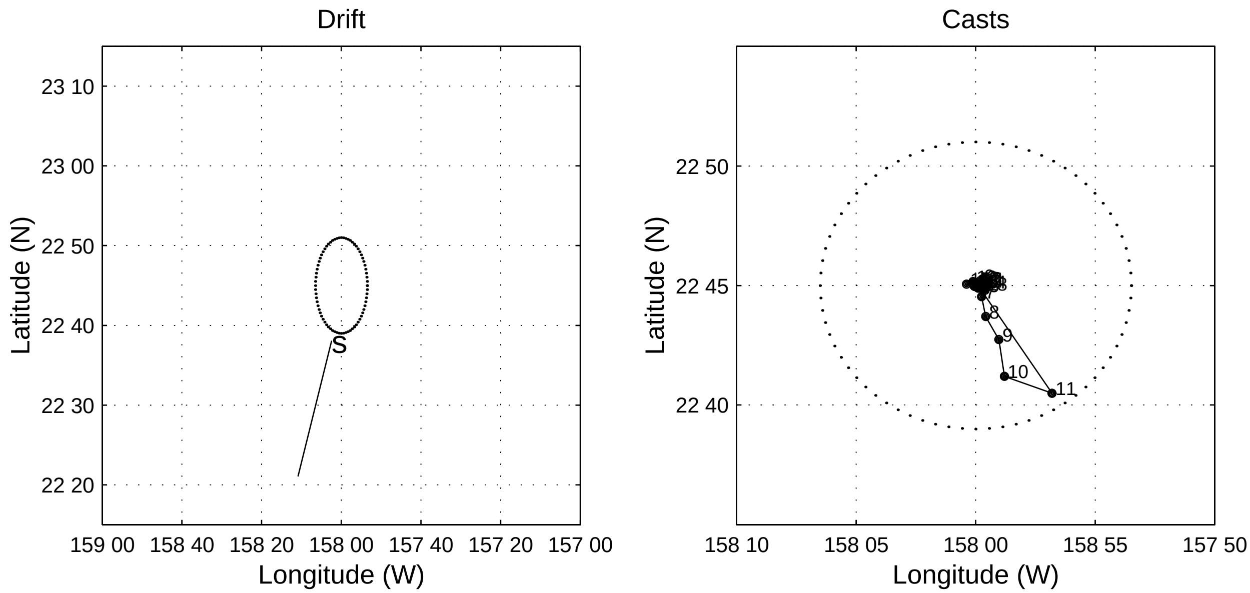

HOT−45

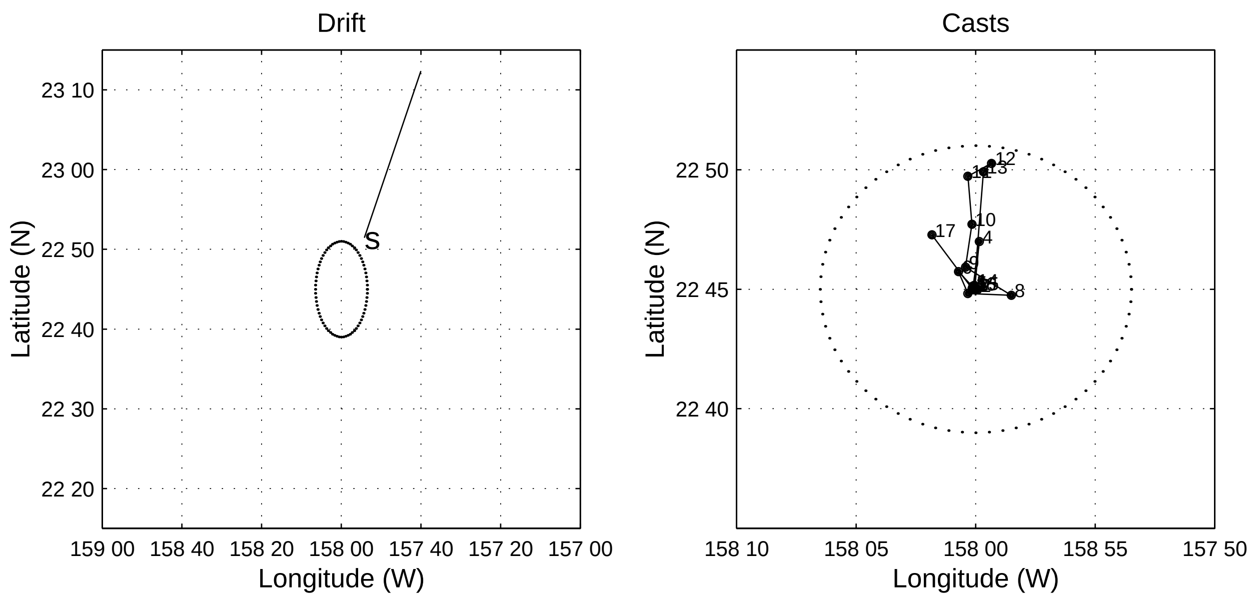

Figure 6.1.1

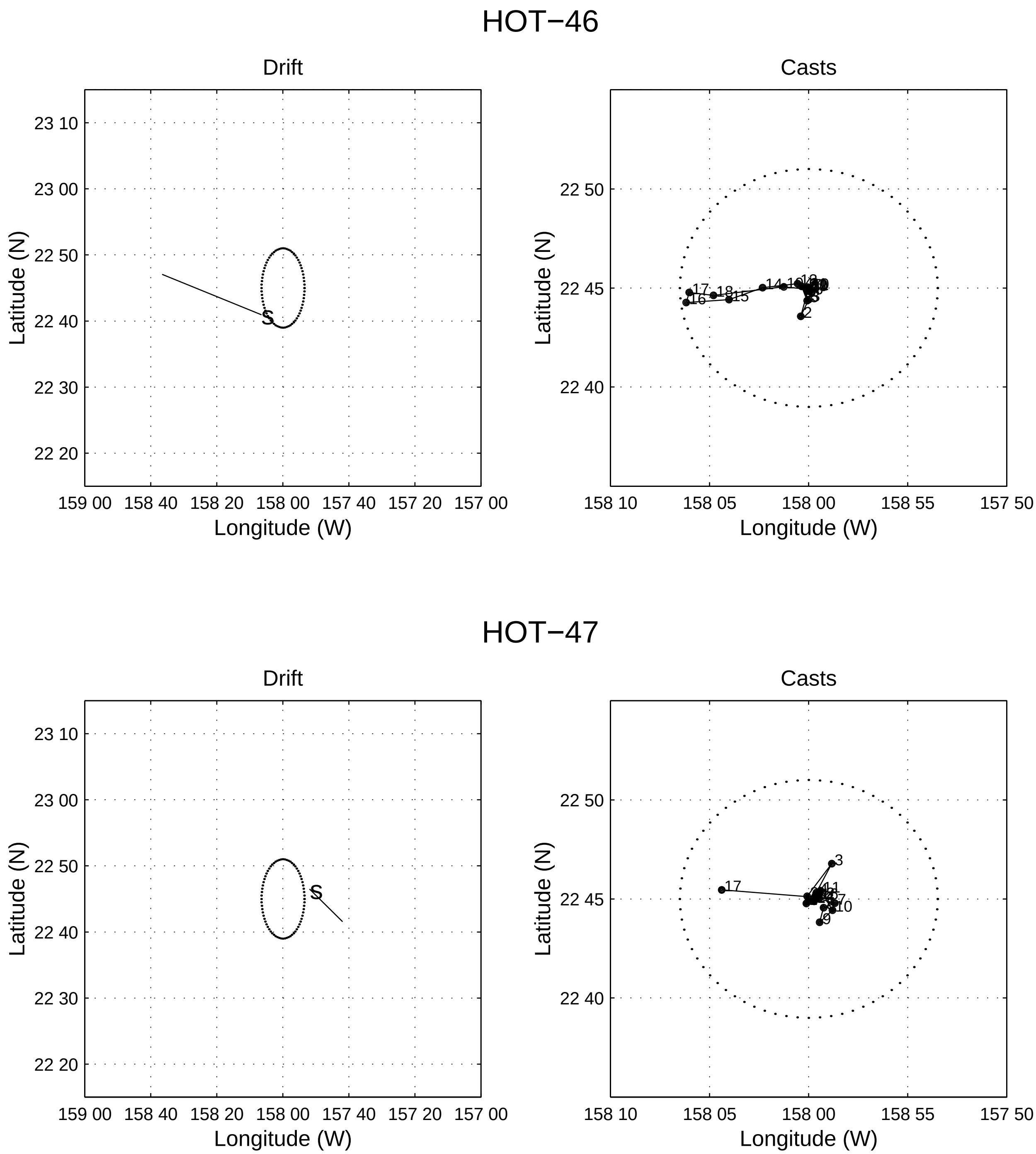
HOT−46
Drift
Casts
Latitude (N)
Longitude (W)
23 10
23 00
22 50
22 40
22 30
22 20
159 00
158 40
158 20
158 00
157 40
157 20
157 00
S
22 45
158 10
158 05
158 55
157 50
HOT−47
S

Figure 6.1.2

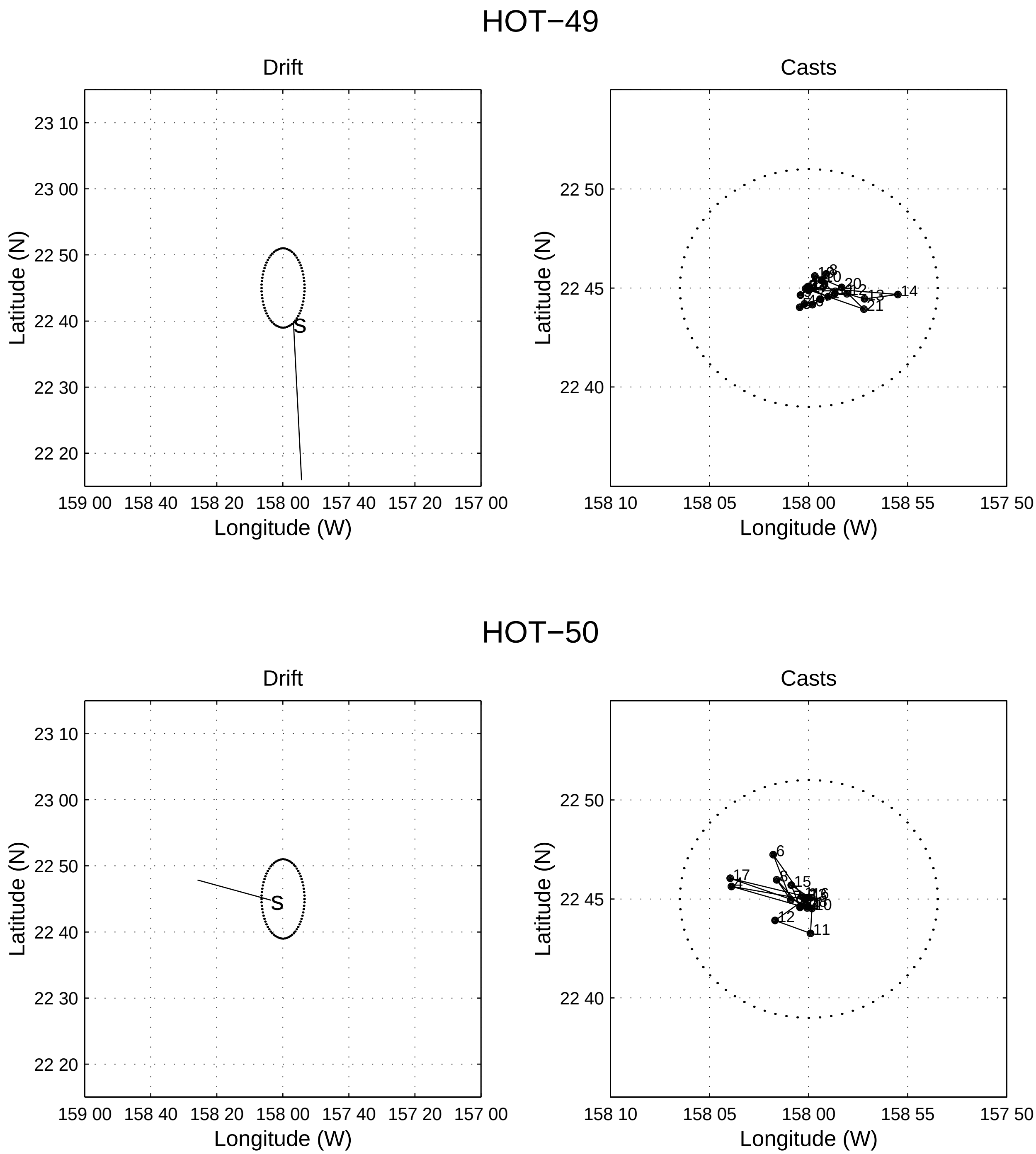
HOT−49
Drift
Casts
Latitude (N)
Longitude (W)
23 10
23 00
22 50
22 40
22 30
22 20
159 00
158 40
158 20
158 00
157 40
157 20
157 00
S
22 45
158 10
158 05
158 55
157 50
14
13
21
20
HOT−50
6
17
4
8
15
12
11
10

Figure 6.1.3

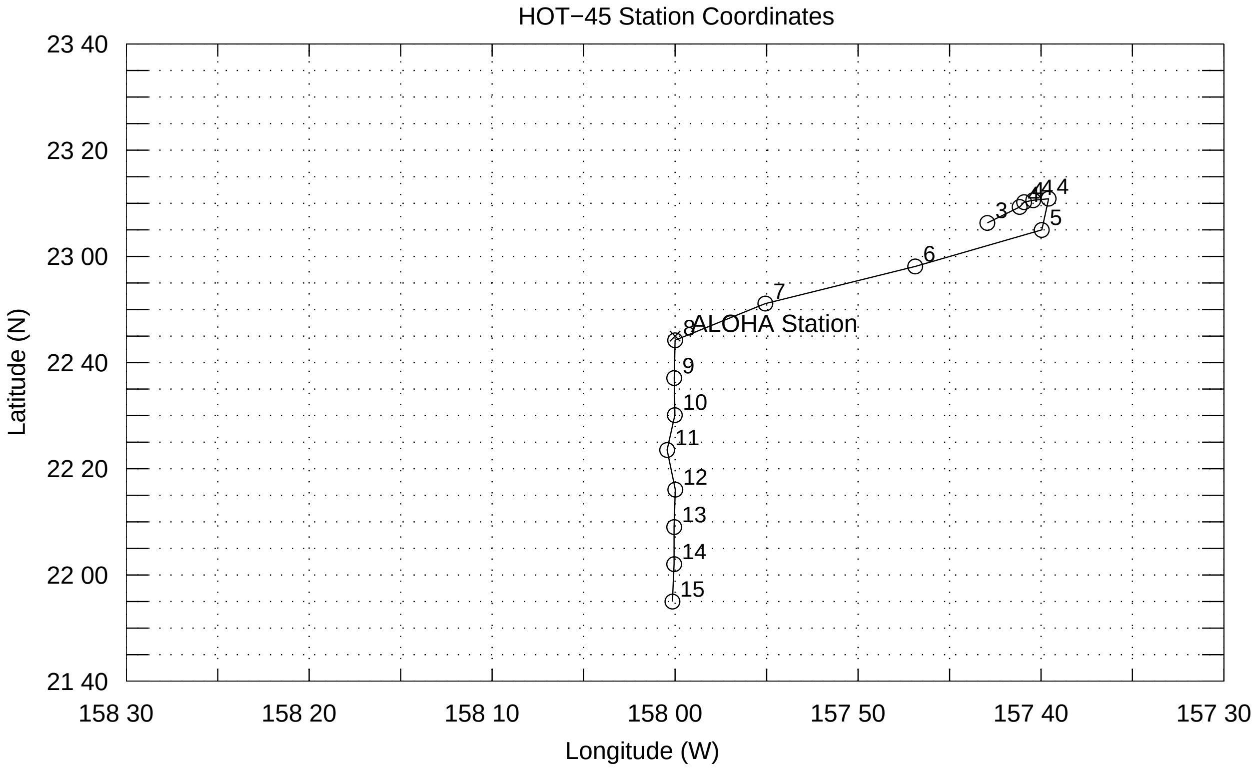
HOT−45 Station Coordinates
Latitude (N)
Longitude (W)
23 40
23 20
23 00
22 40
22 20
22 00
21 40
158 30
158 20
158 10
158 00
157 50
157 40
157 30
ALOHA Station
3
4
5
6
7
8
9
10
11
12
13
14
15

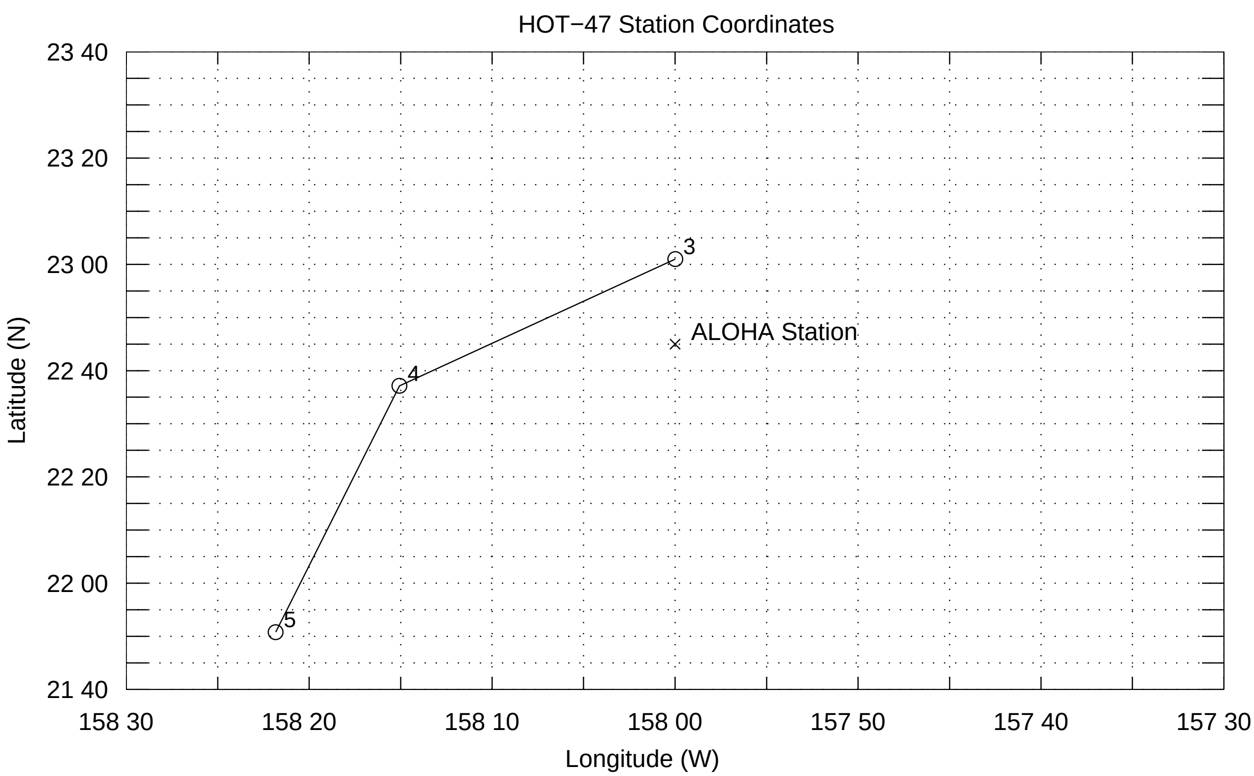
HOT−47 Station Coordinates
Latitude (N)
Longitude (W)
23 40
23 20
23 00
22 40
22 20
22 00
21 40
158 30
158 20
158 10
158 00
157 50
157 40
157 30
ALOHA Station
3
4
5

Figure 6.1.4

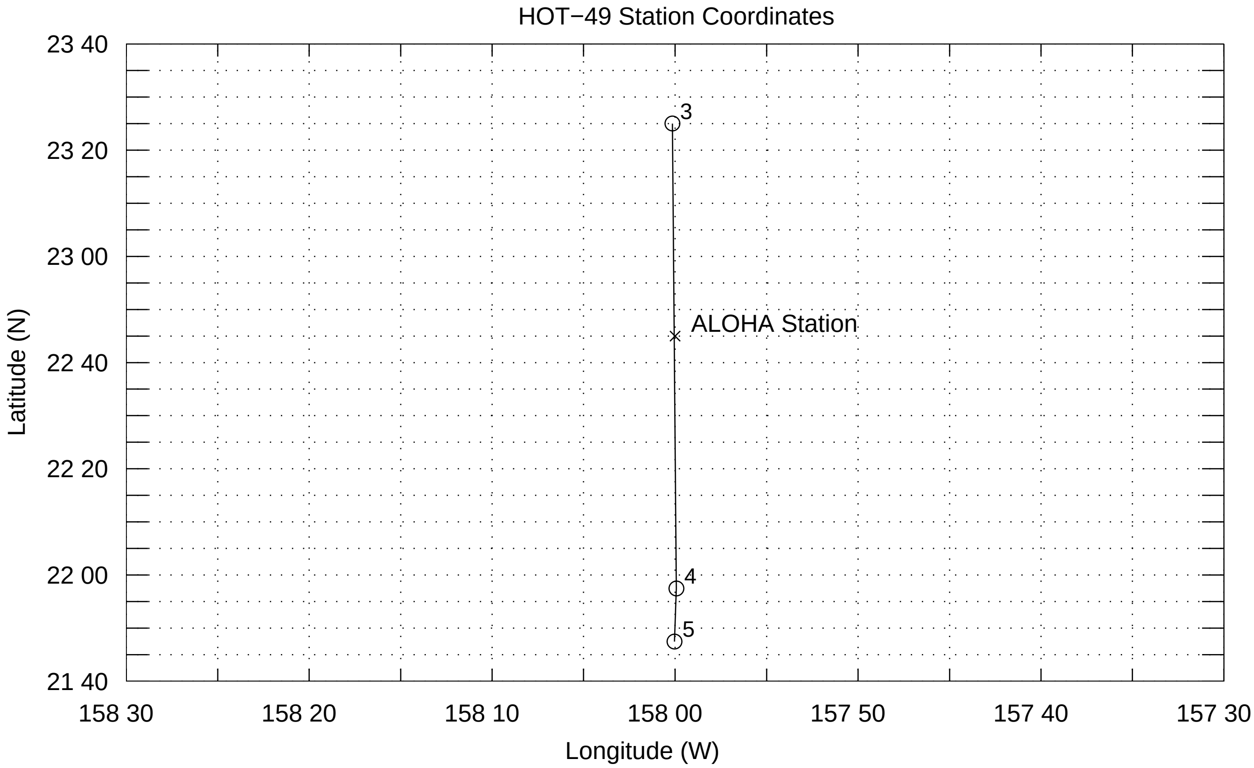
HOT−49 Station Coordinates
23 40
23 20
23 00
22 40
22 20
22 00
21 40
Latitude (N)
158 30
158 20
158 10
158 00
157 50
157 40
157 30
Longitude (W)
ALOHA Station
3
4
5

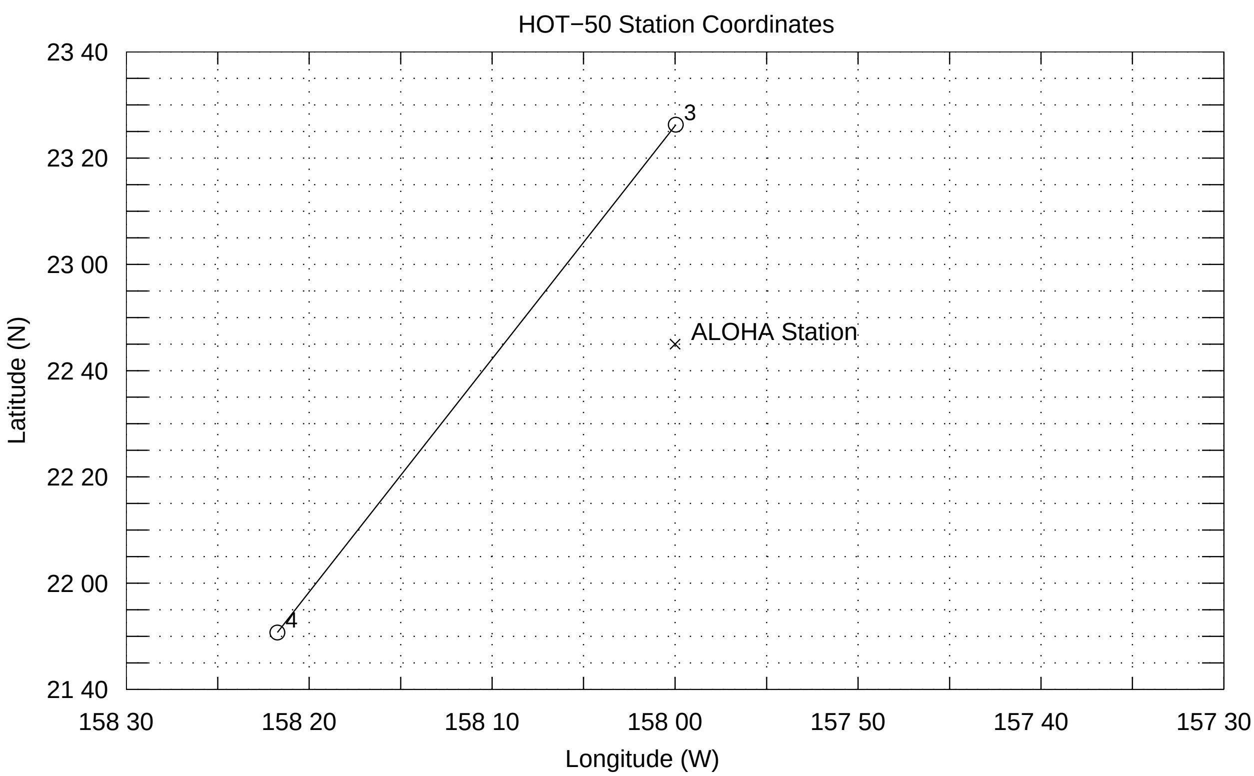
HOT−50 Station Coordinates
23 40
23 20
23 00
22 40
22 20
22 00
21 40
Latitude (N)
158 30
158 20
158 10
158 00
157 50
157 40
157 30
Longitude (W)
ALOHA Station
3
4

Figure 6.1.5

6.2. CTD Profiles

Figures 6.2.1a-f. Upper left panel: Temperature, salinity, oxygen and density (σ_θ) as a function of pressure for WOCE deep cast. Salinity and oxygen water bottle data are also plotted. Upper right panel: Nutrients ([NO_3 + NO_2], PO_4 and silicic acid) and oxygen as a function of potential temperature for all water samples. Lower left panel: CTD temperature and salinity profiles plotted as a function of pressure. Lower right panel: Salinity and oxygen from CTD and water samples plotted as a function of potential temperature.

Figures 6.2.2a-f. Upper panel: Stack plots of potential temperature versus pressure to 1000 dbar. Offset is 2 ºC. Lower panel: Stack plots of salinity versus pressure to 1000 dbar. Offset is 0.1.

Figures 6.2.3a-g: As in 6.1.1 but for Station Kahe.

Figure 6.2.4. Upper panel: Potential temperature versus pressure for all deep casts in 1993. Lower panel: Potential temperature for all deep casts in 1993 plotted from 2500 dbar.

Figure 6.2.5. Upper panel: Potential temperature versus salinity for all deep casts collected during 1993. Lower panel: Potential temperature versus salinity on same casts in the 1-5 °C range.

Figure 6.2.6. Upper panel: Oxygen values derived from calibrated CTD sensor data versus potential temperature for all deep casts collected during 1993. Lower panel: Oxygen versus potential temperature for 1993 deep casts within the 1-5 °C range.

Station ALOHA HOT 44

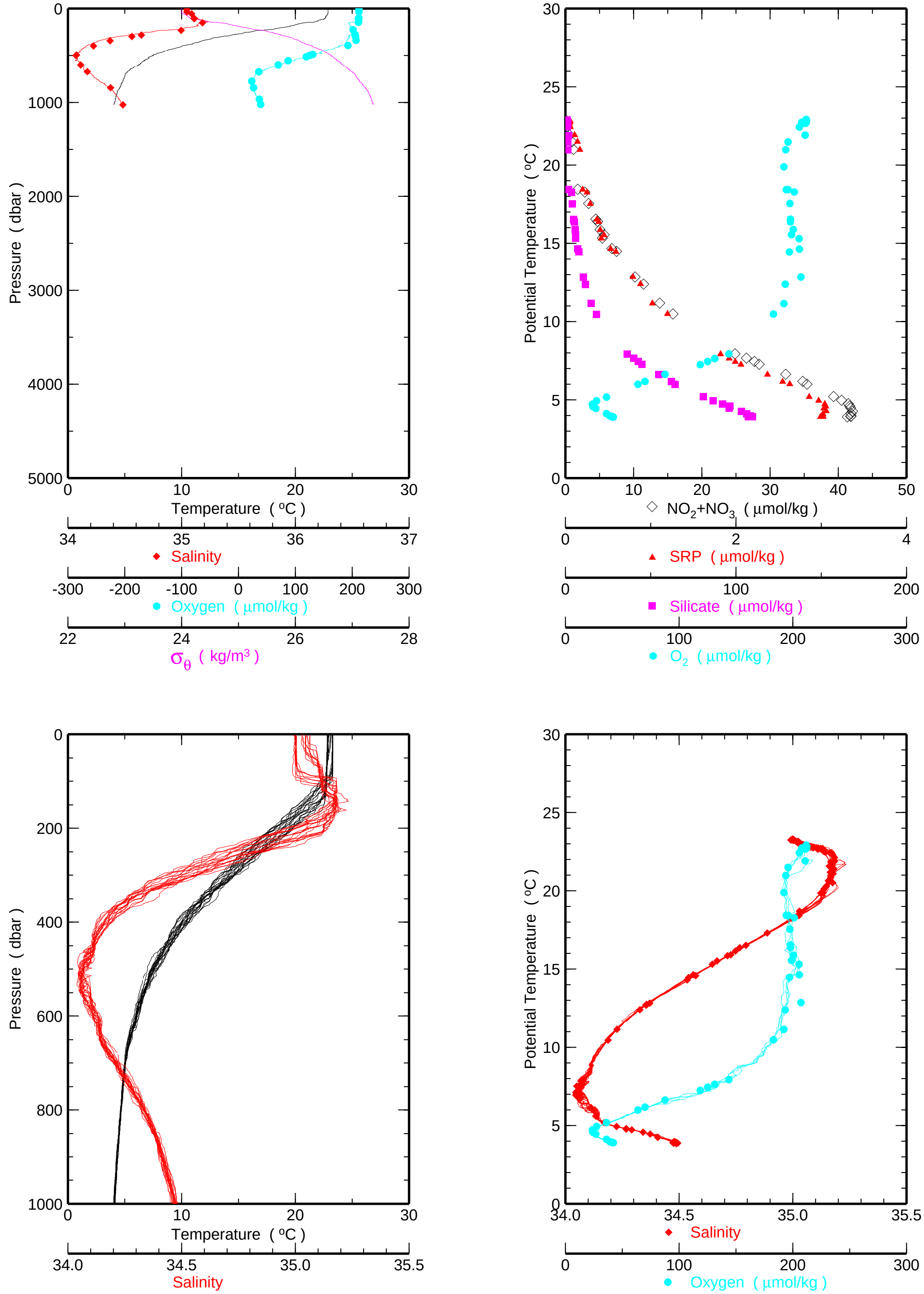

Figure 6.2.1a

Station ALOHA HOT 45

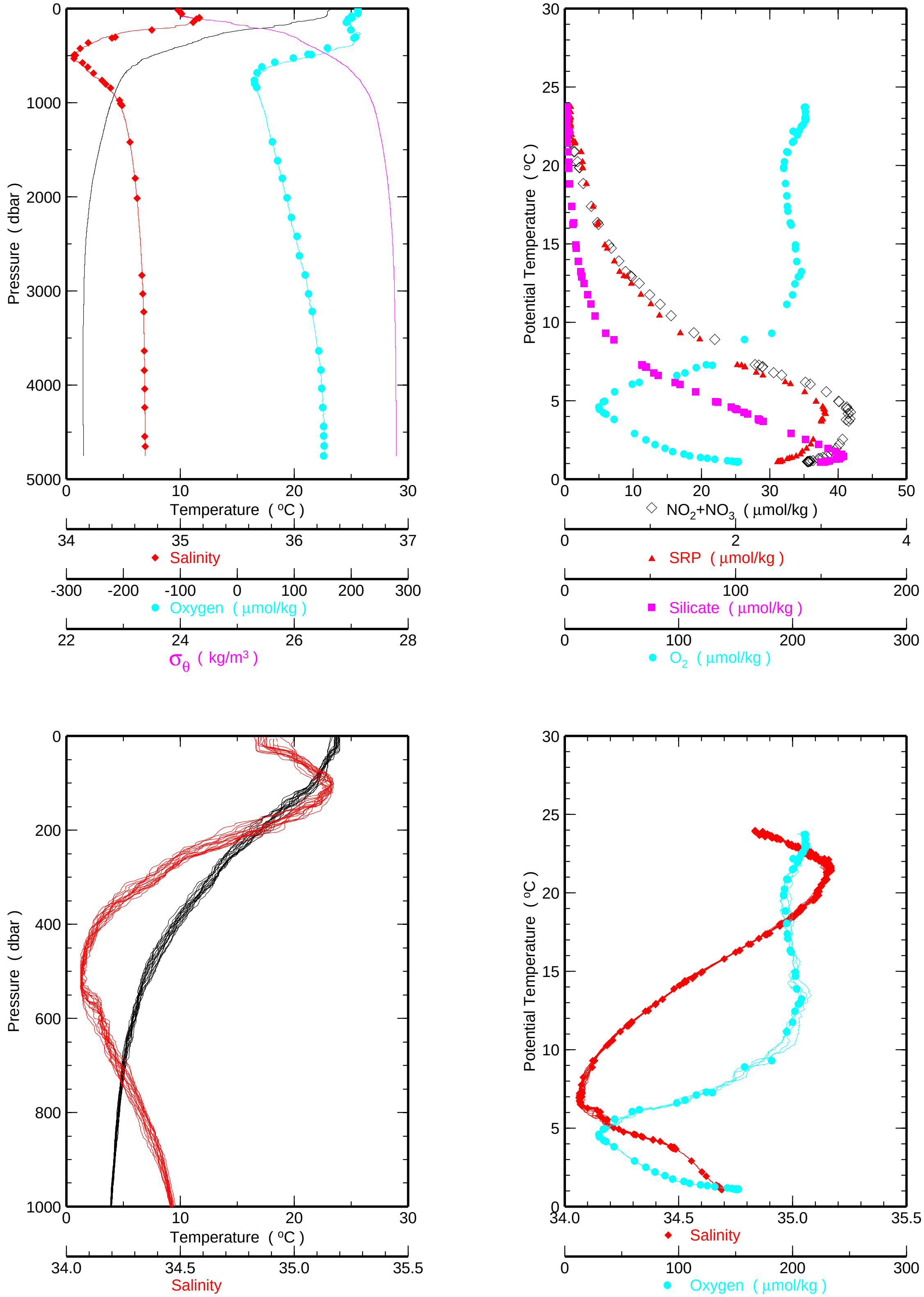

Figure 6.2.1b

Station ALOHA HOT 46

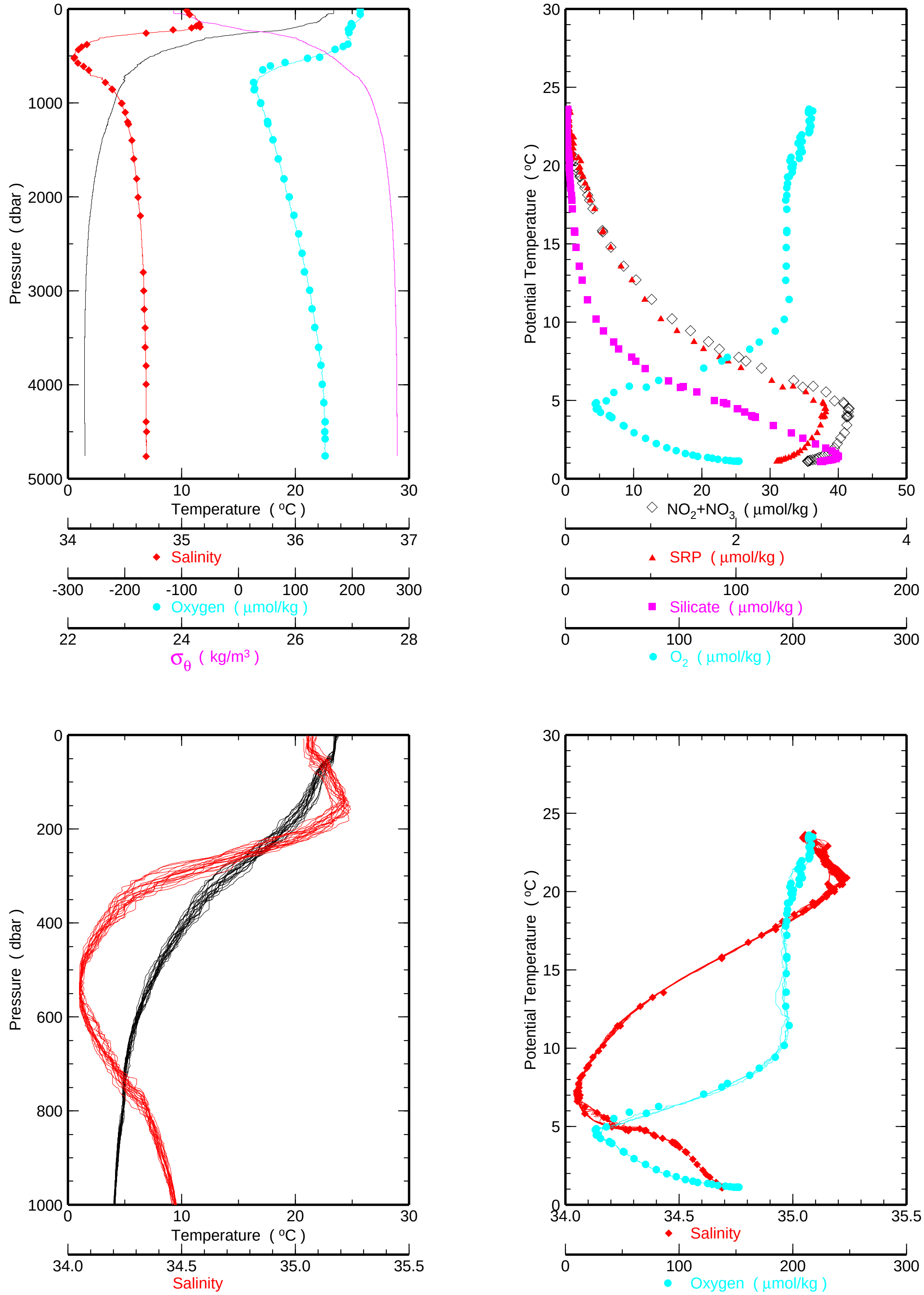

Figure 6.2.1c

Station ALOHA HOT 47

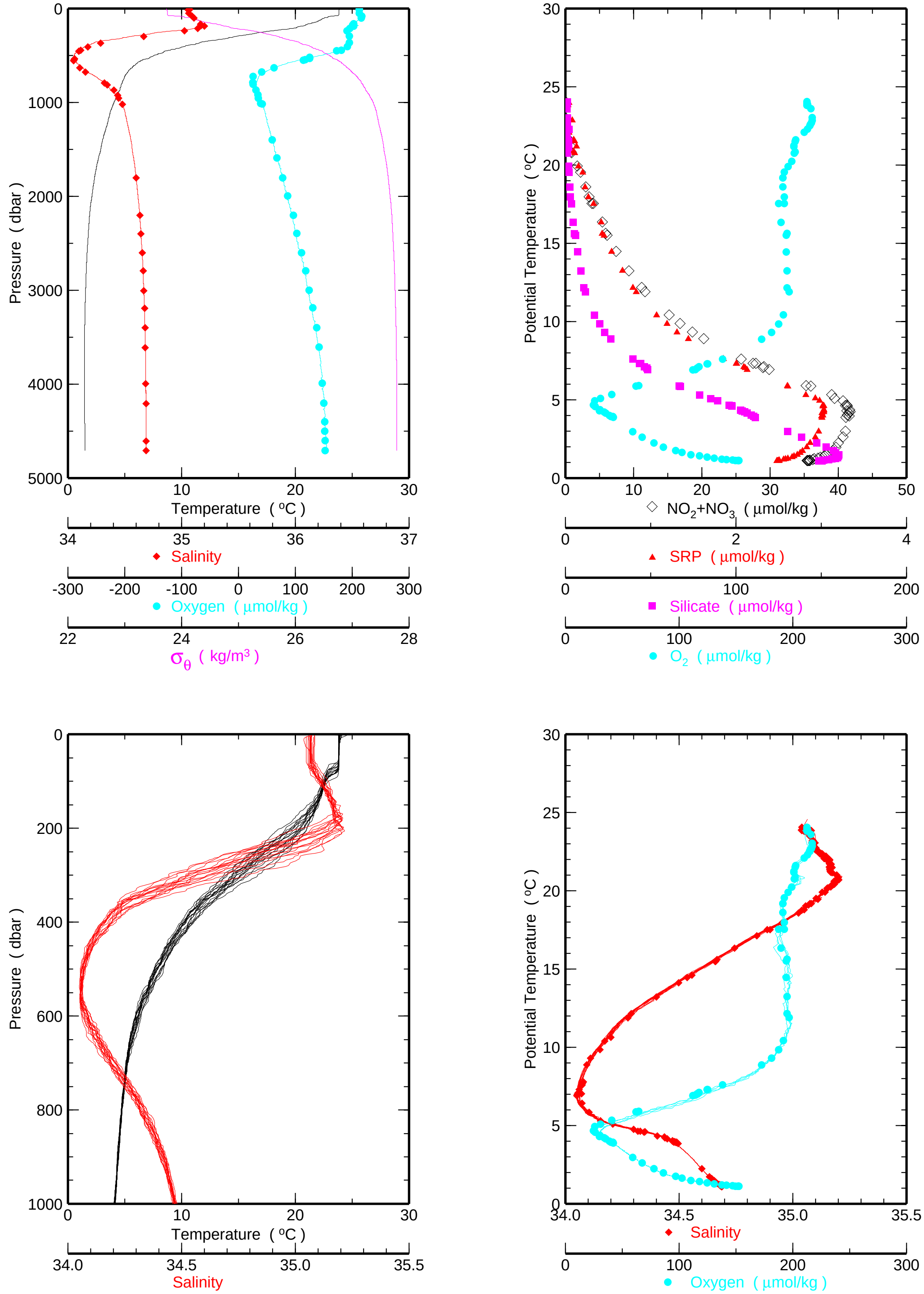

Figure 6.2.1d

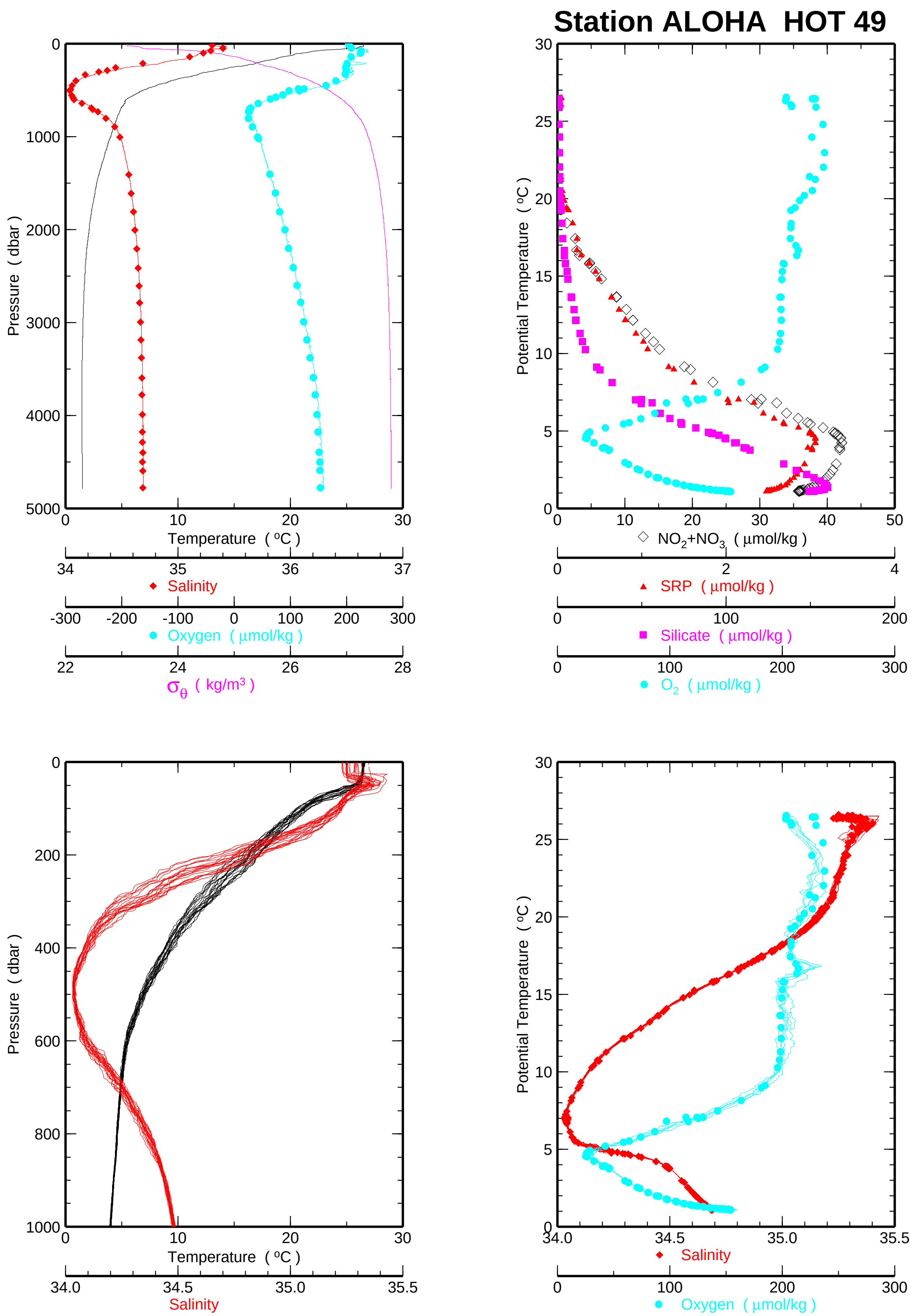

Station ALOHA HOT 49
Pressure (dbar)
Temperature (°C)
Salinity
Oxygen (µmol/kg)
σθ (kg/m³)
Potential Temperature (°C)
NO2+NO3 (µmol/kg)
SRP (µmol/kg)
Silicate (µmol/kg)
O2 (µmol/kg)

Figure 6.2.1e

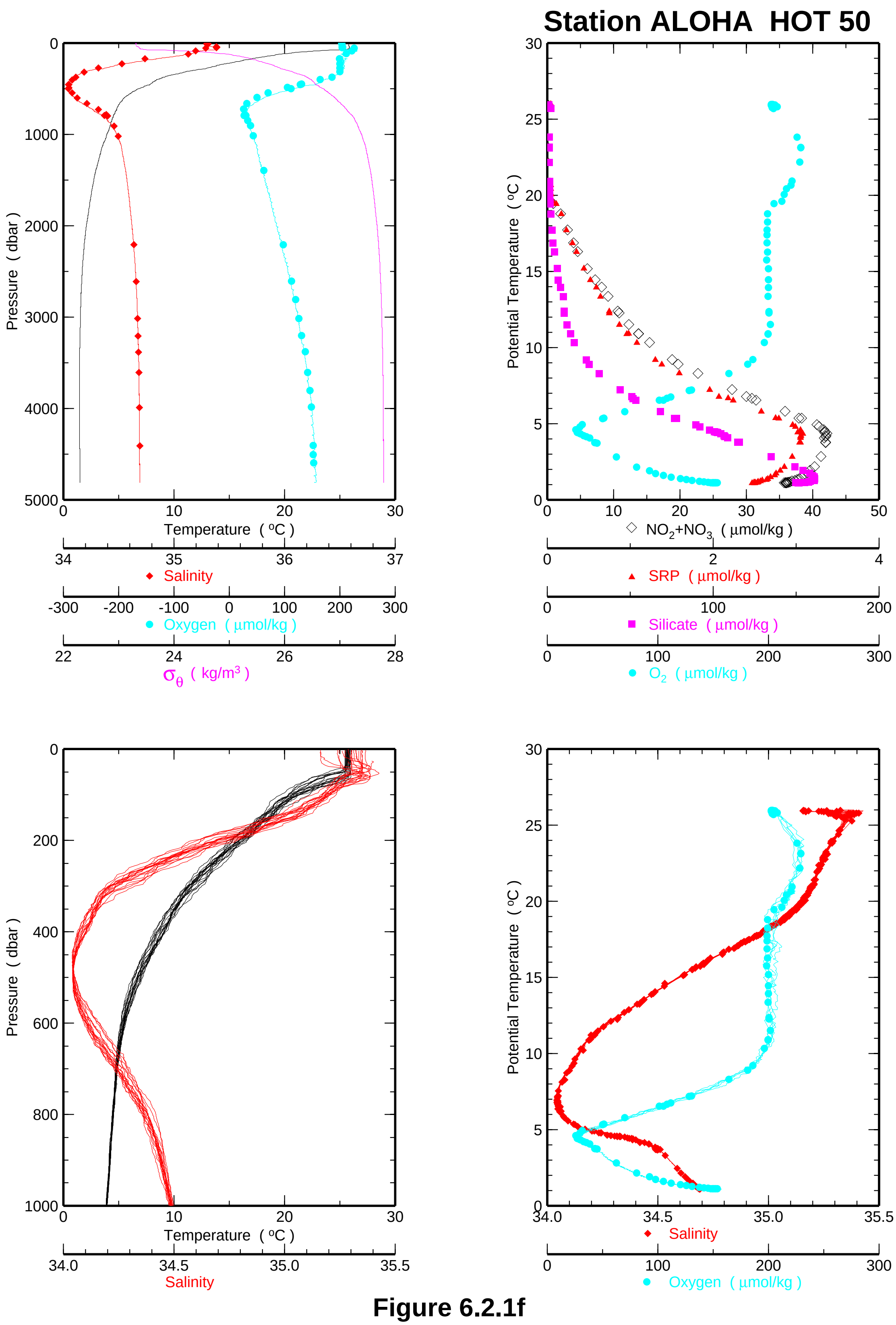
Station ALOHA HOT 50
Pressure (dbar)
Temperature (°C)
Salinity
Oxygen (µmol/kg)
σθ (kg/m³)
Potential Temperature (°C)
NO2+NO3 (µmol/kg)
SRP (µmol/kg)
Silicate (µmol/kg)
O2 (µmol/kg)

Figure 6.2.1f

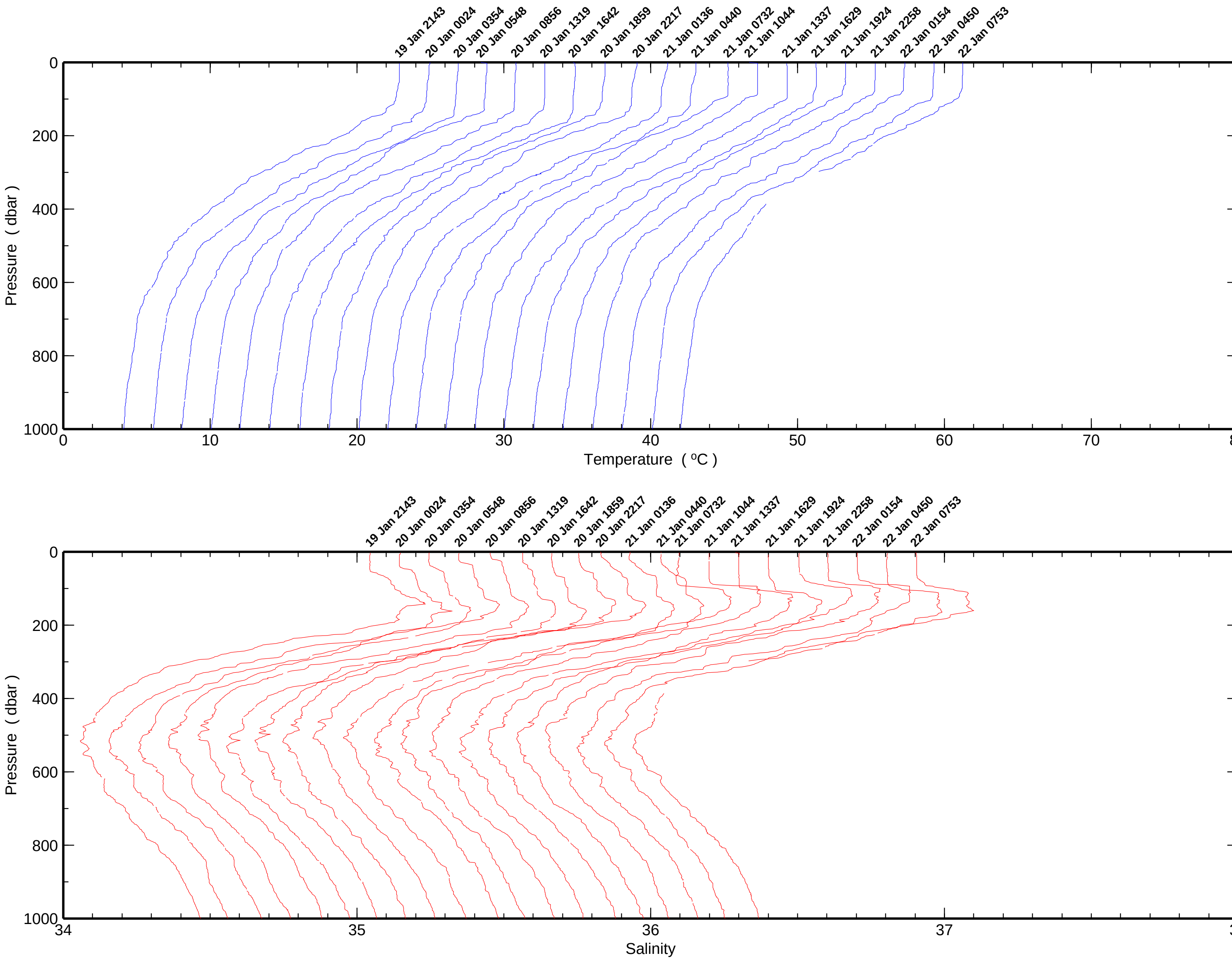

Station ALOHA HOT 44

Figure 6.2.2a

Figure 6.2.2b

Station ALOHA HOT 45

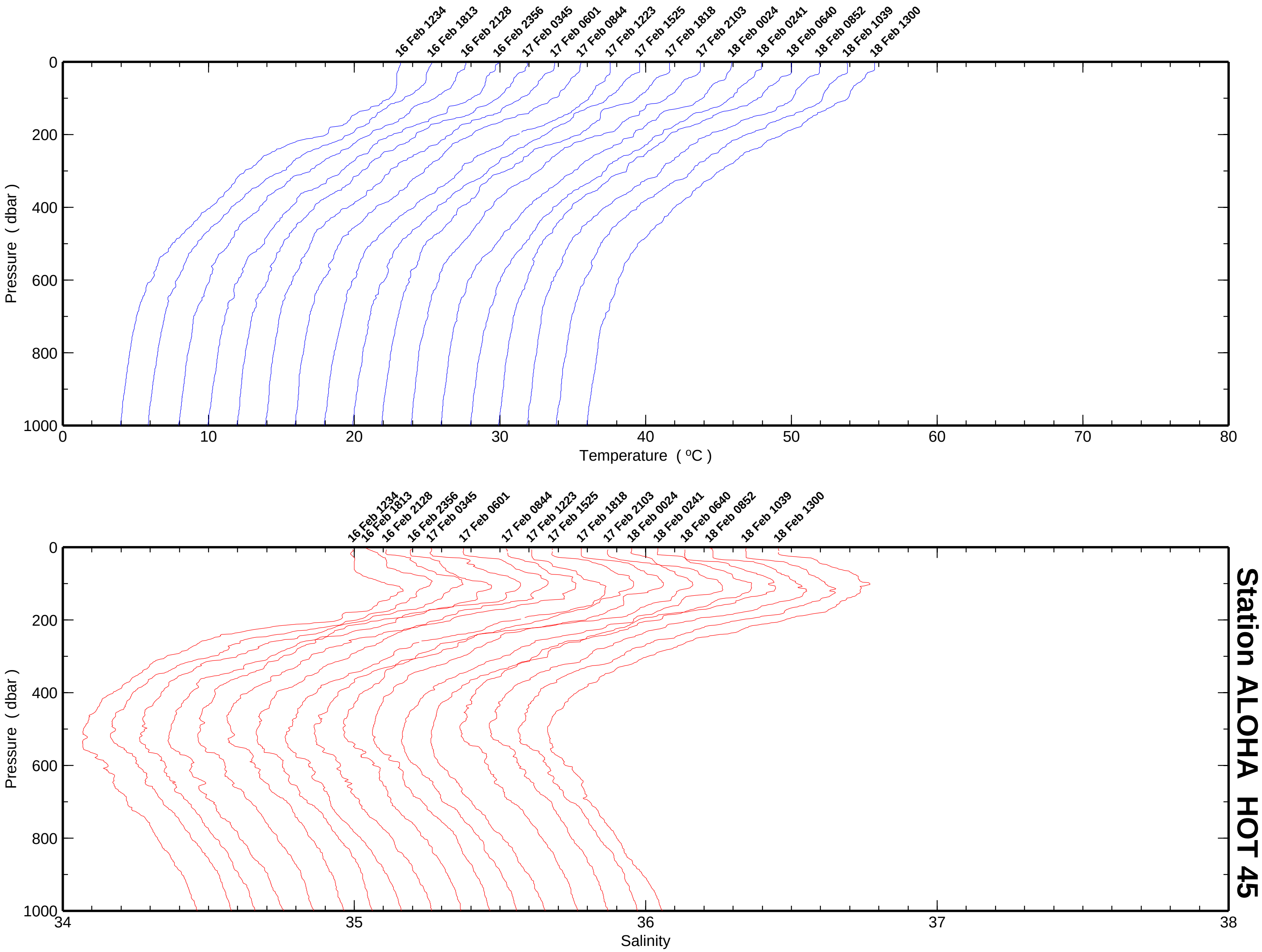

Station ALOHA HOT 46

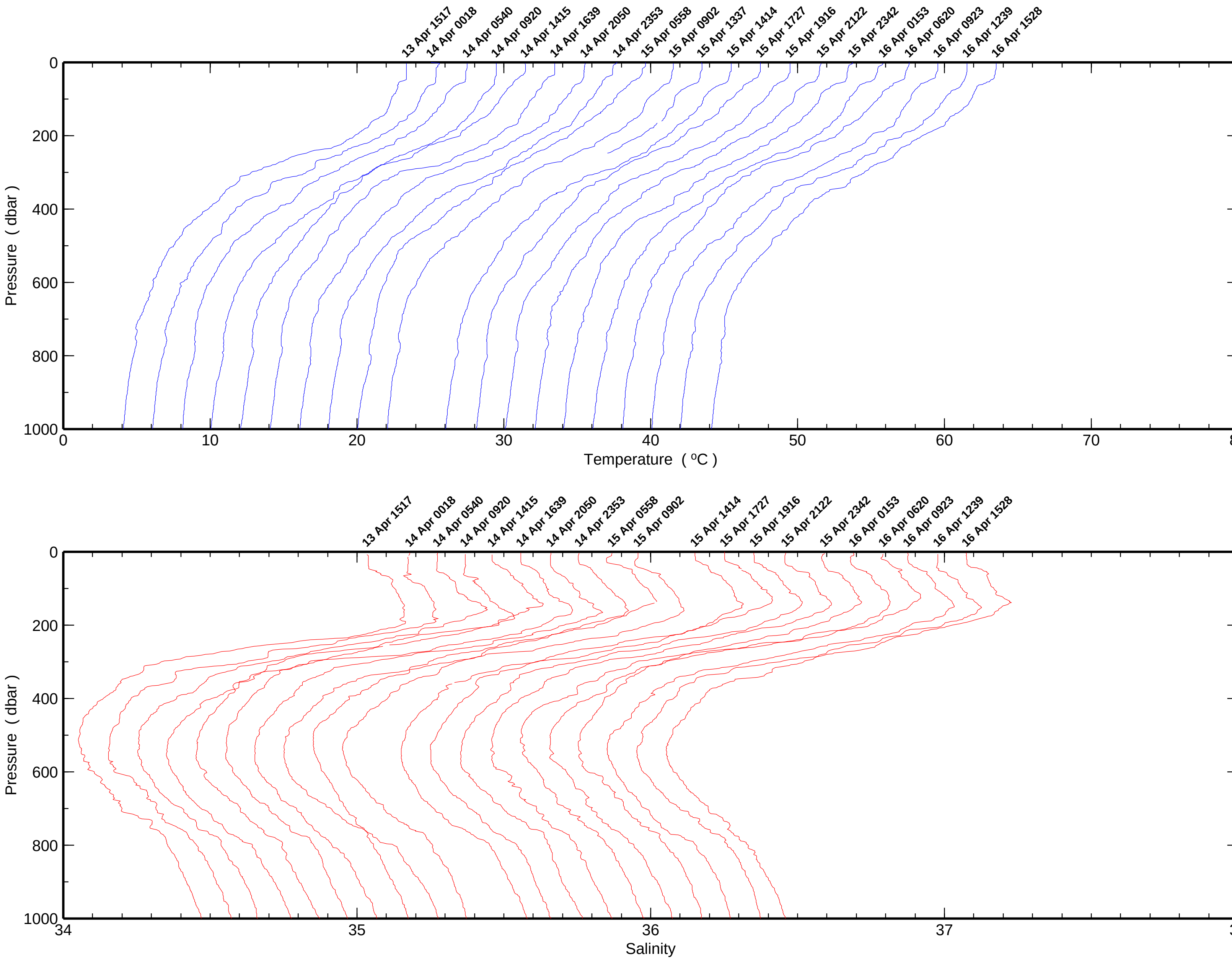

Figure 6.2.2c

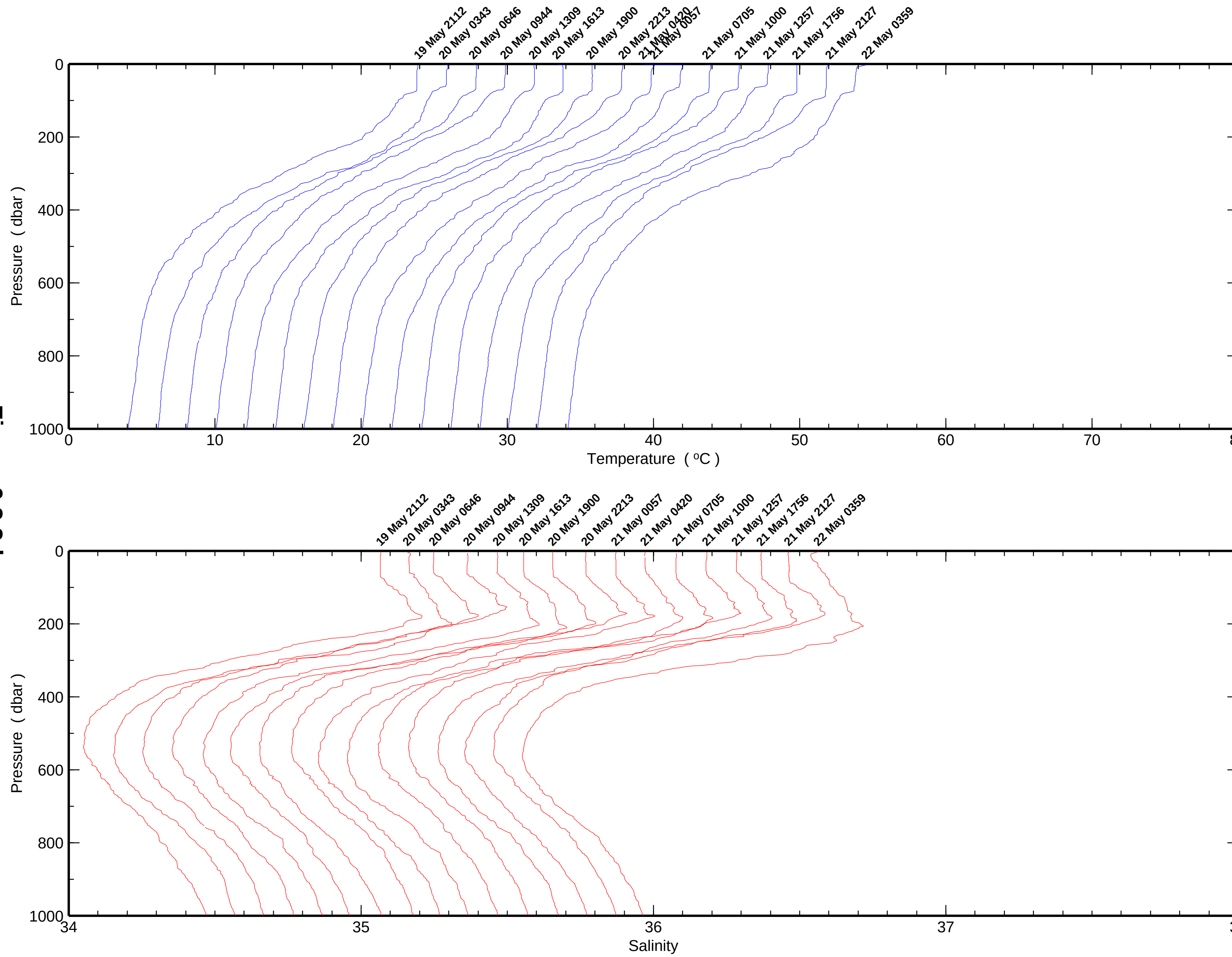
19 May 2112
20 May 0343
20 May 0646
20 May 0944
20 May 1309
20 May 1613
20 May 1900
20 May 2213
21 May 0420
21 May 0057
21 May 0705
21 May 1000
21 May 1257
21 May 1756
21 May 2127
22 May 0359
Pressure (dbar)
Temperature (ºC)
0
200
400
600
800
1000
0
10
20
30
40
50
60
70
80
19 May 2112
20 May 0343
20 May 0646
20 May 0944
20 May 1309
20 May 1613
20 May 1900
20 May 2213
21 May 0057
21 May 0420
21 May 0705
21 May 1000
21 May 1257
21 May 1756
21 May 2127
22 May 0359
Pressure (dbar)
Salinity
34
35
36
37
38

Figure 6.2.2d

Figure 6.2.2e

Station ALOHA HOT 49

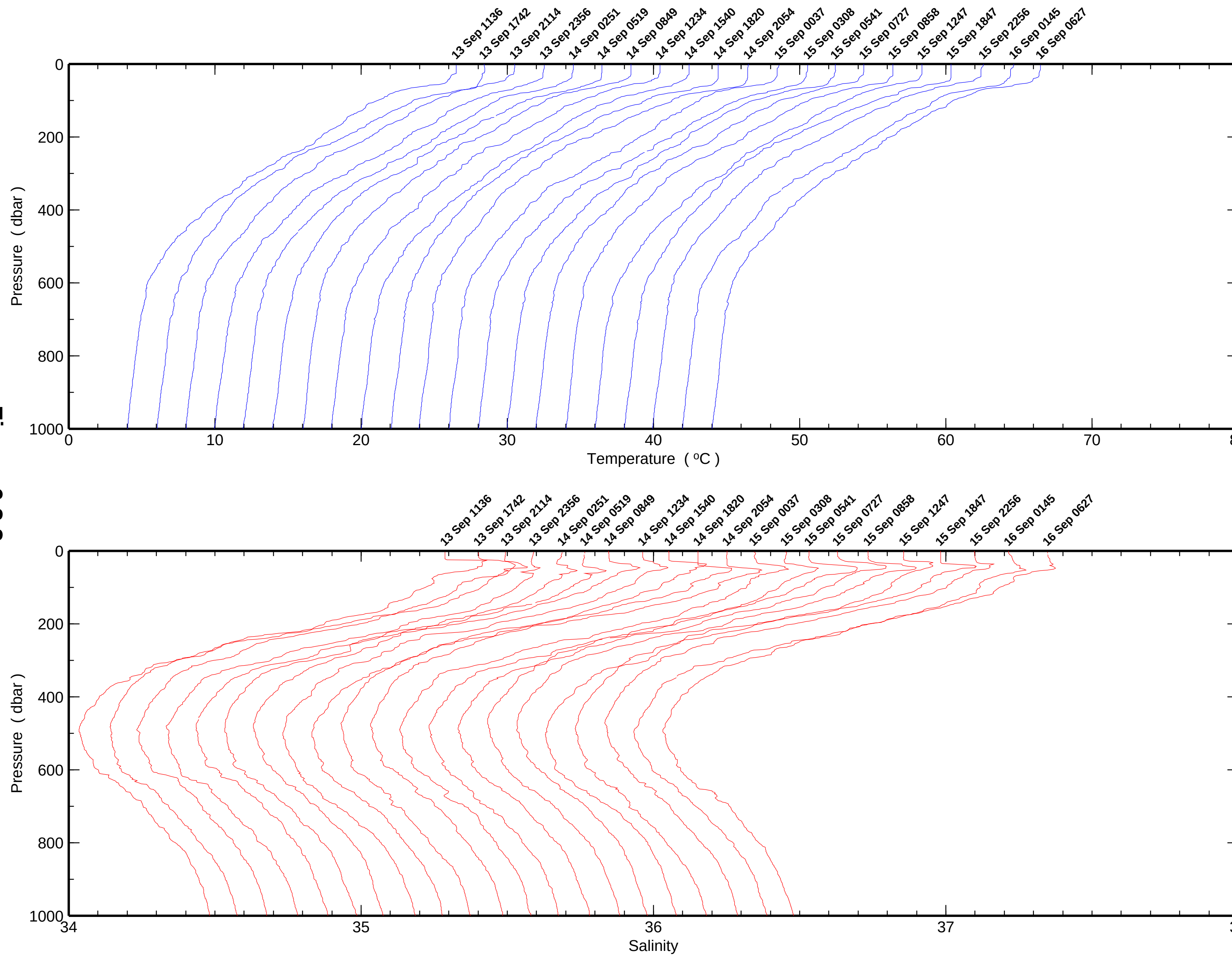

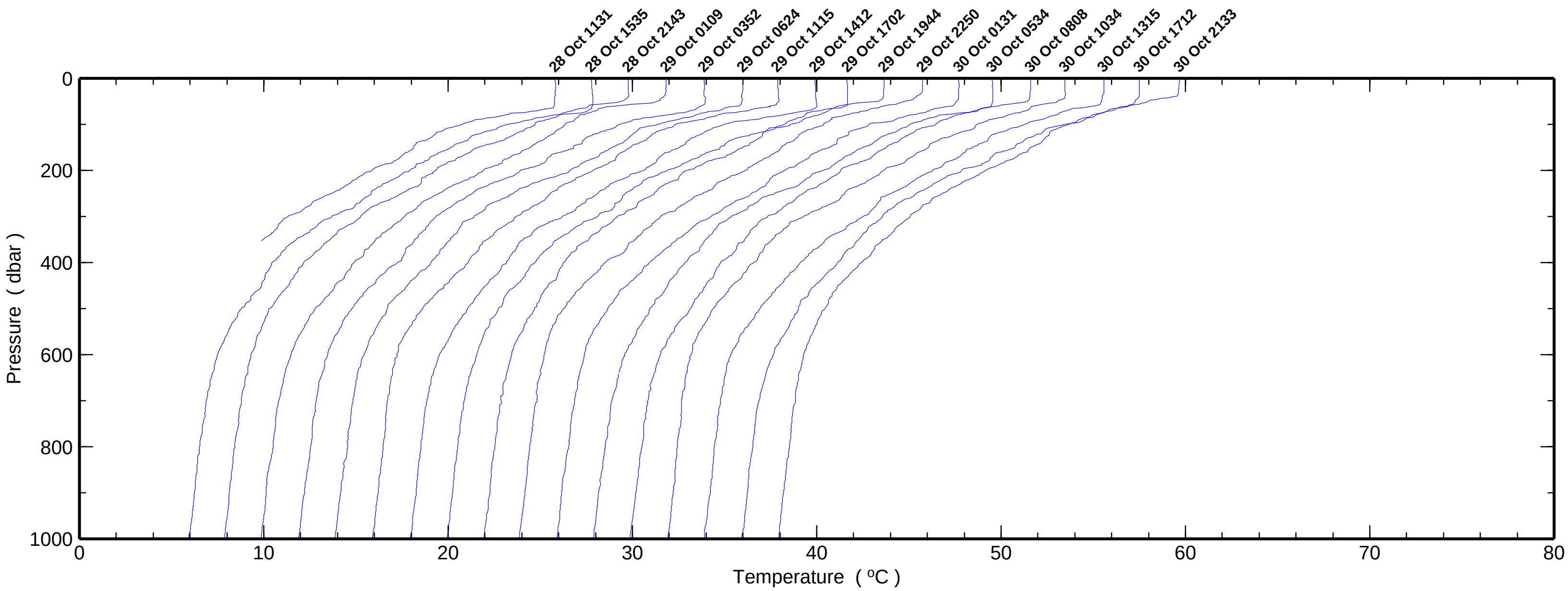

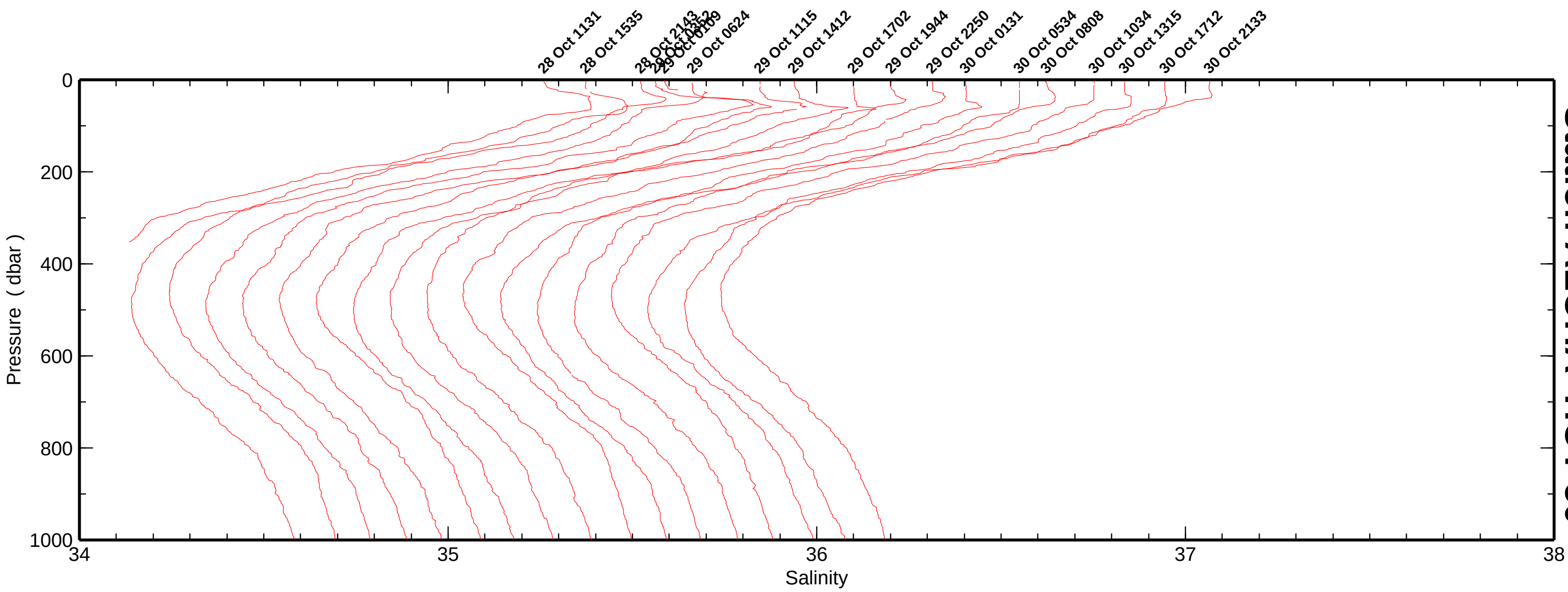

Figure 6.2.2f

Station ALOHA HOT 50

Kahe Pt. HOT 44

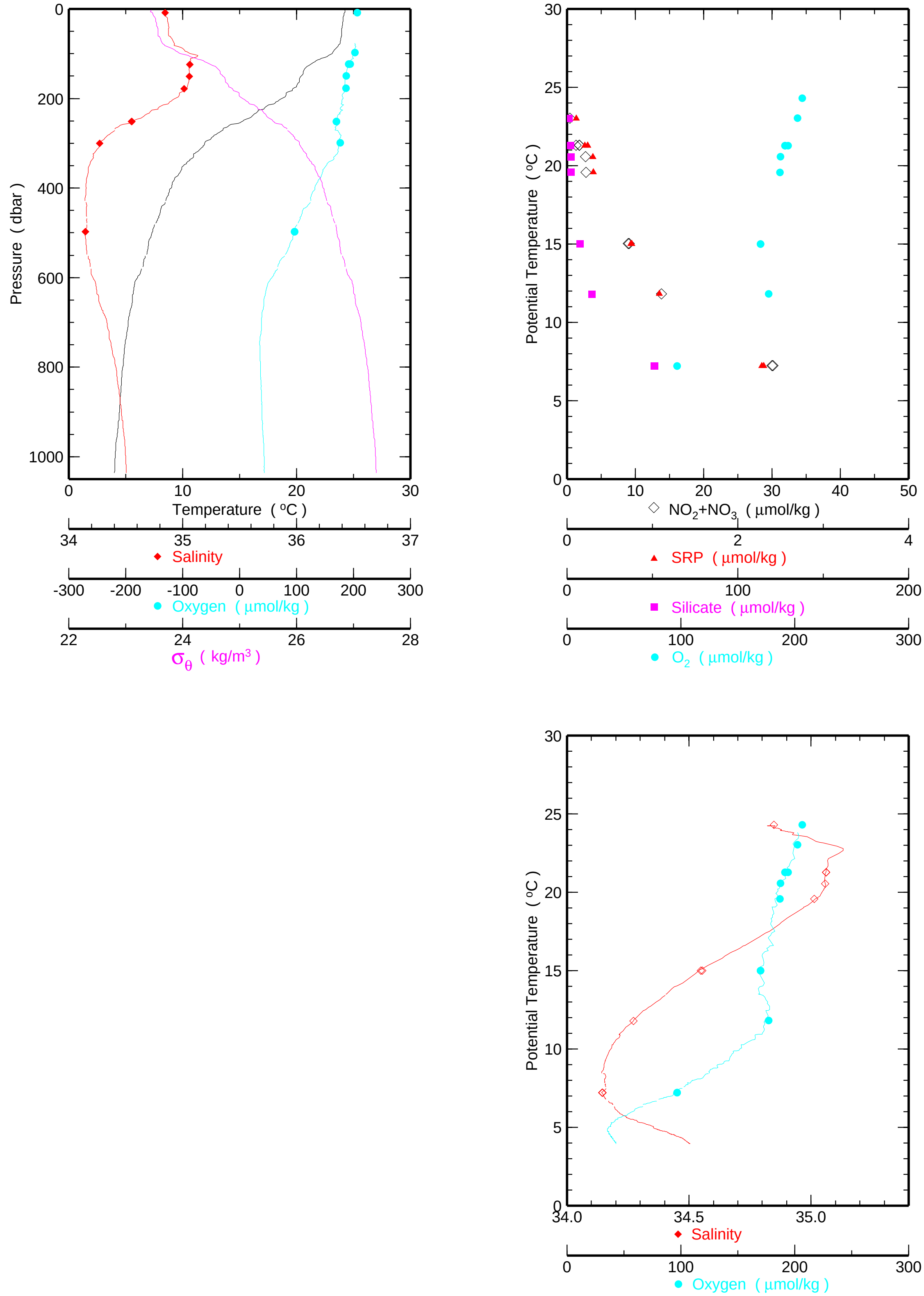

Figure 6.2.3a

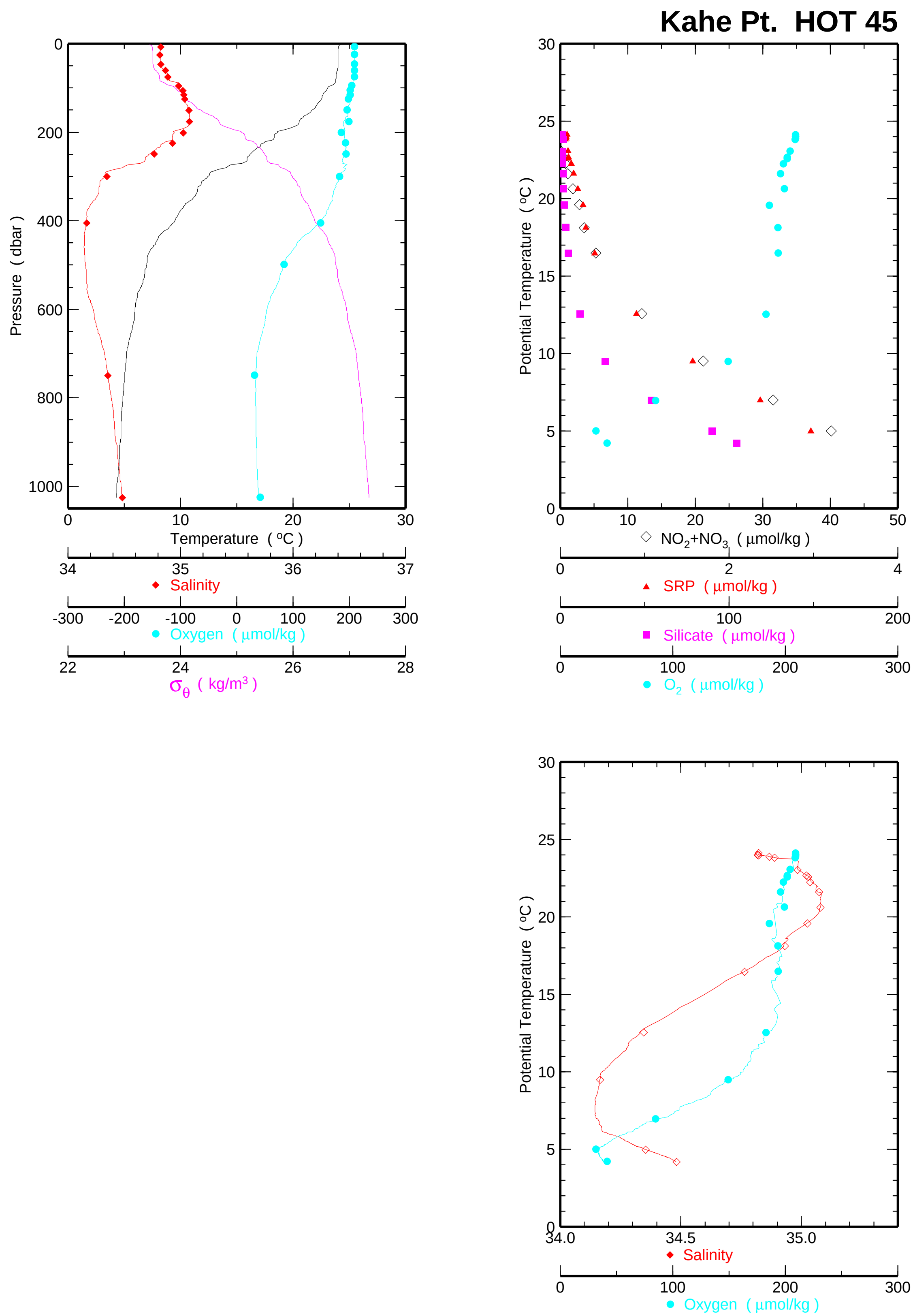

Kahe Pt. HOT 45
Pressure (dbar)
Temperature (°C)
Salinity
Oxygen (µmol/kg)
σθ (kg/m³)
Potential Temperature (°C)
NO2+NO3 (µmol/kg)
SRP (µmol/kg)
Silicate (µmol/kg)
O2 (µmol/kg)
Potential Temperature (°C)
Salinity
Oxygen (µmol/kg)

Figure 6.2.3b

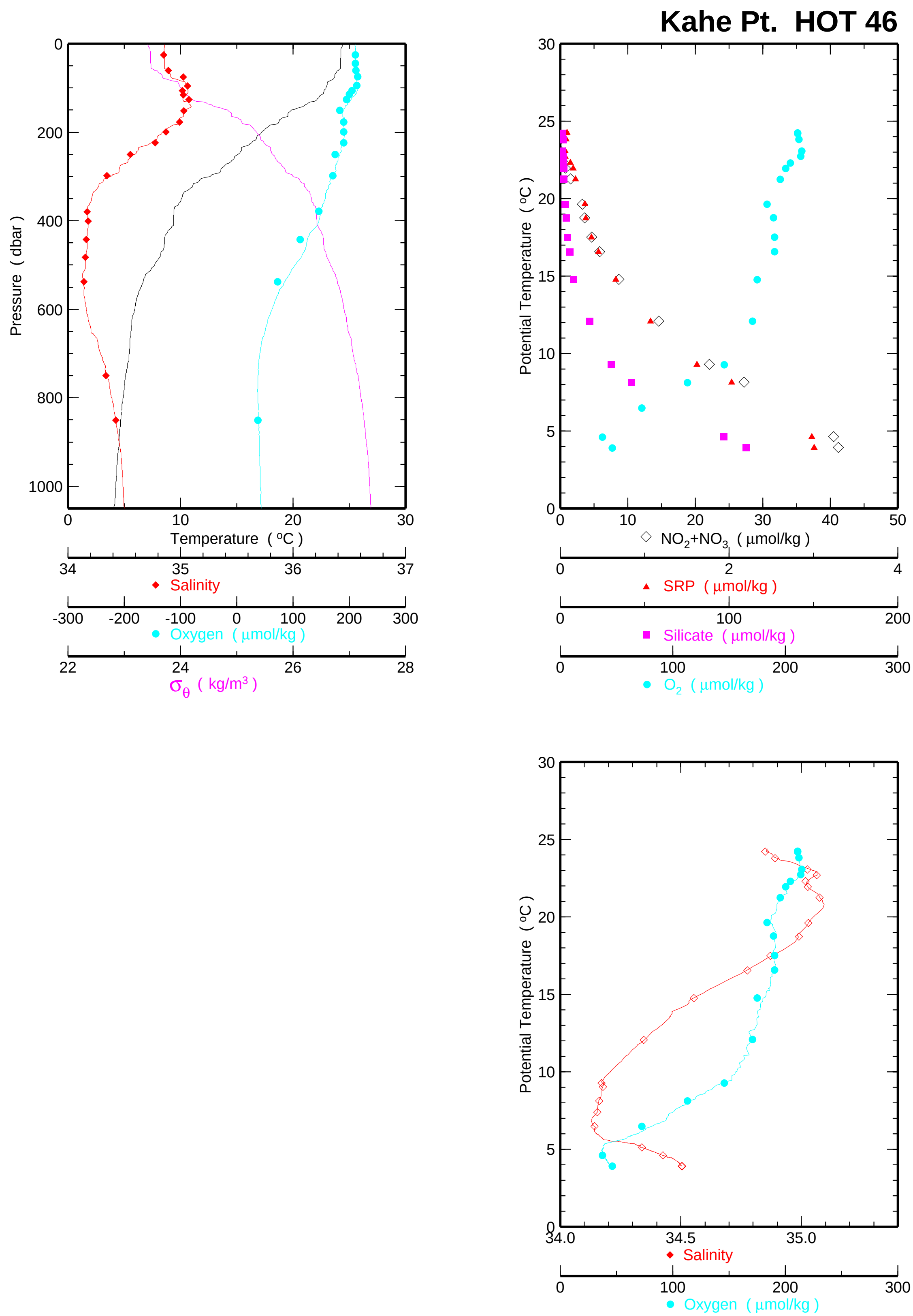

Kahe Pt. HOT 46
Pressure (dbar)
Temperature (°C)
Salinity
Oxygen (µmol/kg)
σ_θ (kg/m^3)
Potential Temperature (°C)
NO_2+NO_3 (µmol/kg)
SRP (µmol/kg)
Silicate (µmol/kg)
O_2 (µmol/kg)
Potential Temperature (°C)
Salinity
Oxygen (µmol/kg)

Figure 6.2.3c

Kahe Pt. HOT 47

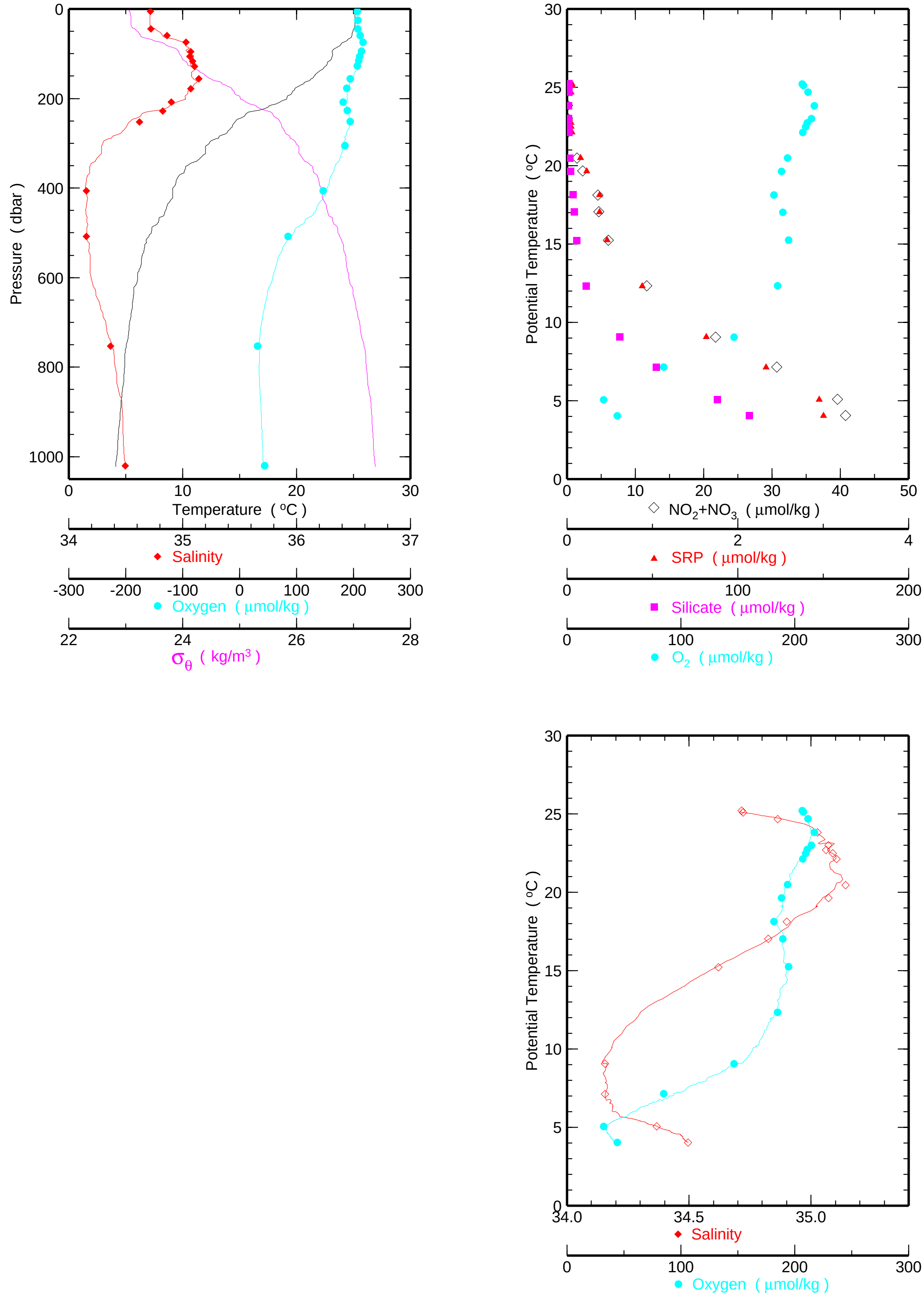

Figure 6.2.3d

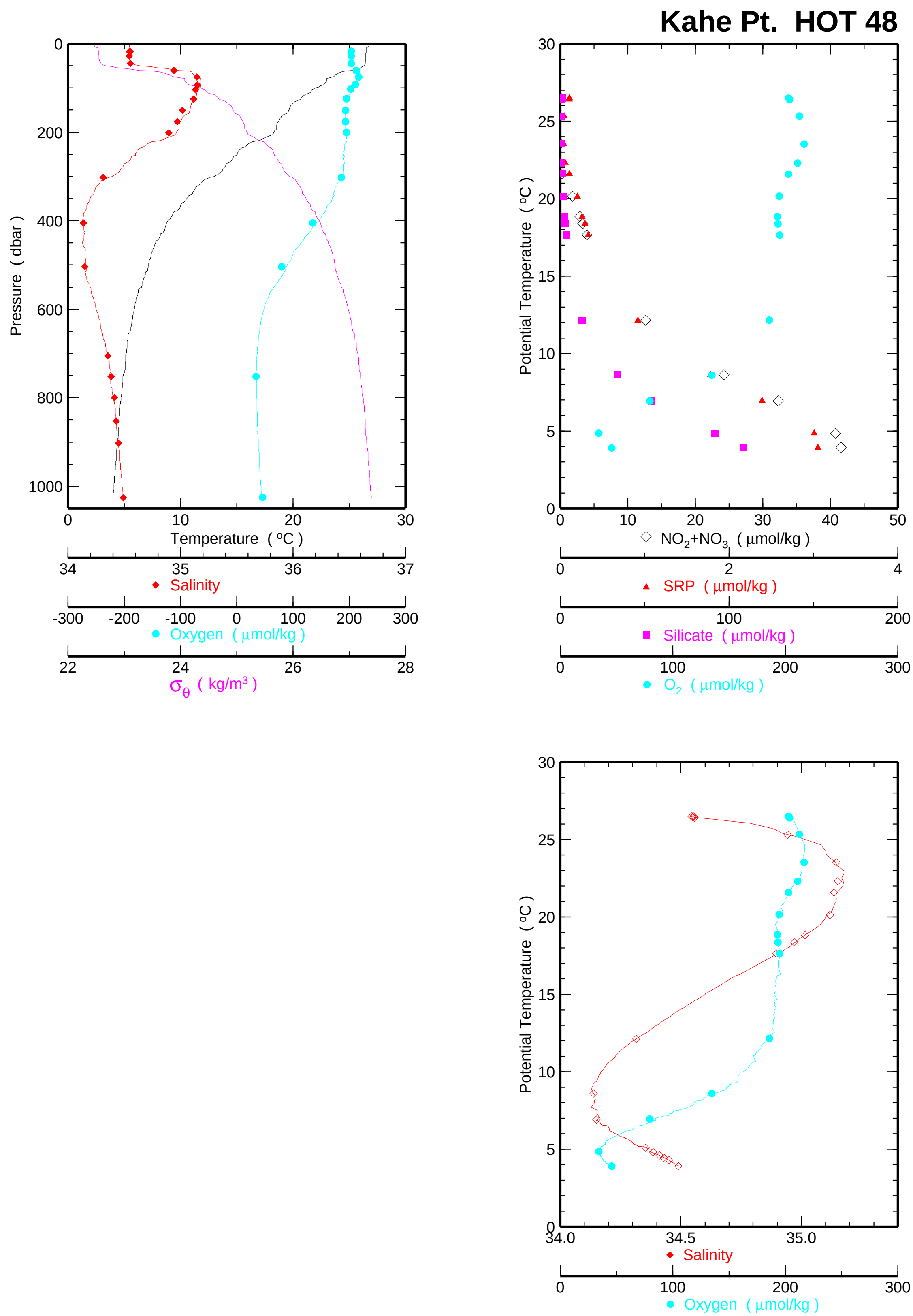

Kahe Pt. HOT 48
Pressure (dbar)
Temperature (°C)
Salinity
Oxygen (µmol/kg)
σθ (kg/m³)
Potential Temperature (°C)
NO2+NO3 (µmol/kg)
SRP (µmol/kg)
Silicate (µmol/kg)
O2 (µmol/kg)
Potential Temperature (°C)
Salinity
Oxygen (µmol/kg)

Figure 6.2.3e

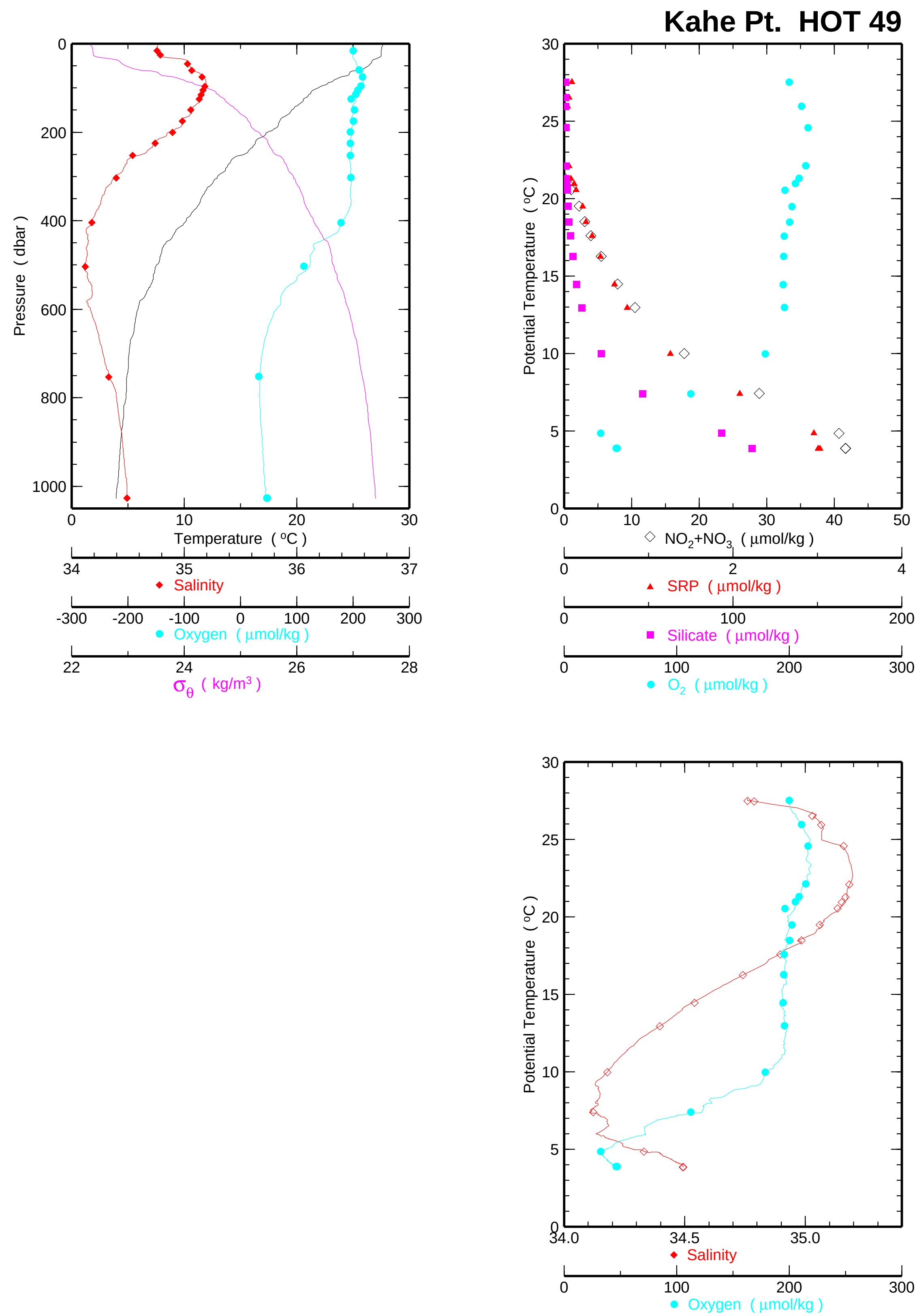
Kahe Pt. HOT 49
Pressure (dbar)
Temperature (ºC)
Salinity
Oxygen (µmol/kg)
σθ (kg/m3)
Potential Temperature (ºC)
NO2+NO3 (µmol/kg)
SRP (µmol/kg)
Silicate (µmol/kg)
O2 (µmol/kg)
Potential Temperature (ºC)
Salinity
Oxygen (µmol/kg)

Figure 6.2.3f

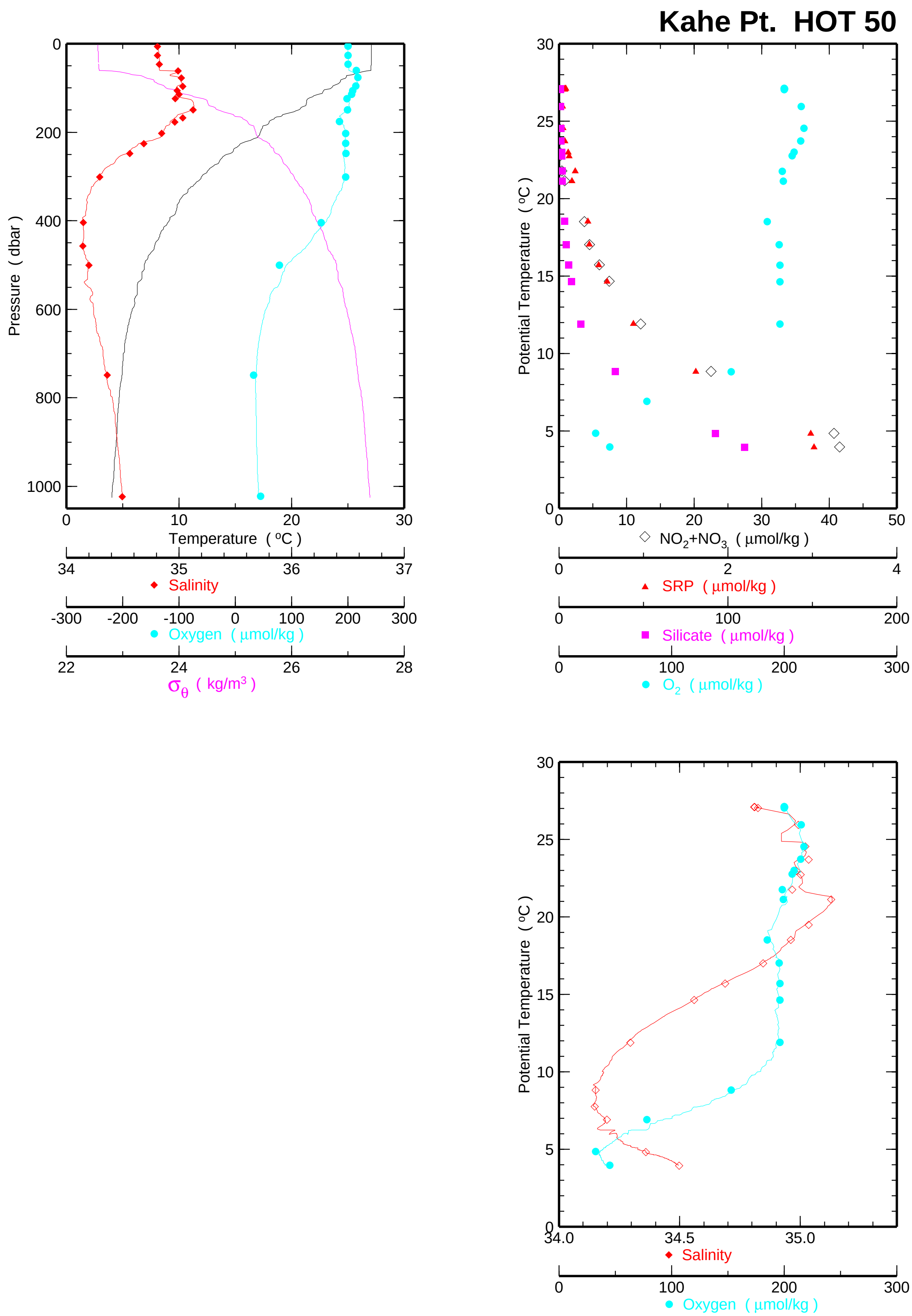
Kahe Pt. HOT 50
Pressure (dbar)
Temperature (ºC)
Salinity
Oxygen (µmol/kg)
σθ (kg/m3)
Potential Temperature (ºC)
NO2+NO3 (µmol/kg)
SRP (µmol/kg)
Silicate (µmol/kg)
O2 (µmol/kg)
Potential Temperature (ºC)
Salinity
Oxygen (µmol/kg)

Figure 6.2.3g

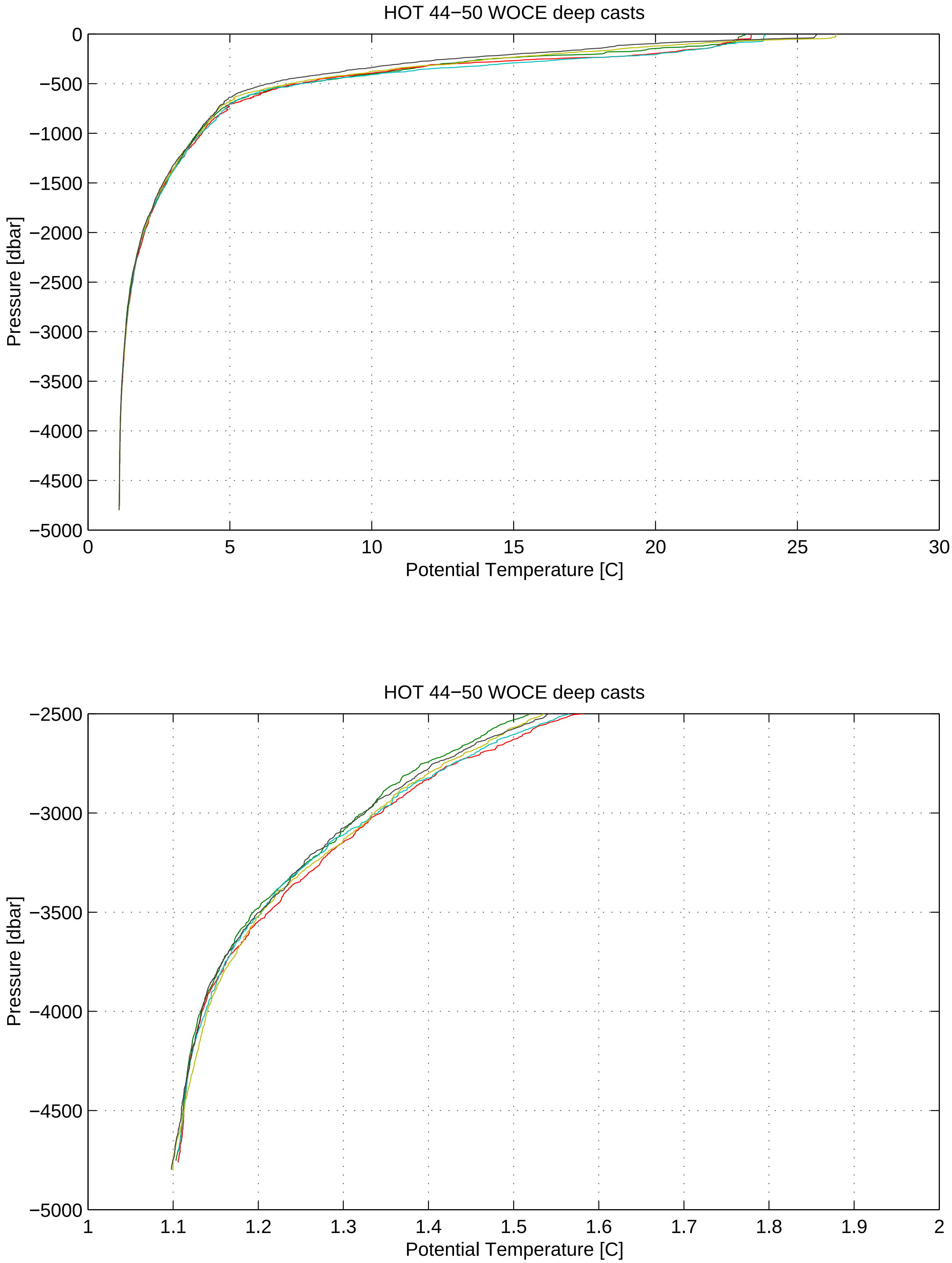

HOT 44−50 WOCE deep casts
Pressure [dbar]
Potential Temperature [C]
0
−500
−1000
−1500
−2000
−2500
−3000
−3500
−4000
−4500
−5000
0
5
10
15
20
25
30
HOT 44−50 WOCE deep casts
Pressure [dbar]
Potential Temperature [C]
−2500
−3000
−3500
−4000
−4500
−5000
1
1.1
1.2
1.3
1.4
1.5
1.6
1.7
1.8
1.9
2

Figure 6.2.4

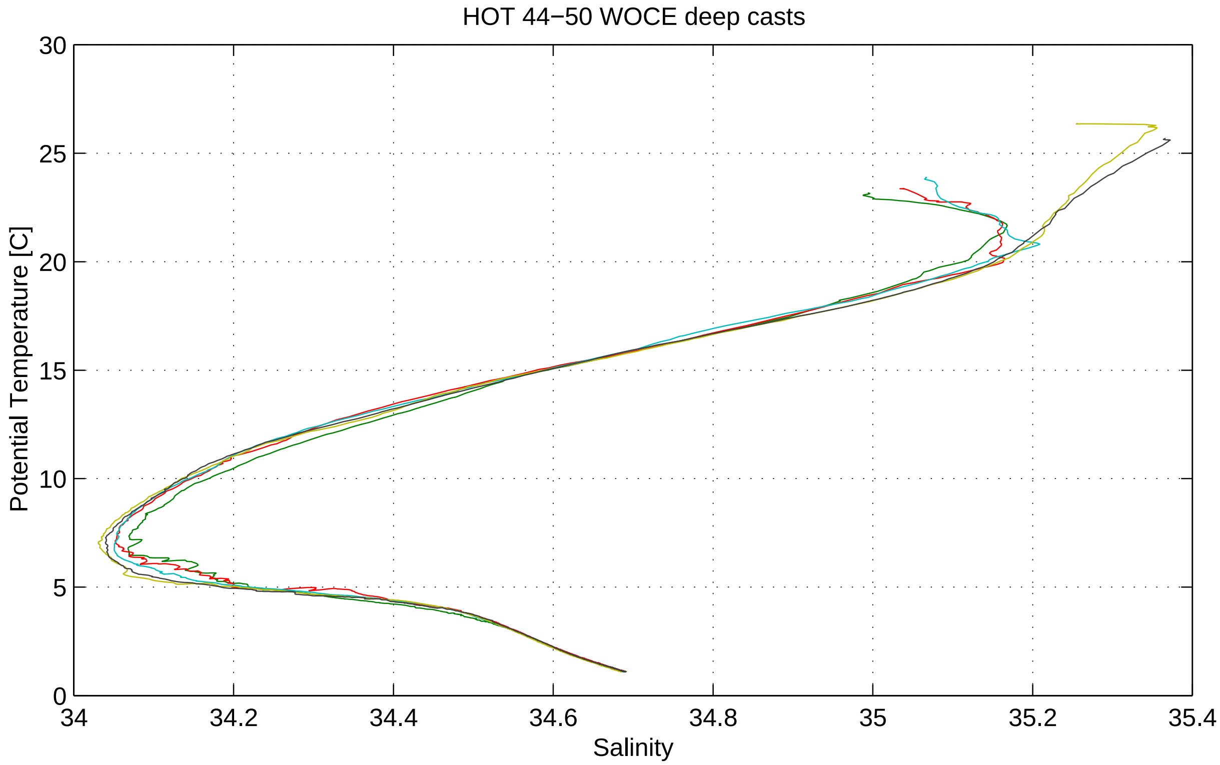

HOT 44−50 WOCE deep casts
Potential Temperature [C]
Salinity
30
25
20
15
10
5
0
34
34.2
34.4
34.6
34.8
35
35.2
35.4

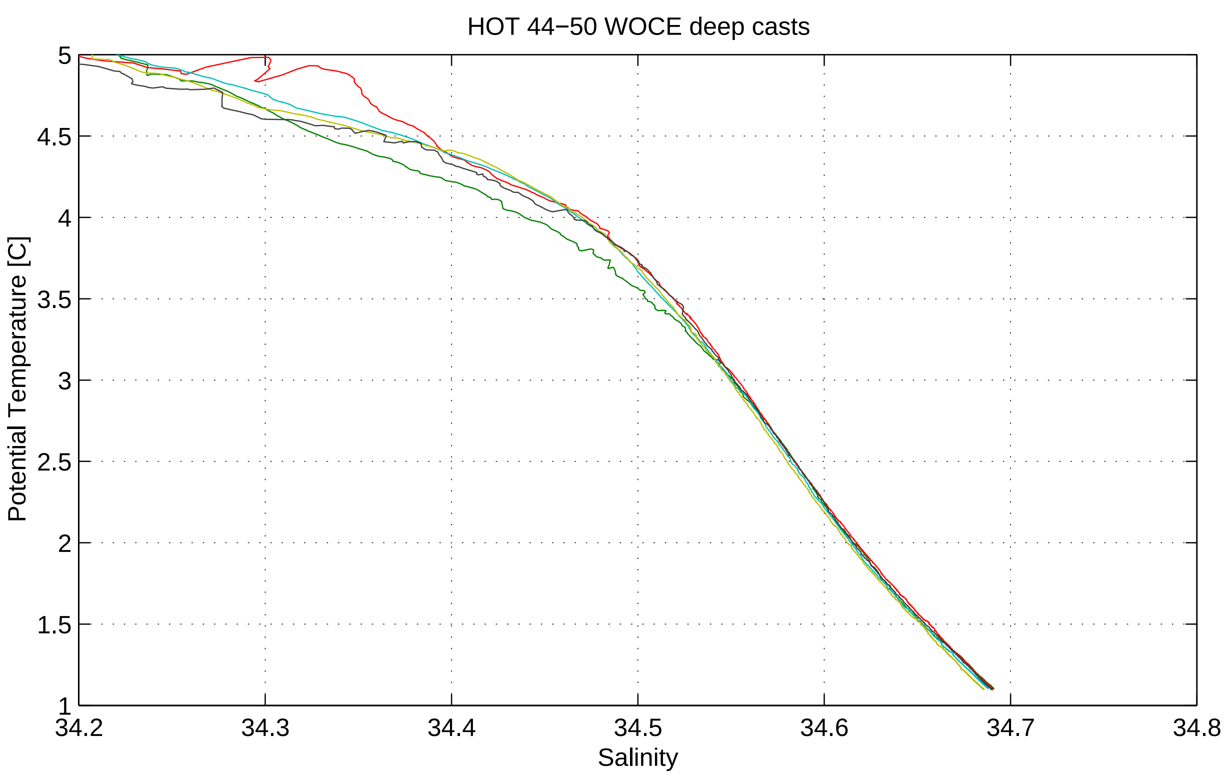

HOT 44−50 WOCE deep casts
Potential Temperature [C]
Salinity
5
4.5
4
3.5
3
2.5
2
1.5
1
34.2
34.3
34.4
34.5
34.6
34.7
34.8

Figure 6.2.5

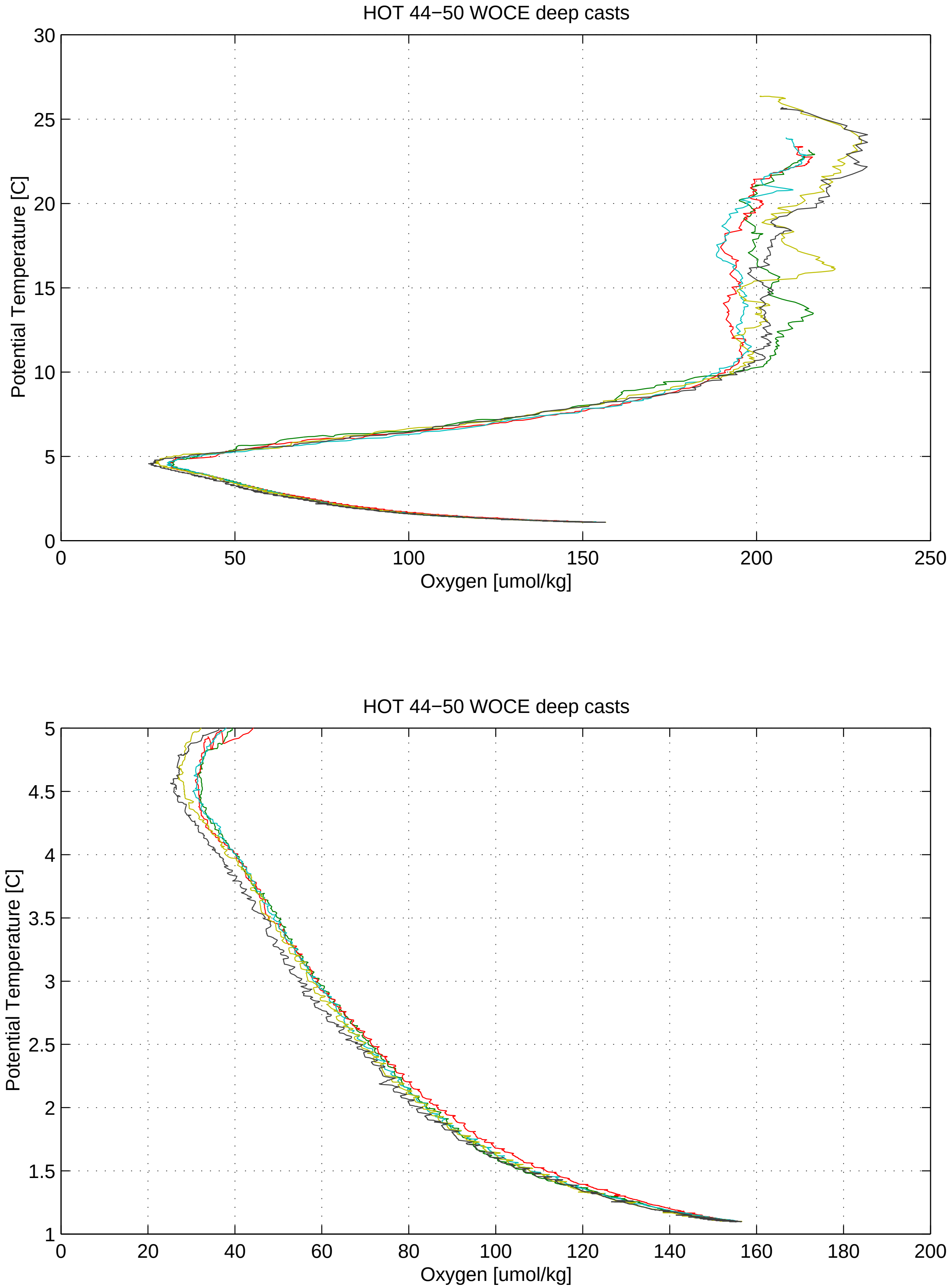

HOT 44−50 WOCE deep casts
Potential Temperature [C]
Oxygen [umol/kg]
30
25
20
15
10
5
0
0
50
100
150
200
250
HOT 44−50 WOCE deep casts
Potential Temperature [C]
Oxygen [umol/kg]
5
4.5
4
3.5
3
2.5
2
1.5
1
0
20
40
60
80
100
120
140
160
180
200

Figure 6.2.6

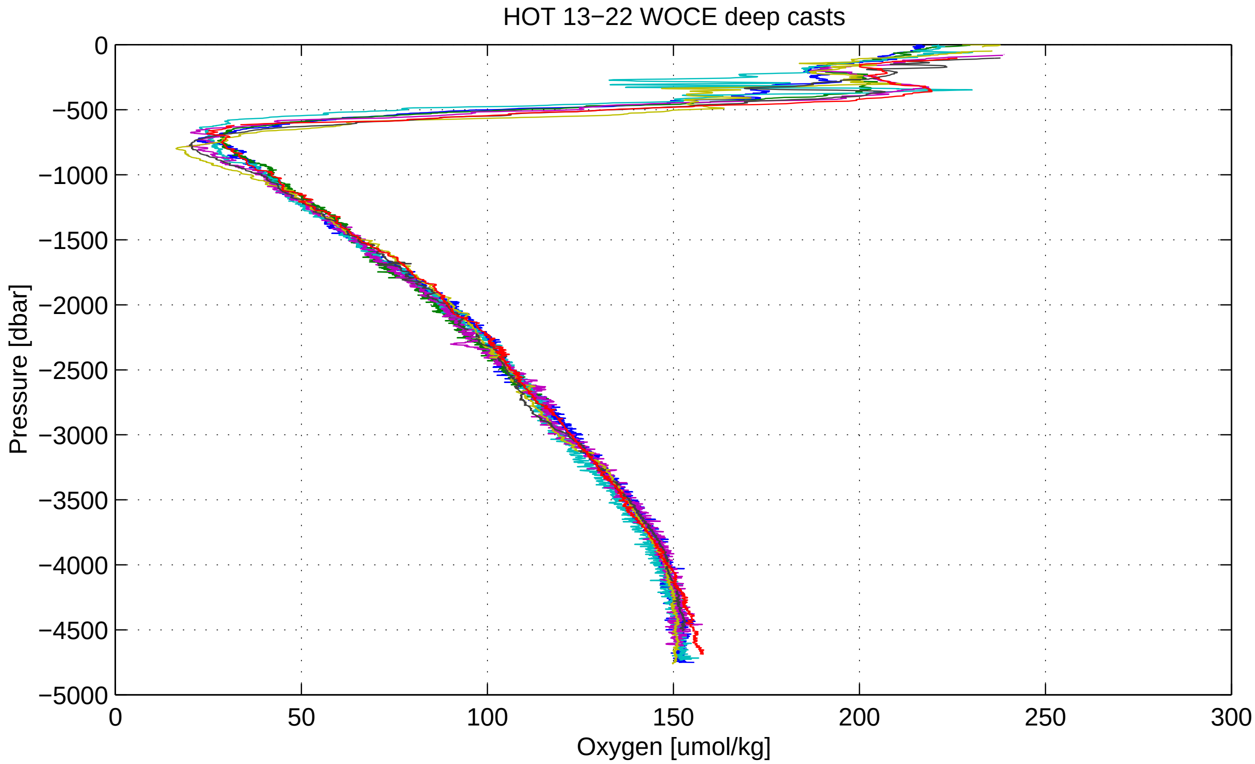
HOT 13−22 WOCE deep casts
Pressure [dbar]
Oxygen [umol/kg]
0
−500
−1000
−1500
−2000
−2500
−3000
−3500
−4000
−4500
−5000
0
50
100
150
200
250
300

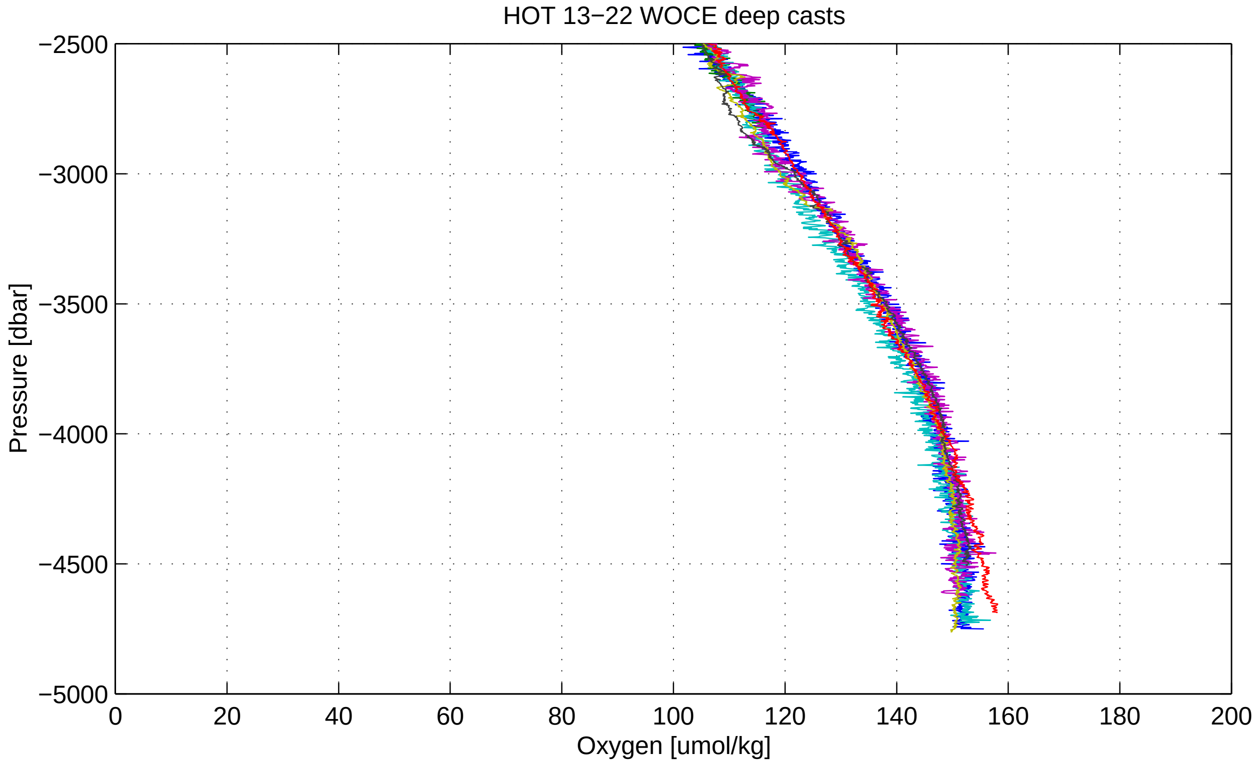
HOT 13−22 WOCE deep casts
Pressure [dbar]
Oxygen [umol/kg]
−2500
−3000
−3500
−4000
−4500
−5000
0
20
40
60
80
100
120
140
160
180
200

6.3. Contour Plots

Figures 6.3.1-14 show data from HOT 1-50. Cruise is indicated by a diamond symbol along the time axis. Data are the average of all casts for each cruise

Figure 6.3.1: Potential temperature measured by CTD versus pressure.

Figure 6.3.2: Potential density, calculated from CTD measurements of pressure, temperature and salinity versus pressure.

Figure 6.3.3: Salinity measured by CTD plotted versus pressure.

Figure 6.3.4: Salinity measured by CTD versus potential density. The average density of the sea surface for each cruise is connected by a heavy line.

Figure 6.3.5: Salinity from discrete water samples plotted versus pressure. Locations of bottle closures are indicated by solid circles.

Figure 6.3.6: Salinity from discrete water samples plotted versus potential density. The average density of the sea surface for each cruise is connected by a heavy line. Locations of bottle closures are indicated by solid circles.

Figure 6.3.7: Oxygen from discrete water samples plotted versus pressure. Locations of bottle closures are indicated by solid circles.

Figure 6.3.8: Oxygen from discrete water samples plotted versus potential density. The average density of the sea surface for each cruise is connected by a heavy line. Locations of bottle closures are indicated by solid circles.

Figure 6.3.9: Nitrate plus nitrite from discrete water samples plotted versus pressure. Locations of bottle closures are indicated by solid circles.

Figure 6.3.10: Nitrate plus nitrite from discrete water samples plotted versus potential density. The average density of the sea surface for each cruise is connected by a heavy line. Locations of bottle closures are indicated by solid circles.

Figure 6.3.11: Phosphate from discrete water samples plotted versus pressure. Locations of bottle closures are indicated by solid circles.

Figure 6.3.12: Phosphate from discrete water samples plotted versus potential density. The average density of the sea surface for each cruise is connected by a heavy line. Locations of bottle closures are indicated by solid circles.

Figure 6.3.13: Silica from discrete water samples plotted versus pressure. Locations of bottle closures are indicated by solid circles.

Figure 6.3.14: Silica from discrete water samples plotted versus potential density. The average density of the sea surface for each cruise is connected by a heavy line. Locations of bottle closures are indicated by solid circles.

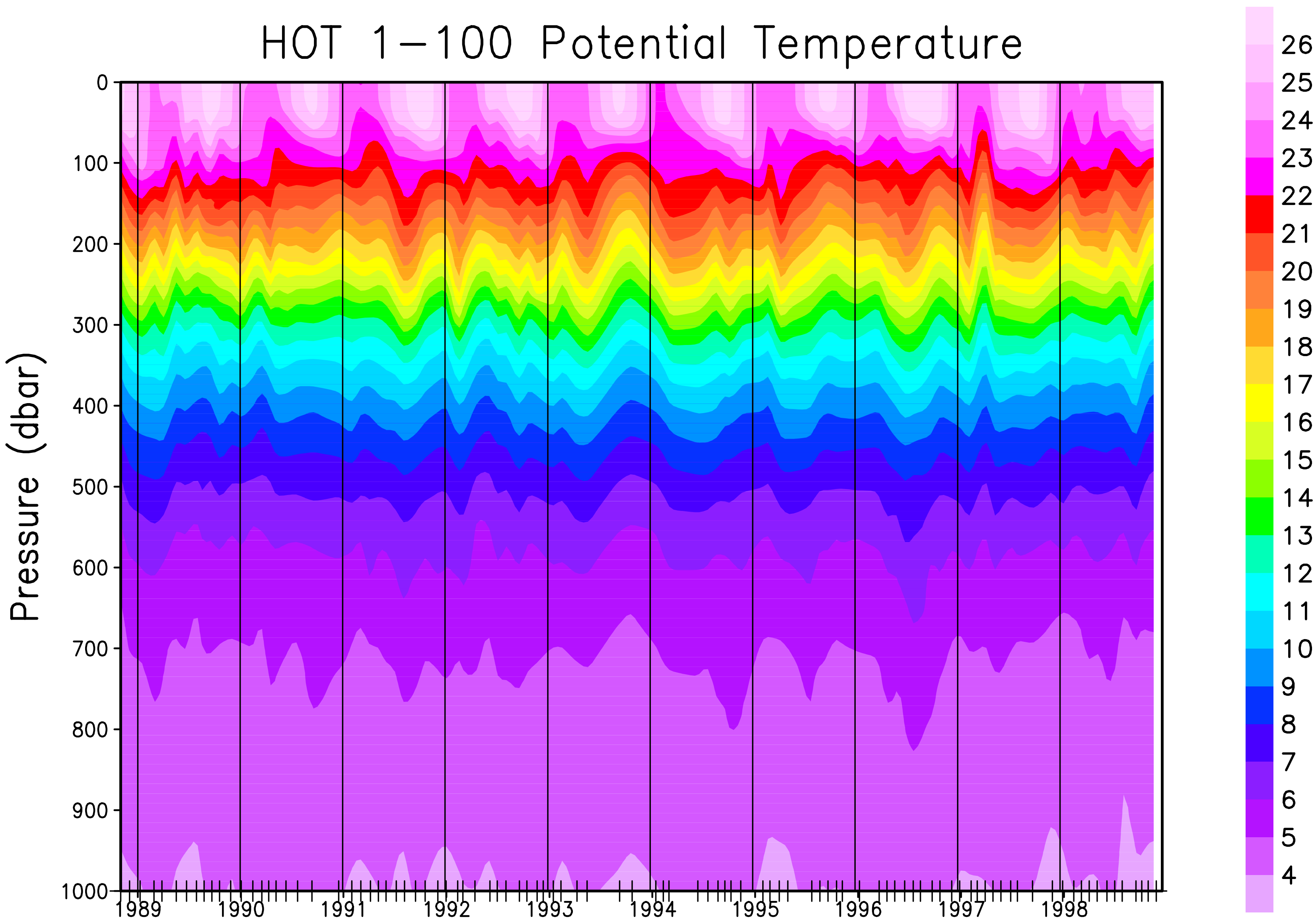

Figure 6.3.1: Contour plot of CTD potential temperature versus pressure for HOT cruises 1-100.

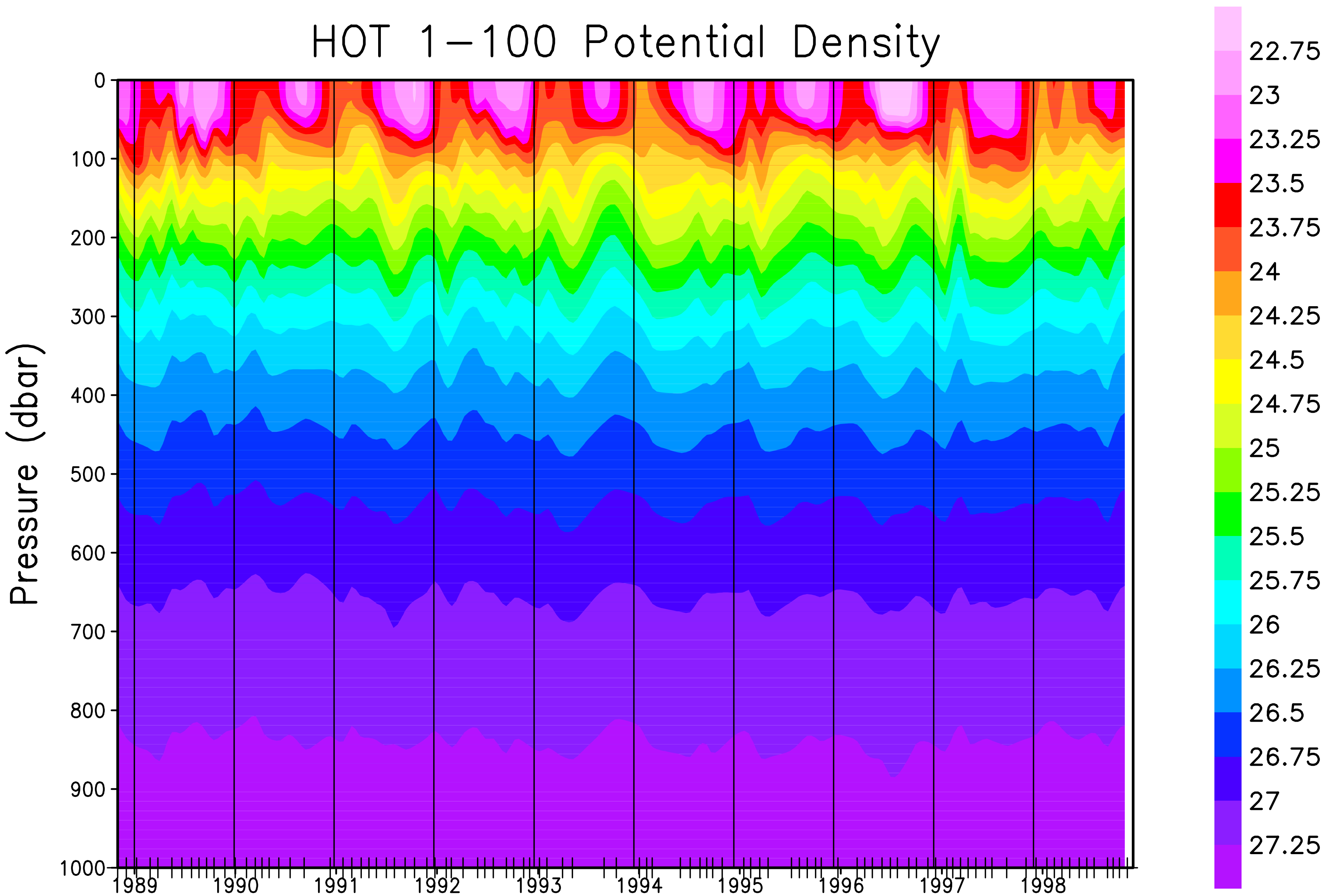

Figure 6.3.2: Contour plot of potential density (σ_θ), calculated from CTD pressure, temperature and salinity, versus pressure for HOT cruises 1-100.

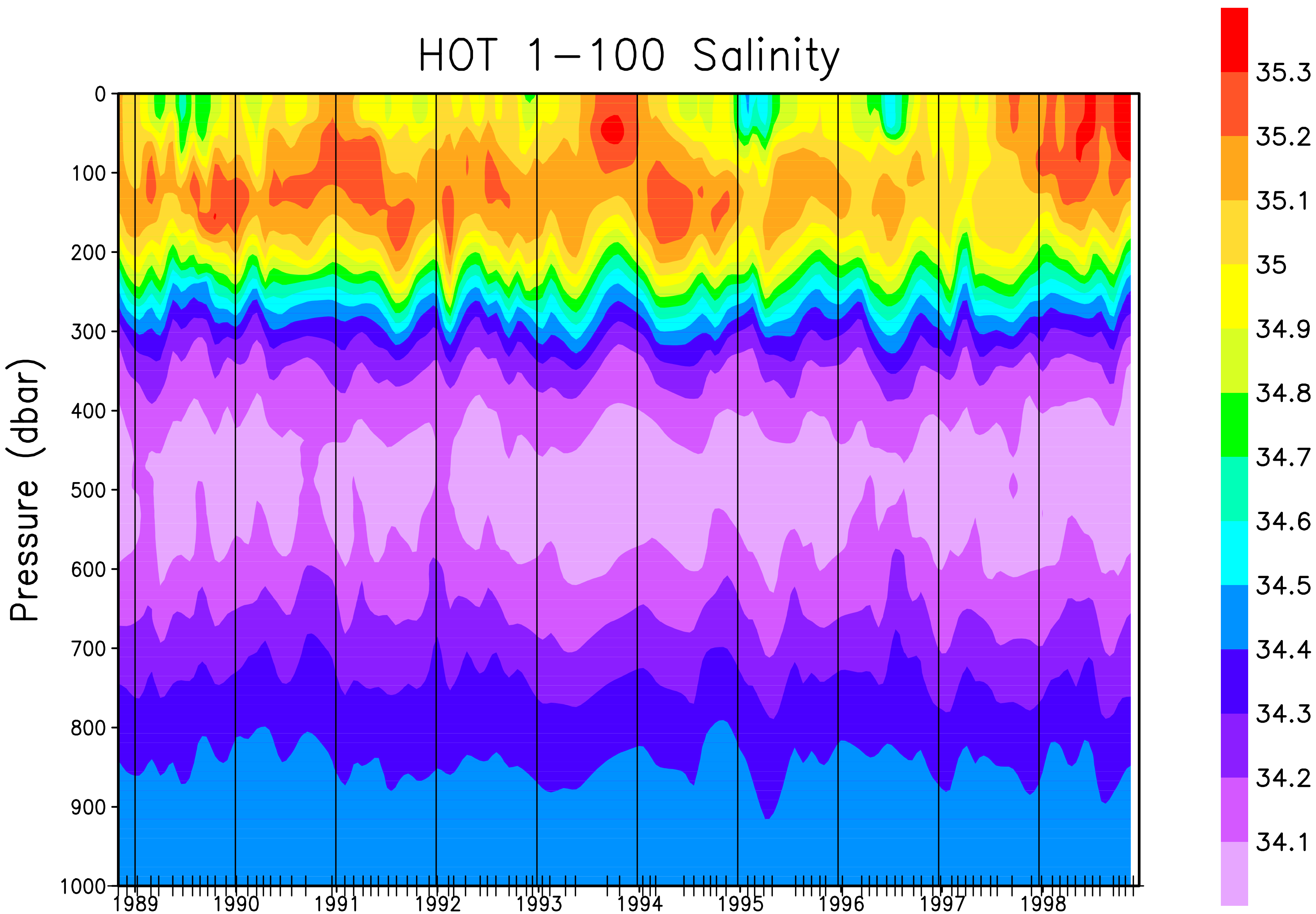

Figure 6.3.3: Contour plot of CTD salinity versus pressure for HOT cruises 1-100.

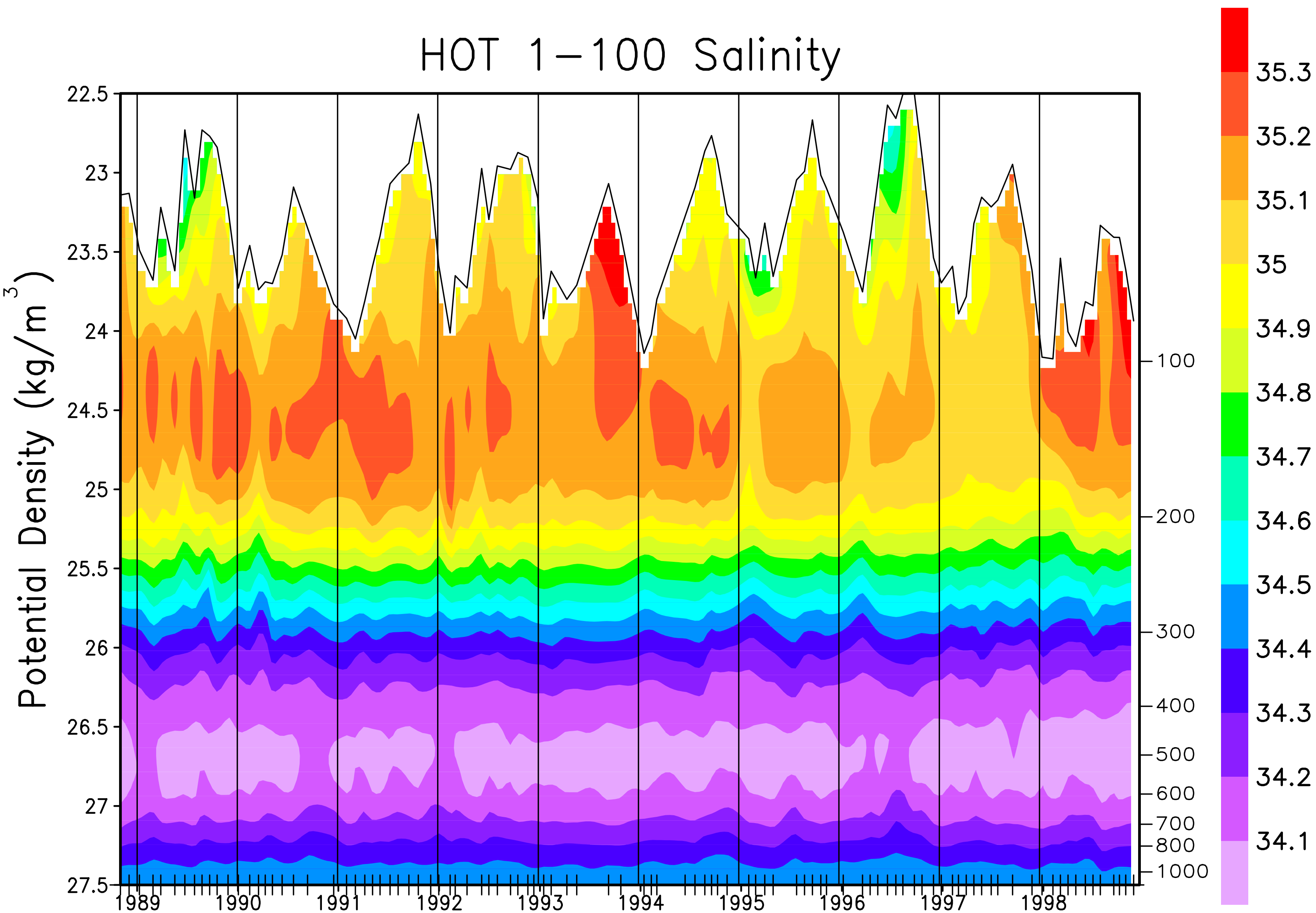

Figure 6.3.4: Contour plot of CTD salinity versus potential density (σ_θ) to 27.5 kg m^{-3} for HOT cruises 1-100. The average density of the sea surface is connected by the heavy line.

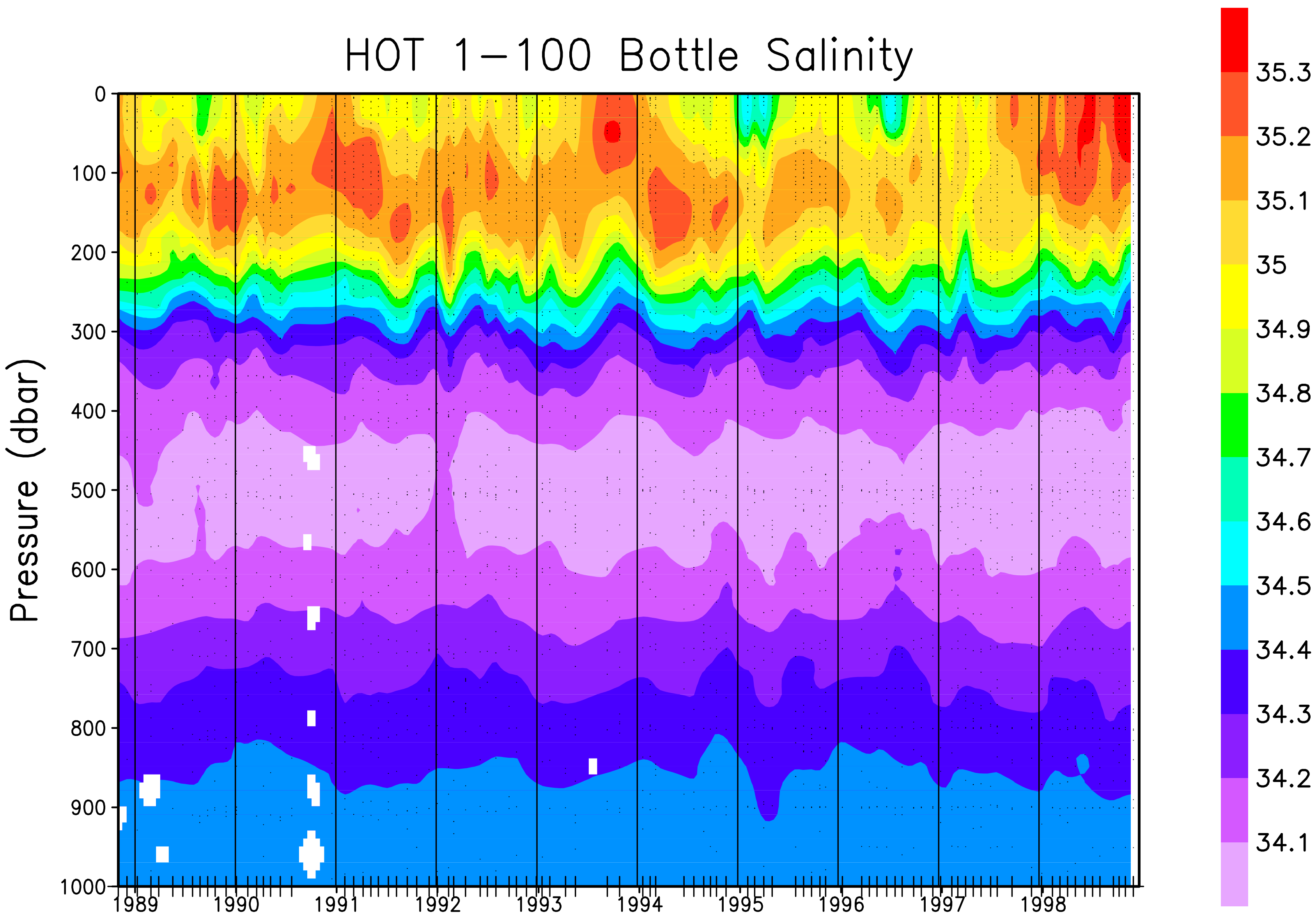

Figure 6.3.5: Contour plot of bottle salinity versus pressure for HOT cruises 1-100. Location of samples in the water column are indicated by the solid circles.

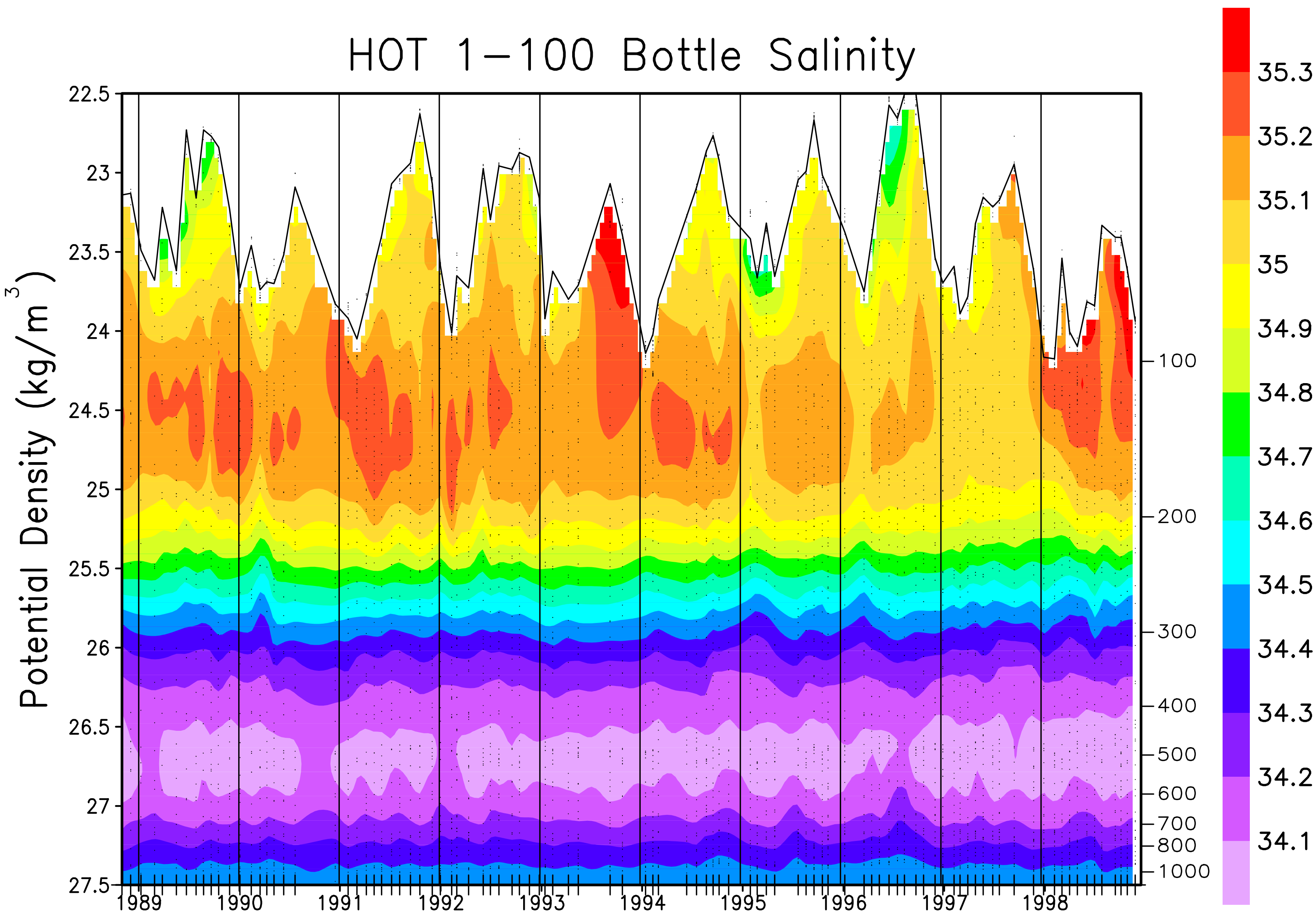

Figure 6.3.6: Contour plot of bottle salinity versus potential density (σ_θ)to 27.5 kg m^{-3} for HOT cruises 1-100. The average density of the sea surface is connected by the heavy line.

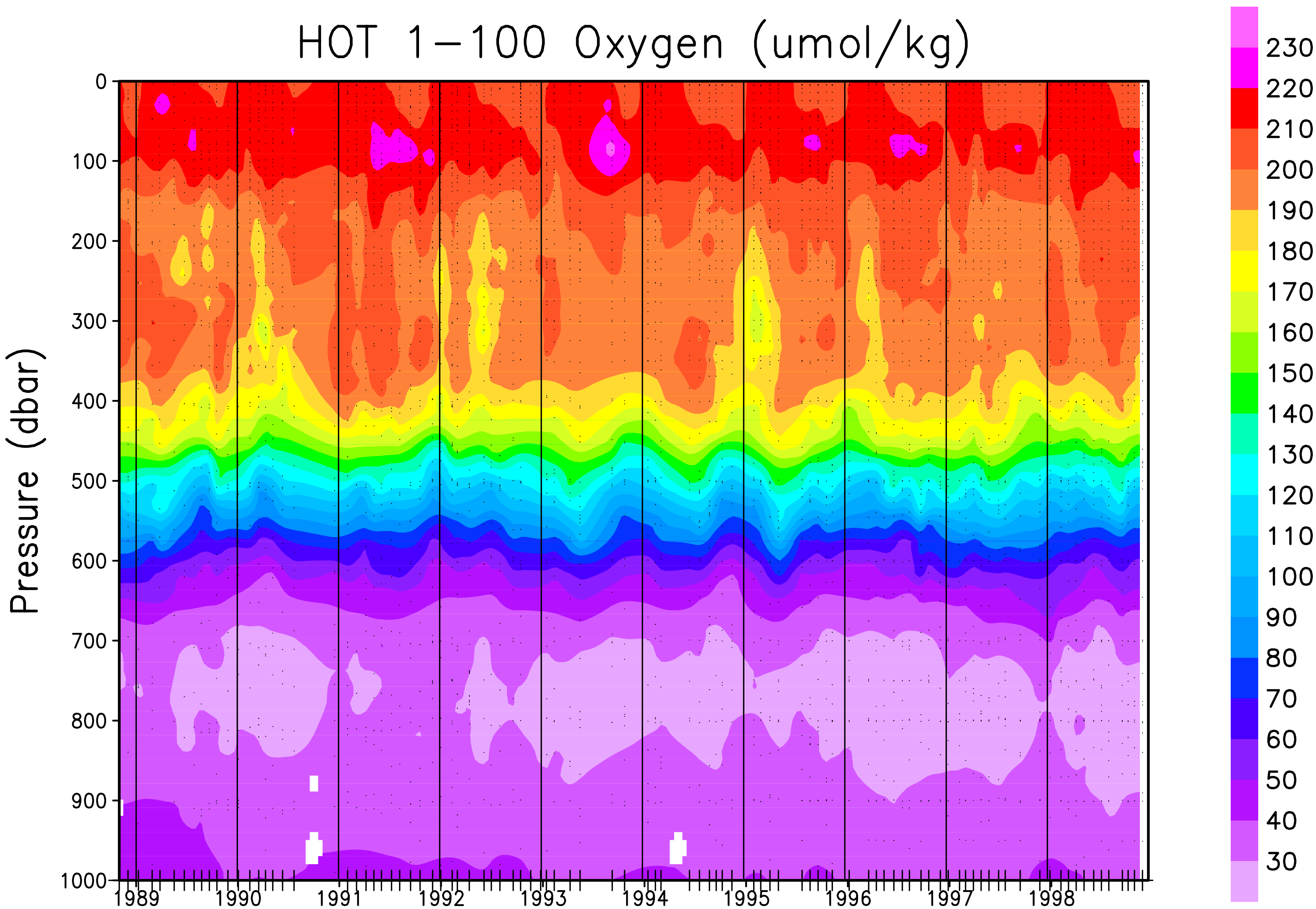

Figure 6.3.7: Contour plot of bottle oxygen versus pressure for HOT cruises 1-100. Location of samples in the water column are indicated by the solid circles.

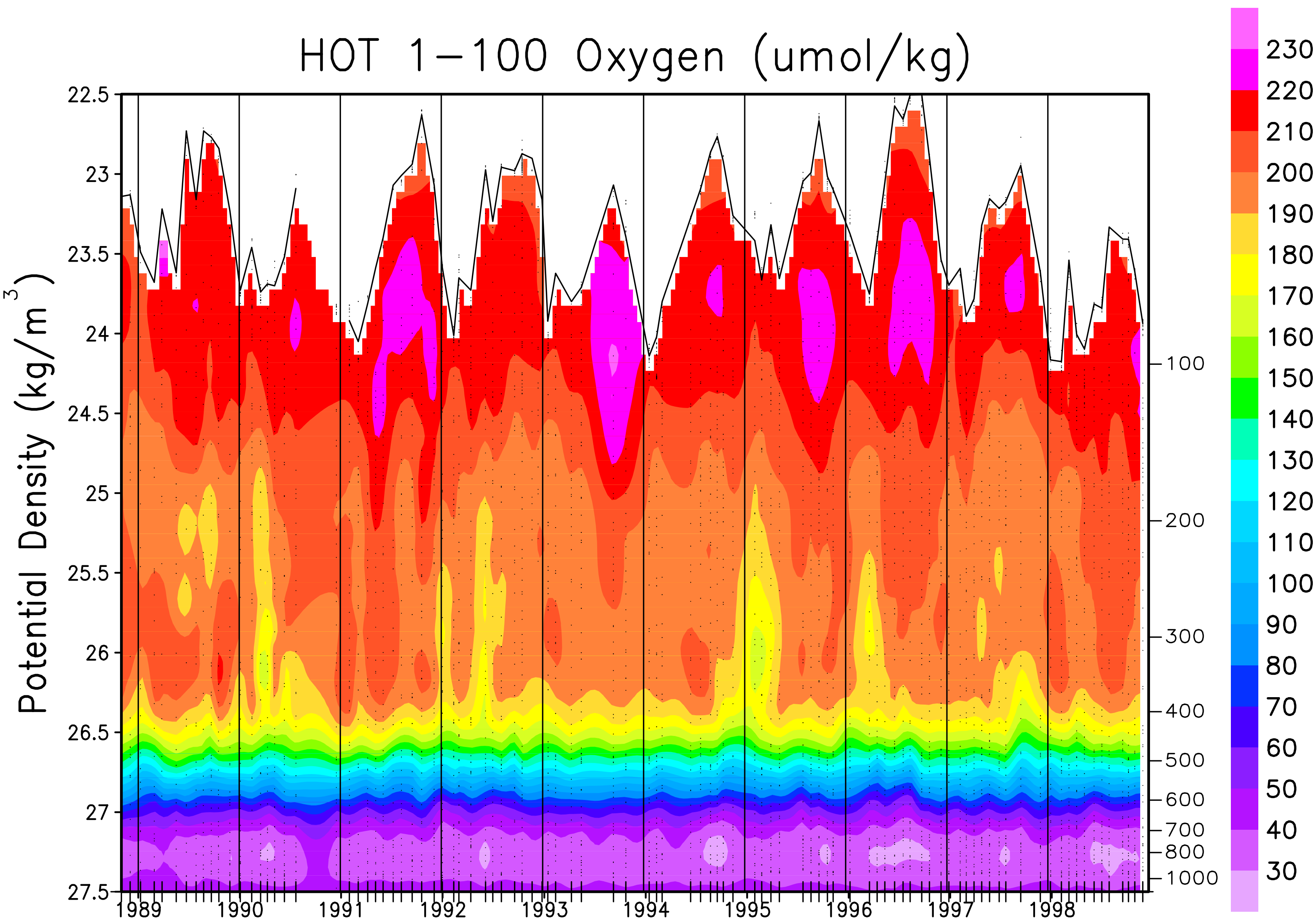

Figure 6.3.8: Contour plot of bottle oxygen versus potential density (σ_θ) to 27.5 kg m^{-3} for HOT cruises 1-100. The average density of the sea surface is connected by the heavy line.

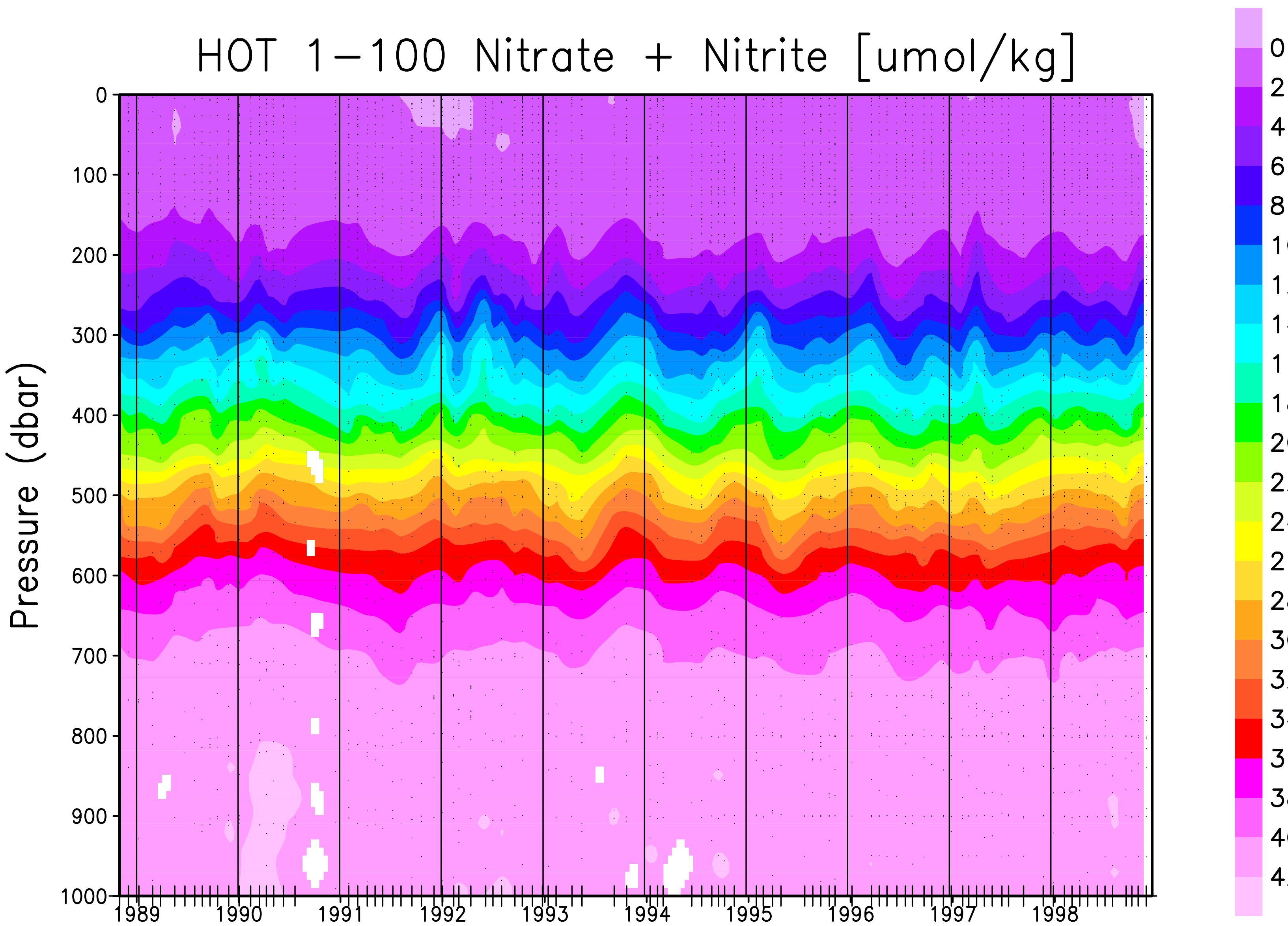

Figure 6.3.9: Contour plot of [nitrate + nitrite] versus pressure for HOT cruises 1-100. Location of samples in the water column are indicated by the solid circles.

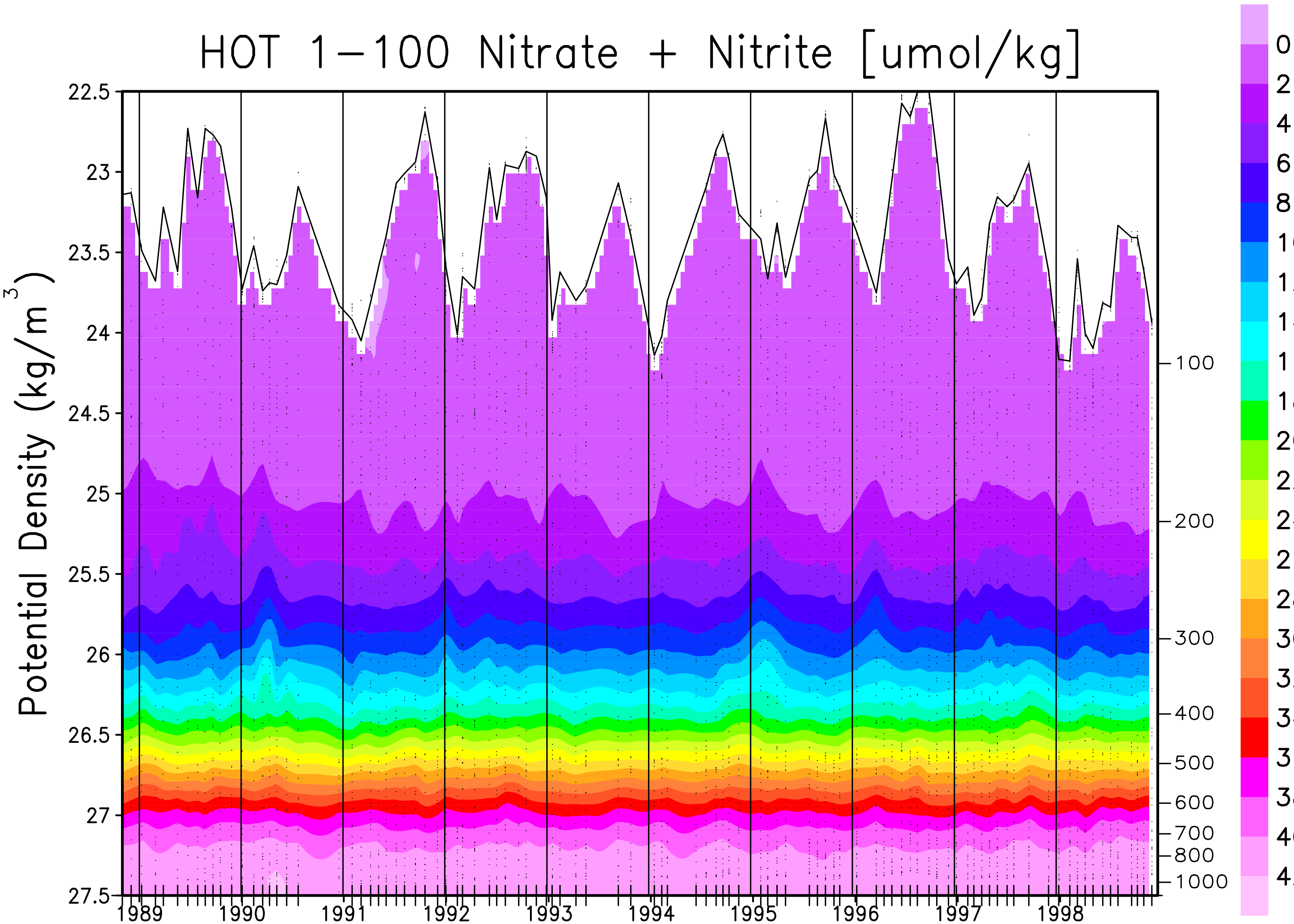

Figure 6.3.10: Contour plot of [nitrate + nitrite] versus potential density (σ_θ) to 27.5 kg m^{-3} for HOT cruises 1-100. The average density of the sea surface is connected by the heavy line.

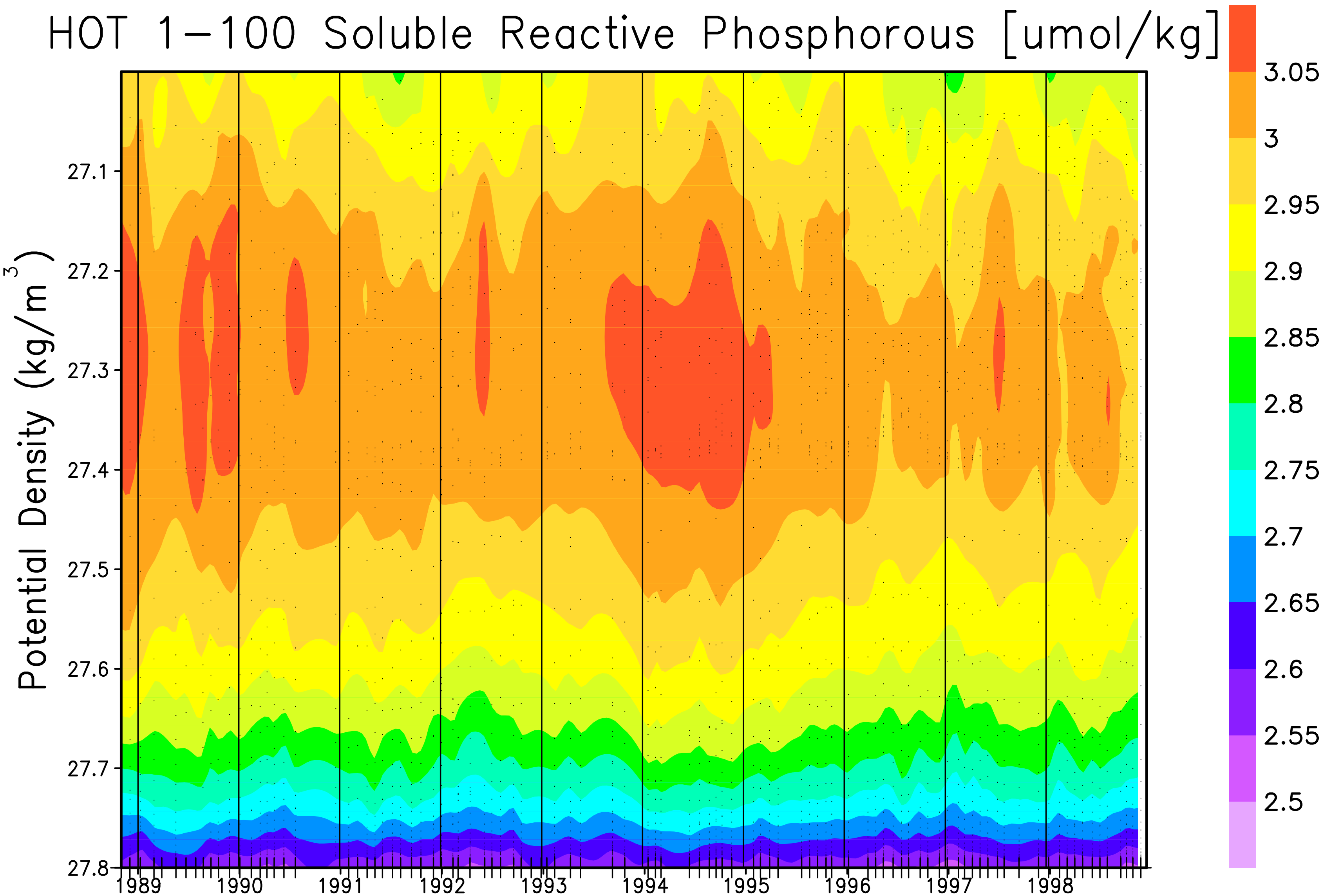

Figure 6.3.11: Contour plot of soluble reactive phosphate versus pressure for HOT cruises 1-100. Location of samples in the water column are indicated by the solid circles.

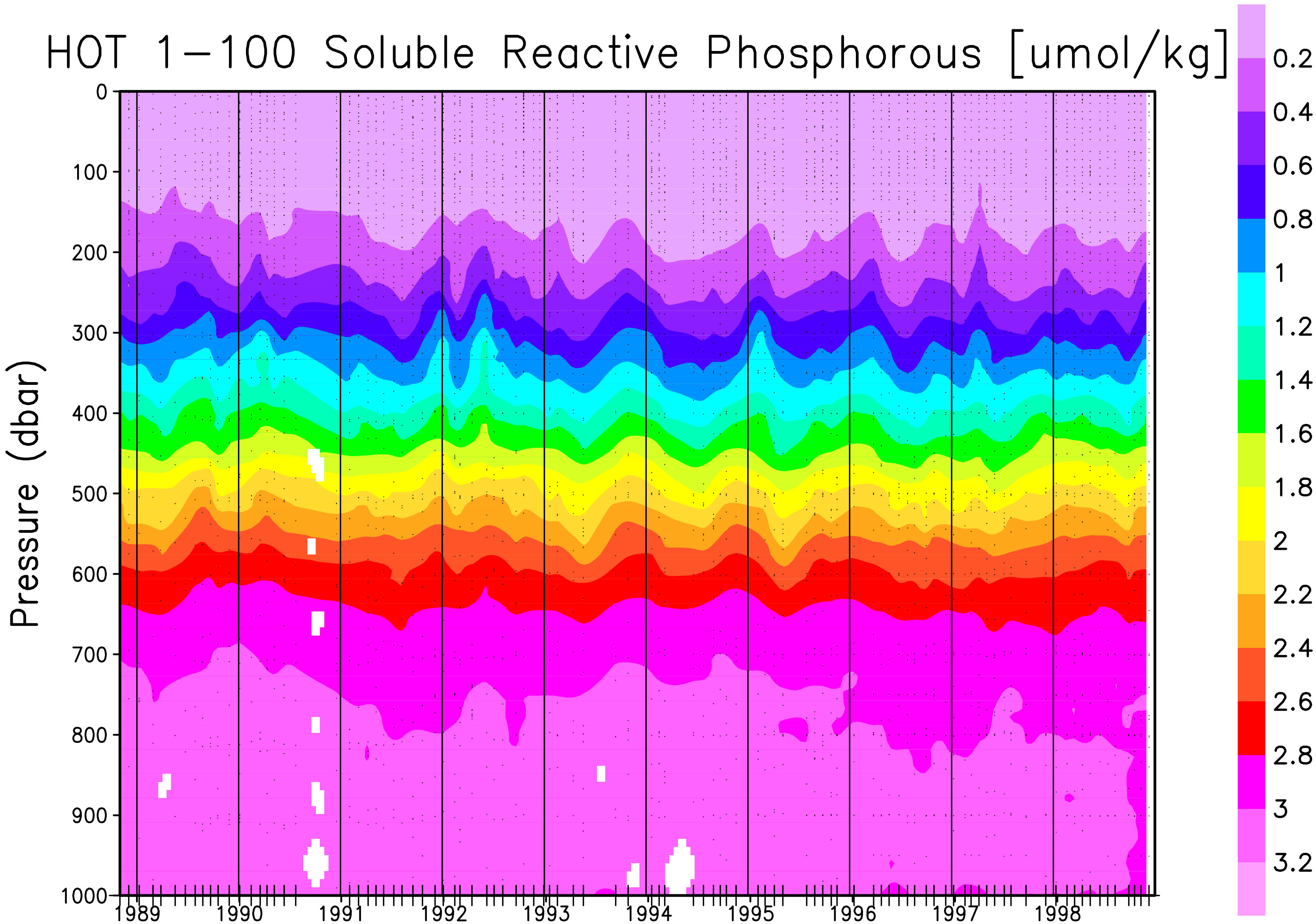

Figure 6.3.12: Contour plot of soluble reactive phosphate versus potential density (σ_θ) to 27.5 kg m^{-3} for HOT cruises 1-100. The average density of the sea surface is connected by the heavy line.

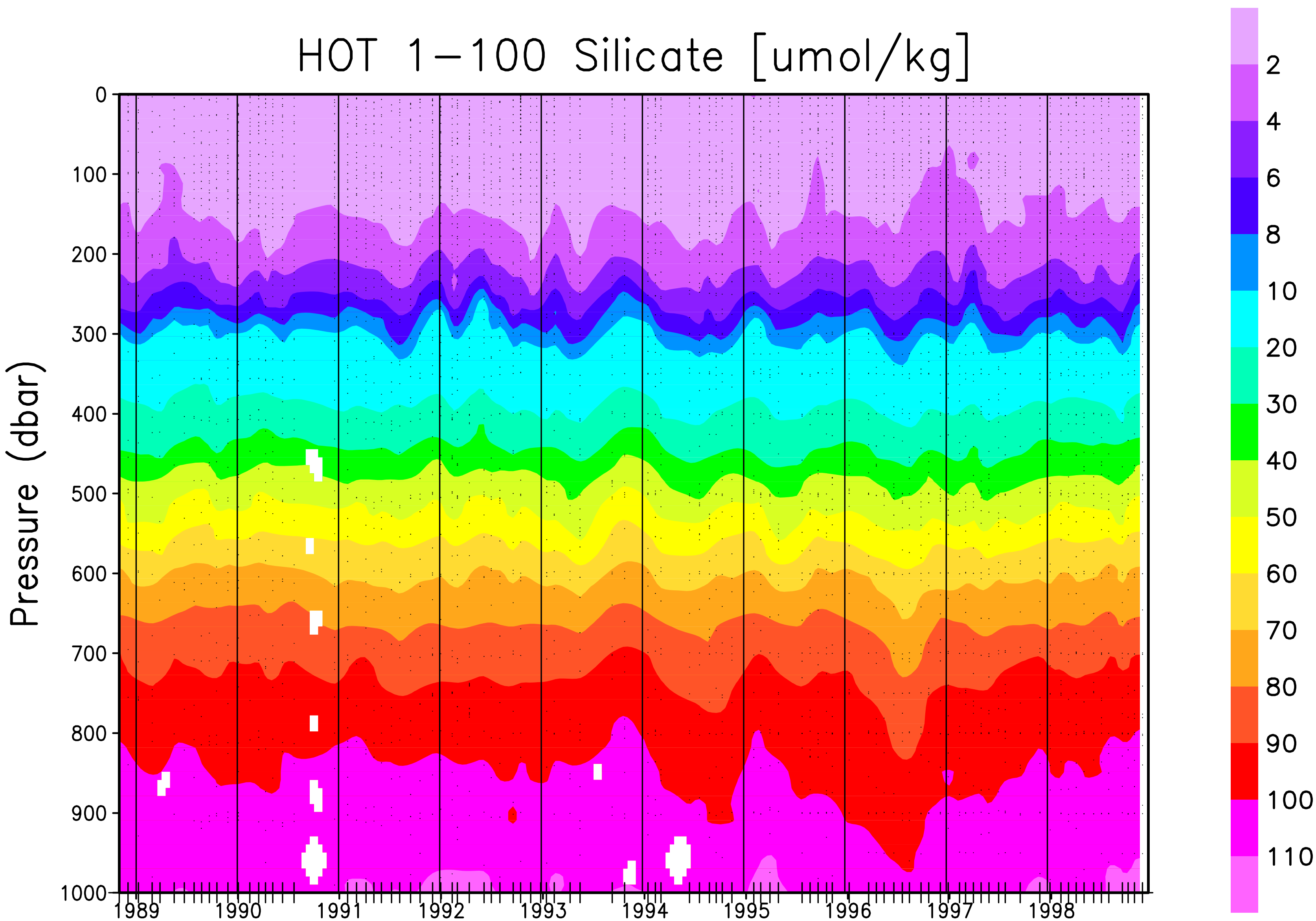

Figure 6.3.13: Contour plot of silicate versus pressure for HOT cruises 1-100. Location of samples in the water column are indicated by the solid circles.

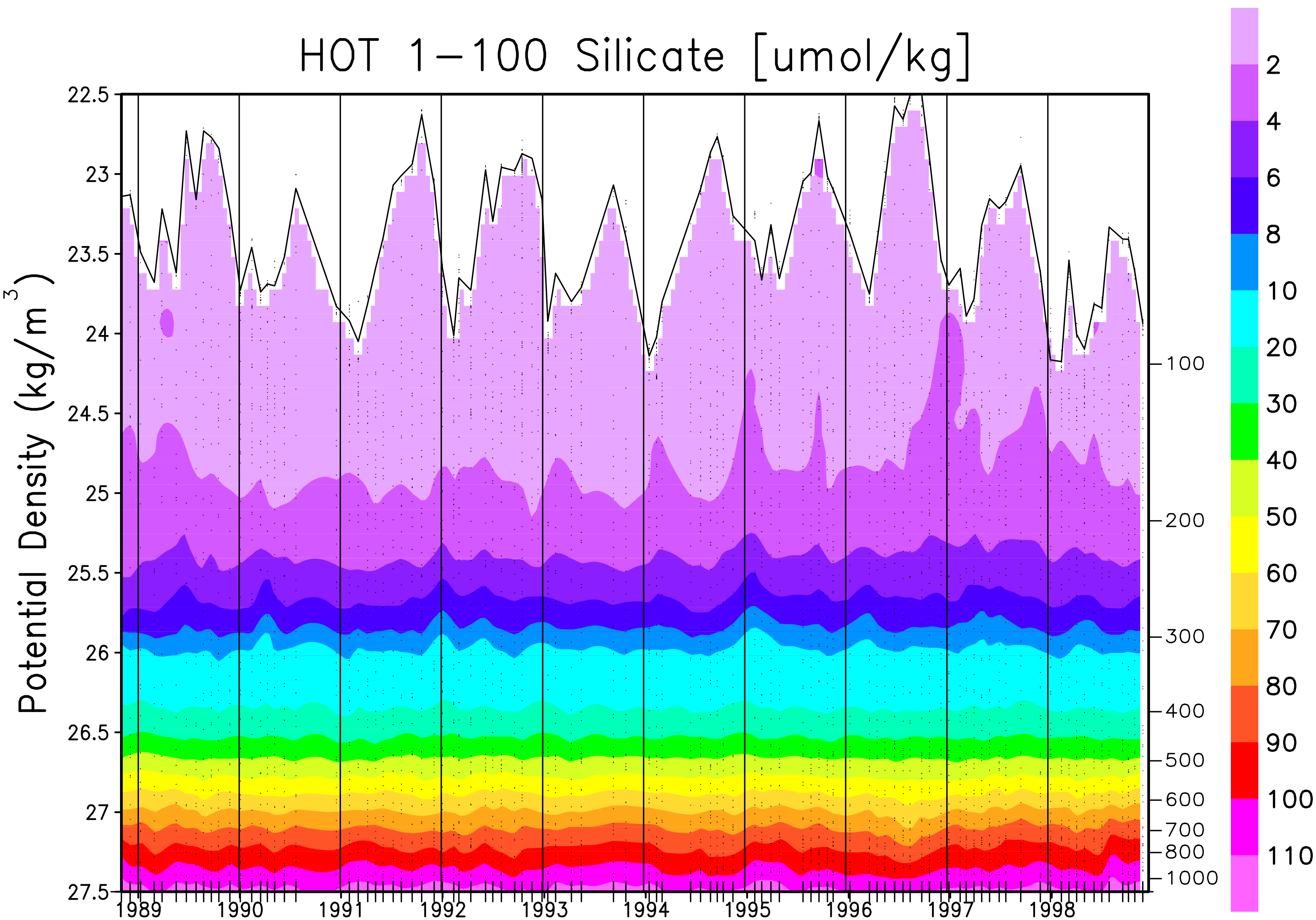

Figure 6.3.14: Contour plot of silicate versus potential density (σ_θ) to 27.5 kg m^{-3} for HOT cruises 1-100. The average density of the sea surface is connected by the heavy line.

6.4. Flash Fluorescence and Beam Transmission

Figures 6.4.1-6: Stack plots of flash fluorescence and beam transmission (when available) collected at Station ALOHA on HOT 44-50. Upper two panels show flash fluorescence data collected on each cruise plotted versus pressure to 250 dbar and potential density at 26 σ_θ. Offset is 20 mvolts. Lower two panels show % transmittance data collected on each cruise plotted versus pressure to 250 dbar and potential density at 26 σ_θ. Offset is 33%.

Figure 6.4.7: Stack plots of averaged night-time fluorescence profiles plotted versus pressure to 250 dbar collected on each HOT cruise from 1988 through 1993. The HOT cruise number is shown at the top of each panel.

Figure 6.4.8: As in 6.4.7, except profiles are plotted versus potential density at 26 σ_θ.

Figure 6.4.9: Stack plots of averaged beam transmission profiles collected in 1991-1993. Upper panel shows profiles plotted versus pressure to 250 dbar. Lower panel shows profiles plotted versus potential density at 26 σ_θ. The HOT cruise number is shown at the top of each panel.

Figure 6.4.10: As in 6.3.9, except profiles are plotted versus potential density at 26 σ_θ.

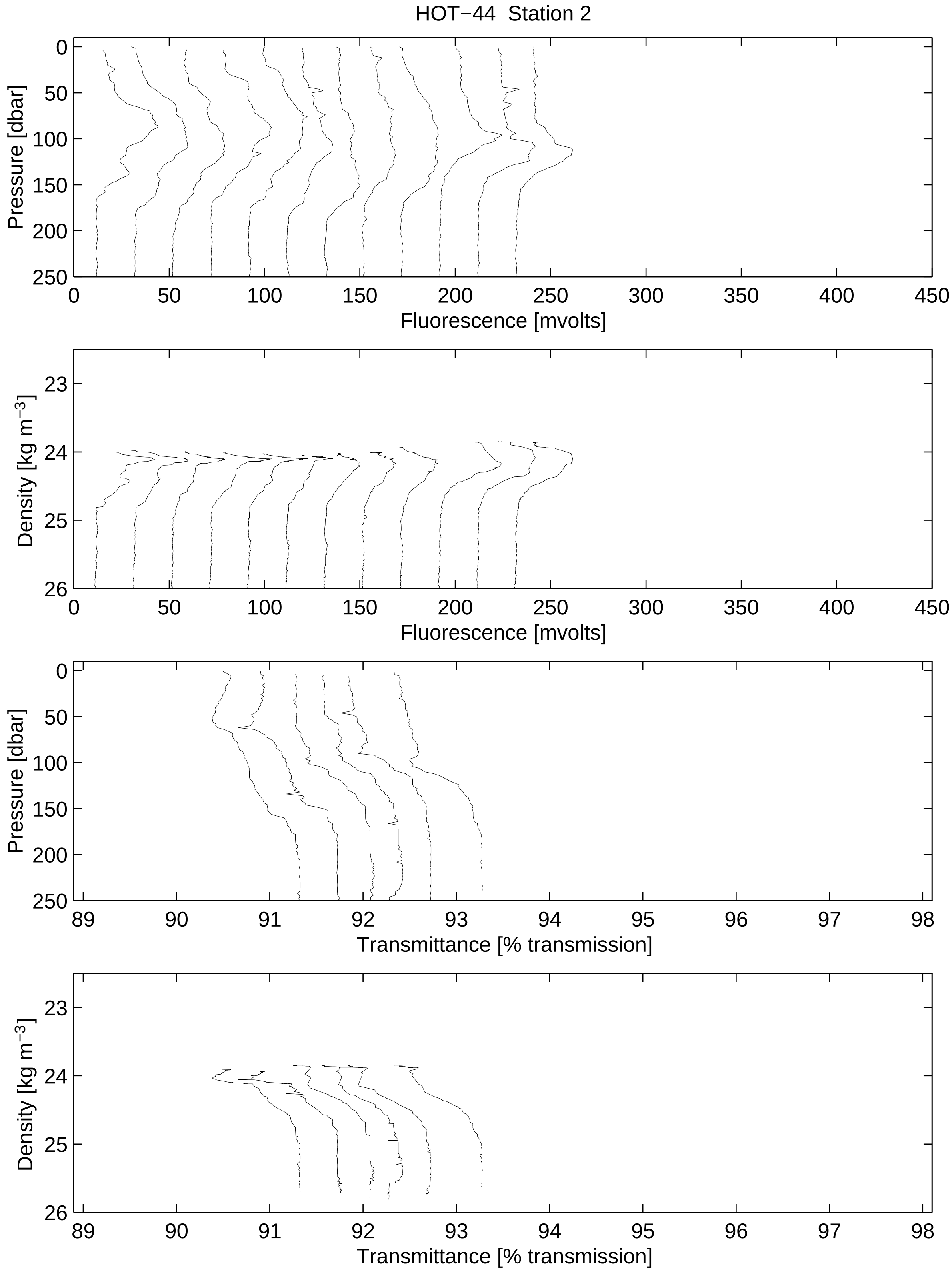
HOT−44 Station 2
Pressure [dbar]
Fluorescence [mvolts]
Density [kg m−3]
Fluorescence [mvolts]
Pressure [dbar]
Transmittance [% transmission]
Density [kg m−3]
Transmittance [% transmission]

Figure 6.4.1

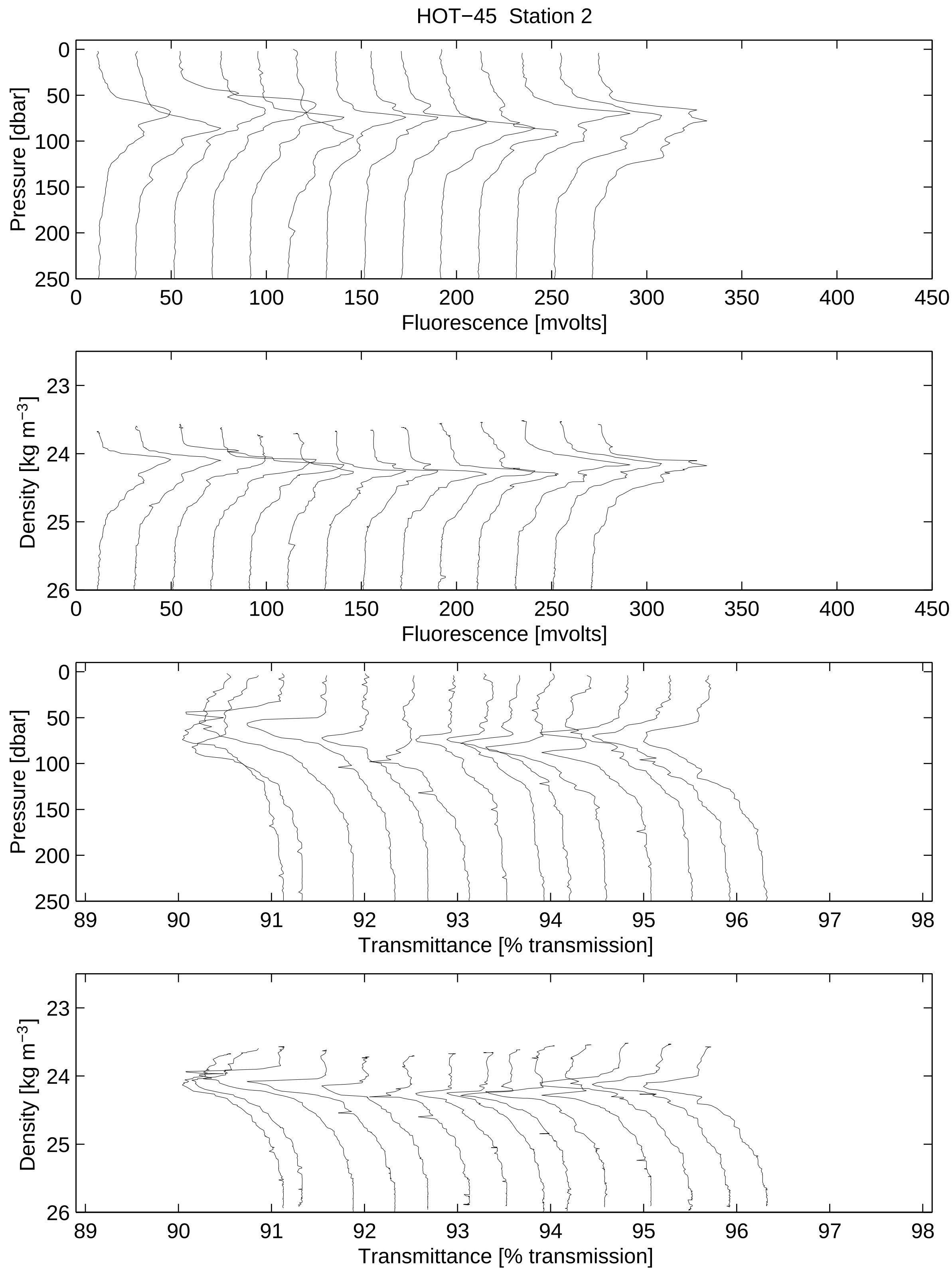

HOT−45 Station 2
Pressure [dbar]
Fluorescence [mvolts]
Density [kg m−3]
Fluorescence [mvolts]
Pressure [dbar]
Transmittance [% transmission]
Density [kg m−3]
Transmittance [% transmission]

Figure 6.4.2

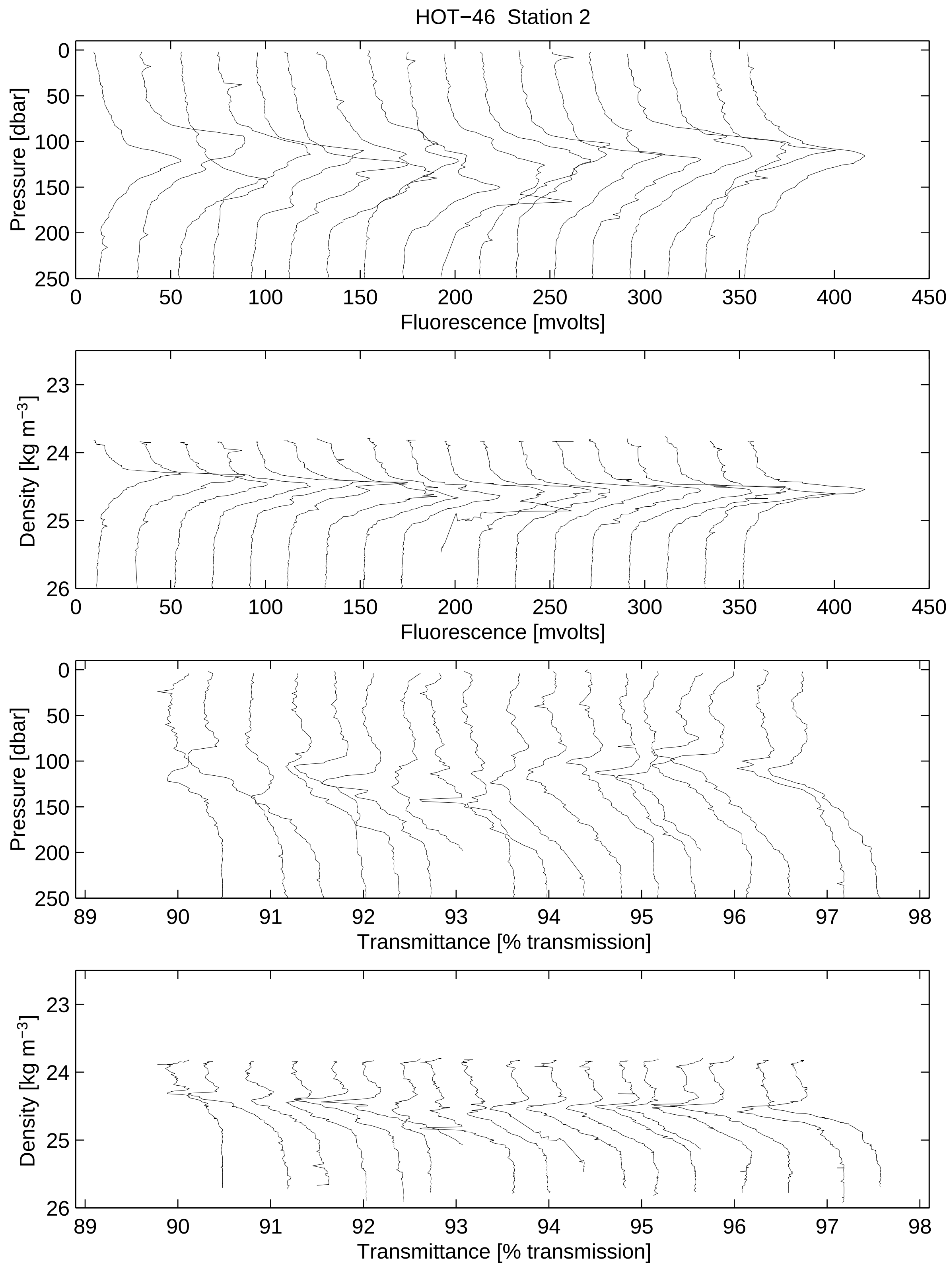

HOT−46 Station 2
Pressure [dbar]
Fluorescence [mvolts]
Density [kg m−3]
Fluorescence [mvolts]
Pressure [dbar]
Transmittance [% transmission]
Density [kg m−3]
Transmittance [% transmission]

Figure 6.4.3

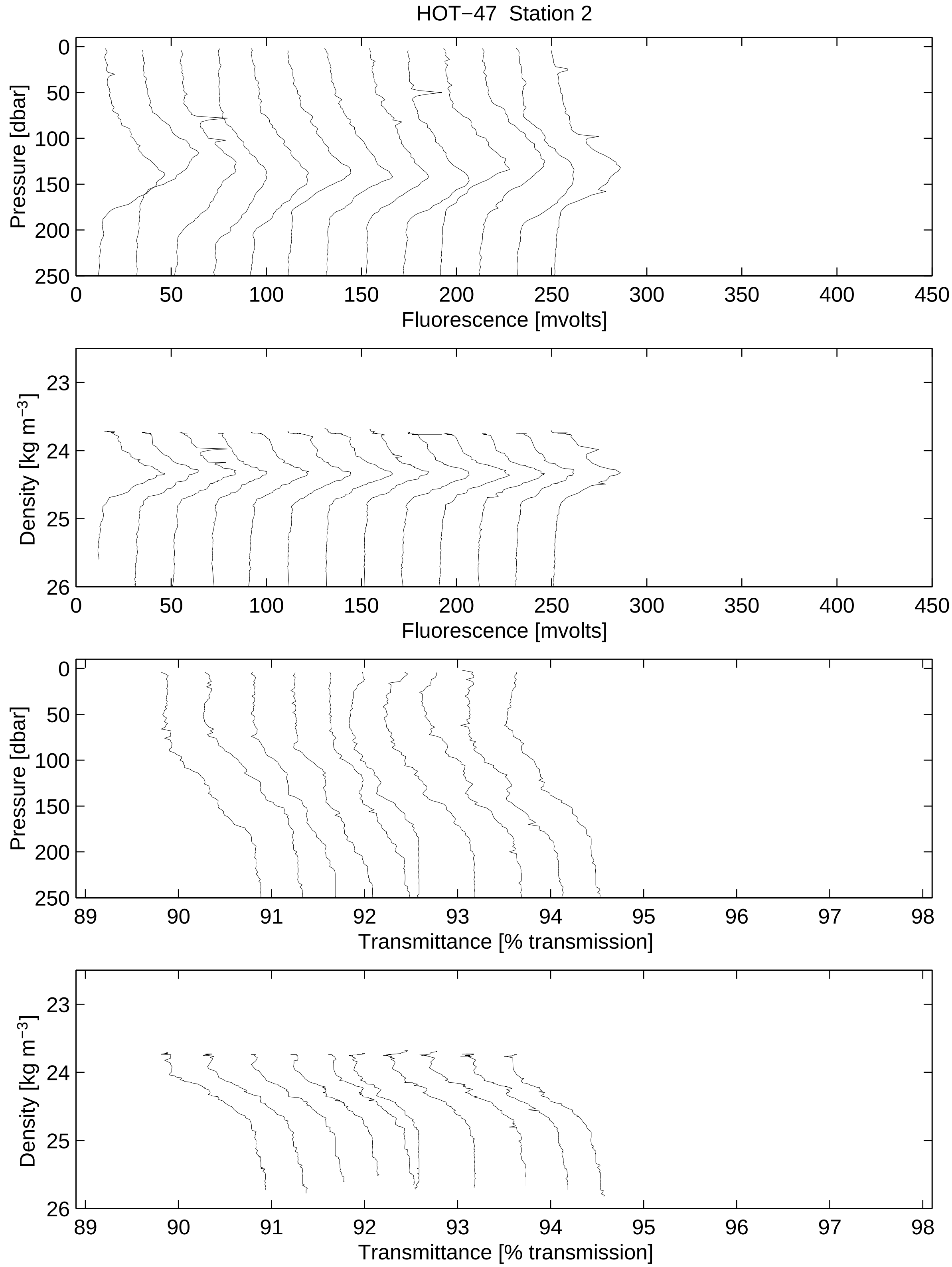

HOT−47 Station 2
Pressure [dbar]
Fluorescence [mvolts]
Density [kg m^{-3}]
Fluorescence [mvolts]
Pressure [dbar]
Transmittance [% transmission]
Density [kg m^{-3}]
Transmittance [% transmission]

Figure 6.4.4

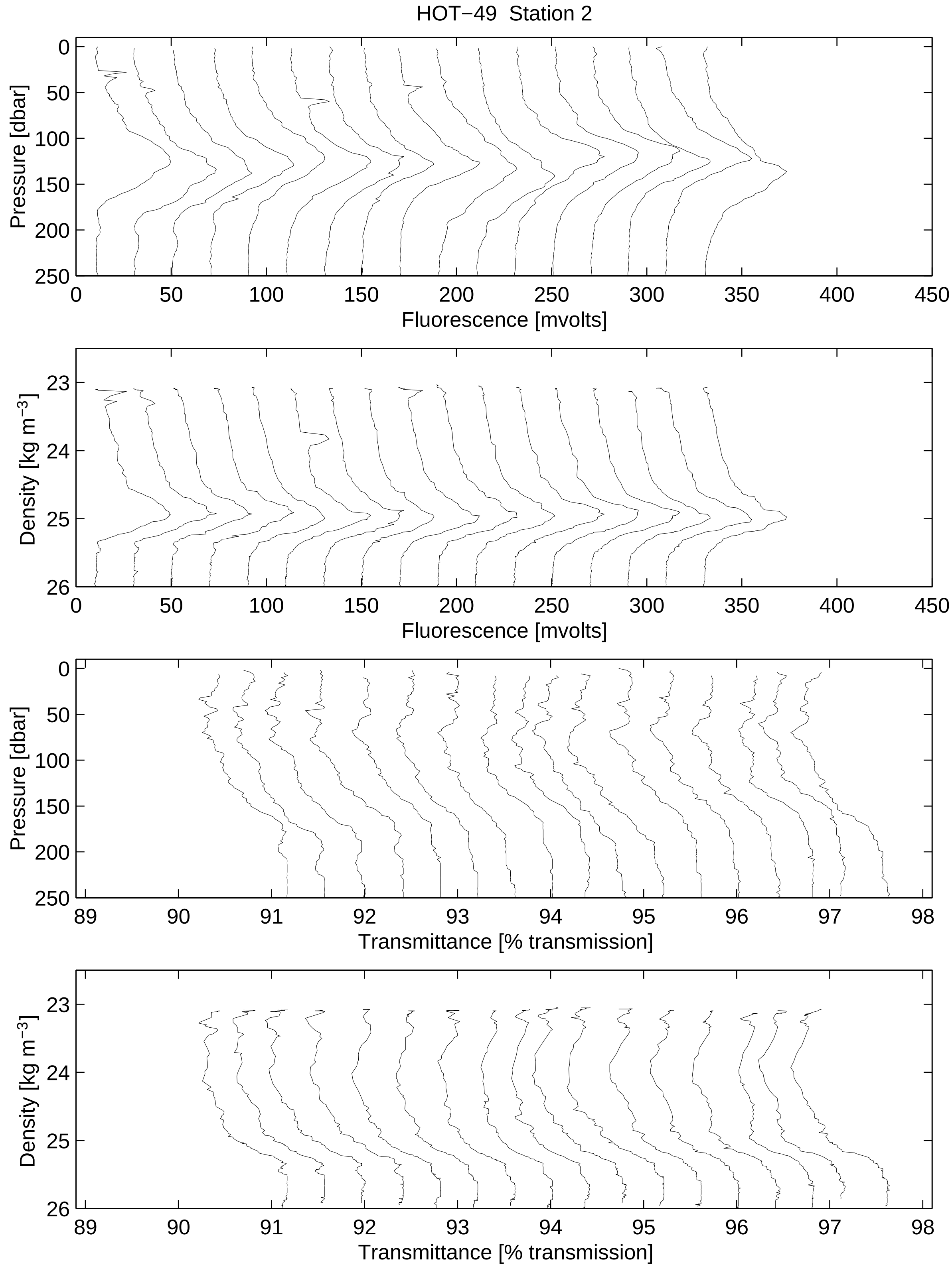
HOT−49 Station 2
Pressure [dbar]
Fluorescence [mvolts]
Density [kg m−3]
Fluorescence [mvolts]
Pressure [dbar]
Transmittance [% transmission]
Density [kg m−3]
Transmittance [% transmission]

Figure 6.4.5

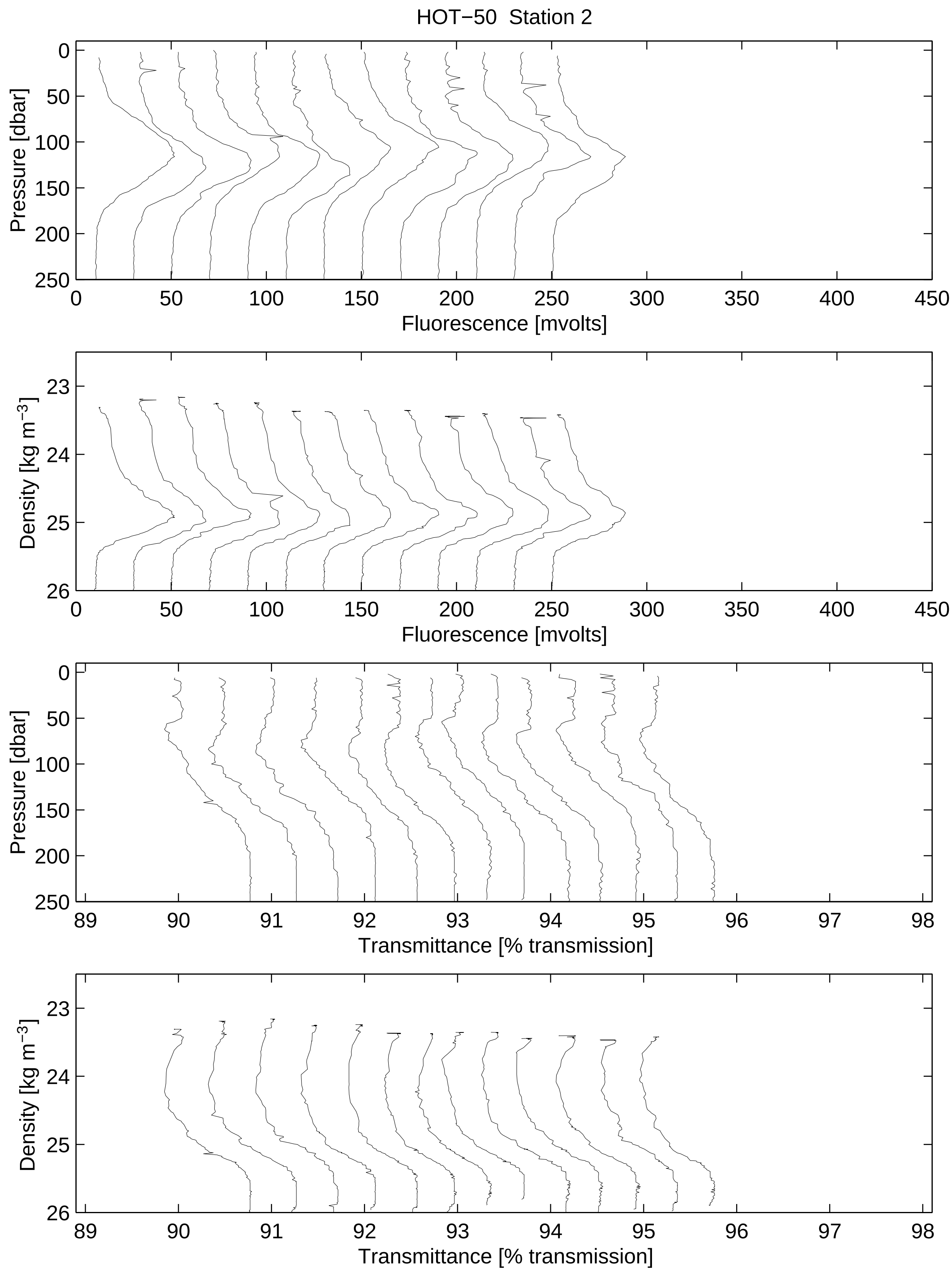
HOT−50 Station 2
Pressure [dbar]
Fluorescence [mvolts]
Density [kg m−3]
Fluorescence [mvolts]
Pressure [dbar]
Transmittance [% transmission]
Density [kg m−3]
Transmittance [% transmission]

Figure 6.4.6

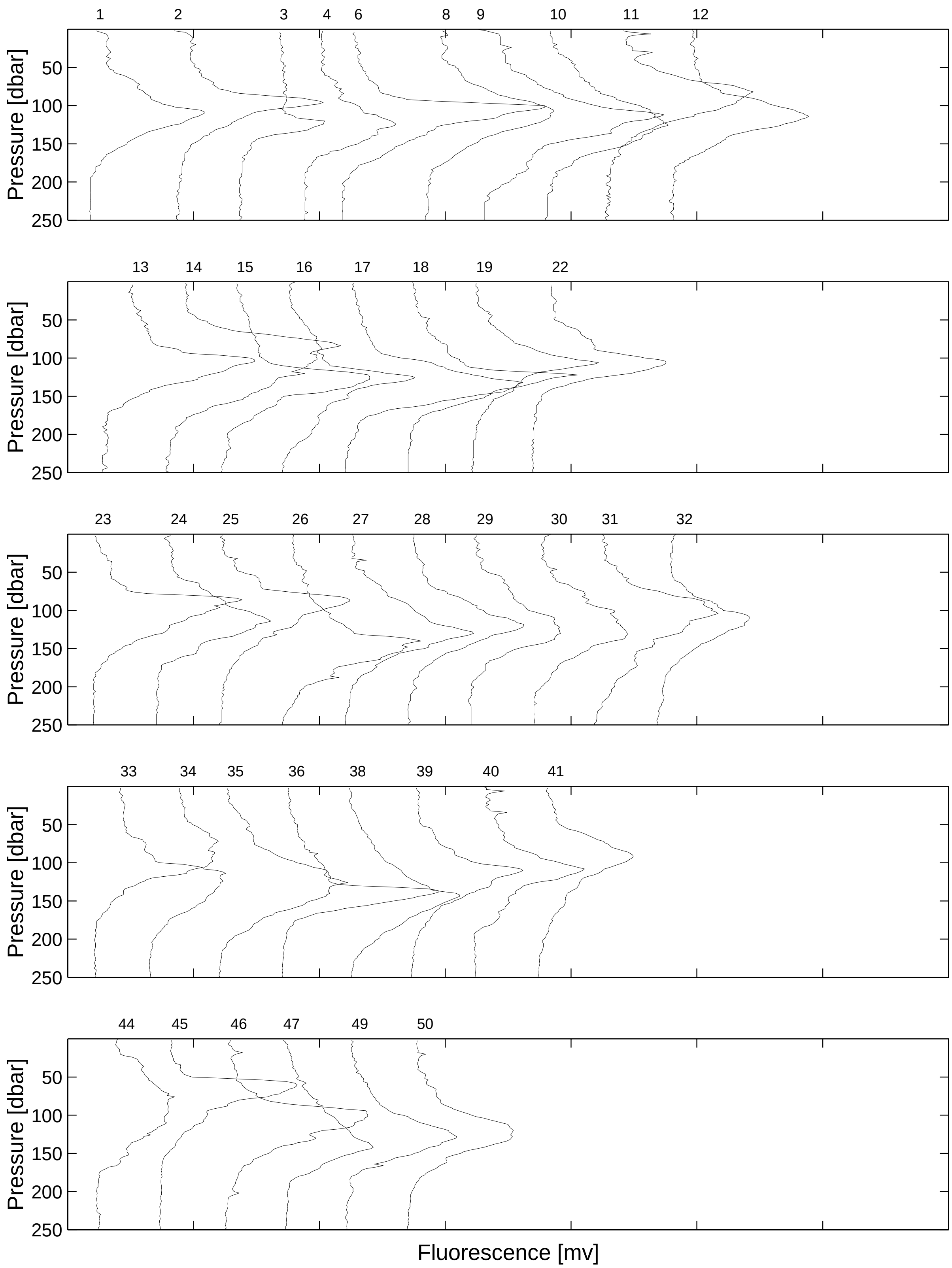
1
2
3
4
6
8
9
10
11
12
13
14
15
16
17
18
19
22
23
24
25
26
27
28
29
30
31
32
33
34
35
36
38
39
40
41
44
45
46
47
49
50
Pressure [dbar]
50
100
150
200
250
Fluorescence [mv]

Figure 6.4.7

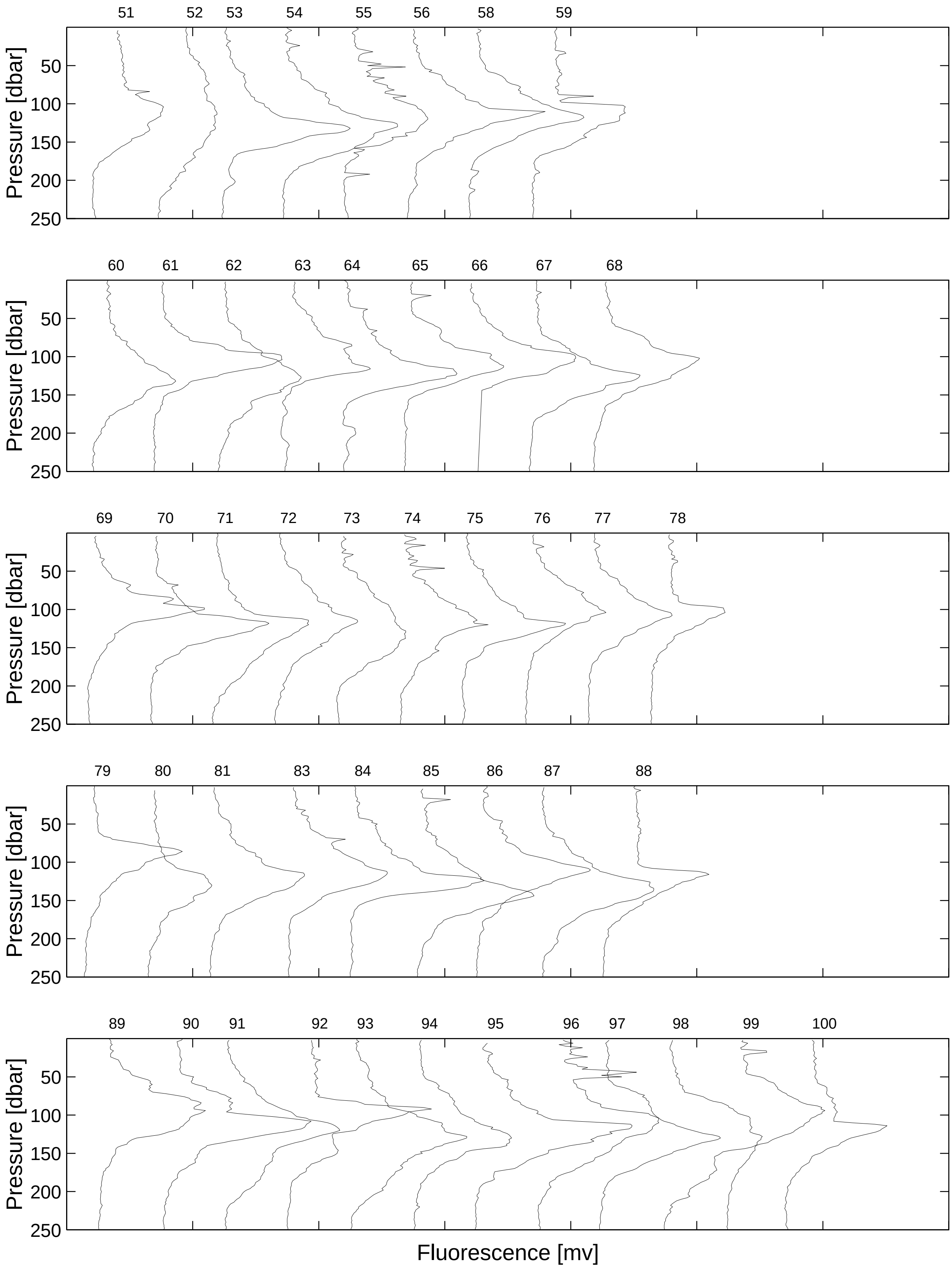
51 52 53 54 55 56 58 59
60 61 62 63 64 65 66 67 68
69 70 71 72 73 74 75 76 77 78
79 80 81 83 84 85 86 87 88
89 90 91 92 93 94 95 96 97 98 99 100
Pressure [dbar]
50
100
150
200
250
Fluorescence [mv]

Figure 6.4.8

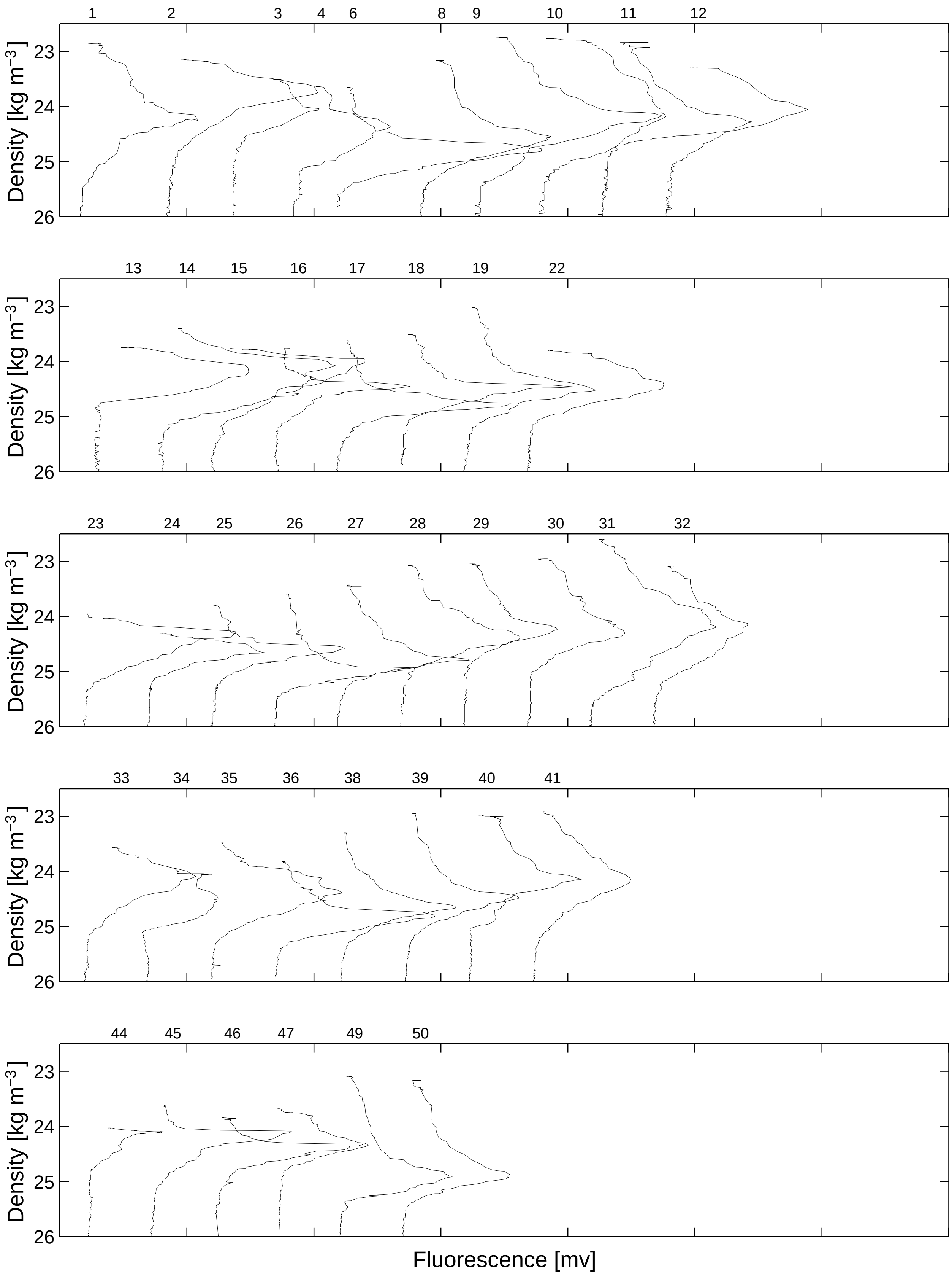
1 2 3 4 6 8 9 10 11 12
13 14 15 16 17 18 19 22
23 24 25 26 27 28 29 30 31 32
33 34 35 36 38 39 40 41
44 45 46 47 49 50
Density [kg m^{-3}]
23
24
25
26
Fluorescence [mv]

Figure 6.4.9

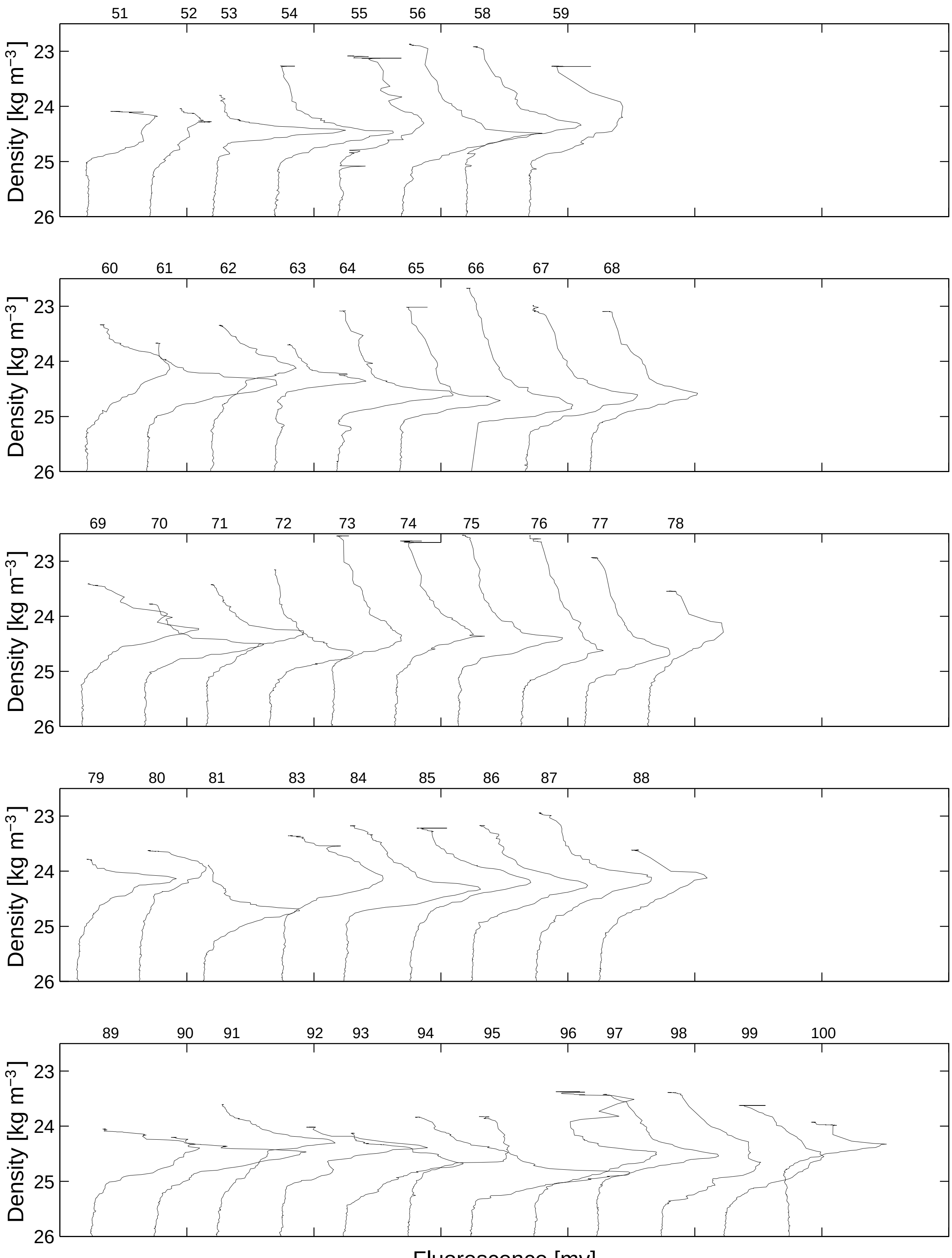
51 52 53 54 55 56 58 59
60 61 62 63 64 65 66 67 68
69 70 71 72 73 74 75 76 77 78
79 80 81 83 84 85 86 87 88
89 90 91 92 93 94 95 96 97 98 99 100
Density [kg m−3]
23
24
25
26
Fluorescence [mv]

Figure 6.4.10

6.5. Biogeochemistry

Figure 6.5.1: Contoured time-series of DIC in the upper 1000 dbar at Station ALOHA normalized to 35 ppt salinity. Location of bottle closure is indicated by solid circle.

Figure 6.5.2: Contoured time-series of titration alkalinity in the upper 1000 dbar at Station ALOHA normalized to 35 ppt salinity. Location of bottle closure is indicated by solid circle

Figure 6.5.3: Mean titration alkalinity and DIC in surface waters (0-50 dbars) at Station ALOHA. Upper Panel: Titration alkalinity plotted versus time for all HOT cruises. Error bars represent standard deviation of pooled samples collected between 0 and 50 dbar. Lower panel: As in upper panel except for DIC.

Figure 6.5.4: Soluble reactive phosphorus measured by the MAGIC procedure in the upper 250 dbar at Station ALOHA in 1993.

Figure 6.5.5: Nitrate plus nitrite measured by the nitrogen oxides analyzer in the upper 250 dbar at Station ALOHA in 1993.

Figure 6.5.6: Contoured time-series of chlorophyll *a* in the upper 200 dbar for all HOT cruises.

Figure 6.5.7: Particulate carbon at Station ALOHA on all HOT cruises. Upper panel: Mean particulate carbon concentration in the upper 50 dbar. Error bar represents the standard deviation of pooled samples collected between 0 and 50 dbar. Lower panel: As in upper panel but for 50 to 100 dbar.

Figure 6.5.8: As in Figure 6.5.7 except for particulate nitrogen.

Figure 6.5.9: As in Figure 6.5.7 except for particulate phosphorus.

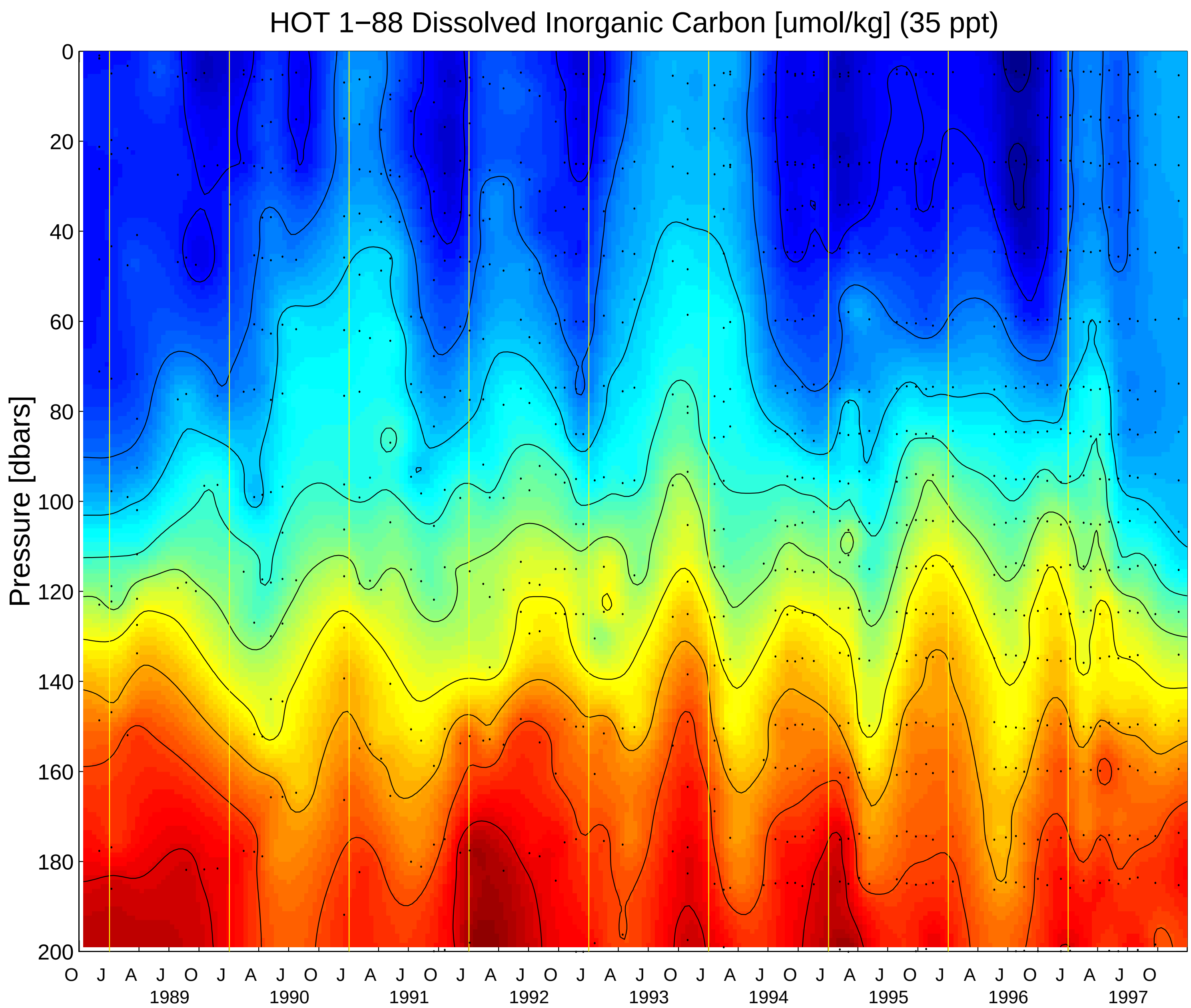
HOT 1−88 Dissolved Inorganic Carbon [umol/kg] (35 ppt)
Pressure [dbars]
0
20
40
60
80
100
120
140
160
180
200
O J A J O J A J O J A J O J A J O J A J O J A J O J A J O J A J O J A J O
1989
1990
1991
1992
1993
1994
1995
1996
1997

Figure 6.5.1

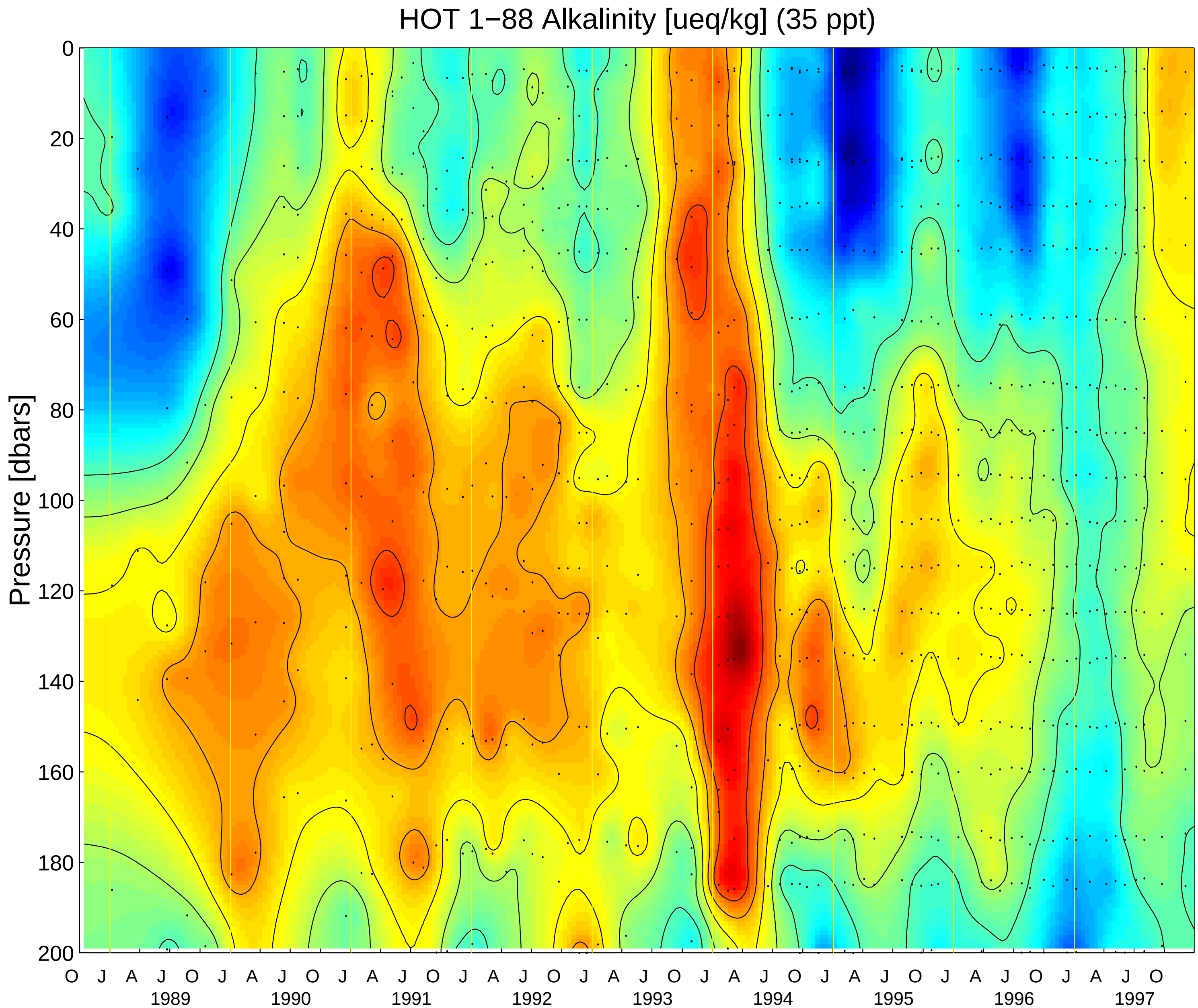
HOT 1−88 Alkalinity [ueq/kg] (35 ppt)
Pressure [dbars]
0
20
40
60
80
100
120
140
160
180
200
O J A J O J A J O J A J O J A J O J A J O J A J O J A J O J A J O J A J O
1989
1990
1991
1992
1993
1994
1995
1996
1997

Figure 6.5.2

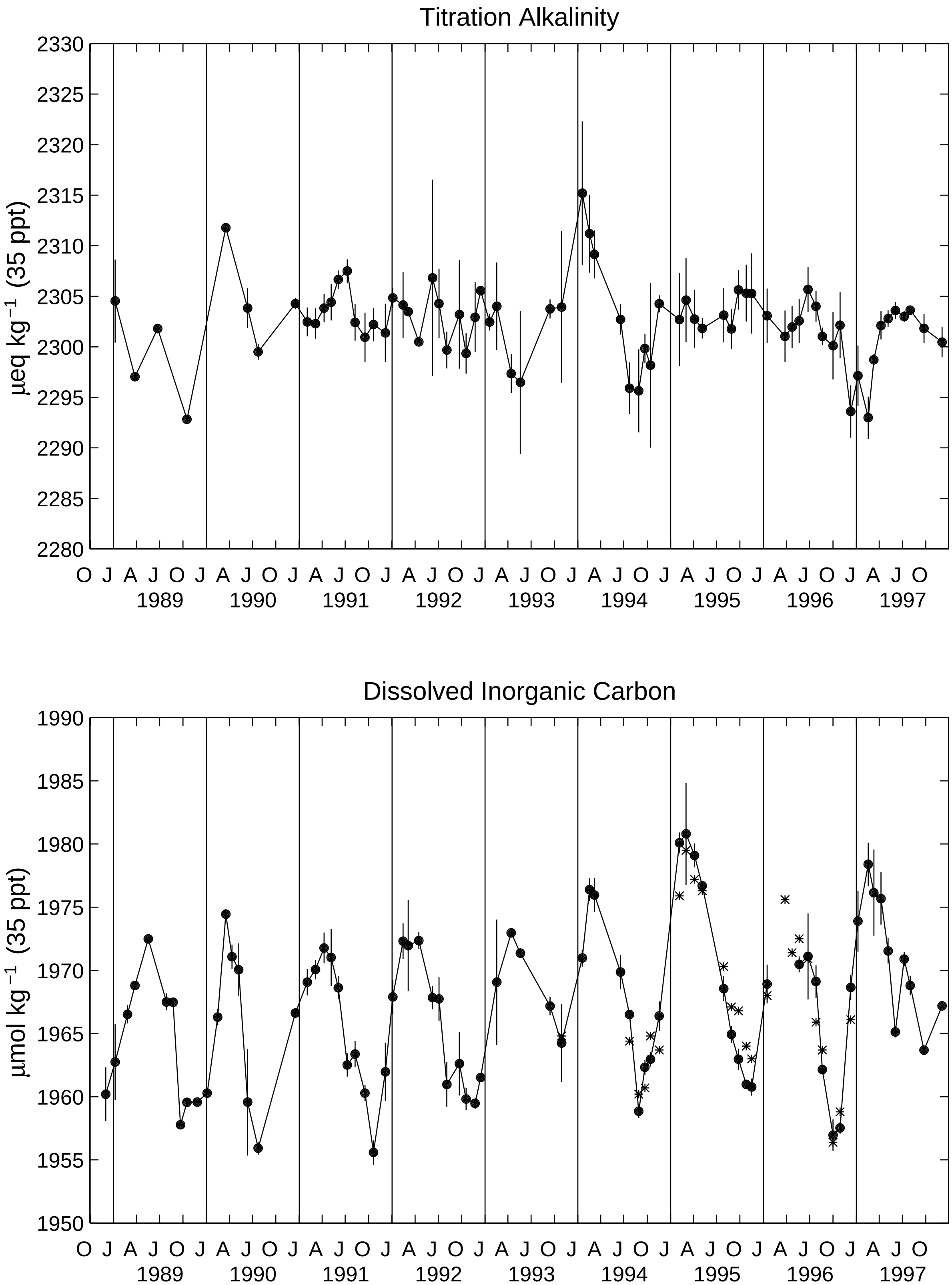

Titration Alkalinity
μeq kg⁻¹ (35 ppt)
2330
2325
2320
2315
2310
2305
2300
2295
2290
2285
2280
O J A J O J A J O J A J O J A J O J A J O J A J O J A J O J A J O J A J O
1989
1990
1991
1992
1993
1994
1995
1996
1997
Dissolved Inorganic Carbon
μmol kg⁻¹ (35 ppt)
1990
1985
1980
1975
1970
1965
1960
1955
1950
O J A J O J A J O J A J O J A J O J A J O J A J O J A J O J A J O J A J O
1989
1990
1991
1992
1993
1994
1995
1996
1997

Figure 6.5.3

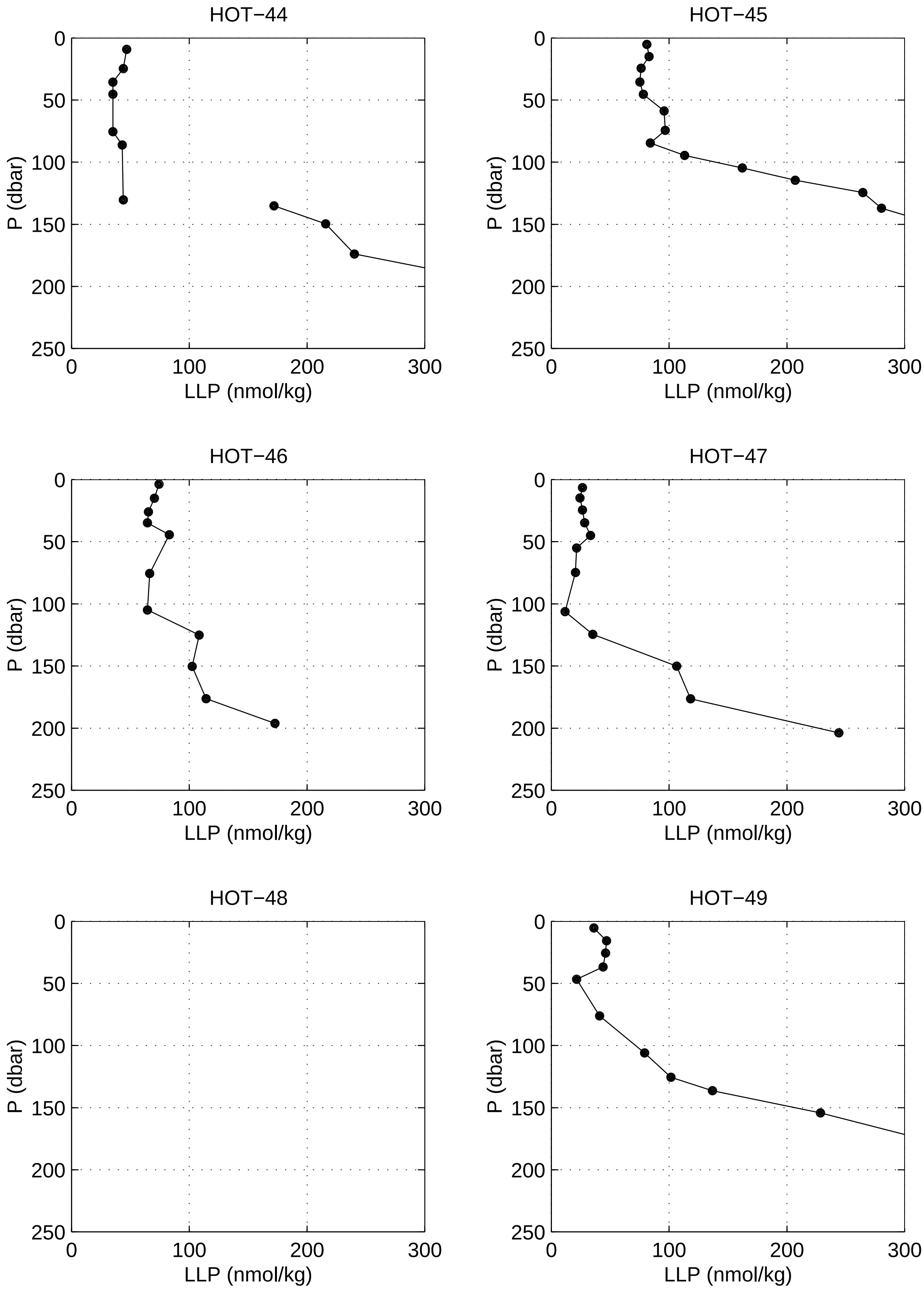
HOT−44
HOT−45
HOT−46
HOT−47
HOT−48
HOT−49
P (dbar)
LLP (nmol/kg)
0
50
100
150
200
250
0
100
200
300

Figure 6.5.4

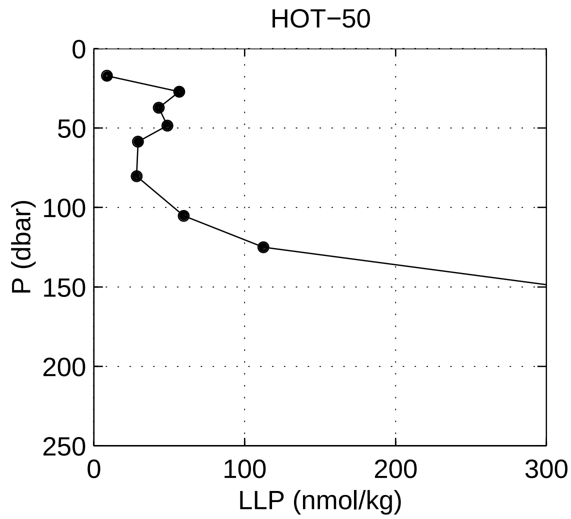

Figure 6.5.4 (continued)

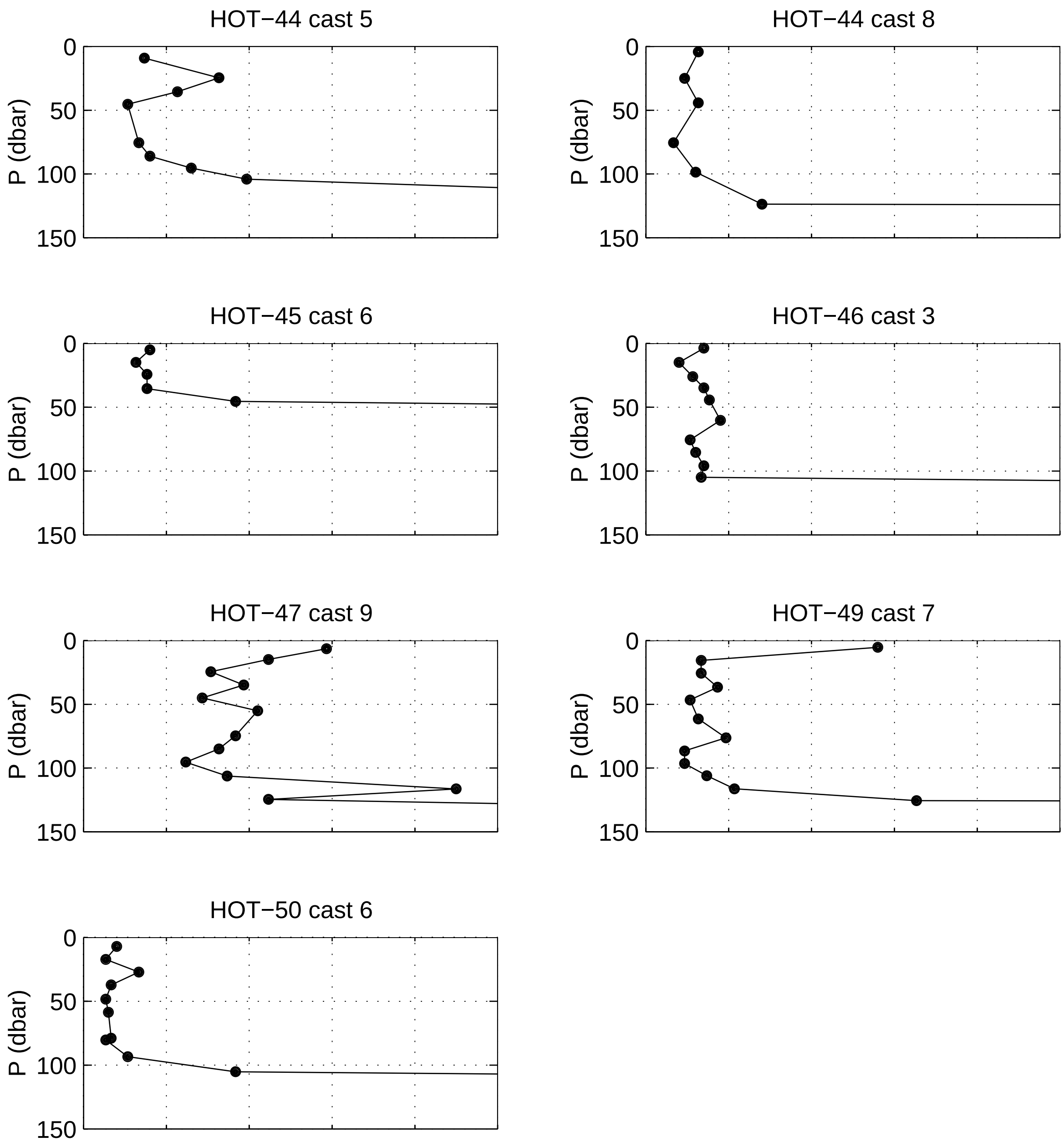
HOT−44 cast 5
HOT−44 cast 8
HOT−45 cast 6
HOT−46 cast 3
HOT−47 cast 9
HOT−49 cast 7
HOT−50 cast 6
P (dbar)
0
50
100
150

Figure 6.5.5

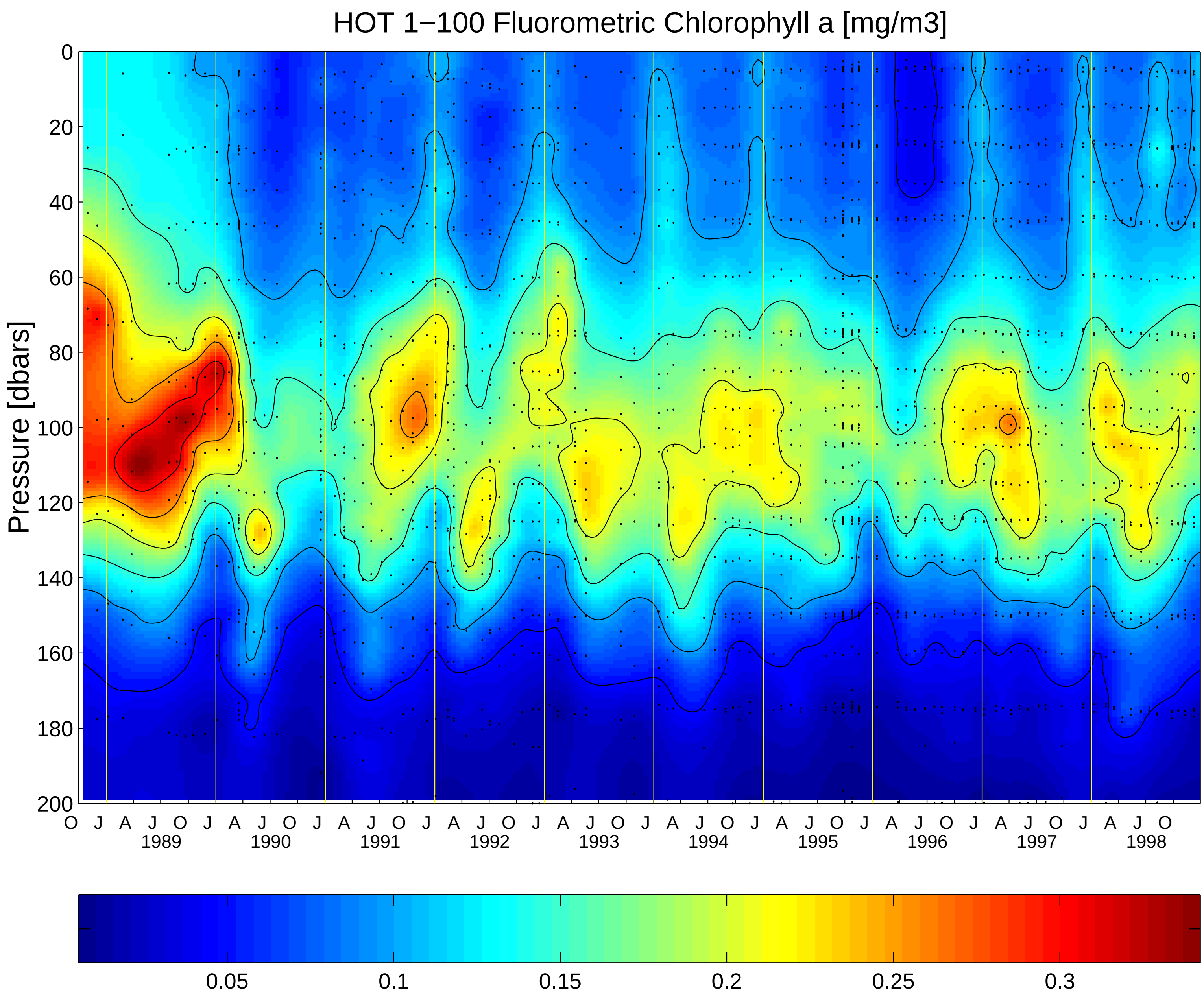
HOT 1−100 Fluorometric Chlorophyll a [mg/m3]
Pressure [dbars]
0
20
40
60
80
100
120
140
160
180
200
O J A J O J A J O J A J O J A J O J A J O J A J O J A J O J A J O J A J O J A J O
1989
1990
1991
1992
1993
1994
1995
1996
1997
1998
0.05
0.1
0.15
0.2
0.25
0.3

Figure 6.5.6

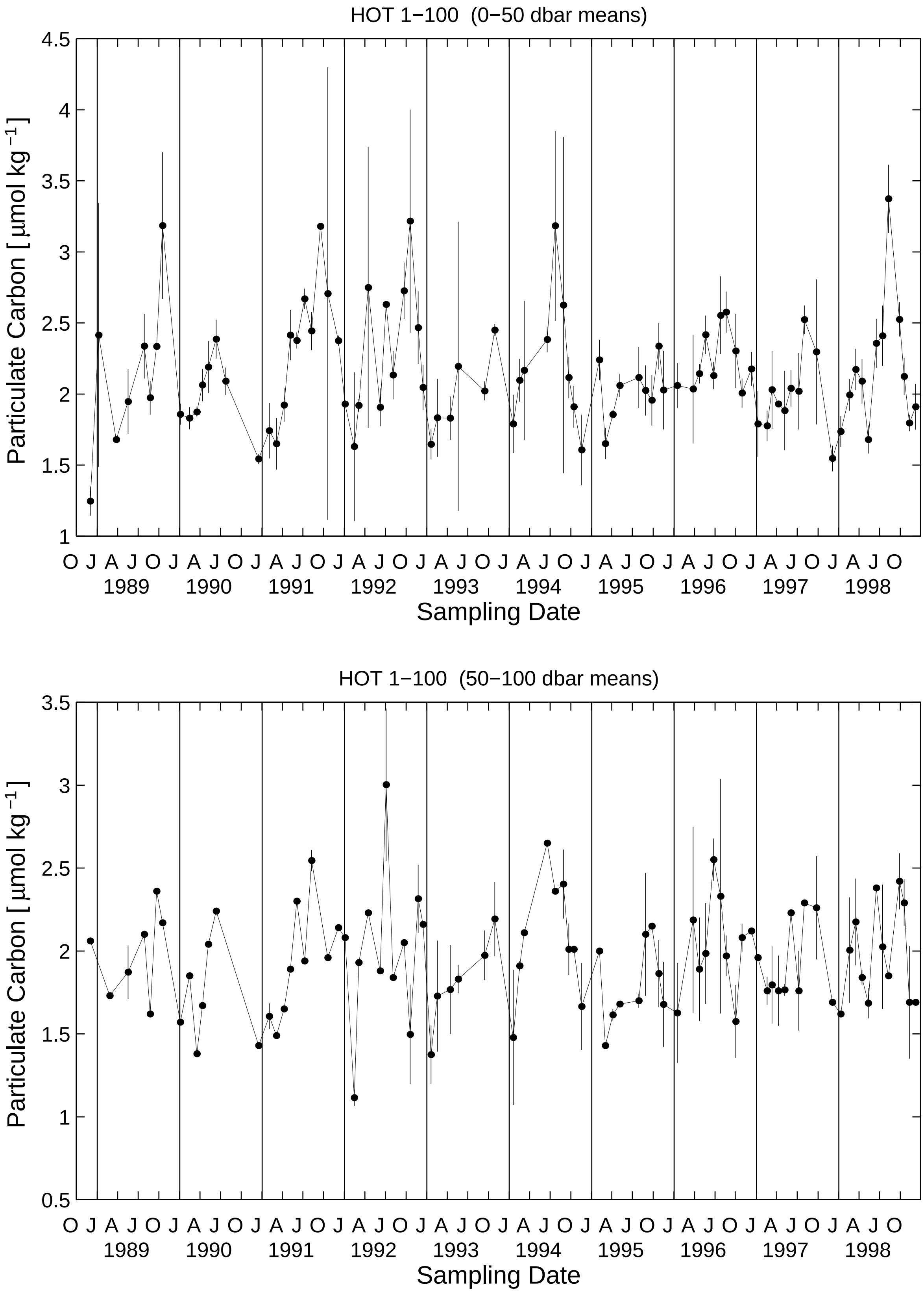
HOT 1−100 (0−50 dbar means)
Particulate Carbon [µmol kg−1]
Sampling Date
1989
1990
1991
1992
1993
1994
1995
1996
1997
1998
HOT 1−100 (50−100 dbar means)
Particulate Carbon [µmol kg−1]
Sampling Date

Figure 6.5.7

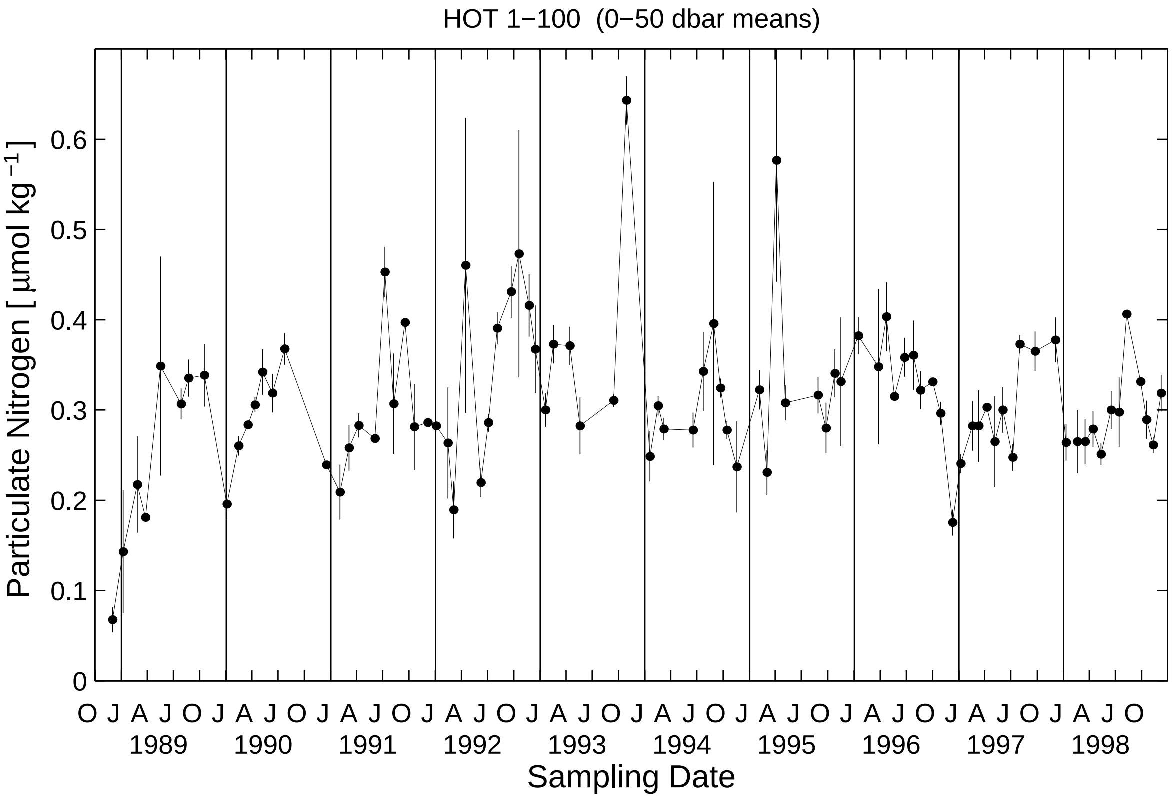
HOT 1−100 (0−50 dbar means)
Particulate Nitrogen [µmol kg⁻¹]
0
0.1
0.2
0.3
0.4
0.5
0.6
O J A J O J A J O J A J O J A J O J A J O J A J O J A J O J A J O J A J O J A J O
1989
1990
1991
1992
1993
1994
1995
1996
1997
1998
Sampling Date

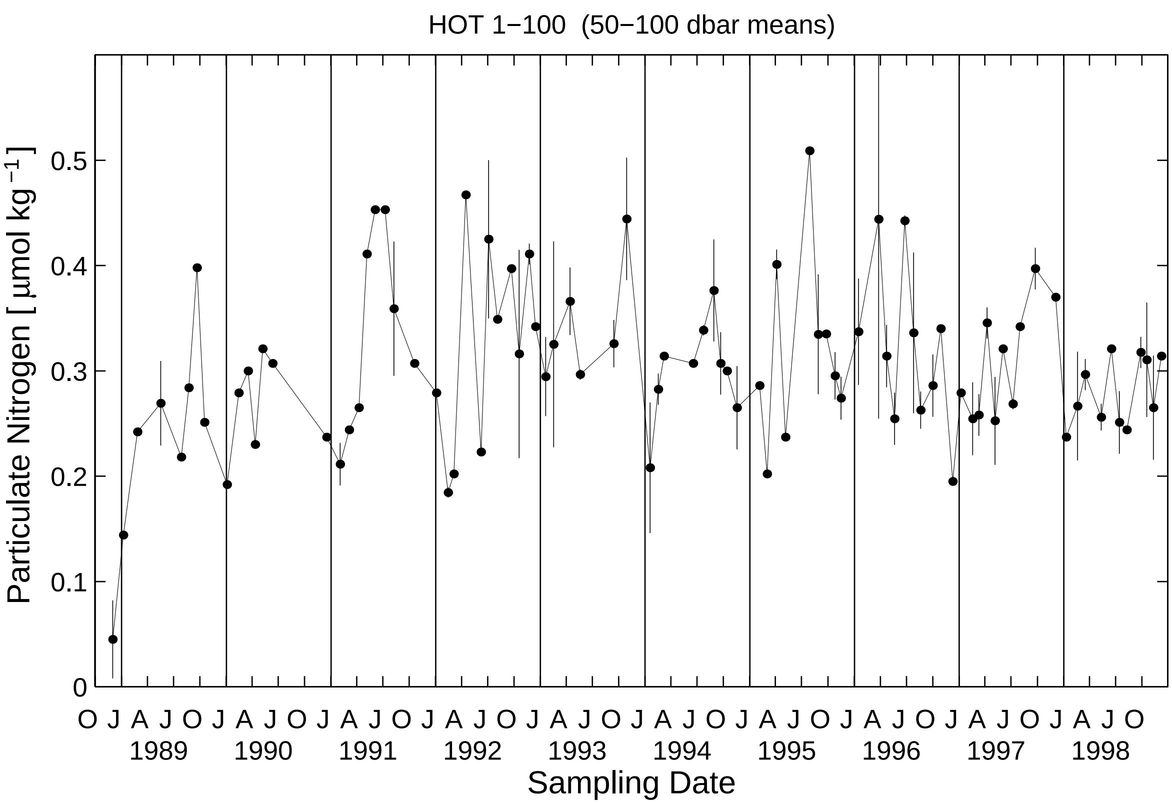
HOT 1−100 (50−100 dbar means)
Particulate Nitrogen [µmol kg⁻¹]
0
0.1
0.2
0.3
0.4
0.5
O J A J O J A J O J A J O J A J O J A J O J A J O J A J O J A J O J A J O J A J O
1989
1990
1991
1992
1993
1994
1995
1996
1997
1998
Sampling Date

Figure 6.5.8

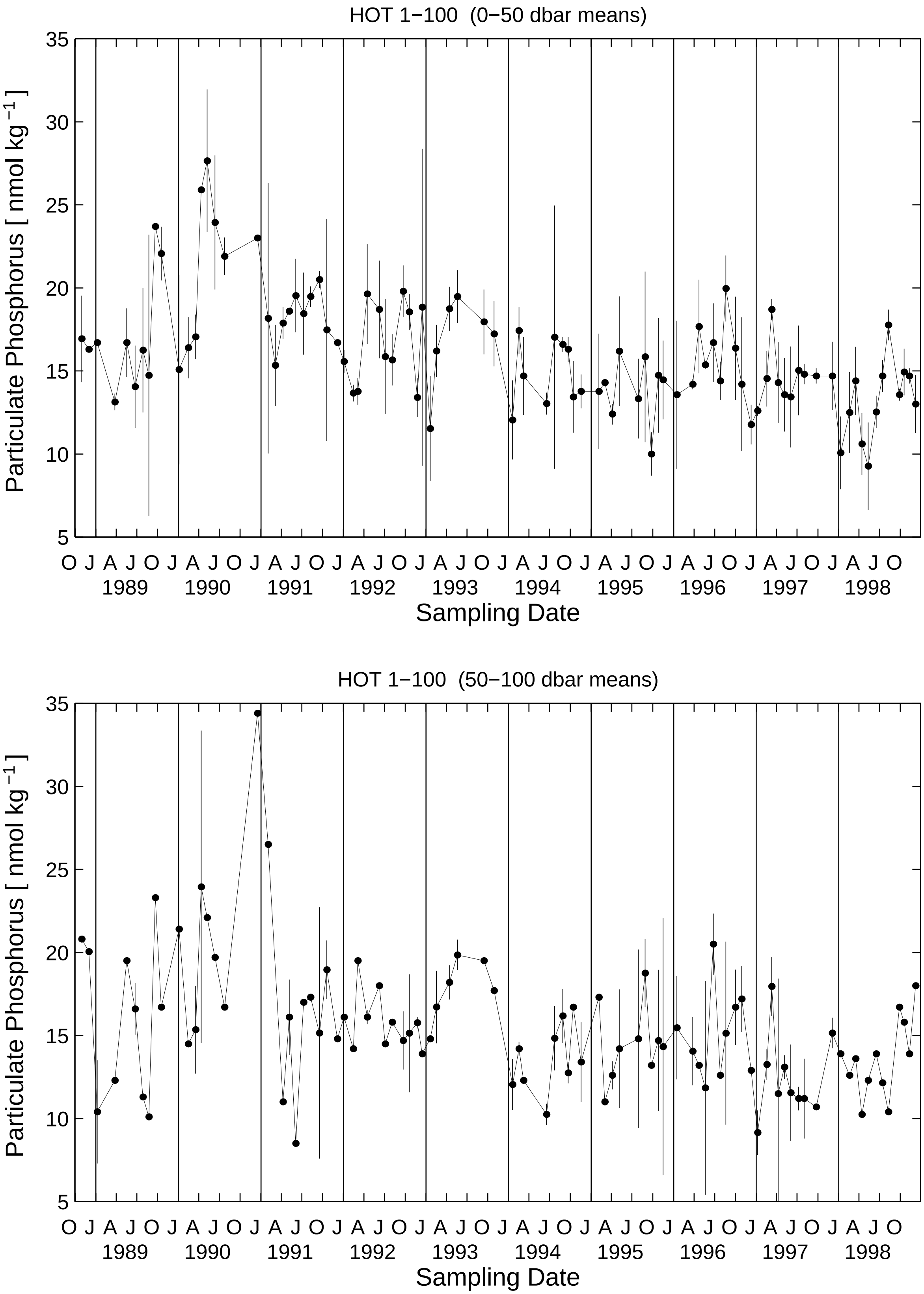
HOT 1−100 (0−50 dbar means)
Particulate Phosphorus [nmol kg⁻¹]
35
30
25
20
15
10
5
O J A J O J A J O J A J O J A J O J A J O J A J O J A J O J A J O J A J O J A J O
1989 1990 1991 1992 1993 1994 1995 1996 1997 1998
Sampling Date
HOT 1−100 (50−100 dbar means)
Particulate Phosphorus [nmol kg⁻¹]
35
30
25
20
15
10
5
O J A J O J A J O J A J O J A J O J A J O J A J O J A J O J A J O J A J O J A J O
1989 1990 1991 1992 1993 1994 1995 1996 1997 1998
Sampling Date

Figure 6.5.9

6.6. Primary Production and Particle Flux

Figure 6.6.1: Integrated (0-200 m) primary production rates measured on all HOT cruises. Data for both in situ and on-deck incubations are presented. On HOT-15 (March 1990) primary production was measured on three consecutive days.

Figure 6.6.2: Carbon flux at 150 m measured on all HOT cruises from 1988 through 1993. Error bars represent the standard deviation of replicate determinations.

Figure 6.6.3: Same as 6.5.2 but for nitrogen.

Figure 6.6.4: Same as 6.5.2 but for phosphorus.

Figure 6.6.5: Same as 6.5.2 but for total mass.

Figure 6.6.6: Contour plot of carbon flux for all cruises from 1988 through 1993.

Figure 6.6.7: Same as 6.6.6 but for nitrogen.

Figure 6.6.8: Same as 6.6.6 but for phosphorus.

Figure 6.6.9: Same as 6.6.6 but for total mass.

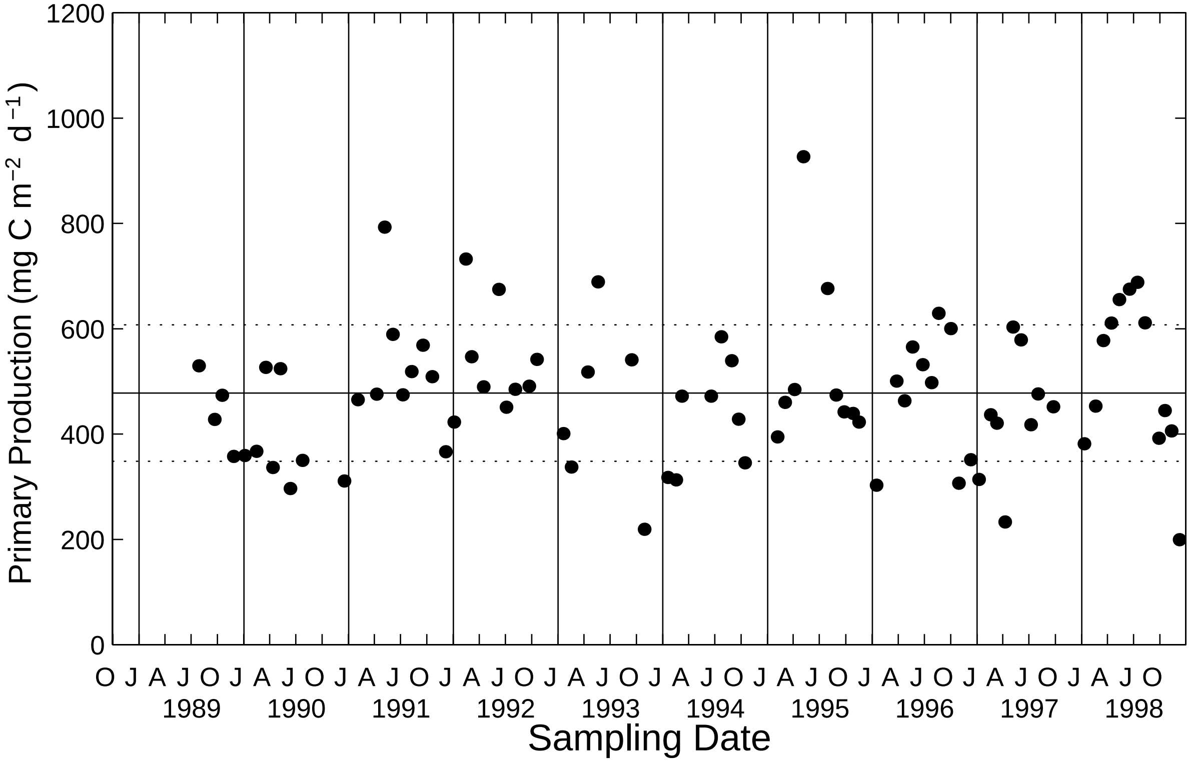

Primary Production (mg C m−2 d−1)
1200
1000
800
600
400
200
0
O J A J O J A J O J A J O J A J O J A J O J A J O J A J O J A J O J A J O J A J O
1989 1990 1991 1992 1993 1994 1995 1996 1997 1998
Sampling Date

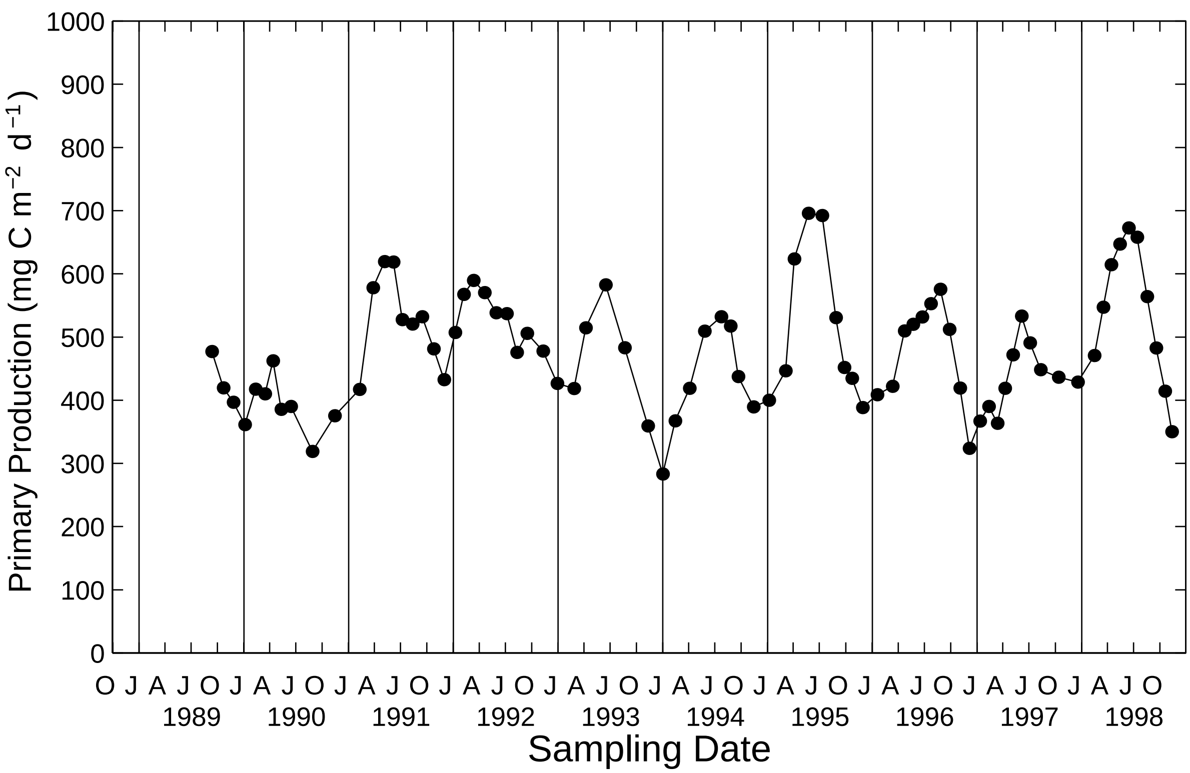

Primary Production (mg C m−2 d−1)
1000
900
800
700
600
500
400
300
200
100
0
O J A J O J A J O J A J O J A J O J A J O J A J O J A J O J A J O J A J O J A J O
1989 1990 1991 1992 1993 1994 1995 1996 1997 1998
Sampling Date

Figure 6.6.1

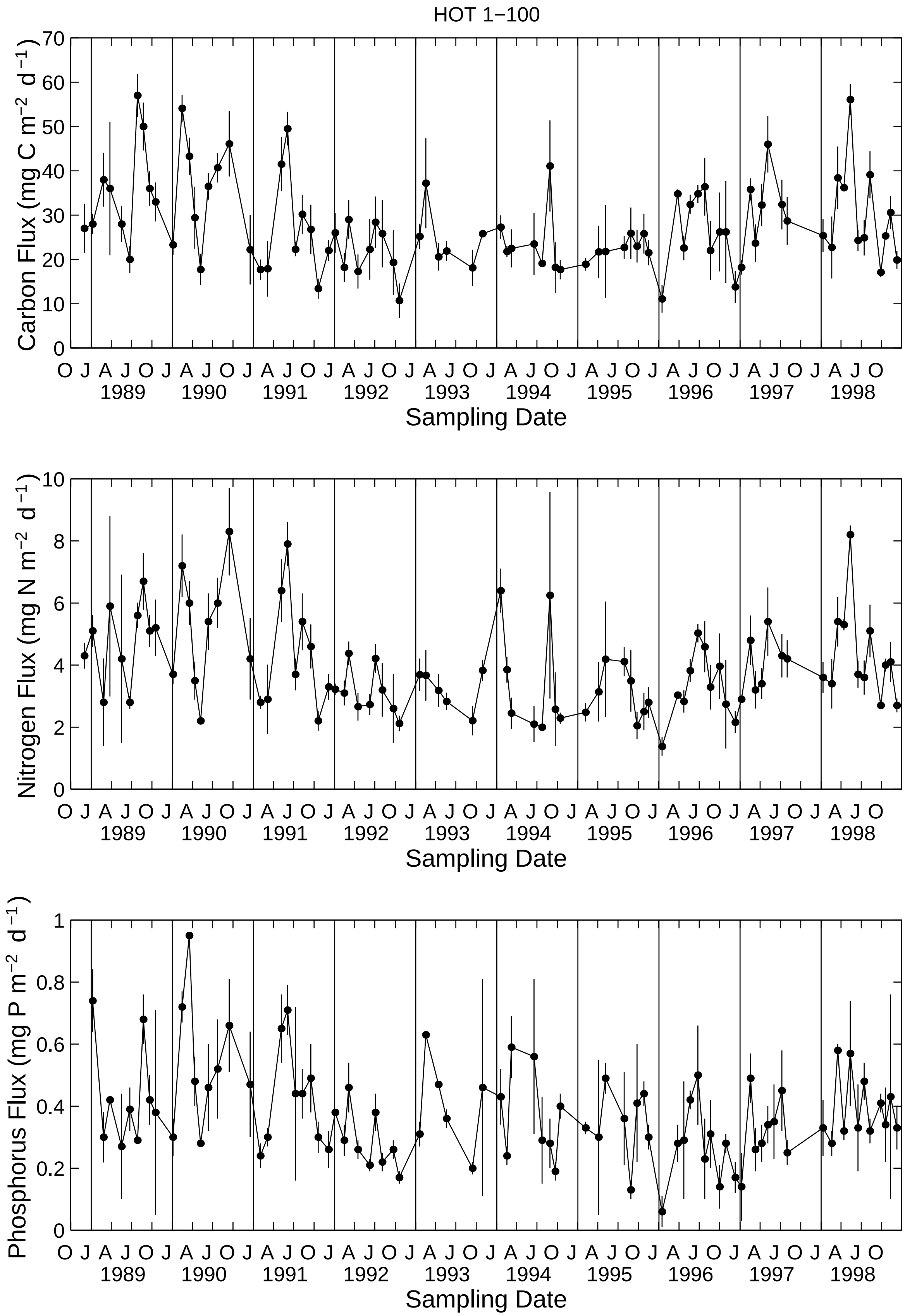

Figure 6.6.2, 6.6.3, 6.6.4

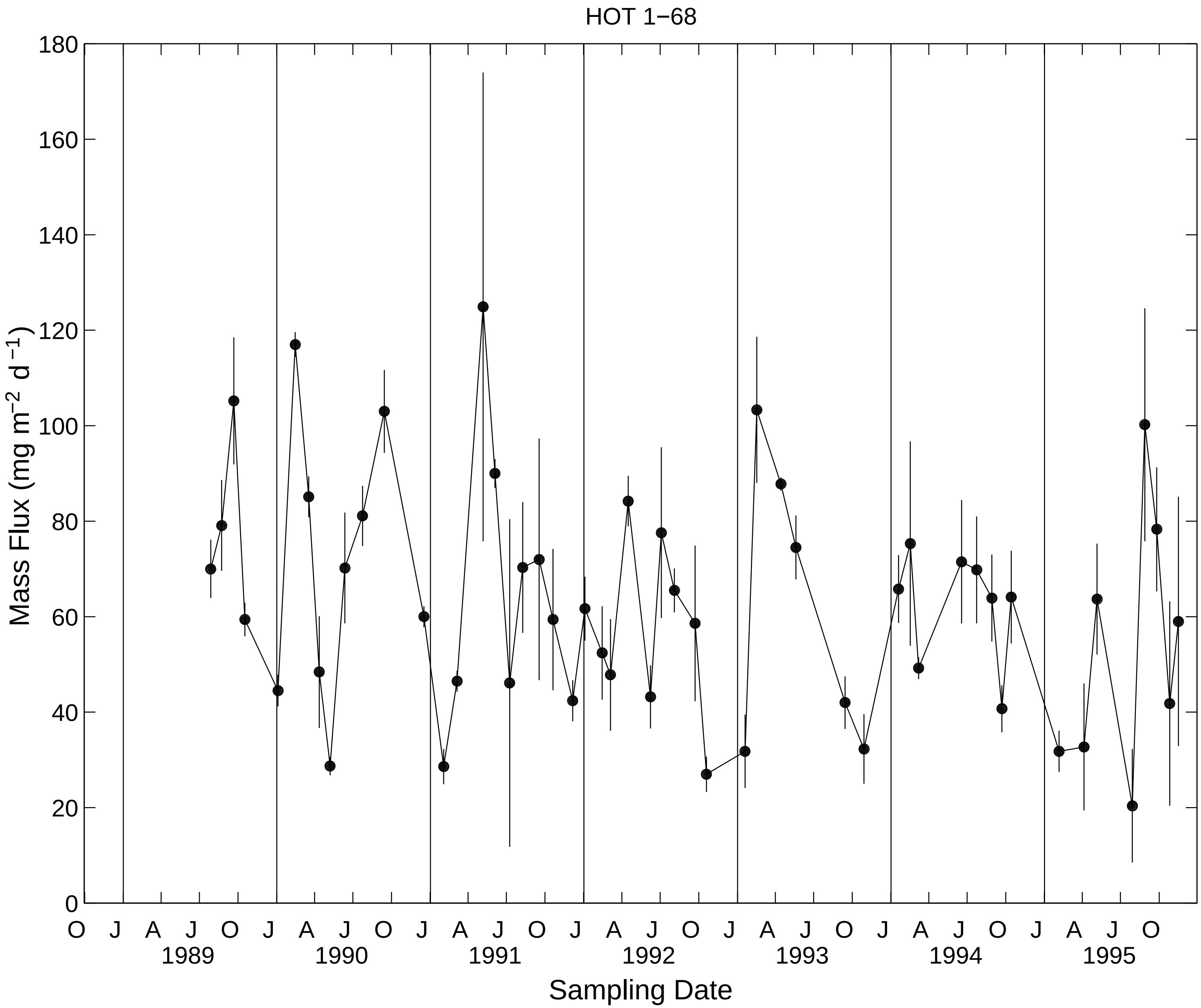
HOT 1−68
Mass Flux (mg m^{-2} d^{-1})
0
20
40
60
80
100
120
140
160
180
O J A J O J A J O J A J O J A J O J A J O J A J O J A J O
1989
1990
1991
1992
1993
1994
1995
Sampling Date

Figure 6.6.5

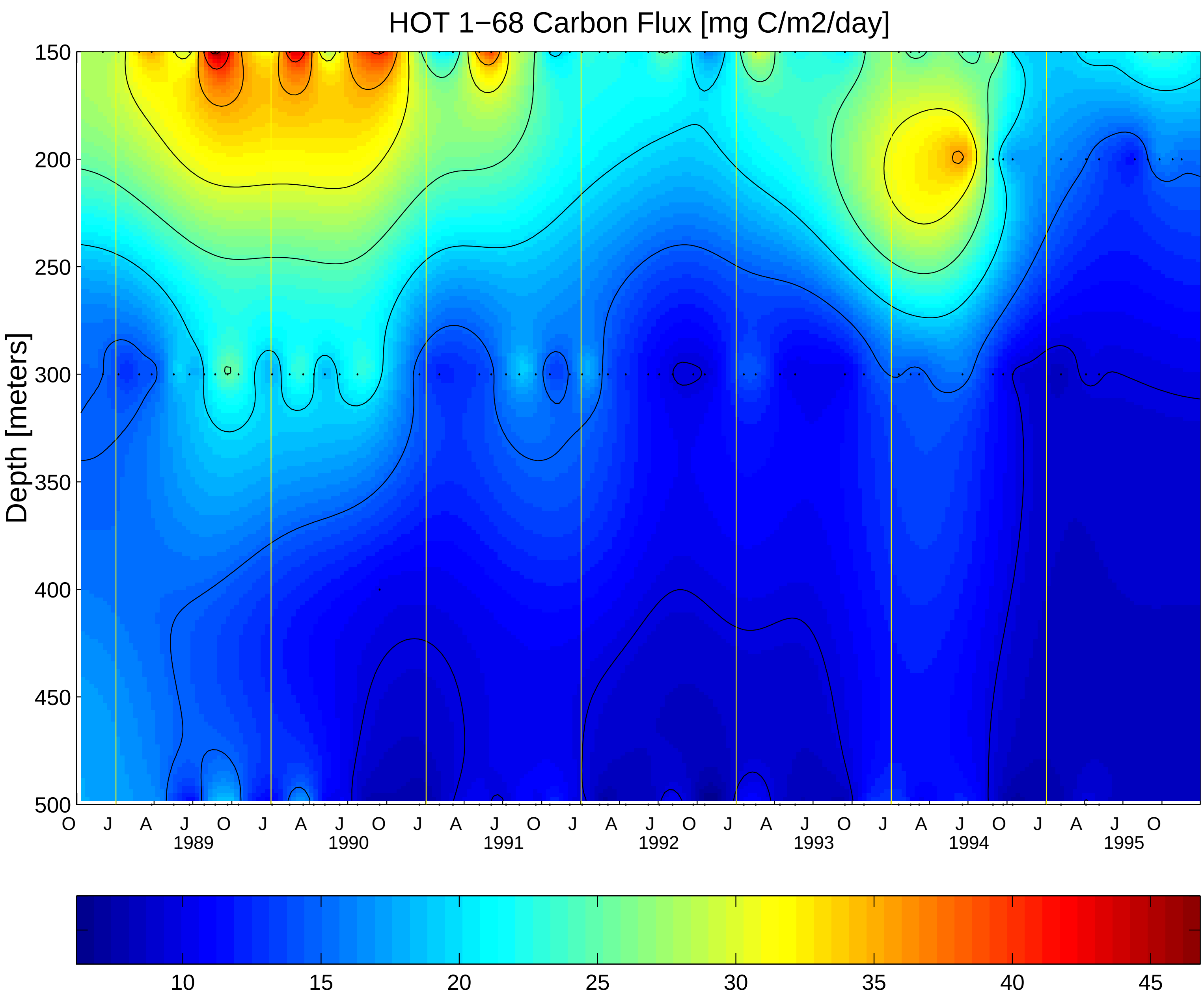
HOT 1−68 Carbon Flux [mg C/m2/day]
Depth [meters]
150
200
250
300
350
400
450
500
O J A J O J A J O J A J O J A J O J A J O J A J O J A J O
1989
1990
1991
1992
1993
1994
1995
10 15 20 25 30 35 40 45

Figure 6.6.6

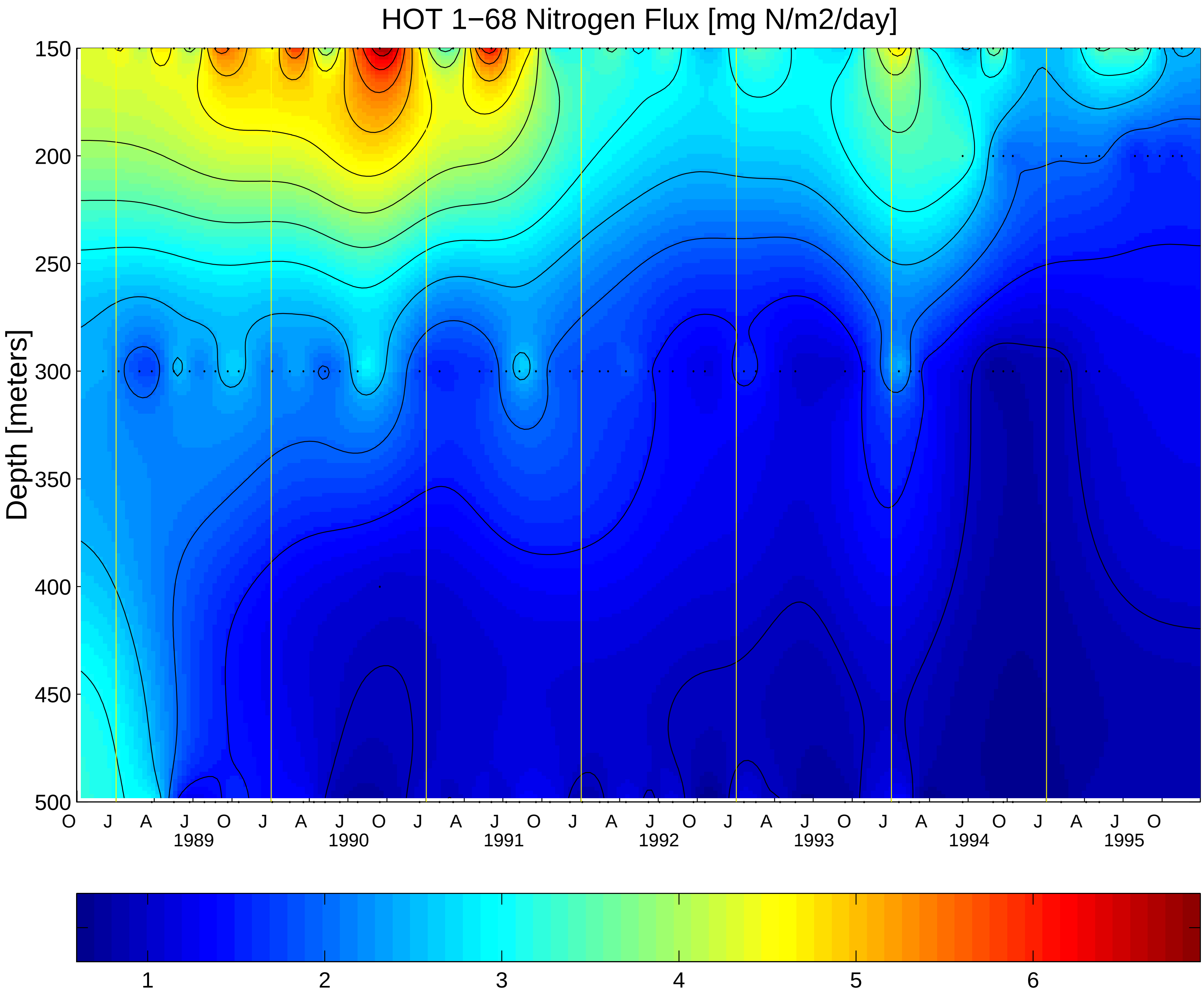
HOT 1−68 Nitrogen Flux [mg N/m2/day]
Depth [meters]
150
200
250
300
350
400
450
500
O J A J O J A J O J A J O J A J O J A J O J A J O J A J O
1989
1990
1991
1992
1993
1994
1995
1
2
3
4
5
6

Figure 6.6.7

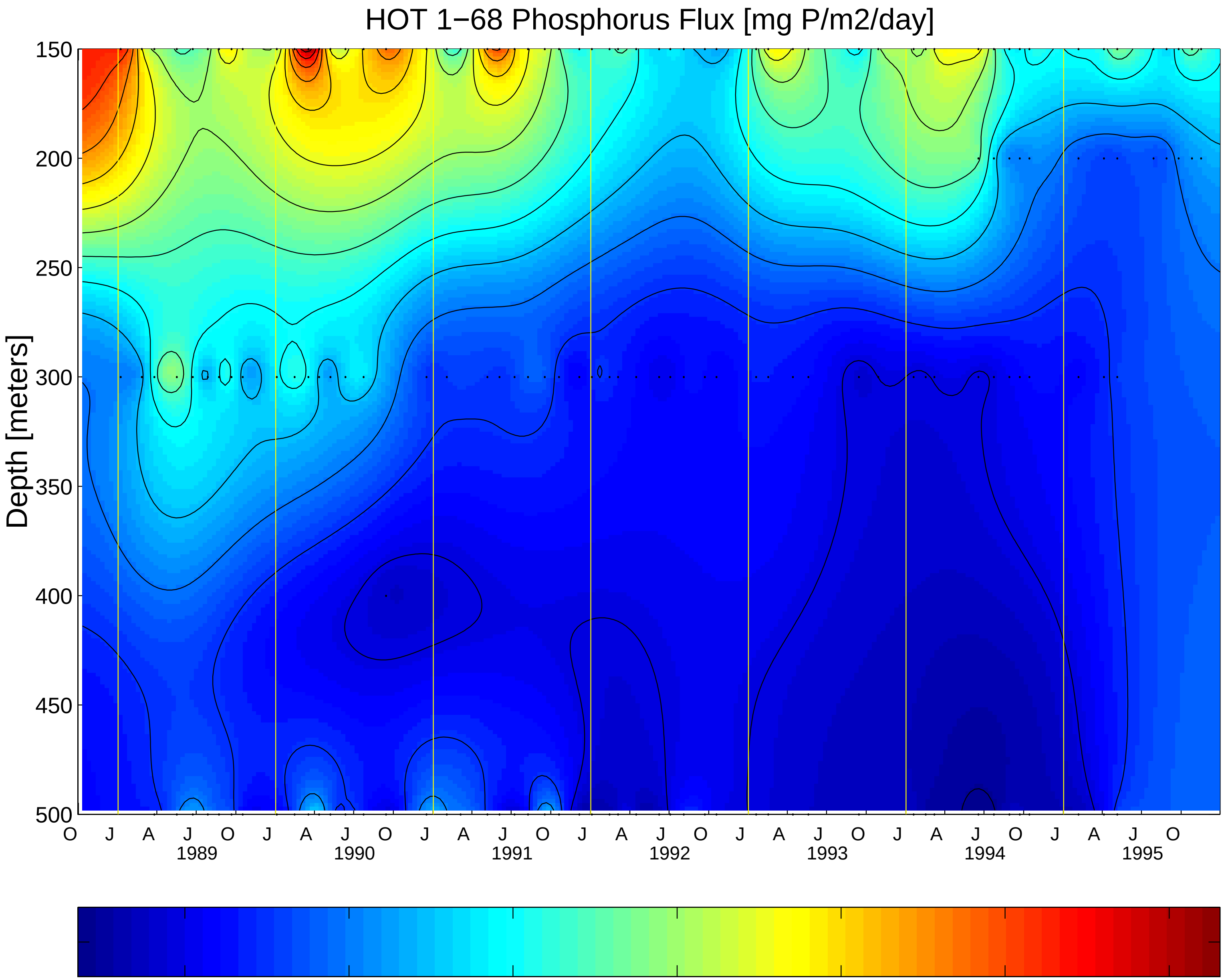

HOT 1−68 Phosphorus Flux [mg P/m2/day]
Depth [meters]
150
200
250
300
350
400
450
500
O J A J O J A J O J A J O J A J O J A J O J A J O J A J O
1989
1990
1991
1992
1993
1994
1995
0.1
0.2
0.3
0.4
0.5
0.6
0.7

Figure 6.6.8

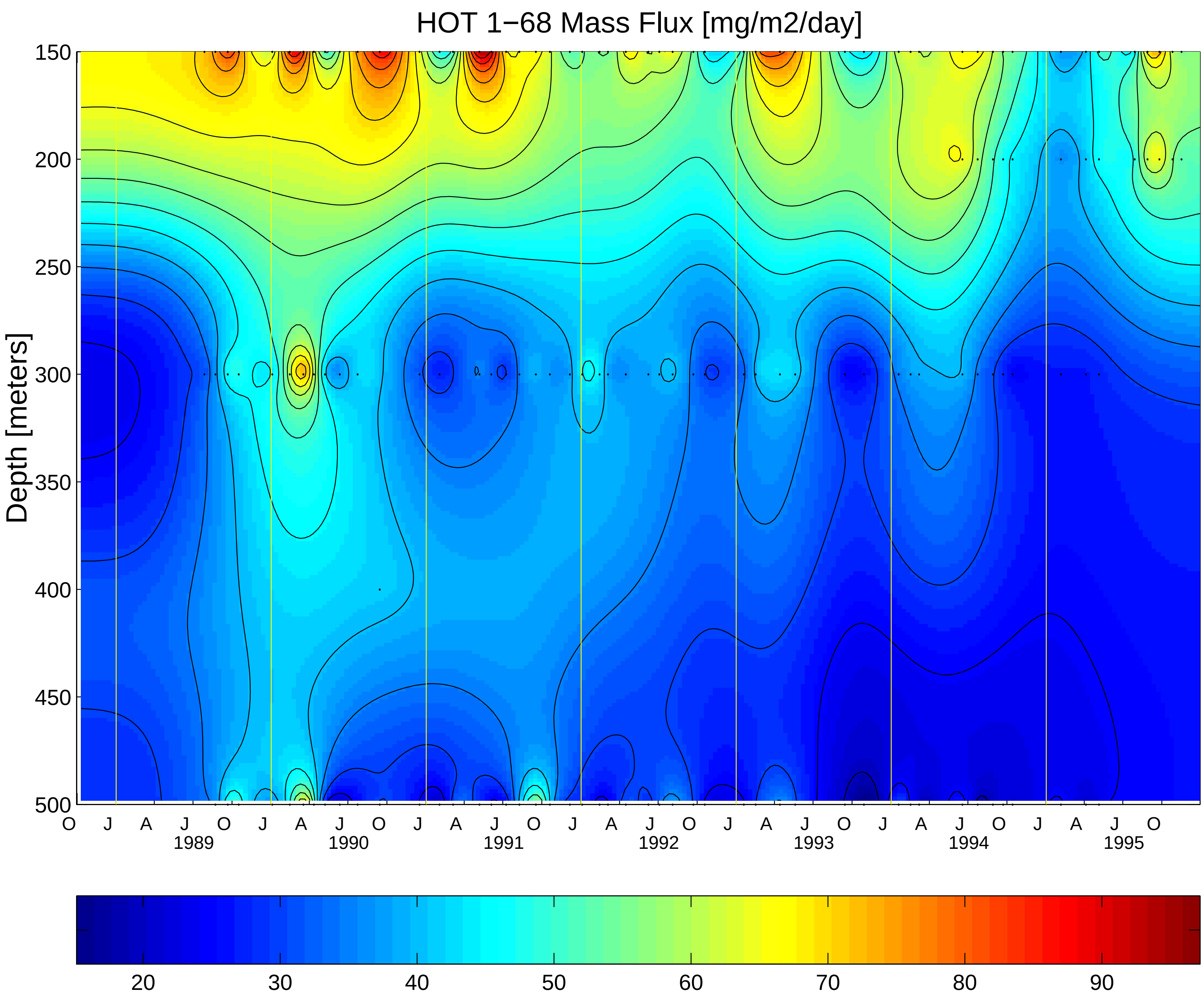
HOT 1−68 Mass Flux [mg/m2/day]
Depth [meters]
150
200
250
300
350
400
450
500
O J A J O J A J O J A J O J A J O J A J O J A J O J A J O
1989
1990
1991
1992
1993
1994
1995
20
30
40
50
60
70
80
90

Figure 6.6.9

6.7. ADCP Measurements

For each cruise with shipboard ADCP, the following figures are provided:

Figures 6.7.1a-f: Velocity fields at Station ALOHA. Top panel shows hourly averages at 20-m depth intervals while the ship was at Station ALOHA. The orientation of each stick gives the direction of the current: up is northward, to the right is eastward. The bottom panel shows the results of a least-squares fit of the hourly averages to a mean, trend, semidiurnal and diurnal tides and an inertial cycle. In the first column, the arrow shows the mean current, and the headless stick shows the sum of the mean plus the trend at the end of the station. For each harmonic, the current ellipse is shown in the first column. The orientation of the stick in the second column shows the direction of that harmonic component of the current at the beginning of the station, and the arrowhead at the end of the stick shows the direction of rotation of the current vector around the ellipse.

Figures 6.7.2a-f: Velocity field on the transits to and from the Station ALOHA. Velocity is shown as a function of latitude, averaged in 10-minute time intervals. Because HOT-49 was conducted in two segments, ADCP data are available for both legs on this cruise.

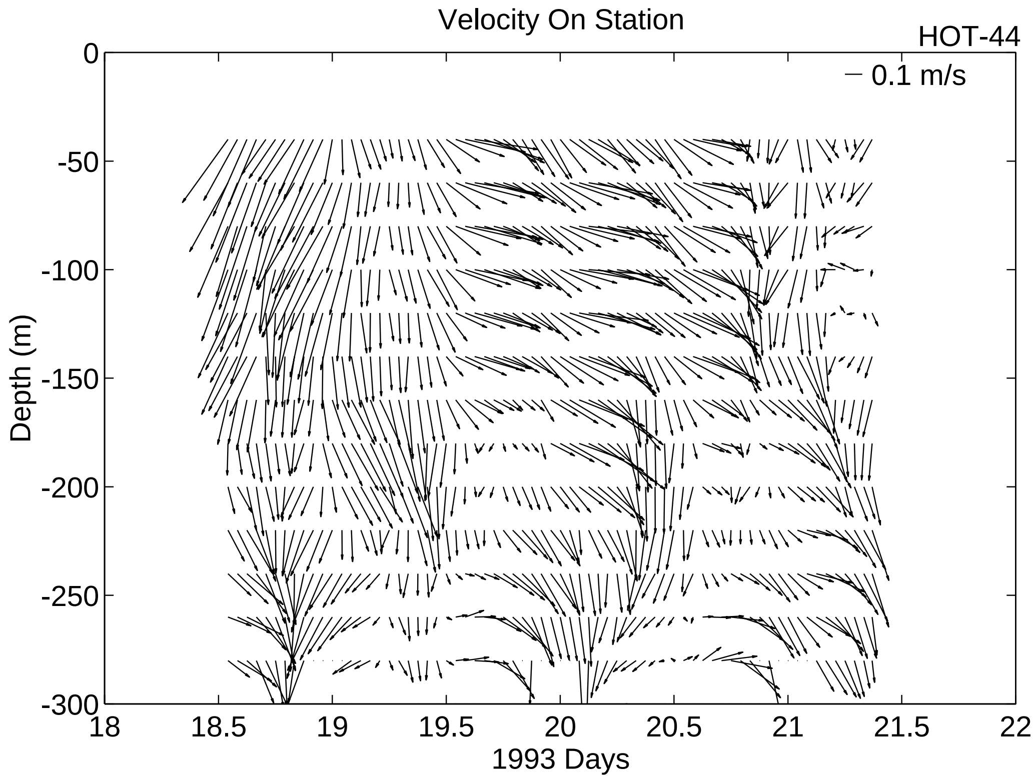

Velocity On Station
HOT-44
0.1 m/s
Depth (m)
0
-50
-100
-150
-200
-250
-300
18
18.5
19
19.5
20
20.5
21
21.5
22
1993 Days

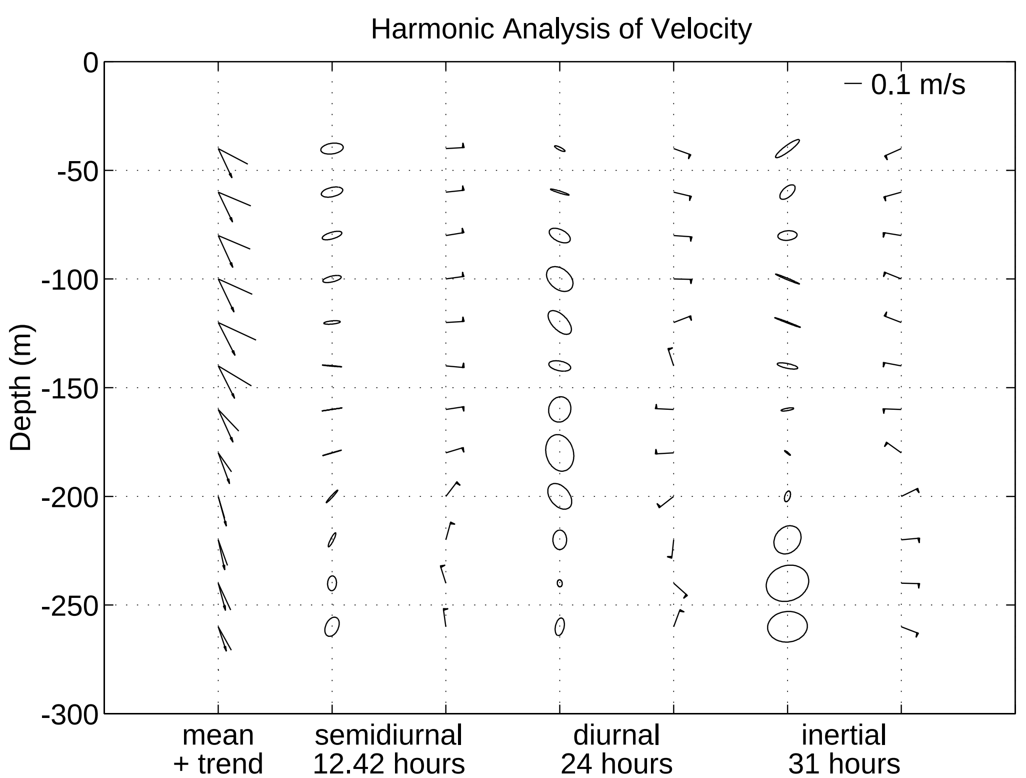

Harmonic Analysis of Velocity
0.1 m/s
Depth (m)
0
-50
-100
-150
-200
-250
-300
mean
+ trend
semidiurnal
12.42 hours
diurnal
24 hours
inertial
31 hours

Figure 6.7.1a

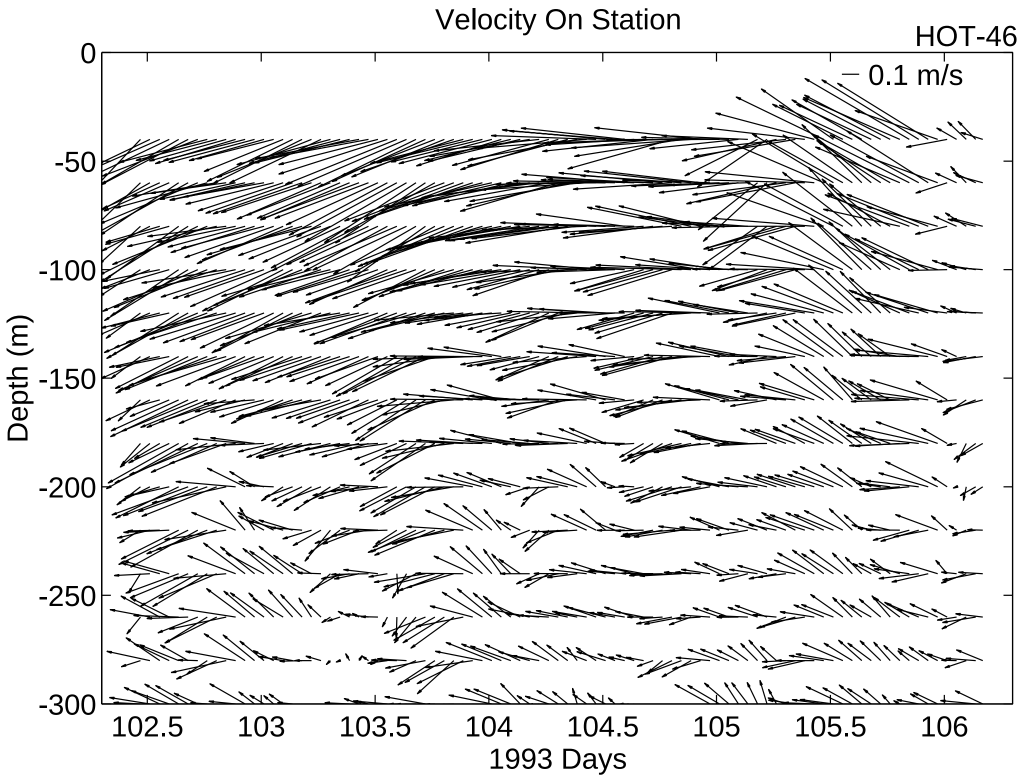
Velocity On Station
HOT-46
0.1 m/s
Depth (m)
0
-50
-100
-150
-200
-250
-300
102.5
103
103.5
104
104.5
105
105.5
106
1993 Days

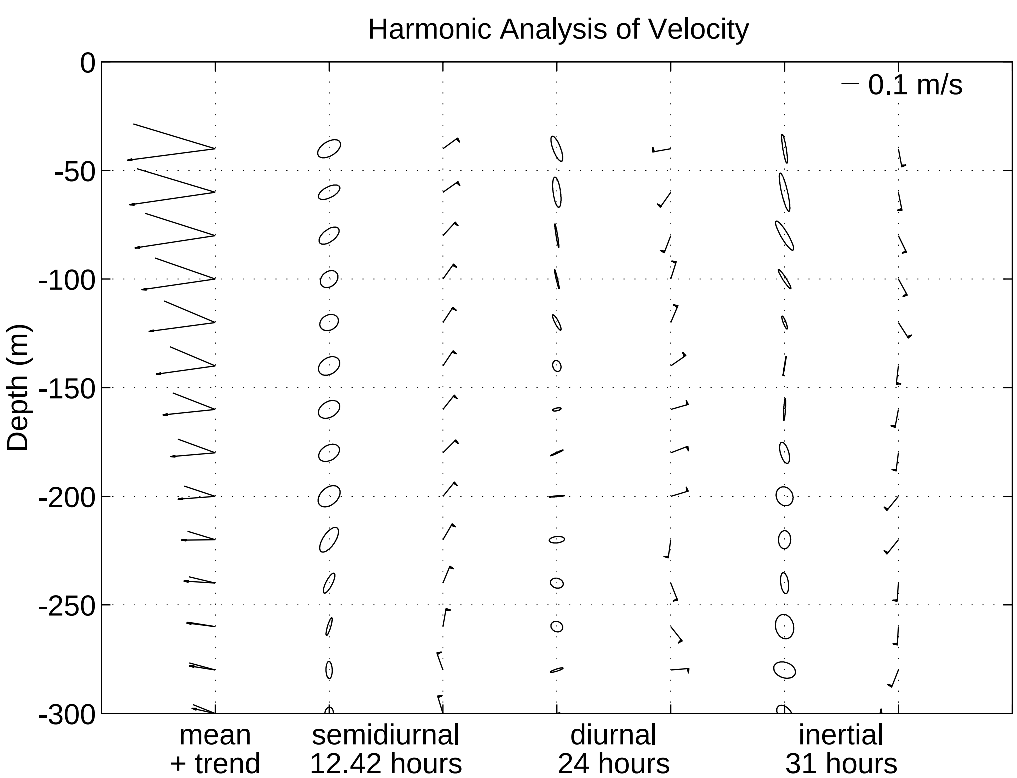
Harmonic Analysis of Velocity
0.1 m/s
Depth (m)
0
-50
-100
-150
-200
-250
-300
mean
+ trend
semidiurnal
12.42 hours
diurnal
24 hours
inertial
31 hours

Figure 6.7.1b

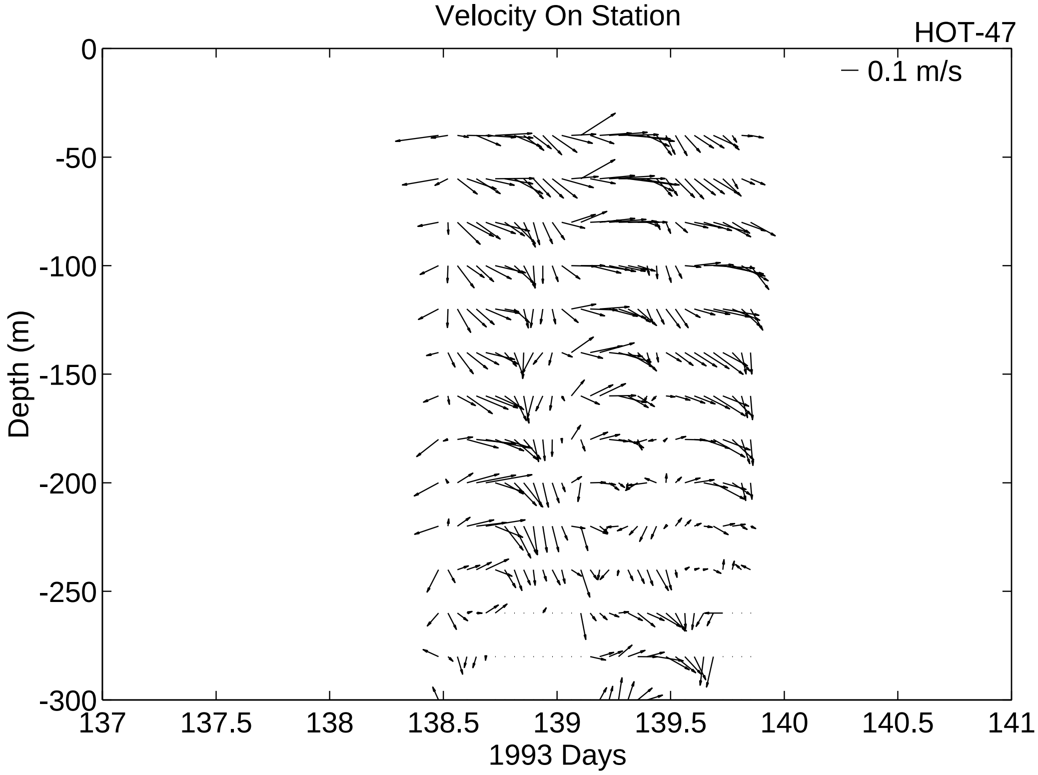

Velocity On Station
HOT-47
0.1 m/s
Depth (m)
0
-50
-100
-150
-200
-250
-300
137
137.5
138
138.5
139
139.5
140
140.5
141
1993 Days

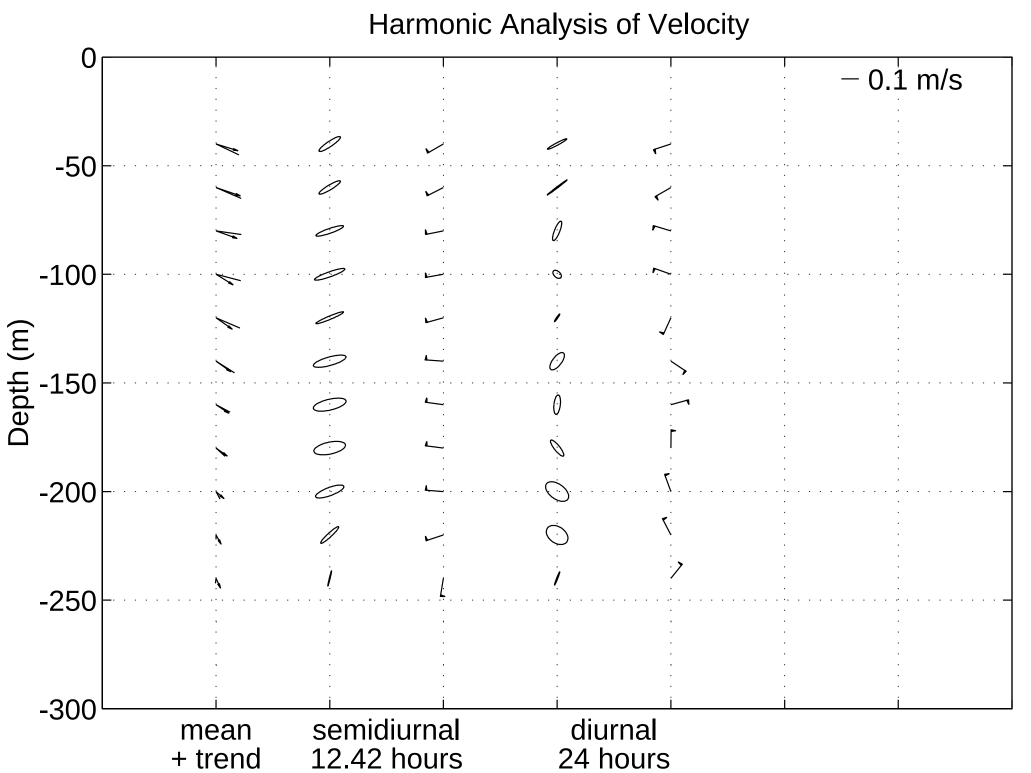

Harmonic Analysis of Velocity
0.1 m/s
Depth (m)
0
-50
-100
-150
-200
-250
-300
mean
+ trend
semidiurnal
12.42 hours
diurnal
24 hours

Figure 6.7.1c

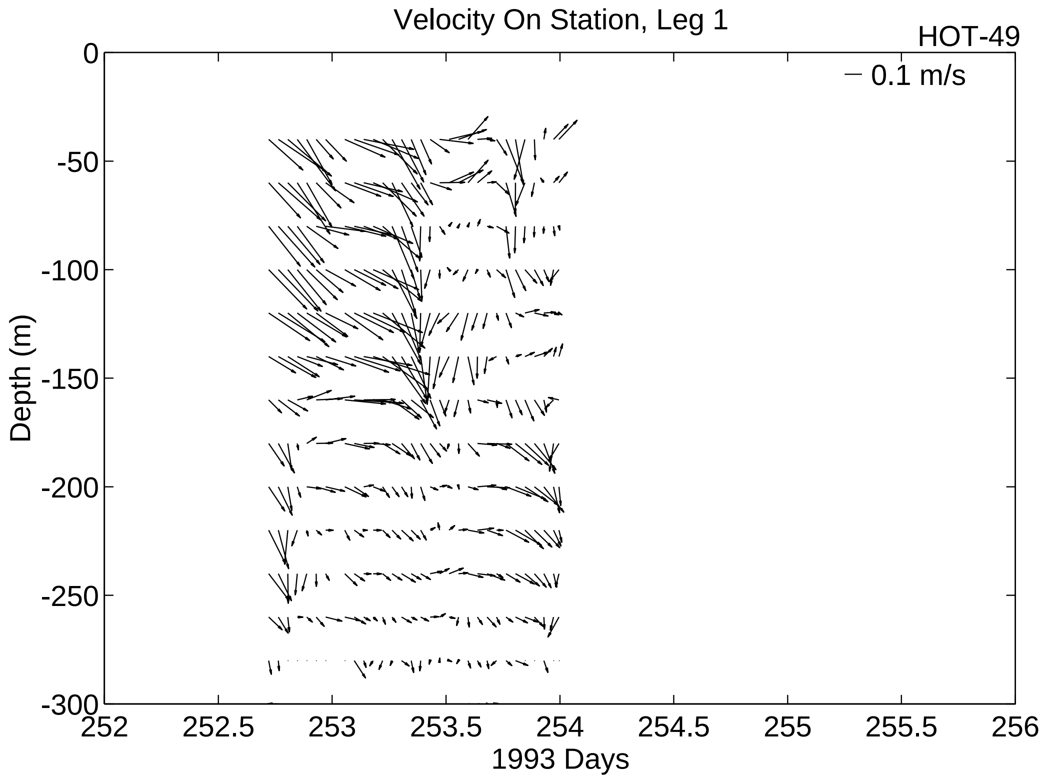

Velocity On Station, Leg 1
HOT-49
0.1 m/s
Depth (m)
0
-50
-100
-150
-200
-250
-300
252
252.5
253
253.5
254
254.5
255
255.5
256
1993 Days

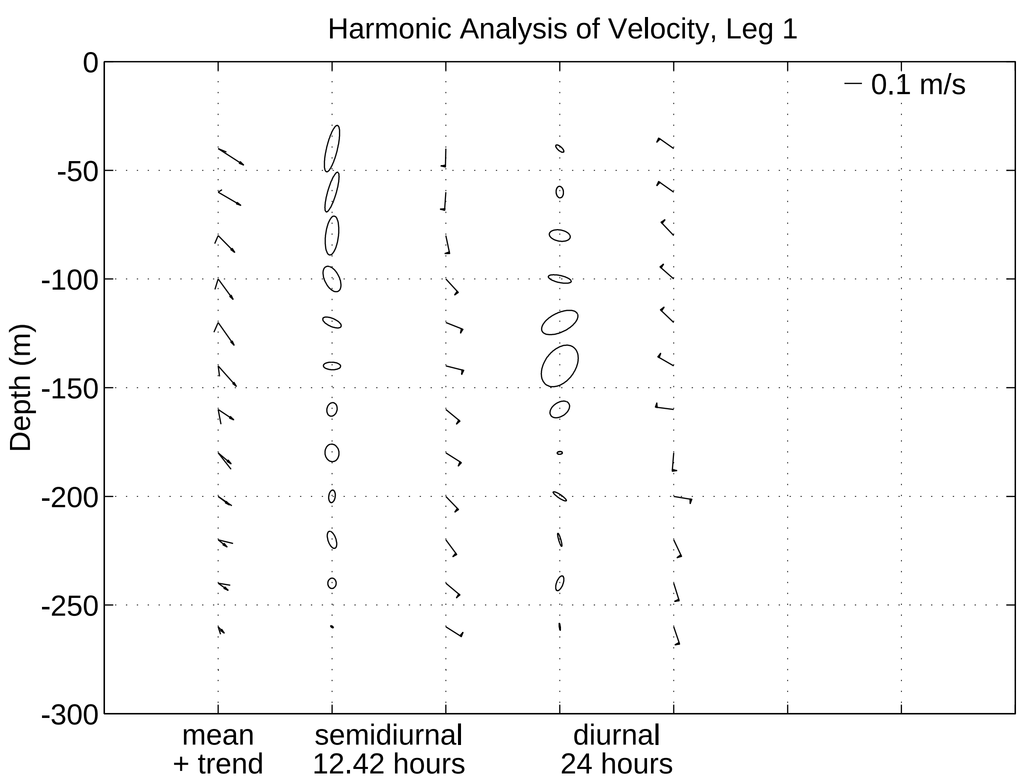

Harmonic Analysis of Velocity, Leg 1
0.1 m/s
Depth (m)
0
-50
-100
-150
-200
-250
-300
mean
+ trend
semidiurnal
12.42 hours
diurnal
24 hours

Figure 6.7.1d

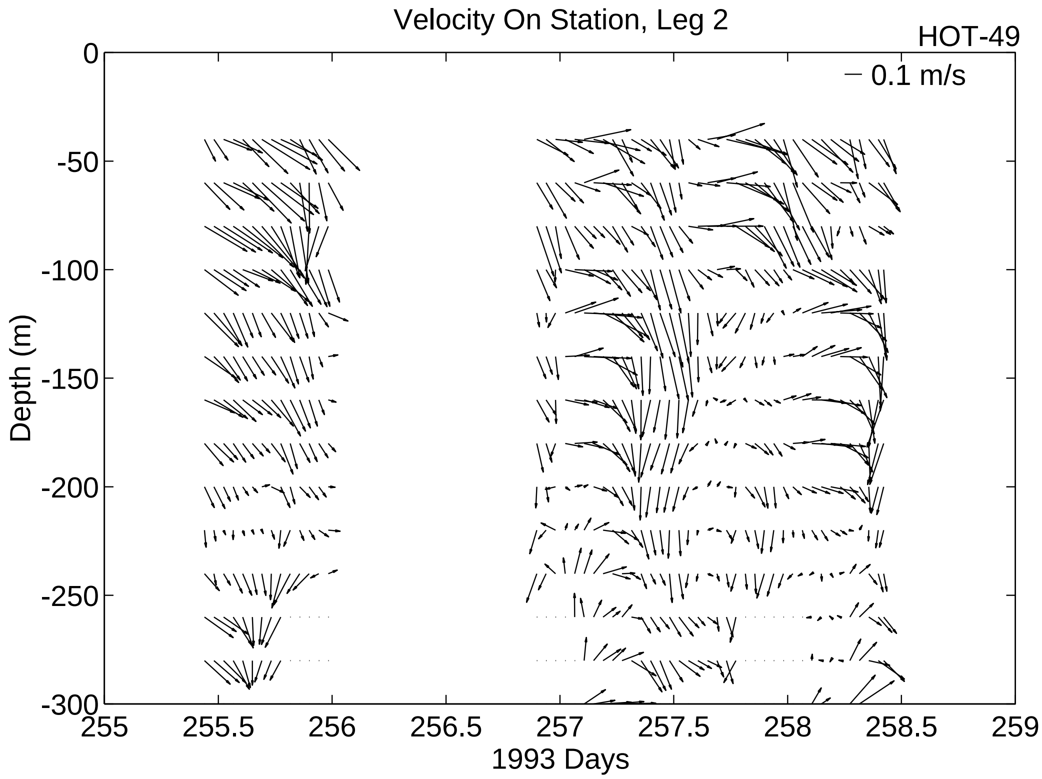

Velocity On Station, Leg 2
HOT-49
0.1 m/s
Depth (m)
0
-50
-100
-150
-200
-250
-300
255
255.5
256
256.5
257
257.5
258
258.5
259
1993 Days

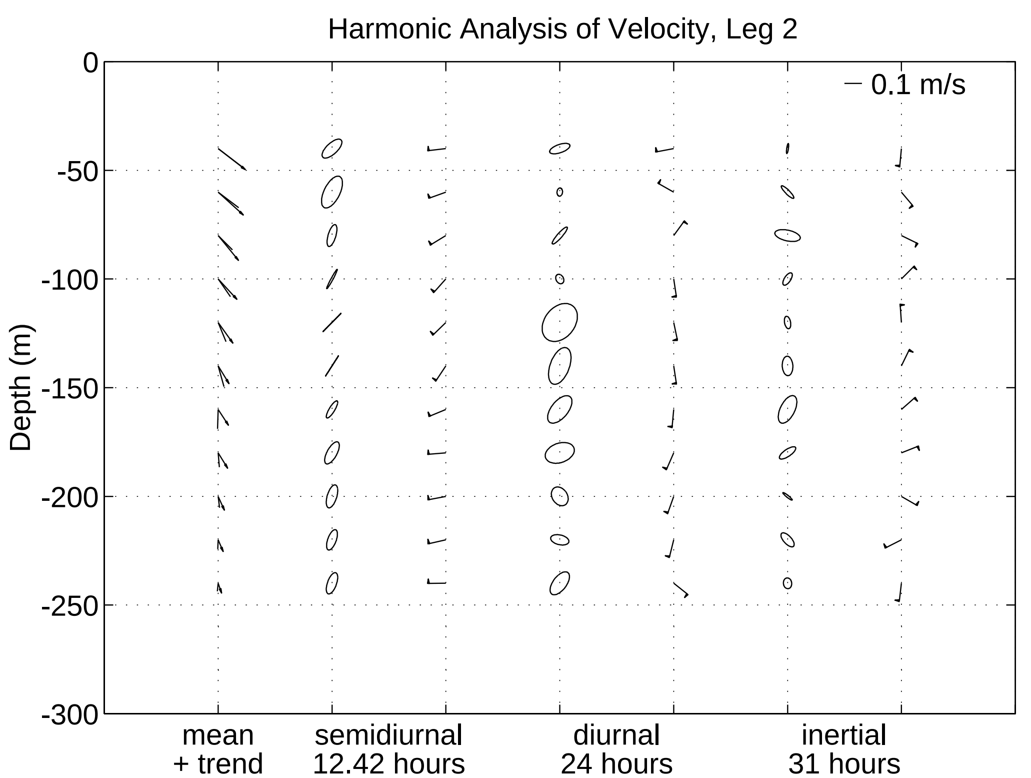

Harmonic Analysis of Velocity, Leg 2
0.1 m/s
Depth (m)
0
-50
-100
-150
-200
-250
-300
mean
+ trend
semidiurnal
12.42 hours
diurnal
24 hours
inertial
31 hours

Figure 6.7.1e

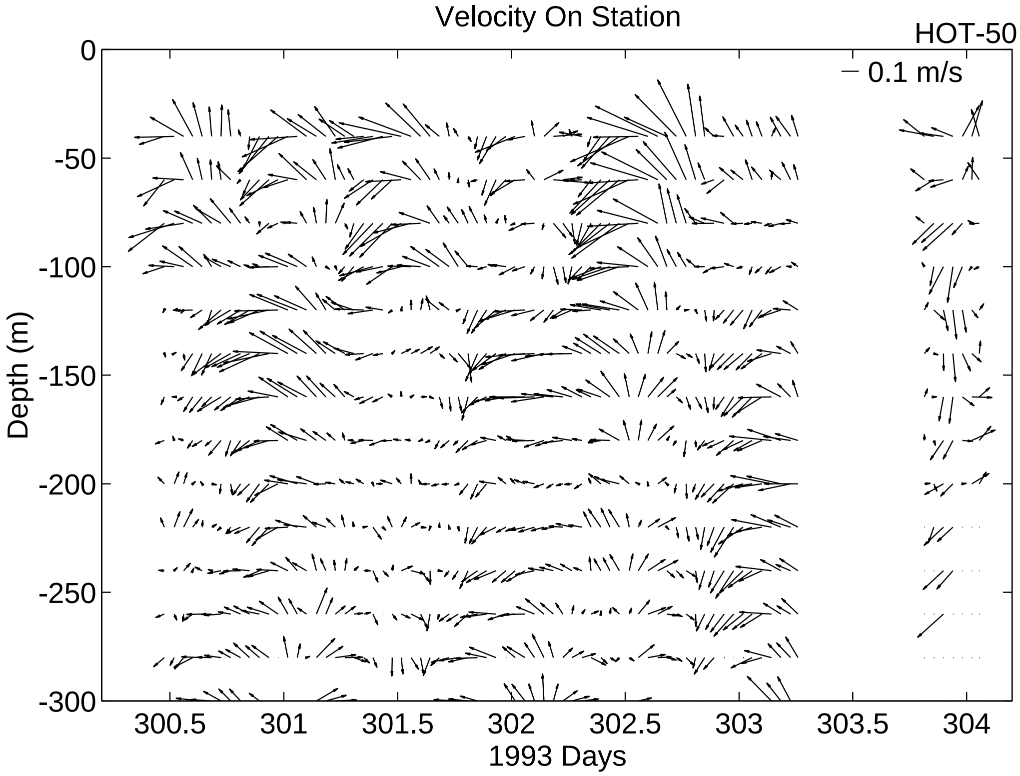

Velocity On Station
HOT-50
0.1 m/s
0
-50
-100
-150
-200
-250
-300
Depth (m)
300.5
301
301.5
302
302.5
303
303.5
304
1993 Days

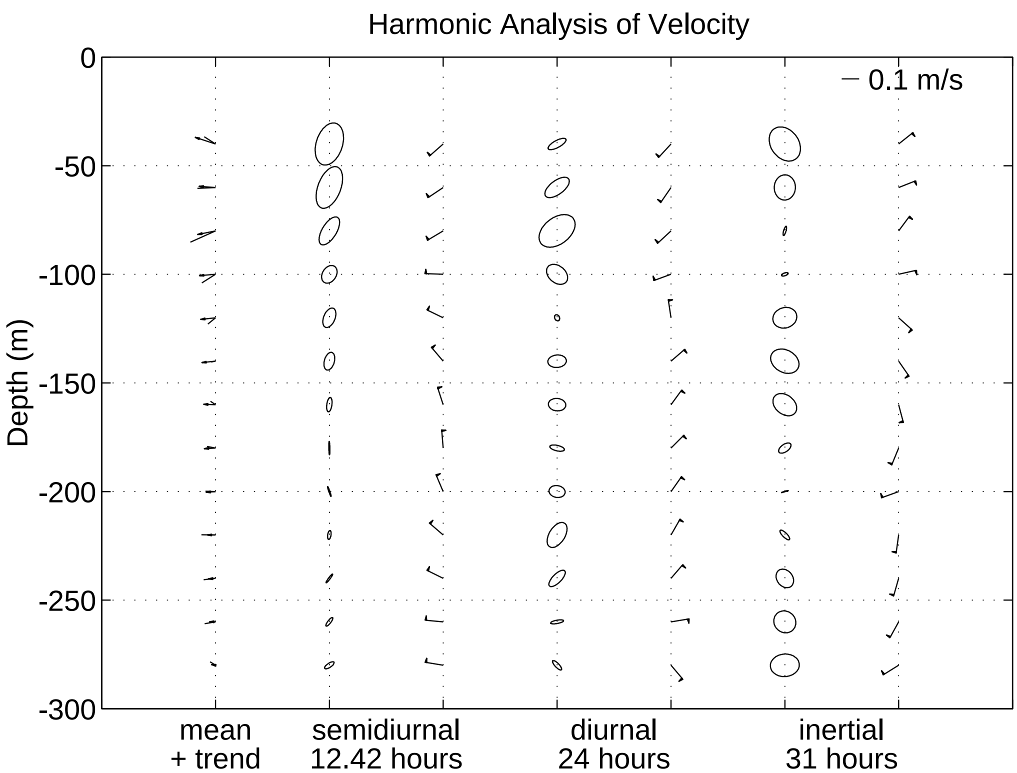

Harmonic Analysis of Velocity
0.1 m/s
0
-50
-100
-150
-200
-250
-300
Depth (m)
mean
+ trend
semidiurnal
12.42 hours
diurnal
24 hours
inertial
31 hours

Figure 6.7.1f

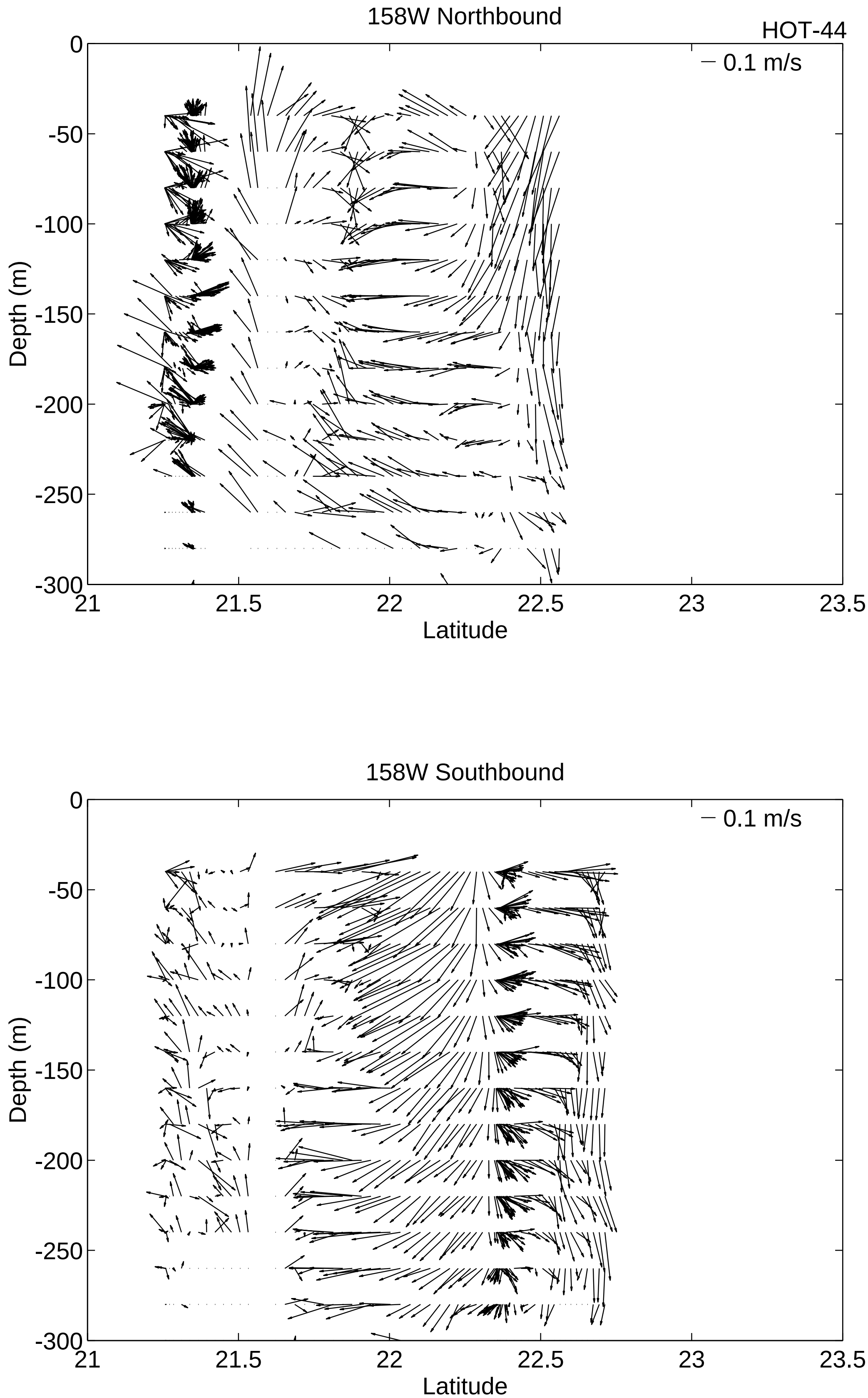
158W Northbound
HOT-44
0.1 m/s
Depth (m)
0
-50
-100
-150
-200
-250
-300
21
21.5
22
22.5
23
23.5
Latitude
158W Southbound
0.1 m/s
Depth (m)
0
-50
-100
-150
-200
-250
-300
21
21.5
22
22.5
23
23.5
Latitude

Figure 6.7.2a

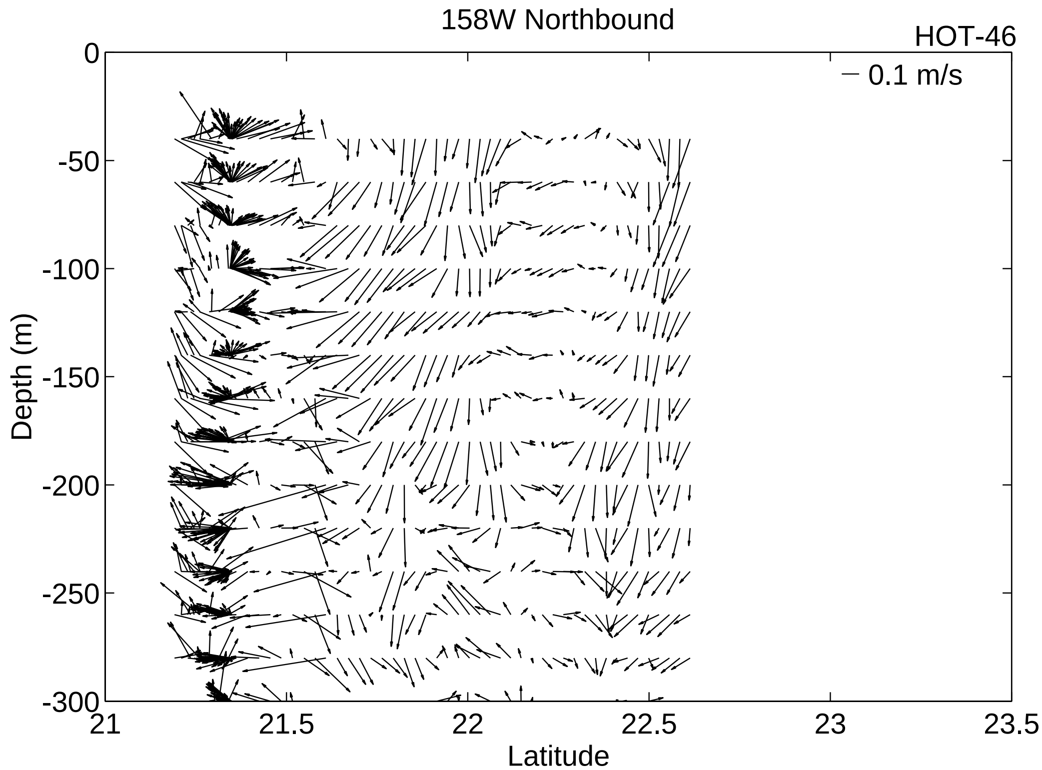

158W Northbound
HOT-46
0.1 m/s
Depth (m)
0
-50
-100
-150
-200
-250
-300
21
21.5
22
22.5
23
23.5
Latitude

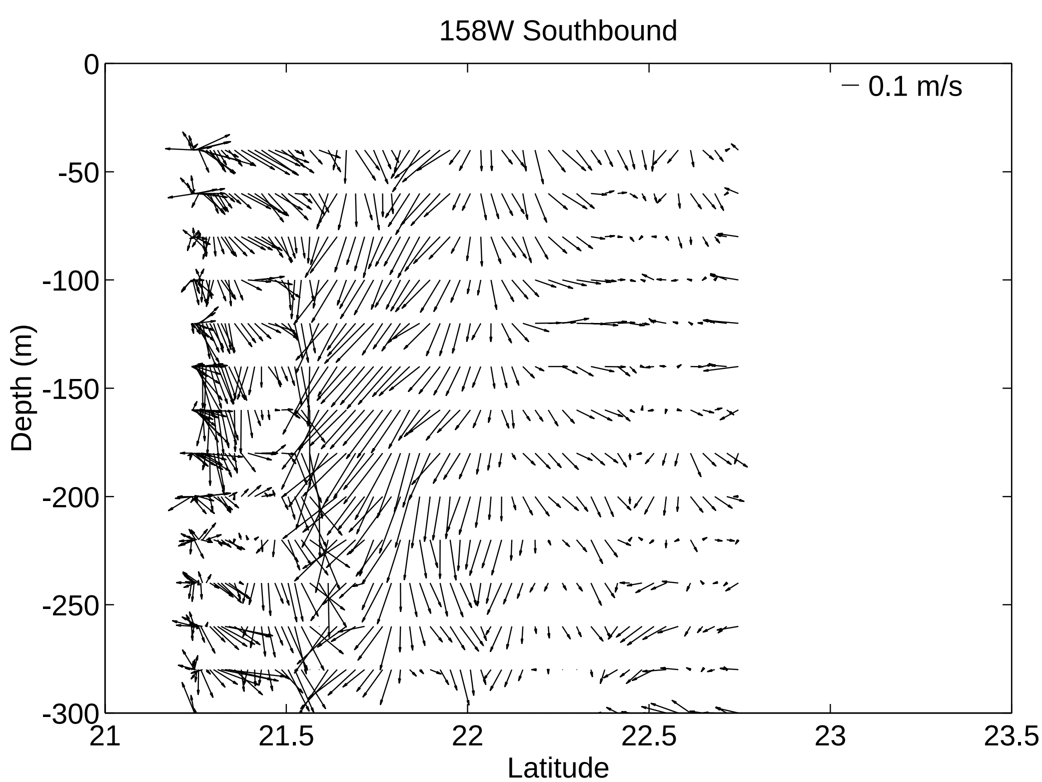

158W Southbound
0.1 m/s
Depth (m)
0
-50
-100
-150
-200
-250
-300
21
21.5
22
22.5
23
23.5
Latitude

Figure 6.7.2b

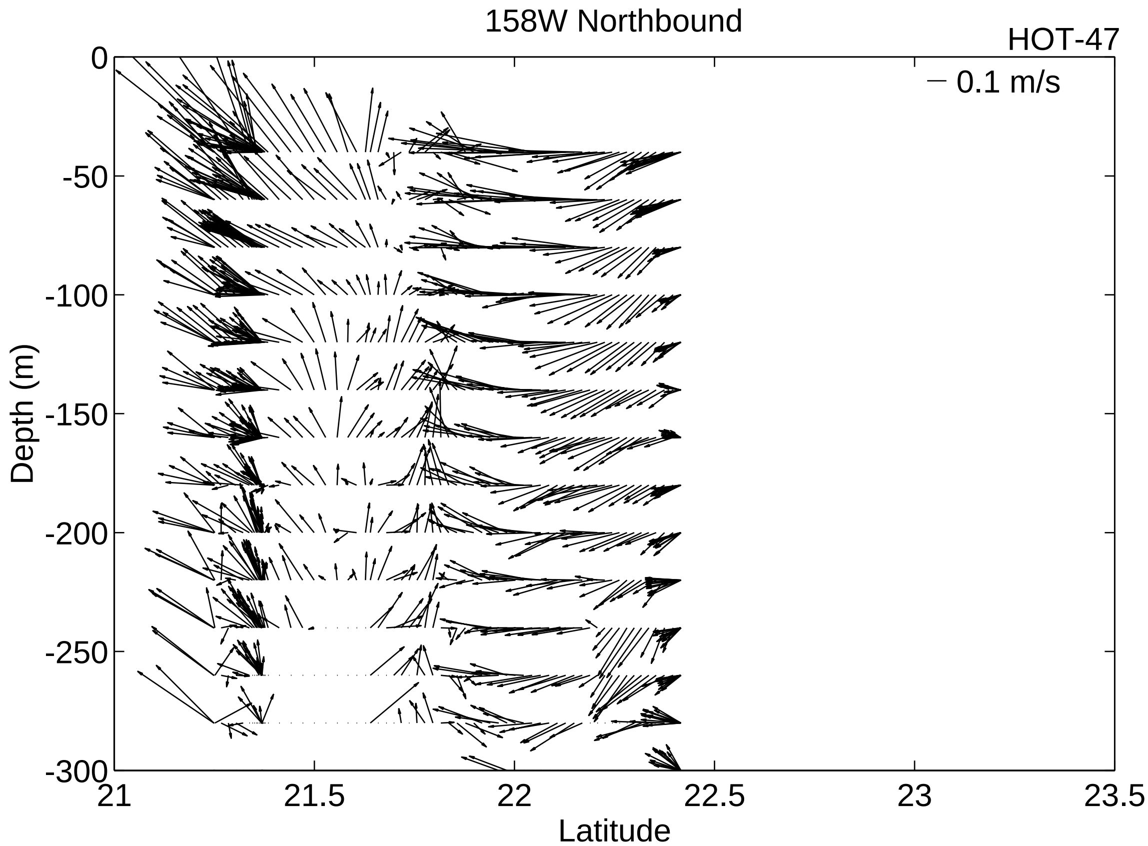

158W Northbound
HOT-47
0.1 m/s
Depth (m)
0
-50
-100
-150
-200
-250
-300
21
21.5
22
22.5
23
23.5
Latitude

Figure 6.7.2c

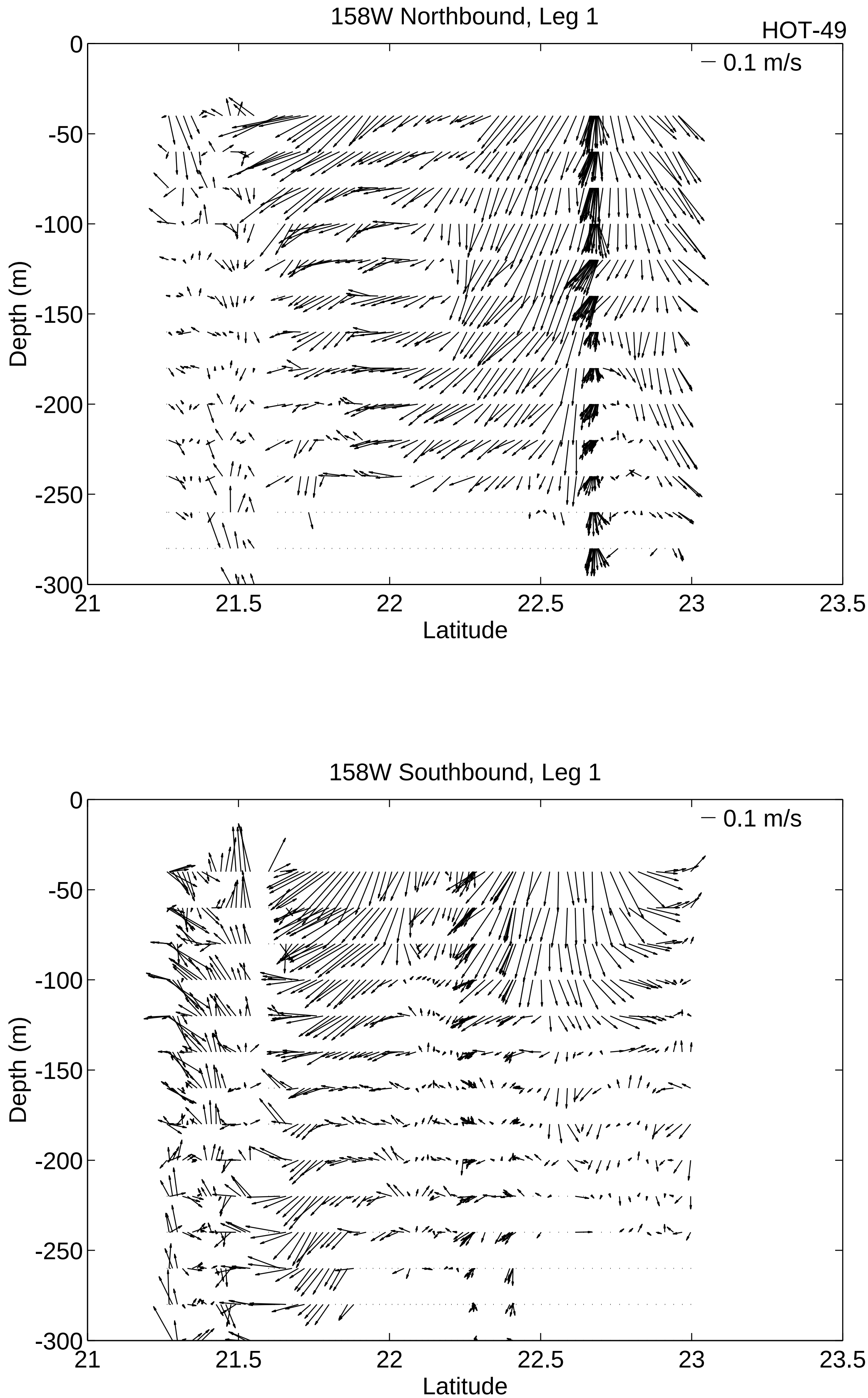

158W Northbound, Leg 1
HOT-49
0.1 m/s
Depth (m)
0
-50
-100
-150
-200
-250
-300
21
21.5
22
22.5
23
23.5
Latitude
158W Southbound, Leg 1
0.1 m/s
Depth (m)
0
-50
-100
-150
-200
-250
-300
21
21.5
22
22.5
23
23.5
Latitude

Figure 6.7.2d

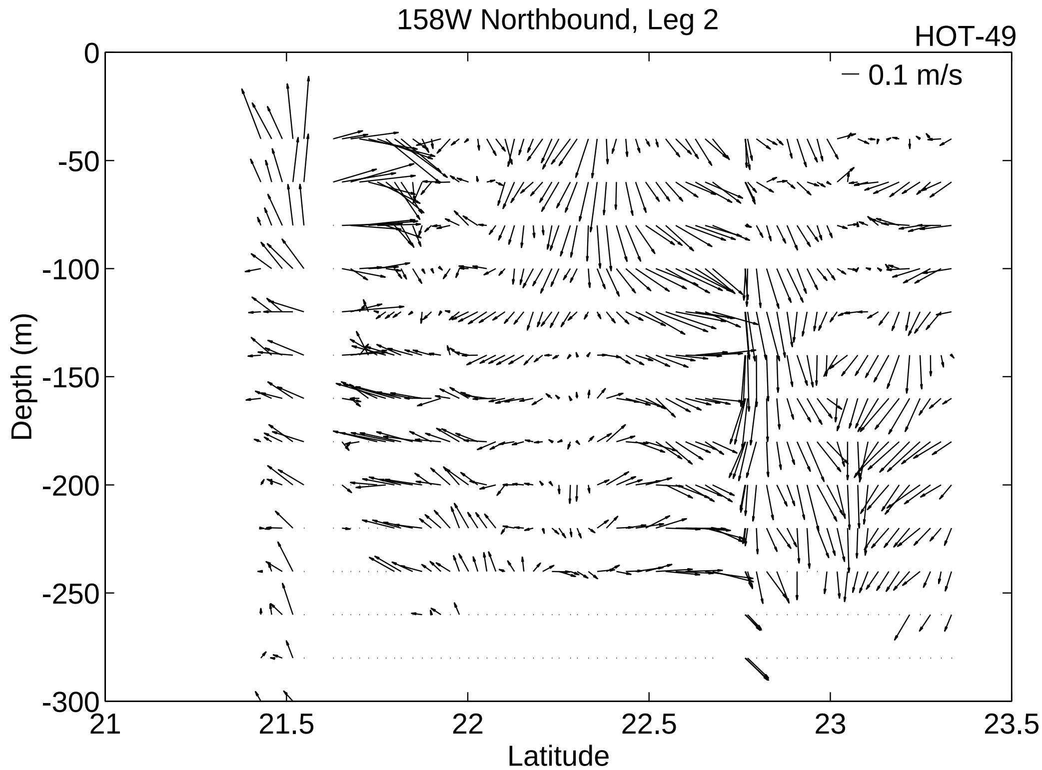

158W Northbound, Leg 2
HOT-49
0.1 m/s
Depth (m)
Latitude
0
-50
-100
-150
-200
-250
-300
21
21.5
22
22.5
23
23.5

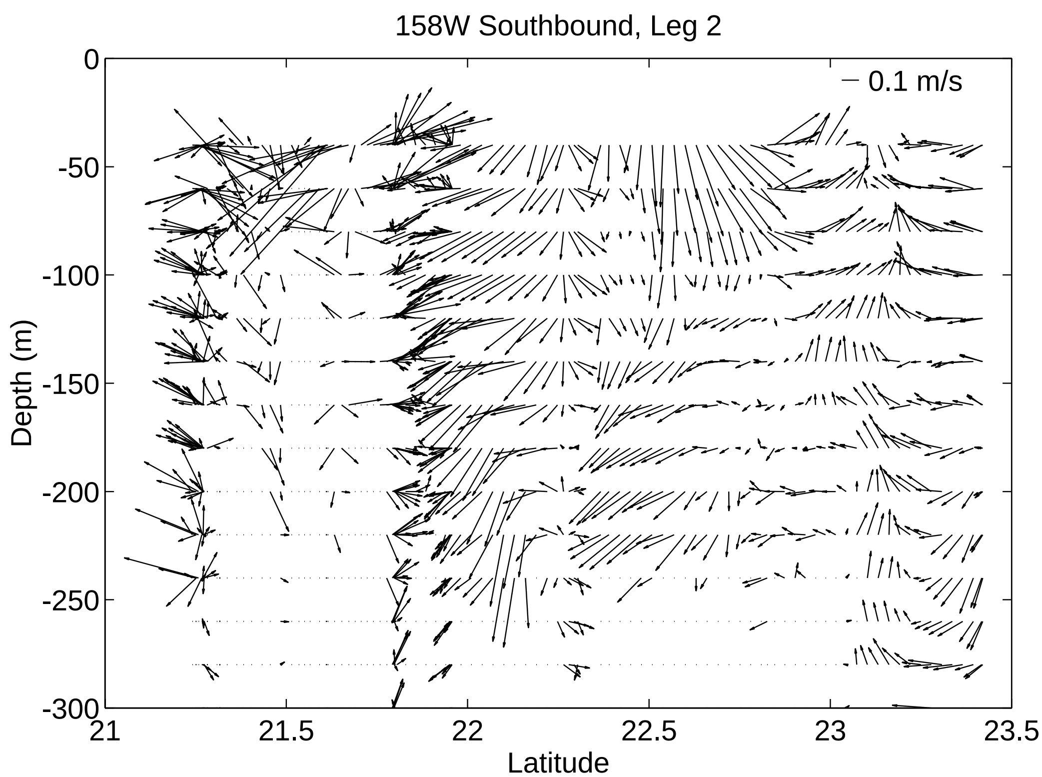

158W Southbound, Leg 2
0.1 m/s
Depth (m)
Latitude
0
-50
-100
-150
-200
-250
-300
21
21.5
22
22.5
23
23.5

Figure 6.7.2e

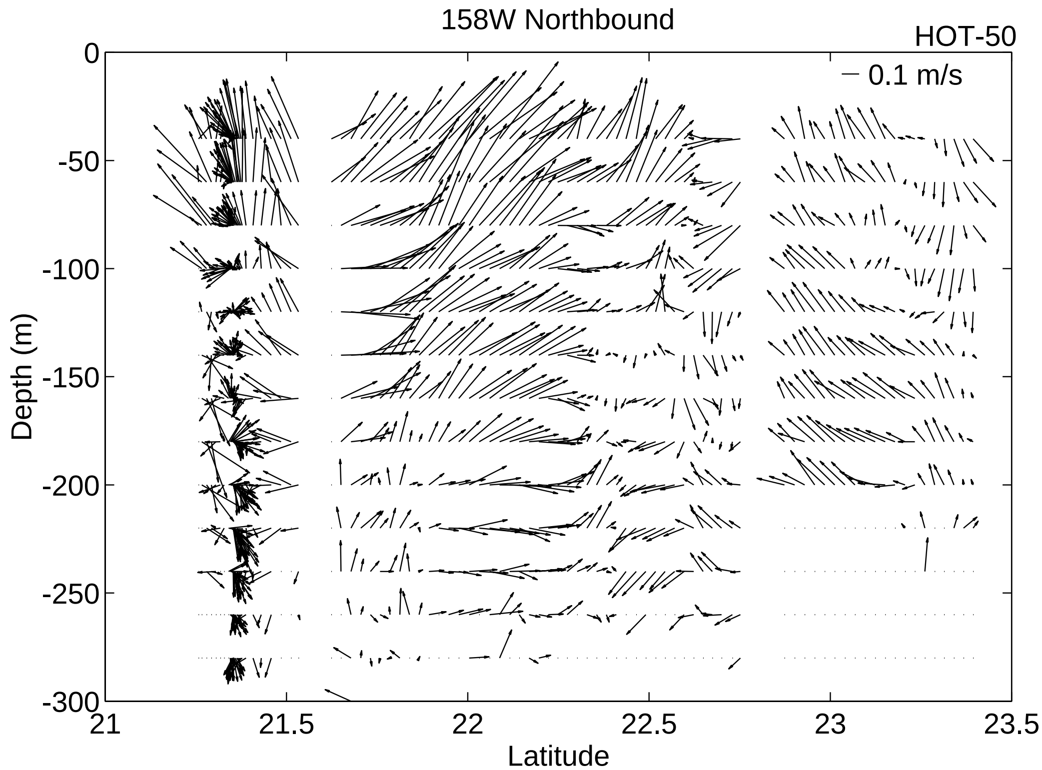

158W Northbound
HOT-50
0.1 m/s
0
-50
-100
-150
-200
-250
-300
Depth (m)
21
21.5
22
22.5
23
23.5
Latitude

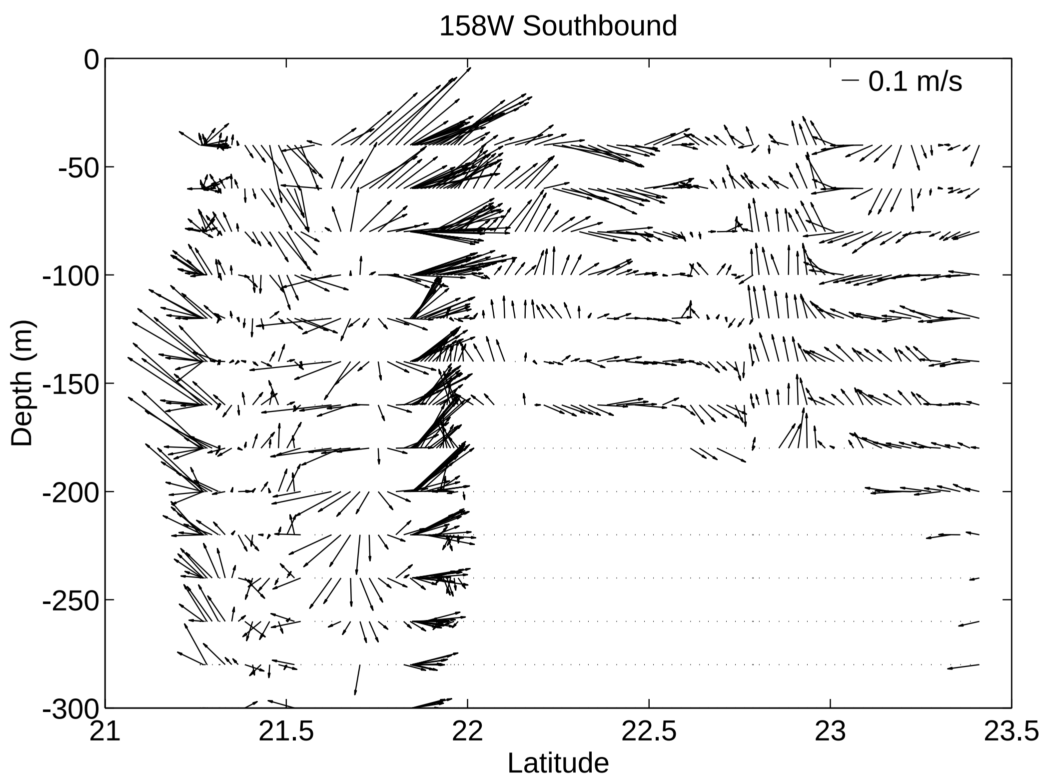

158W Southbound
0.1 m/s
0
-50
-100
-150
-200
-250
-300
Depth (m)
21
21.5
22
22.5
23
23.5
Latitude

Figure 6.7.2f

6.8. Meteorology

Figure 6.8.1. Upper panel: Atmospheric pressure measured while at Station ALOHA during 1993. Open circles represent individual measurements. Lower panel: Sea surface temperature measured from bucket sample while at Station ALOHA during 1993.

Figure 6.8.2. Upper panel: Dry bulb temperature measured while on station during 1993. Lower panel: Wet bulb air temperature measure while as Station ALOHA during 1993.

Figure 6.8.3. Upper panel: Dry air temperature measured at Station ALOHA during 1993. Lower panel: Dry-wet air temperature measured at Station ALOHA during 1993.

Figure 6.8.4. Upper panel: True winds measured at Station ALOHA during HOT-44. Lower panel: True winds collected by NDBC Buoy 51001 during HOT-44.

Figure 6.8.5: As in Figure 6.8.4, except for HOT-45.

Figure 6.8.6: As in Figure 6.8.4, except for HOT-46.

Figure 6.8.7: As in Figure 6.8.4, except for HOT-47.

Figure 6.8.8: As in Figure 6.8.4, except for HOT-49.

Figure 6.8.9: As in Figure 6.8.4, except for HOT-50.

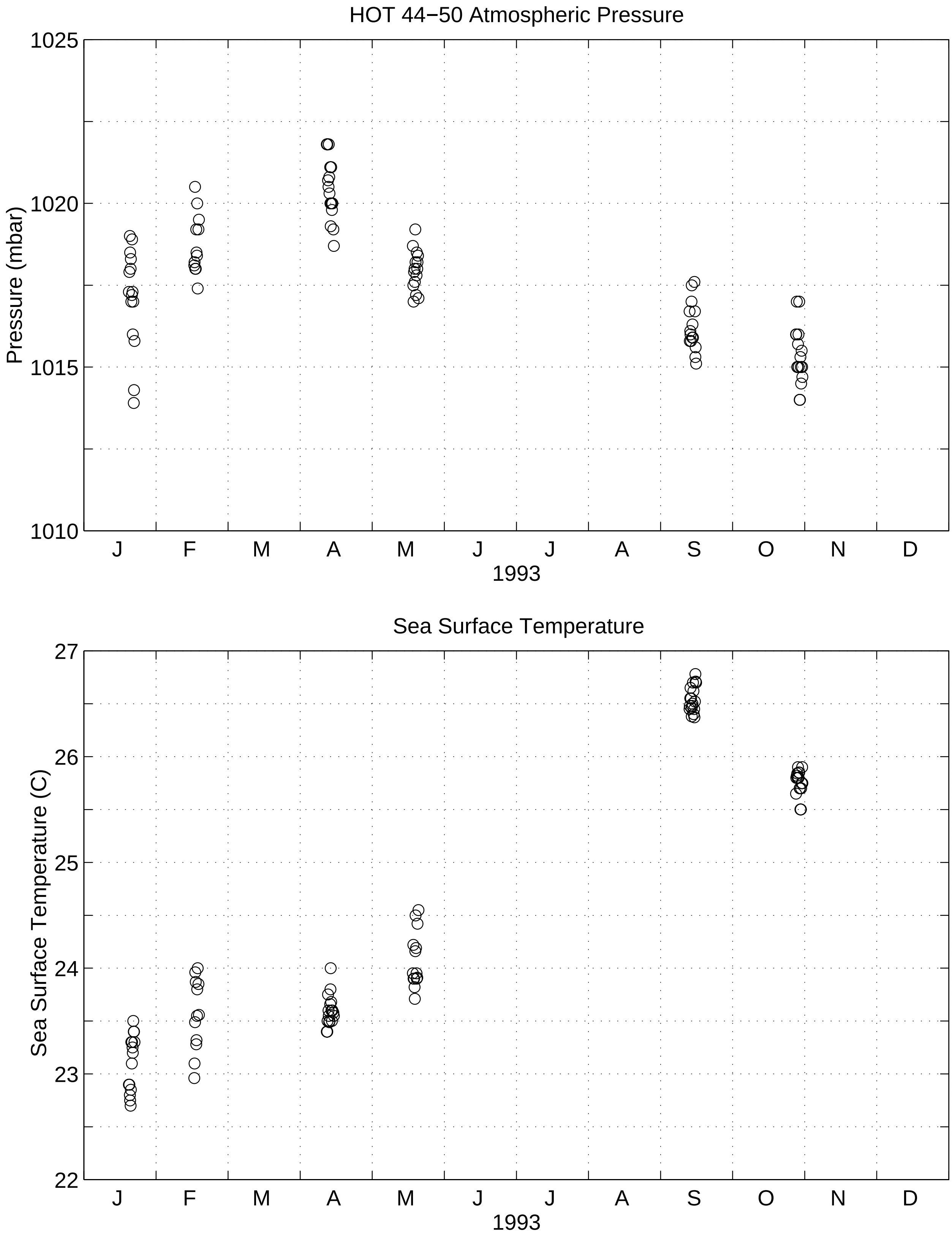
HOT 44−50 Atmospheric Pressure
1025
1020
1015
1010
Pressure (mbar)
J F M A M J J A S O N D
1993
Sea Surface Temperature
27
26
25
24
23
22
Sea Surface Temperature (C)
J F M A M J J A S O N D
1993

Figure 6.8.1

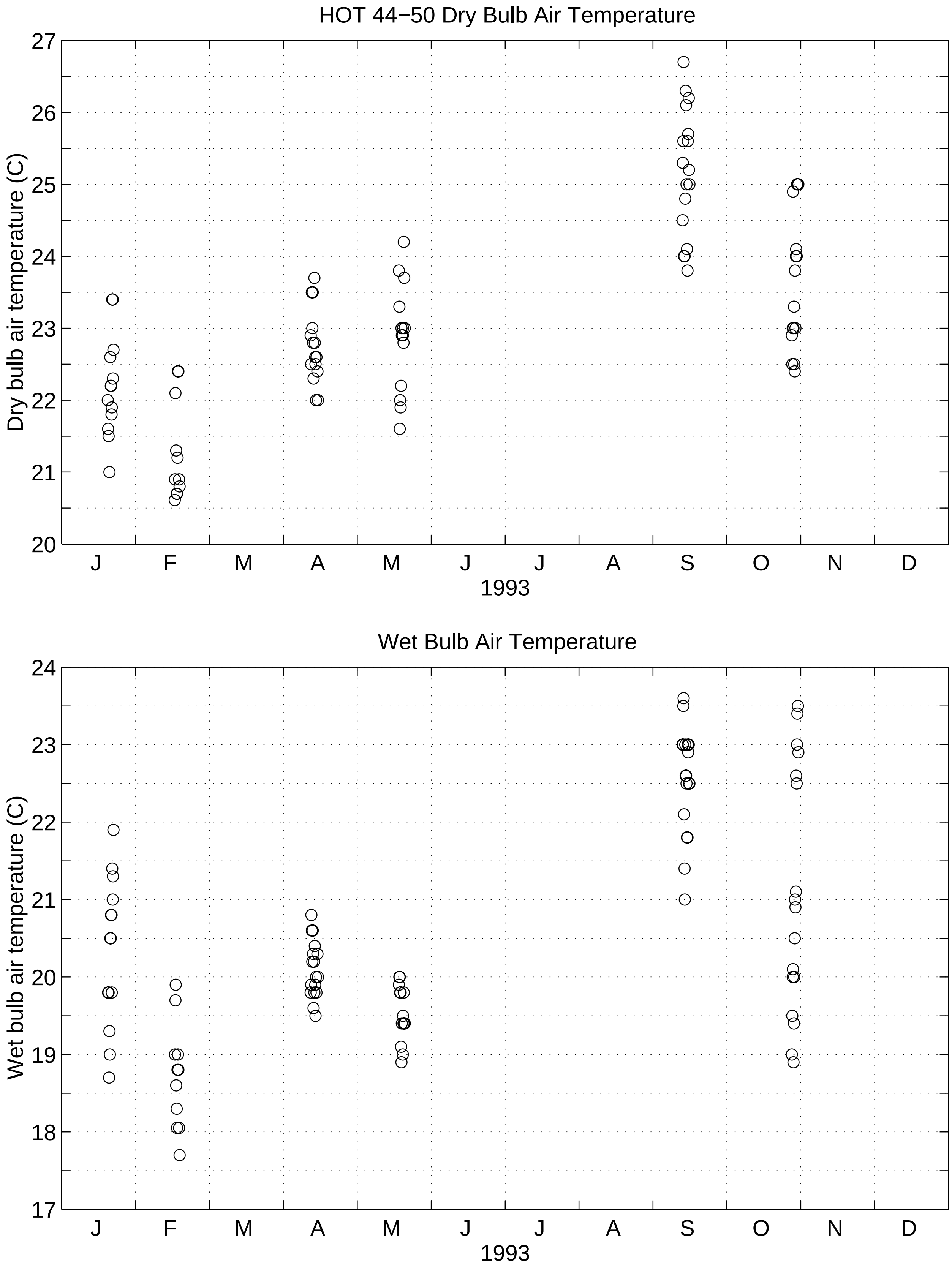

HOT 44−50 Dry Bulb Air Temperature
Dry bulb air temperature (C)
27
26
25
24
23
22
21
20
J
F
M
A
M
J
J
A
S
O
N
D
1993
Wet Bulb Air Temperature
Wet bulb air temperature (C)
24
23
22
21
20
19
18
17
J
F
M
A
M
J
J
A
S
O
N
D
1993

Figure 6.8.2

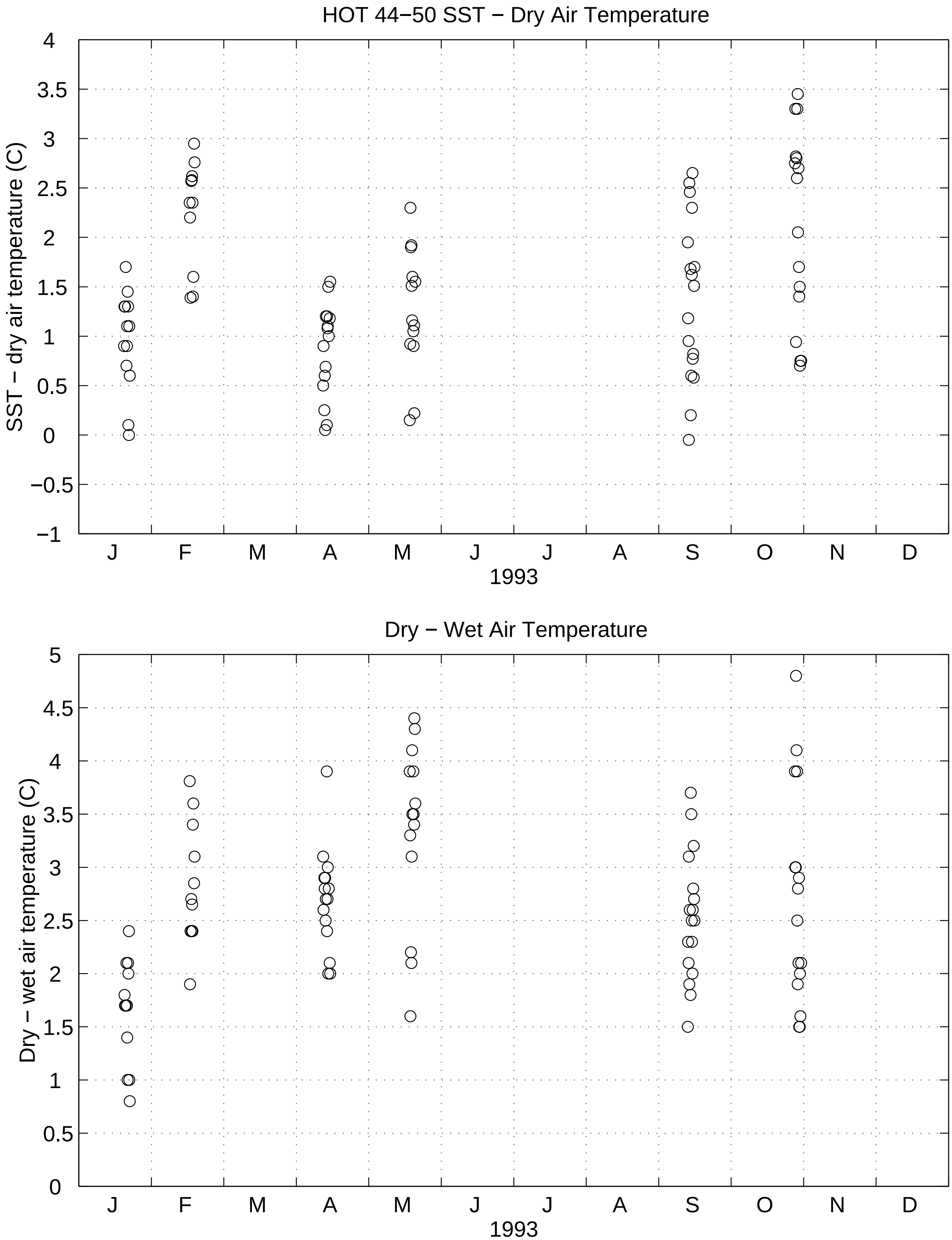
HOT 44−50 SST − Dry Air Temperature
SST − dry air temperature (C)
4
3.5
3
2.5
2
1.5
1
0.5
0
−0.5
−1
J F M A M J J A S O N D
1993
Dry − Wet Air Temperature
Dry − wet air temperature (C)
5
4.5
4
3.5
3
2.5
2
1.5
1
0.5
0
J F M A M J J A S O N D
1993

Figure 6.8.3

HOT 44 Shipboard True Winds

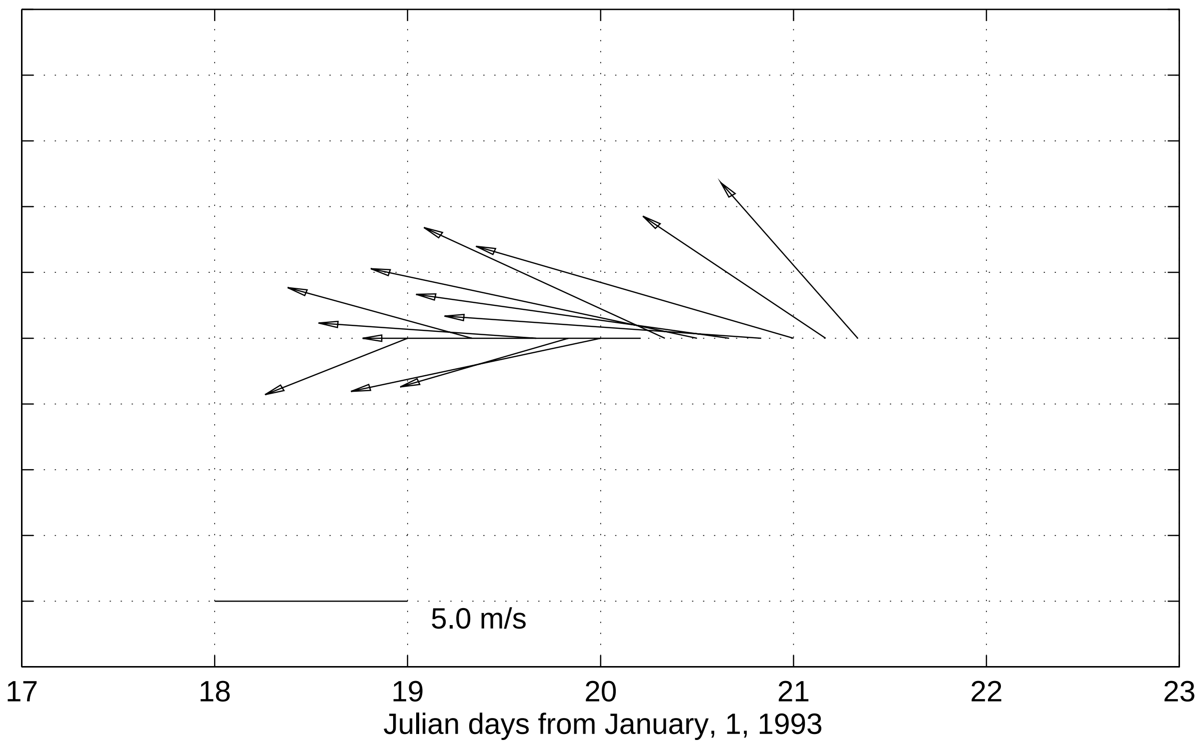

HOT 44 − True Winds, buoy data (23 24N, 162 18W)

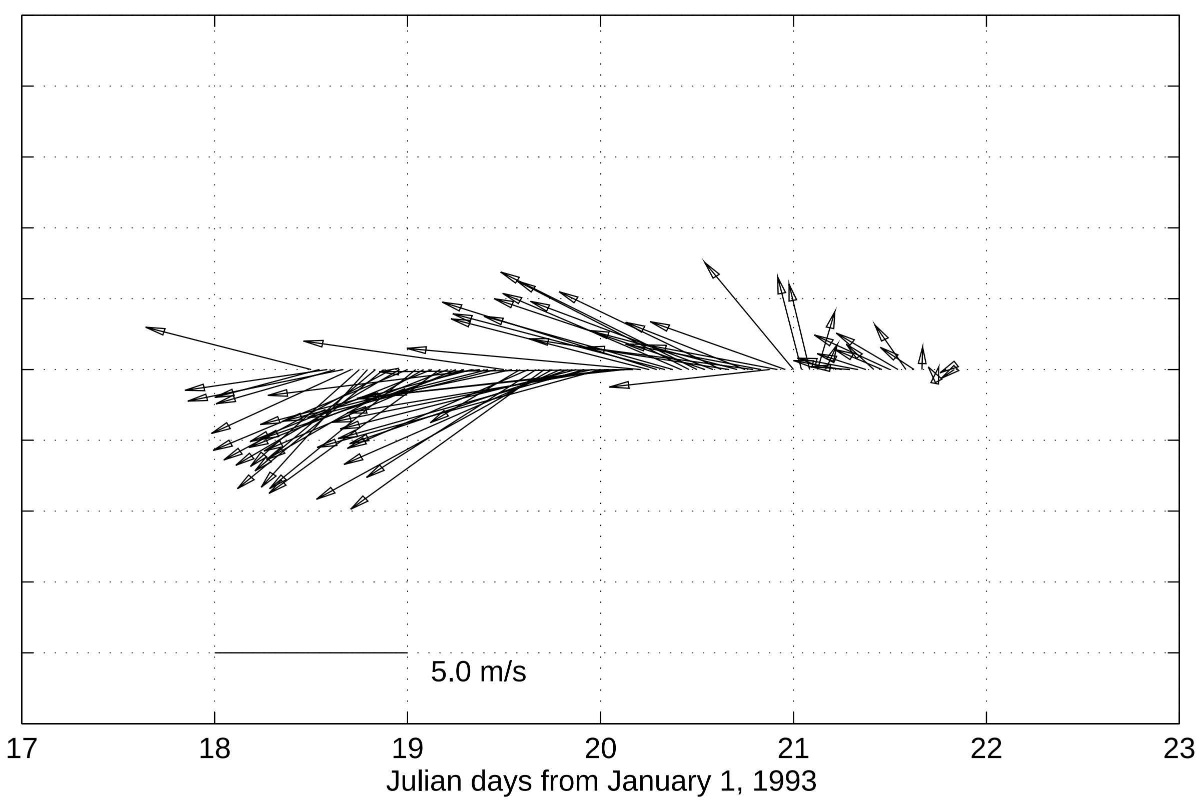

Figure 6.8.4

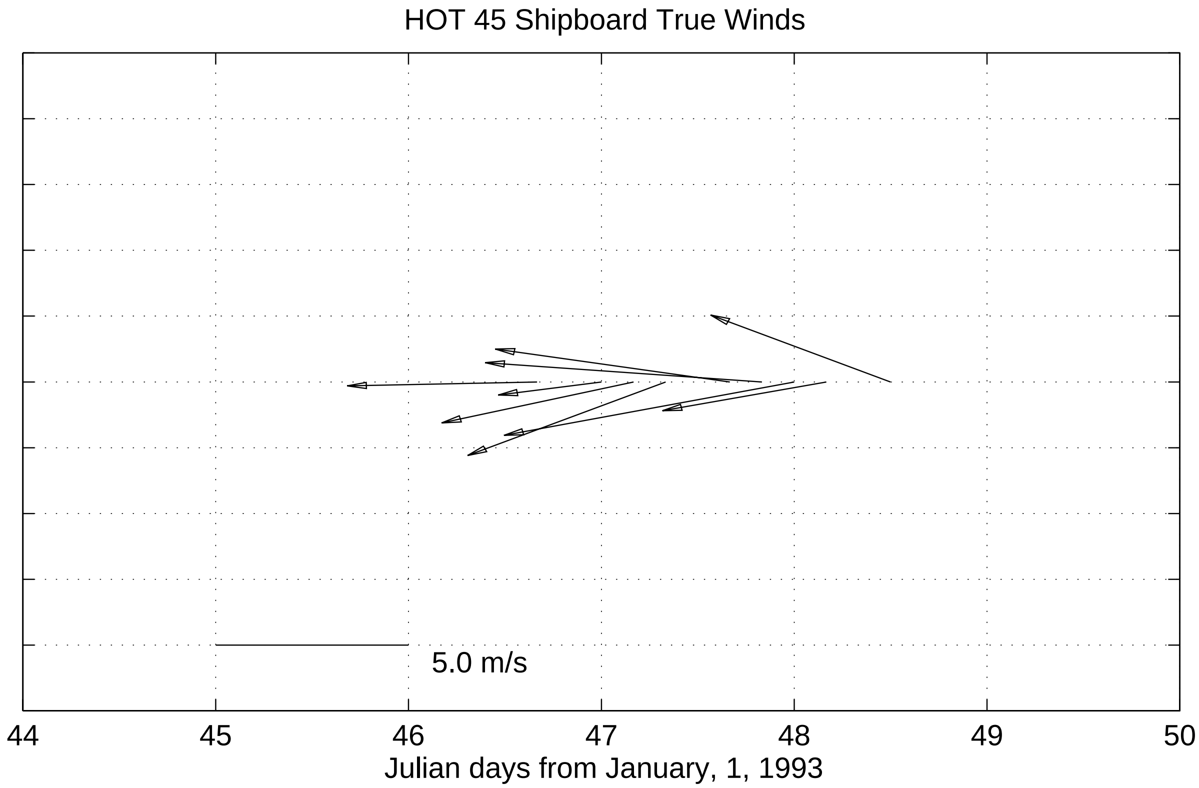
HOT 45 Shipboard True Winds
5.0 m/s
44
45
46
47
48
49
50
Julian days from January, 1, 1993

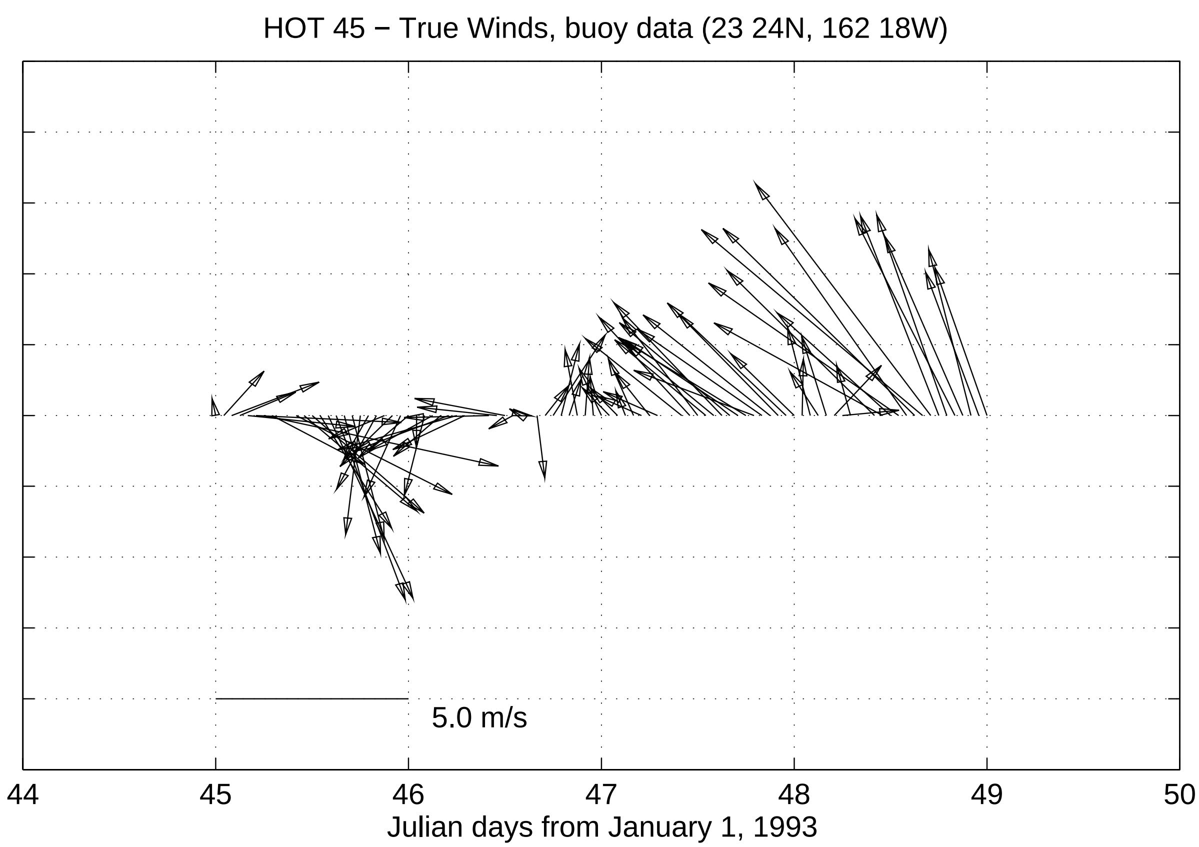
HOT 45 − True Winds, buoy data (23 24N, 162 18W)
5.0 m/s
44
45
46
47
48
49
50
Julian days from January 1, 1993

Figure 6.8.5

HOT 46 Shipboard True Winds

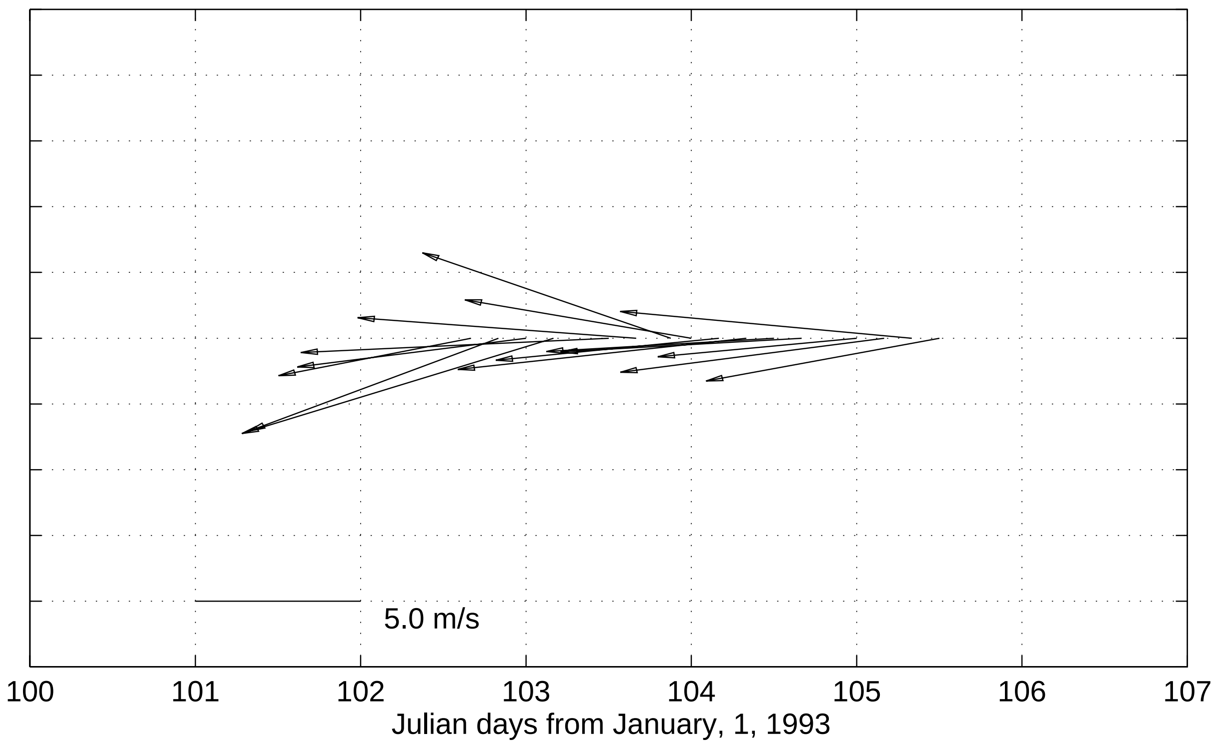

HOT 46 − True Winds, buoy data (23 24N, 162 18W)

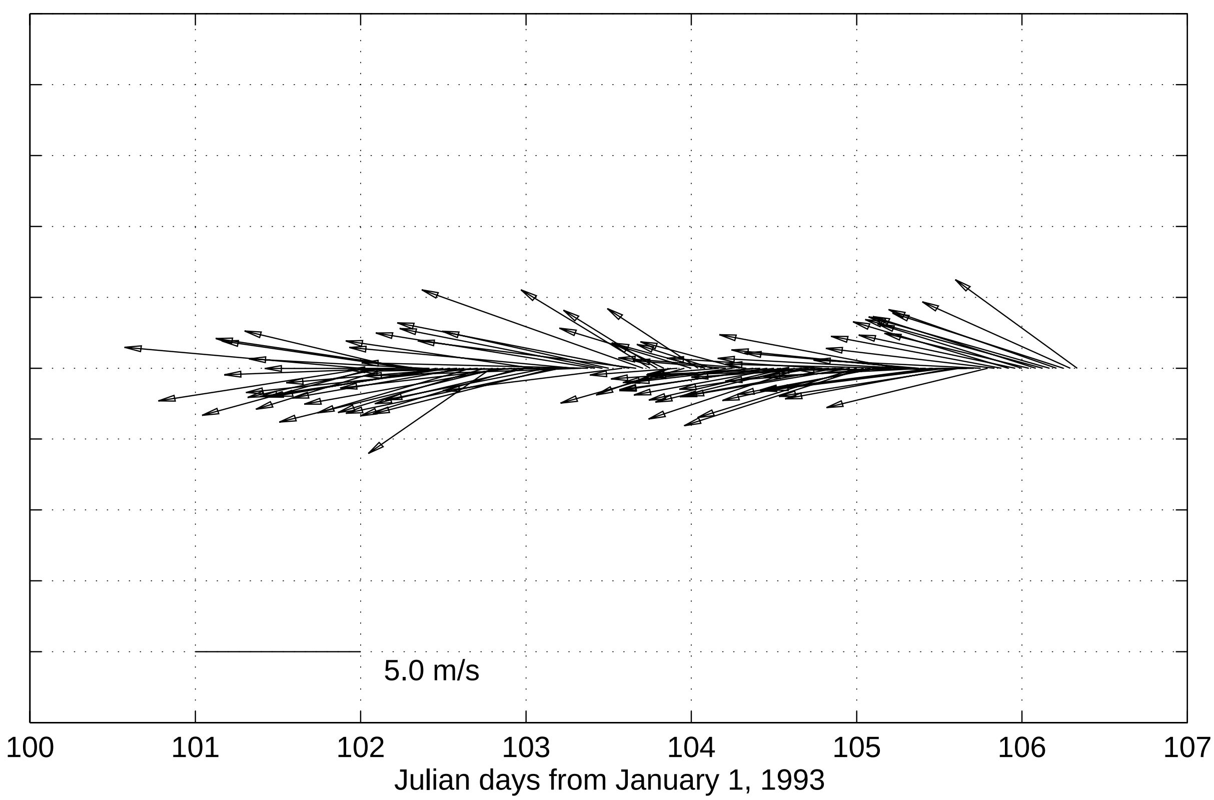

Figure 6.8.6

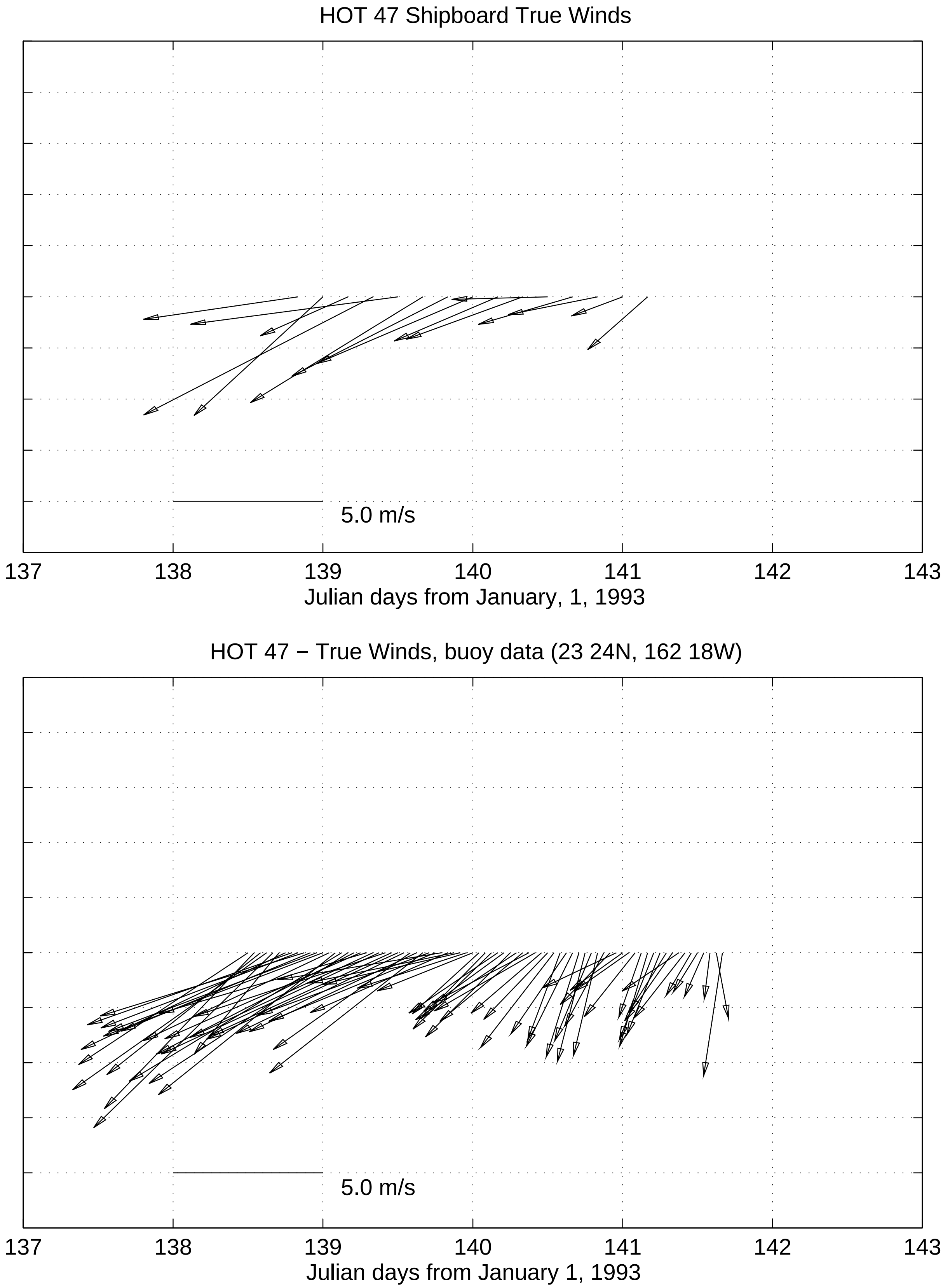

HOT 47 Shipboard True Winds
5.0 m/s
137
138
139
140
141
142
143
Julian days from January, 1, 1993
HOT 47 − True Winds, buoy data (23 24N, 162 18W)
5.0 m/s
137
138
139
140
141
142
143
Julian days from January 1, 1993

Figure 6.8.7

HOT 49 Shipboard True Winds

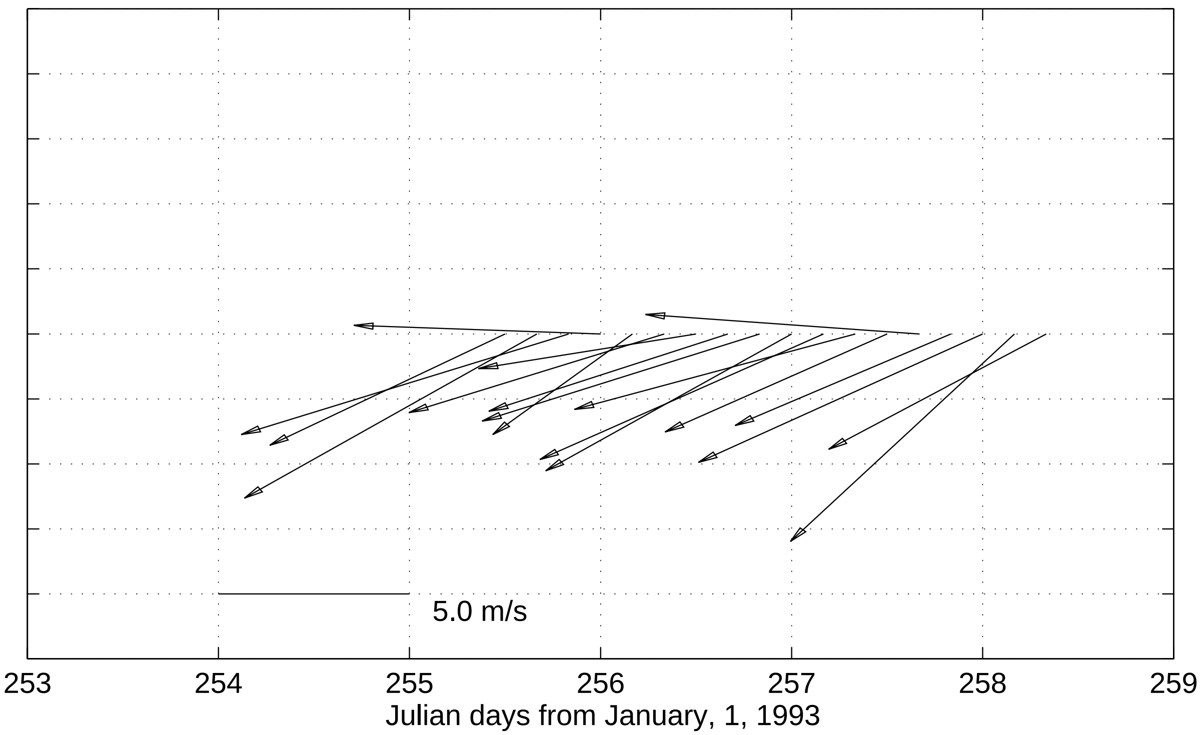

HOT 49 − True Winds, buoy data (23 24N, 162 18W)

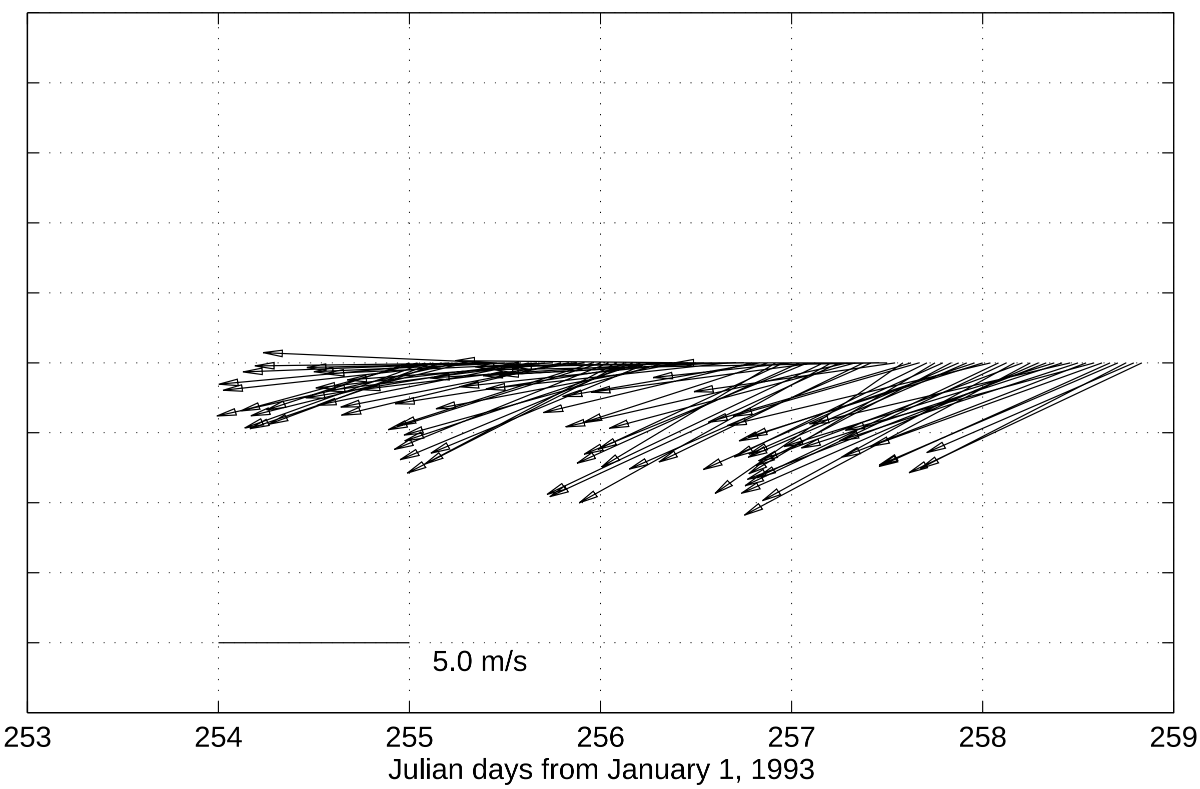

Figure 6.8.8

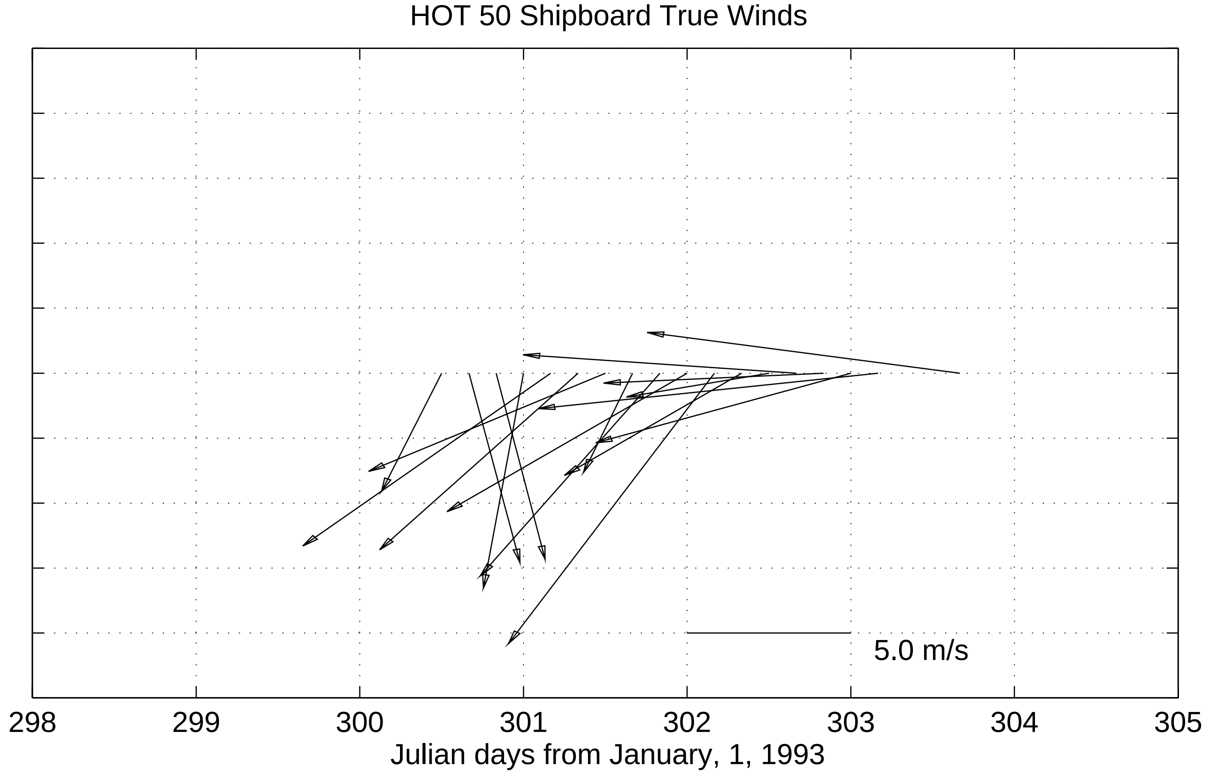
HOT 50 Shipboard True Winds
5.0 m/s
298
299
300
301
302
303
304
305
Julian days from January, 1, 1993

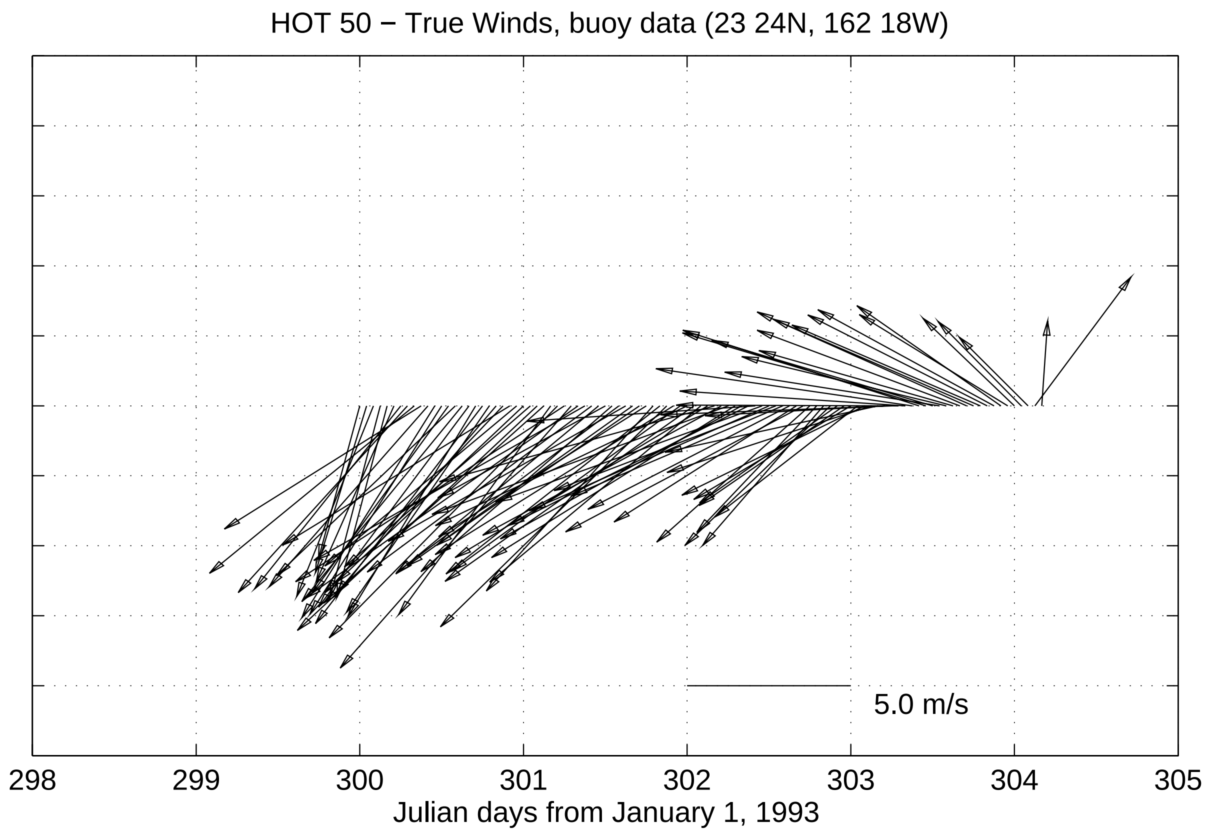
HOT 50 − True Winds, buoy data (23 24N, 162 18W)
5.0 m/s
298
299
300
301
302
303
304
305
Julian days from January 1, 1993

Figure 6.8.9

7. Hawaii Ocean Time-series Publications
Abstracts

1989 Winn, C. D., S. Chiswell, D. M. Karl and R. Lukas. Long time-series research in the Central Pacific Ocean. The Oceanography Society 1st Annual Meeting, Monterey, California.

1990 Chiswell, S. M. and R. Lukas. The Hawaii Ocean Time-series (HOT). EOS, *Transactions of the American Geophysical Union* 1, 1397.

1990 Karl, D., R. Letelier, D. Bird, D. Hebel, C. Sabine and C. Winn. An *Oscillatoria* bloom in the oligotrophic North Pacific Ocean near the GOFS Station ALOHA. *EOS, Transactions of the American Geophysical Union* 71, 177-178.

1990 Winn, C. D., D. Hebel, R. Letelier, D. Bird and D. Karl. Variability in biogeochemical fluxes in the oligotrophic central Pacific: Results of the Hawaii Ocean Time-Series Program. *EOS, Transactions of the American Geophysical Union* 71, 190.

1991 Karl, D. The Hawaii Ocean Time-series program: Carbon production and particle flux. The Oceanography Society 2nd Annual Meeting, St. Petersburg, Florida, March 1991.

1991 Karl, D. *Trichodesmium* blooms and new nitrogen in the North Pacific gyre. NATO Symposium on Biology and Ecology of Diazotrophic Marine Organisms, Bamberg, Germany, May 1991.

1991 Letelier, R., D. Karl, R. Bidigare, J. Christian, J. Dore, D. Hebel and C. Winn. Temporal variability of phytoplankton pigments at the U.S.-JGOFS Station ALOHA (22°45'N, 158°W). *EOS, Transactions of the American Geophysical Union* 72, 74.

1991 Winn, C., C. Sabine, D. Hebel, F. Mackenzie and D. M. Karl. Inorganic carbon system dynamics in the central Pacific Ocean: Results of the Hawaii Ocean Time-series program. *EOS, Transactions of the American Geophysical Union* 72, 70.

1992 Anbar, A. D. Rhenium in seawater: Confirmation of generally conservative behavior. *EOS, Transactions of the American Geophysical Union* 3, 278.

1992 Karl, D. Initial results from the JGOFS Hawaii Ocean Time-series (HOT) experiment. IGBP International Symposium on Global Change, Oceanic ecosystem variability, Tokyo, Japan, March 1992.

1992 Karl, D. The U.S.-JGOFS Hawaii Ocean Time-Series (HOT) Program: Biogeochemical Vignettes from the Oligotrophic North Pacific Ocean. Conoco Topics Seminar Series, Woods Hole, Massachusetts, May 1992.

1992 Karl, D. Temporal Variability in Bioelement Flux at Station ALOHA (22°45'N, 158°W). Conoco Topics Seminar Series, Woods Hole, Massachusetts, May 1992.

1992 Karl, D., C. Winn, D. Hebel, R. Letelier, J. Dore and J. Christian. The U.S.-JGOFS Hawaii Ocean Time-Series (HOT) program. American Society for Limnology and Oceanograph, Santa Fe, NM, February 1992.

1992 Lukas, R. Water mass variability observed in the Hawaii Ocean Time Series. *EOS, Transactions of the American Geophysical Union* **72**: 70.

1992 Winn, C.D., D. Hebel, R. Letelier, J. Christian, J. Dore, R. Lukas and D.M. Karl. Long time-series measurements in the central North Pacific: Results of the Hawaii Ocean Time-series program. PACON conference, Kona, Hawaii, June 1992.

1992 Campbell, L., R.R. Bidigare, R. Letelier, M. Ondrusek, S. Hall, B Tsai and C. Winn. Phytoplankton population structure at the Hawaii Ocean Time-series station. American Society of Limnology and Oceanography Meeting, Santa Fe, NM, February 1992.

1992 Bidigare, R.R., L. Campbell, M. Ondrusek, R. Letelier and D. Vaulot. Characterization of picophytoplankton at Station ALOHA (22 45'N, 158W) using HPLC, flow cytometry and immunofluorescence techniques. PACON 1992 Meeting, June 1992.

1992 Shudlich, R. and S.R. Emerson. Modelling dissolved gases in the subtropical ocean: JGOFS/WOCE Hawaiian Ocean Time-series. *EOS, Transactions of the American Geophysical Union* **73**: 287.

1993 Winn, C.D., C.J. Carrillo, F.T. MacKenzie and D.M. Karl. Variability in the inorganic carbon system parameters in the North Pacific subtropical gyre. The Oceanography Society Meeting, Seattle, WA, April 1993.

1993 Moyer, C.L., L. Campbell, D.M. Karl and J. Wilcox. Restriction fragment length polymorphism (RFLP) and DNA sequence analysis PCR-generated clones to assess diversity of picoeukaryotic algae in the subtropical central North Pacific Ocean (Station ALOHA). American Society of Limnology and Oceanography Meeting, Edmonton, Alberta, May 1993.

1993 Christian, J.R. and D.M. Karl. Bacterial exoenzymes in marine waters: Implications for global biogeochemical cycles. American Society of Limnology and Oceanography Meeting, Edmonton, Alberta, May 1993.

1993 Campbell, L., H.A. Nolla and D. Vaulot. Microbial biomass in the subtropical central North Pacific Ocean (Station ALOHA): The importance of Prochlorococcus. The Oceanography Society Third Scientific Meeting, Seattle,WA, April 1993.

1993 Emerson, S., P. Quay, C. Stump, D. Wilbur and R. Shudlich. Determining primary production form the mesoscale oxygen field. ICES Marine Science Symposium **197**: 196-206.

1993 Emerson, S., P. Quay, C. Stump, D. Wilbur and R. Shudlich. Oxygen cycles and productivity in the oligotrophic subtropical Pacific Ocean. The Oceanography Society Meeting. Seattle, WA, April 1993.

1993 Sharp, J.H., R. Benner, L. Bennett, C.A. Carlson, S.E. Fitzwater, E.T. Peltzer and L.M. Tupas. The Equatorial Pacific intercalibration analyses of dissolved organic carbon in seawater. American Society of Limnology and Oceanography Meeting, Edmonton, Alberta, May 1993.

1993 Sharp, J.H., R. Benner, L. Bennett, C.A. Carlson, S.E. Fitzwater, E.T. Peltzer and L.M. Tupas. Dissolved organic carbon: intercalibration analyses with Equatorial Pacific samples. The Oceanography Society Meeting. Seattle, WA, April 1993.

1993 Atkinson, M.J. A potentiostatic solid state sensor for oceanic CTD's. The Oceanography Society Meeting. Seattle, WA, April 1993.

1994 Winn, C., F.T. MacKenzie, C. Carrillo, T. Westby and D.M. Karl. Air-sea carbon diozide exchange at Station ALOHA. *EOS, Transactions of the American Geophysical Union* **75**, 112.

1994 Lukas, R., F. Bingham, and A. Mantyla. An anomalous cold event in the bottom water observed north of Oahu. *EOS, Transactions of the American Geophysical Union* **75**, 205.

1994 Measures, C.I., J. Yuan and J.A. Resing. The rapid determination of iron in seawater at sub-nanomolar concentrations using in-line preconcentration and spectrophometric detection. Sixth Winter Conference on Flow Injection Analysis, San Diego, CA.

1994 Measures, C.I., J. Yuan and J.A. Resing. Determination of iron in seawater using in-line preconcentration and spectrophotometric detection. Workshop on Iron Speciation and its Biological Activity. Bermuda Biological Station for Research, Bermuda.

1994 Yuan, J., C.I. Measures and J.A. Resing. Rapid determination of iron in seawater: In-line preconcentration flow injection analysis with spectrophometric detection *EOS, Transactions of the Amercian Geophysical Union* **75**: 25.

1994 Smith, C.R., S. Garner, D. Hoover and R. Pope. Macrobenthos, mechanisms of bioturbation and carbon flux proxies at the abyssal seafloor along the JGOFS Equatorial Pacific Transect, *EOS, Transactions of the American Geophysical Union* **75**: 70.

1994 Campbell, L., C.D. Winn, R. Letelier, D. Hebel and D.M. Karl. Temporal variability in phytoplankton fluorescence at Station ALOHA. *EOS, Transactions of the Americal Geophysical Union* **75**: 100.

1994 Campbell, L., H. Liu, R.R. Bidigare and D. Vaulot. Immunochemical characterization of *Prochlorococcus*. American Society of Limnology and Oceanography Meeting, Edmonton, Alberta, May 1993.

1994 Liu, H. and L. Campbell. Measurement of growth and mortality rate of *Prochlorococcus and Synechococcus at Station ALOHA* using a new selective inhibitor technique. Fifth International Phycological Congress, Qingdao, China, July 1994.

1994 Farrenkopf, A.M., G.W. Luther, III and C.H. Van Der Weijden. Vertical distribution of dissolved iodine species in the northwest Indian Ocean. *EOS, Transactions of the American Geophysical Union* **75**: 78.

1994 Tupas, L.M., B.N. Popp and D.M. Karl. Dissolved organic carbon in oligotrophic waters; experiments on sample preservation, storage and analysis. *EOS, Transactions of the American Geophysical Union* **73**: 287.

Newsletters

1991 Lukas, R. and S. Chiswell. Submesoscale water mass variations in the salinity minimum of the North Pacific. *WOCE Notes*, 3(1), 6-8.

1992 Chiswell, S. Inverted echo sounders at the WOCE deep-water station. *WOCE Notes*, 4(4), 1-6.

1992 Firing, E. and P. Hacker. ADCP results from WHP P16/P17. *WOCE Notes*, 4(3), 6- 12.

plus a periodic column entitled "HOT Stuff", written by D. Karl, which appears in the U.S. JGOFS Program newsletter

Publications

1990 Giovannoni, S.J., E.F. DeLong, T.M. Schmidt and N.R. Pace. Tangential flow filtration and preliminary phylogenetic analysis of marine picoplankton. *Applied and Environmental Microbiology* **56**, 2572-2575.

1990 Collins, D. J., W. J. Rhea and A. van Tran. Bio-optical profile data report: HOT-3. National Aeronautics and Space Administration JPL Publ. #90-36.

1990 Firing, E. and R.L. Gordon. Deep ocean acoustic Doppler current profiling. In: G. F. Appell and T. B. Curtin (eds.), Proceedings of the Fourth IEEE Working Conference on Current Measurements, pp. 192-201. IEEE, New York.

1991 Karl, D.M., W.G. Harrison, J. Dore et al. Chapter 3. Major bioelements workshop report. In: D. C. Hurd and D. W. Spencer (eds.), Marine Particles: Analysis and Characterization, pp. 33-42. American Geophysical Union, Geophysical Monograph 63.

1991 Karl, D. M., J. E. Dore, D.V. Hebel and C. Winn. Procedures for particulate carbon, nitrogen, phosphorus and total mass analyses used in the US-JGOFS Hawaii Ocean Time-Series Program. In: D. Spencer and D. Hurd (eds.), Marine Particles: Analysis and Characteriation, pp. 71-77. American Geophysical Union, Geophysical Monograph 63.

1991 Karl, D. M. and C.D. Winn. A sea of change: Monitoring the oceans' carbon cycle. *Environmental Science & Technology* **25**, 1976-1981.

1991 Sabine, C.L. and F.T. Mackenzie. Oceanic sinks for anthropogenic CO_2. International *Journal of Energy, Environment, Economics* **1**, 119-127.

1991 Schmidt, T. M., E.F. DeLong and N.R. Pace. Analysis of a marine picoplankton community by 16S rRNA gene cloning and sequencing. *Journal of Bacteriology* **173**, 4371- 4378.

1991 Chiswell, S. M. Dynamic response of CTD pressure sensors to temperature. *Journal of*

Atmospheric and Oceanic Technology **8**, 659-668.

1992 Karl, D.M., R. Letelier, D.V. Hebel, D.F. Bird and C.D. Winn. *Trichodesmium* blooms and new nitrogen in the North Pacific gyre. In: E. J. Carpenter et al. (eds.), Marine Pelagic Cyanobacteria: Trichodesmium and Other Diazotrophs, pp. 219-237. Kluwer Academic Publishers, Netherlands.

1992 Karl, D.M. and G. Tien. MAGIC: A sensitive and precise method for measuring dissolved phosphorus in aquatic environments. *Limnology and Oceanography* **37**, 105-116.

1992 Chen, R.F. and J.L. Bada. The fluorescence of dissolved organic matter in seawater. *Marine Chemistry* **37**, 191-221.

1992 Quay, P.D., B. Tilbrook and C.S. Wong. Oceanic uptake of fossil fuel CO_2: Carbon-13 evidence. *Science* **256**, 74-78.

1992 Karl, D.M. The oceanic carbon cycle: Primary production and carbon flux in the oligotrophic North Pacific Ocean. Proceedings of the IGBP Symposium on Global Change, pp. 203-219. Tokyo, Japan

1992 Benner, R., J. D. Pakulski, M. McCarthy, J.I. Hedges and P.G. Hatcher. Bulk chemical characteristics of dissolved organic matter in the ocean. *Science* **255**, 1561-1564.

1993 Anbar, A.D., R.A. Creaser, D.A. Papanastassiou and G.J. Wasserburg. Rhenium in seawater: Confirmation of generally conservative behavior. *Geochimica et Cosmochimica Acta* **56**, 4099-4103.

1993 Karl, D.M., G. Tien, J. Dore and C.D. Winn. Total dissolved nitrogen and phosphorus concentrations at US-JGOFS Station ALOHA: Redfield reconciliation. *Marine Chemistry* **41**, 203-208.

1993 Selph, K.E., D.M. Karl, M.R. Landry. Quantification of Chemiluminescent DNA probes using liquid scintillation counting. *Analytical Biochemistry* **210**, 394-401.

1993 Karl, D.M. Total microbial biomass estimation derived from the measurement of particulate adenosine-5'-triphosphate. In: P.F. Kemp, B.F. Sherr, E.B. Sherr and J.J. Cole (eds.), Handbook of Methods in Aquatic Microbial Ecology, pp. 359-368. Lewis Publishers, Boca Raton.

1993 Hedges, J.I., B.A. Bergamaschi and R. Benner. Comparative analyses of DOC and DON in natural waters. *Marine Chemistry* **41**, 121-134.

1993 Mopper, K. and C.A. Schultz. Fluorescence as a possible tool for studying the nature and water column distribution of DOC components. *Marine Chemistry* **41**, 229-238.

1993 Coble, P. G., C. A. Schultz and K. Mopper. Fluorescence contouring analysis of DOC intercalibration experiment samples: a comparison of techniques. *Marine Chemistry* **41**, 173-178.

1993 Winn, C.D., R. Lukas, D. Hebel, C. Carrillo, R. Letelier and D.M. Karl. The Hawaii Ocean Time- series program: Resolving variability in the North Pacific. In: N. Saxena (ed.), Recent advances in marine science and technology, 92, Proceedings of the Pacific Ocean Congress (PACON), pp. 139-150.

1993 Letelier, R.M., R.R. Bidigare, D.V. Hebel, C.D. Winn and D.M. Karl. Temporal variability of phytoplankton community structure at the US-JGOFS Time-series Station ALOHA (22°45'N, 158°00'W) based on pigment analyses. *Limnology and Oceanography* **38**, 1420-1437.

1993 Campbell, L. and D. Vaulot. Photosynthetic picoplankton community structure in the subtropical North Pacific Ocean near Hawaii (Station ALOHA). *Deep-Sea Research* **40**, 2043-2060.

1993 Campbell, L. and D. Vaulot. Photosynthetic picoplankton community structure in the subtropical central North Pacific Ocean near Hawaii (Station ALOHA). *Deep Sea Research* **40**: 2043-2060.

1993 Keeling, C.D. 1993. Lecture 2: Surface Ocean C02. NATO ASI Series Vol. I(**15**) 413-429.

1994 Baines, S.B., M.L. Pace and D.M. Karl. Why does the relationship between sinking flux and planktonic primary production differ between lakes and oceans? *Limnology and Oceanography* **39**, 213-216.

1994 Christian, J.R. and D.M. Karl. Microbial community structure at the U.S. - Joint Global Ocean Flux Study Station ALOHA: Inverse methods for estimating biochemical indicator ratios. *Journal of Geophysical Research* **99**, 14269-14276.

1994 Winn, C.D., F.T. MacKenzie, C.J. Carrillo, C.L. Sabine and D.M. Karl. Air-sea carbon dioxide exchange in the North Pacific Subtropical Gyre: Implications for the global carbon budget. *Global Biogeochemical Cycles* **82**, 157-163.

1994 Chiswell, S.M. Using an array of inverted echo sounders to measure dynamic height and geostrophic current in the North Pacific Subtropical Gyre. *Journal of Atmospheric and Oceanic Technology*: in press.

1994 Campbell, L., L.P. Shapiro and E.M. Haugen. Immunochemical characterization of the eukaryotic ultraplankton in the Atlantic and Pacific oceans. *Journal of Plankton Research* **16**: 35-51.

1994 Campbell, L., H.A. Nolla and D. Vaulot. The importance of Prochlorococcus to community structure in the central North Pacific Ocean. *Limnology and Oceanography* **39**: 954-961.

1994 Sharp, J.H., R. Benner, L. Bennett, C.A. Carlson, S.E. Fitzwater, E.T. Peltzer and L.M. Tupas. Analyses of dissolved organic carbon in seawater: The JGOFS EQPAC methods comparison. *Marine Chemistry*: in press.

1994 Tupas, L.M., B.N. Popp and D.M. Karl. Dissolved organic carbon in oligotrophic waters: experiments on sample preservation, storage and analysis. *Marine Chemistry* **45**: 207-216.

1994 Thomas, F.I.M., S.A. McCarthy, J. Bower, S. Krothapalli, M.J. Atkinson and P. Flament. Response characteristics of two oxygen sensors for oceanic CTD's. *Journal of Atmospheric and Oceanographic Technology*: in press.

1994 Atkinson, M.J., F.I.M. Thomas, N. Larson, E. Terrill, K. Morita and C.C. Liu. A micro-hole potentiostatic oxygen sensor for oceanic CTD's. *Deep-Sea Research*: in press.

1994 Thomas, F.I.M. and M.J. Atkinson. Calibration protocol for a micro-hole potentiostatic sensor for oceanic CTD's. *Journal of Atmospheric and Oceanographic Technology*: in press.

1994 Atkinson, M.J., F.I.M. Thomas and N. Larson. Effects of pressure on oxygen sensors: a new pressure term for calibration equations. *Journal of Atmospheric and Oceanographic Technology*: in press.

1994 Sabine, C.L., F.T. MacKenzie, C.D. Winn and D.M. Karl. Geochemistry of particulate and dissolved inorganic carbon at the Hawaii Ocean Time-series station, ALOHA. *Global Biogeochemical Cycles*: in press

1994 Chavez, F.P., K.R. Buck, R.R. Bidigare, D.M. Karl, D.V. Hebel, M. Latasa, L. Campbell and J. Newton. On the Chlorophyll a retention properties of glass fiber GF/F filters: *Limnology and Oceanography*: in press

1994 Karl, D.M. Accurate estimation of microbial loop processes and rates. *Microbial Ecology*: in press.

Theses and Dissertations

1992 Sabine, C. L. Geochemistry of particulate and dissolved inorganic carbon in the central North Pacific. Ph.D. Dissertation, May 1992.

1993 Kennan, S. Variability of the intermediate water north of Oahu. M.S. Thesis, December 1993.

1994 Letelier, R. M. Studies on the Ecology of *Trichodesmium* spp. (Cyanophyceae) in the Central North Pacific Gyre. Ph.D. Dissertation, May 1994.

1994 Liu, H. B. Growth and Mortality Rates of *Prochlorococcus* and *Synechococcus* measured by a selective inhibitor technique. M.S. Thesis, May 1994.

Data Reports

1990 Karl, D. M., C. D. Winn, D. V. W. Hebel and R. Letelier. Hawaii Ocean Time-series Program Field and Laboratory Protocols, September 1990. School of Ocean and Earth Science and Technology, Univ. of Hawaii, Honolulu, HI, 72 pp.

1990 Chiswell, S., E. Firing, D. Karl, R. Lukas and C. Winn. Hawaii Ocean Time-series Program

Data Report 1, 1988-1989. School of Ocean and Earth Science and Technology, Univ. of Hawaii, Honolulu, HI, 269 pp.

1991 Winn, C., S. Chiswell, E. Firing, D. Karl and R. Lukas. Hawaii Ocean Time-series Program Data Report 2, 1990. School of Ocean and Earth Science and Technology, Univ. of Hawaii, Honolulu, HI, 175 pp.

1993 Winn, C., R. Lukas, D. Karl, E. Firing. Hawaii Ocean Time-series Program Data Report 3, 1991. School of Ocean and Earth Science and Technology Report 3, University of Hawaii, 228 pp.

1993 Tupas, L., F. Santiago-Mandujano, D. Hebel, R. Lukas, D. Karl and E. Firing. Hawaii Ocean Time-series Program Data Report 4. 1992. School of Ocean and Earth Science and Technology, University of Hawaii, 248 pp.

Hawaii Ocean Time-Series Golden Anniversary Science Symposium
University of Hawaii, November 1993

Lukas, R. and F. Bingham. Annual and interannual variations of hydrographic properties observed in the Hawaii Ocean Time-series (HOT).

Bingham, F. The oceanographic context of HOT.

Firing, E. The north Hawaiian ridge current and other flows near ALOHA.

Kennan, S. Possibilities for stirring along the Hawaiian ridge.

Lukas, R. and F. Bingham. An anomalous cold event in the bottom water observed at station ALOHA.

Winn, C. Air-sea carbon dioxide exchange at station ALOHA.

Sadler, D. Time Series measurement of pH at station ALOHA.

Letelier, R. Inorganic carbon assimilation at station ALOHA: possible evidence of a change in carbon fluxes.

Campbell, H. Nolla, H. Liu and D. Vaulot. Phytoplankton population dynamics at the Hawaii Ocean Time Series station ALOHA.

Letelier, R. Spatial and temporal distribution of *Trichodesmium* sp. at Station ALOHA: how important are they?

Campbell, L. H. Nolla and D. Vaulot. The importance of *Prochlorococcus* to Community Structure in the Central North Pacific Ocean.

Liu, H and L. Campbell. Measurement of Growth and Mortality Rates of *Prochlorococcus* and *Synechococcus* at station ALOHA using a new selective inhibitor technique.

Moyer, C., L. Campbell, D. Karl, and J. Wilcox. Restriction fragment length polymorphism (RFLP) and DNA sequence analysis of PCR-generated clones to assess diversity of picoekaryotic algae in the subtropical Central North Pacific Ocean (station ALOHA).

Karl, D. R. Letelier, L. Tupas, J. Dore, D. Hebel and C. Winn. N_2 fixation as a contributor to new production at station ALOHA.

Dore, J. Nitrate diffusive flux cannot support new production during quiescent periods at station ALOHA.

Karl, D., G. Tien and K. Yanagi. Phosphorus dynamics at station ALOHA.

Yuan, J. and C. Measures. Sampling and analysis of dissolved iron.

Dore, J. Nitrification in the lower euphotic zone at station ALOHA: patterns and significance.

Tupas, L. B. Popp and D. Karl. Dissolved organic carbon in oligotrophic waters: experiments on sample preservation, storage and analysis.

Hebel, D. Temporal distribution, abundance and variability of suspended particulate matter (particulate carbon, nitrogen and phosphorus) at station ALOHA - observations of a seasonal cycle.

Karl, D., D. Hebel, L. Tupas, J. Dore and C. Winn. Station ALOHA particle fluxes and estimates of export production.

Krothapalli, Y. Li and F. Mackenzie. What controls the temporal variability of carbon flux at station ALOHA?

Christian, J. Vertical fluxes of carbon and nitrogen at station ALOHA.

Smith, C., D. DeMaster, R. Pope, S. Garner, D. Hoover and S. Doan. Seabed radionuclides, bioturbation and benthic community structure at the Hawaii Ocean Time-Series station ALOHA.

Polovina, J. and D. Kobayashi. HOT and Hawaii's fisheries landings: complementary or independent Time-Series?

The Oceanography Society Pacific Basin Meeting
Honolulu, HI, July 1994

Karl, D. M. HOT: a time-series study of carbon cycling in the oligotrophic North Pacific.

Lukas, R., F. Bingham and E. Firing. Seasonal-to-interannual variability observed in the Hawaii Ocean Time-Series.

Winn, C., F. Mackenzie, C. Carrillo and D. Karl. Air-sea carbon dioxide exchange at station ALOHA.

Bidigare, R., L. Campbell, M. Ondrusek, R. Letelier, D. Vaulot and D. Karl. Phytoplankton community structure at station ALOHA (22º 45'N, 158ºW) during fall 1991.

Liu, H. and L. Campbell. Growth and grazing rates of Prochlorococcus and Synechococcus at station ALOHA measured by the selective inhibitor technique.

Karl, D. M. The Hawaii Ocean Time-Series (HOT) program: the first five years.

Letelier, R., J. Dore, C. Winn and D. Karl. Temporal variations in photosynthetic carbon assimilation efficiencies at station ALOHA (22º 45'N; 158º 00'W).

Dore, J. E. and D. M. Karl. Nitrite distributions and dynamics at station ALOHA.

Fujieki, L. A., D. V. Hebel, L. M. Tupas and D. M. Karl. Hawaii Ocean Time-Series data organization and graphical system (HOT-DOGS)

Christian, J. and D. Karl. Vertical fluxes of carbon and nitrogen at station ALOHA.

Houlihan, T., J. Dore, L. Tupas, D. Hebel, G. Tien and D. Karl. Freezing as a method of preservation for seawater dissolved nutrient and organic carbon samples.

Hebel, D. V., F. P. Chavez, K. R. Buck, R. R. Bidigare, D. M. Karl, M. Latasa, M. E. Ondrusek, L. Campbell and J. Newton. Do GF/F filters underestimate particulate chlorophyll *a* and primary production in the oligotrophic ocean?

Tupas, L., B. Popp, D. Hebel, G. Tien and D. Karl. Dissolved organic carbon measurements at station ALOHA measured by high temperature catalytic oxidation: characteristics and variation in the water column.

Bingham, F. and B. Qiu. Interannual variability of surface and mixed-layer properties observed in the Hawaii Ocean Time-Series.

Bingham, F. and R. Lukas. Seasonal cycles of temperature, salinity and dissolved oxygen observed in the Hawaii Ocean Time-Series.

Firing, E. Currents observed north of Oahu during the first five years of HOT.

Kennan, S. and R. Lukas. Saline intrusions in the intermediate waters north of Oahu.

Lukas, R. Interannual variability of Pacific deep and bottom waters observed in the Hawaii Ocean Time-Series.

8. Data Availability and Distribution

Data collected by HOT program scientist are made available to the oceanographic community as soon after processing as possible. In order to provide easy access to our data, we have provided summaries of our CTD and water column chemistry data on the enclosed IBM PC 3.5" high-density floppy diskette. CTD data at NODC standard pressures for temperature, potential temperature, salinity, oxygen and potential density are provided in ASCII files; water column chemistry data are provided in Lotus 1-2-3™ files. The pressure and temperature reported for each water column sample are derived from CTD temperature and pressure readings at the time of bottle trip. Densities are calculated from calibrated CTD temperature, pressure and salinity values. These densities are used, where appropriate, to express chemical concentrations on a per kilogram basis. With the exception of the results of replicate analysis, all water column chemical data collected during 1992 are given in these data sets.

The data included in the Lotus 1-2-3™ files have been quality controlled and the flags associated with each value indicate our estimate of the quality of each value. The text file `readme.txt` gives a description of data formats and quality flags.

A more complete data set, containing data collected since year 1 of the HOT program, as well as 2 dbar averaged CTD data, are available from two sources. The first is through NODC in the normal manner. The second source is via the world-wide Internet system. The data reside in a data base on a workstation at the University of Hawaii, and may be accessed using anonymous ftp on Internet.

In order to maximize ease of access, the data are in ASCII files. File names are chosen so that they may be copied to DOS machines without ambiguity. (DOS users should be aware that Unix is case-sensitive, and Unix extensions may be longer than 3 characters.)

The data are in a subdirectory called /pub/hot. More information about the data base is given in several files called `Readme.*` at this level. The file `Readme.first` gives general information on the data base; we encourage users to read it first.

The following is an example of how to use ftp to obtain HOT data. The user's command are denoted by underlined text. The workstation's Internet address is hokulea.soest.hawaii.edu, or 128.171.154.47 (either address should work).

1. At the Prompt >, type ftp 128.171.154.47. or ftp hokulea.soest.hawaii.edu.

2. When asked for your login name, type anonymous.

3. When asked for a password, type your email address.

4. To change to the HOT database, type cd /pub/hot.

   To view files type ls. A directory of files and subdirectories will appear.

4a. To obtain a list of publications, type cd publication-list then get hotpub.lis

4b. To obtain the JGOFS protocol manual, type cd protocols then get 1142.asc.

4c. To obtain water column data, type cd water, then get <filename> where the filename is hot#.gof (JGOFS data) or hot#.sea (WOCE data) and # is the HOT cruise of interest.

5. To obtain further information about the database type get Readme.first. This will transfer an ASCII file to your system. Use any text editor to view it.

6. To exit type bye.

7. Data on optical parameters are located on another server. To obtain light data, at the prompt type ftp 128.171.154.13 or ftp hahana.soest.hawaii.edu then follow steps 2 to 4.